2012

Designing Direct and Indirect Factor Xa Inhibitors

Rami Al-Horani
Virginia Commonwealth University

School of Pharmacy
Virginia Commonwealth University

This is to certify that the dissertation prepared by Rami A. Al-Horani entitled "DESIGNING DIRECT AND INDIRECT FACTOR Xa INHIBITORS" has been approved by his committee as satisfactory completion of the dissertation requirement for the degree of Doctor of Philosophy

_____
Umesh R. Desai, PhD, Department of Medicinal Chemistry, School of Pharmacy

_____
Glen E. Kellogg, PhD, Department of Medicinal Chemistry, School of Pharmacy

_____
Keith C. Ellis, PhD, Department of Medicinal Chemistry, School of Pharmacy

_____
Scott Gronert, PhD, Department of Chemistry, College of Humanities and Sciences

_____
H. Tonie Wright, PhD, Department of Biochemistry, School of Medicine

_____
Richard R. Glennon, PhD, Chairman of Department of Medicinal Chemistry

_____
Victor A. Yanchick, PhD, Dean of School of Pharmacy

_____
F. Douglas Boudinot, PhD, Dean of School of Graduate Studies

May 7, 2012

DESIGNING DIRECT AND INDIRECT FACTOR Xa INHIBITORS

A Dissertation submitted in partial fulfillment of the requirements for the degree of Doctor of Philosophy at Virginia Commonwealth University

by

RAMI A. AL-HORANI
MS Pharmaceutical Sciences, University of Jordan, Amman, Jordan, 2003
B Pharm., University of Jordan, Amman, Jordan, 2000

Director: UMESH R. DESAI
PROFESSOR, DEPARTMENT OF MEDICINAL CHEMISTRY

Virginia Commonwealth University
Richmond, Virginia

May 2012

Acknowledgment

I would like to thank my supervisor Dr. Umesh R. Desai for his relentless support at all times, all stages, and in all aspects of my five–year graduate work. His sincere mentorship, excellent academic guidance, and generous financial support have helped me not only to gain a compelling scientific knowledge and high standards of professional skills, but also to truly enjoy this thrilling phase of my life which was full of fun, science, and friendship.

I would also like to thank my committee members Drs. Glen E. Kellogg, Keith C. Ellis, Scott Gronert, H. Tonie Wright, and Martin K. Safo (Dean Rep.) for the time they had invested in reading, advising, and discussing my independent research proposal as well as the practical aspects of my graduate work which I have documented in this dissertation. Furthermore, I would like to express my sincere thanks to Drs. Glen E. Kellogg, Scott Gronert, H. Tonie Wright, and Donald F. Brophy for reviewing and recommending my postdoctoral fellowship application to the American Heart Association. In addition, genuine gratitude goes to all who recommended and voted for me with respect to the J. Doyle Smith award and School of Pharmacy Dean's award.

In Dr Desai's laboratory, I have had the privilege of working with endowed graduate students and postdoctoral scholars. I thank the Desai group postdoctoral scholars – Drs. Phil Mosier, Aiye Liang, and Rajesh Karuturi. I also thank all current and previous graduate students in Dr Desai's laboratory who contributed to my graduate work in one way or another particularly Akul Mehta, May Abdel Aziz, Jenson Verghese, Shrenik Mehta, Rio Boothello, and Malaika Argade.

My words cannot describe my heartwarming thanks that go to my parents – Halemah and AbdulRahamn – for their endless love and prayers. I wish also to express my gratitude to all of my beloved sisters, brothers, and friends for their support and advice. Finally, I am certainly in debit for my long life love, my wife Kholoud, who was there all the time to support me in this scientific endeavor. Kholoud was more than competent to carry the responsibility by herself when it was needed and to take care of me and the joy of our life, our son Elias.

Table of Contents

Lists of Tables

Lists of Figures

Lists of Abbreviations

ABH3CA	2-azabicyclo [2.2.1]heptane-3-carboxylic acid
APTT	Activated Partial Thromboplastin Time
AT	Antithrombin
CE	Capillary Electrophoresis
EHBS	Extended Heparin Binding Site
FID	Free Induction Decay
FLH	Full Length Heparin
FIIa	Factor IIa (Thrombin)
FXa	Factor Xa
FVIIa	Factor VIIa
FIXa	Factor IXa
FXIa	Factor XIa
FXIIa	Factor XIIa
GAG	Glycosaminoglycan
H	Heparin
HBS	Heparin Binding Site
HS	Hill Slope
I	Ionic Strength
LMWH	Low Molecular Weight Heparin
NMR	Nuclear Magnetic Resonance
P2CA	Piperidine–2–Carboxylic Acid
P3CA	Piperidine–3–Carboxylic Acid
PA	Phenylalanine
PBS	Pentasaccharide Binding Site
PT	Prothrombin Time
SAR	Structure–Activity Relationship
THIQ	1,2,3,4–Tetrahydroisoquinoline
THIQ3CA	1,2,3,4–Tetrahydoisoquinoline–3–Carboxylic Acid
THP2CA	1,2,3,6–Tetrahydropyridine–2–Carboxylic Acid

Abstract

DESIGNING DIRECT AND INDIRECT FACTOR Xa INHIBITORS

A Dissertation submitted in partial fulfillment of the requirements for the degree of Doctor of Philosophy at Virginia Commonwealth University

By Rami A. Al-Horani, PhD

Virginia Commonwealth University, 2012

Director: Umesh R. Desai
Professor, Department of Medicinal Chemistry

Anticoagulants are the basis for treatment and prevention of thrombotic diseases. The currently available medicines are associated with a wide range of adverse reactions that mandates developing new anticoagulants. Several lines of evidence support the superiority of factor Xa (FXa) as a promising target to develop novel anticoagulants. This work focuses on the design of direct and indirect FXa inhibitors using an interdisciplinary approach. As indirect FXa inhibitors, a focused library of tetrasulfated *N*–arylacyl tetrahydroisoquinoline (THIQ) non–saccharide allosteric antithrombin activators was designed, synthesized, and biochemically evaluated to establish their structure–activity relationship (SAR). An *N*–arylacyl THIQ analog having carboxylate at position–3, two sulfate groups at positions–5 and –8 of THIQ moiety, butanoyl linker, and two sulfate groups at positions–2 and –5 of the phenolic monocyclic moiety

was identified as the most promising nonsaccharide antithrombin activator with K_D of 1322 ± 237 μM and acceleration potential of 80–fold. Its biochemical profile indicates a strong possibility that it activates antithrombin by the pre–equilibrium pathway rather than the induced–fit mechanism utilized by heparin analogs. A similar interdisciplinary approach was exploited to design direct FXa inhibitors that possess high selectivity and are potentially orally bioavailable. Structurally, the designed direct FXa inhibitors are neutral THIQ dicarboxamides. THIQ dicarboxamide is a privileged structure with a semi–rigid character, a structural feature that potentially offers high selectivity for targeting FXa over other coagulation and digestive proteases. It can also be thought of as an amino acid–like structure, which affords accessibility to a large number of compounds using well established peptide chemistry. Mechanistically, the designed inhibitors were expected to bind to FXa in the active site and function as orthosteric inhibitors. These direct FXa active site inhibitors are also likely to inhibit clot–bound enzyme. Nearly 60 THIQ dicarboxamides were synthesized and biochemically evaluated. Through detailed SAR analysis, the most potent analog was designed and found to exhibit an IC_{50} of 270 nM (Ki = 135 nM), an improvement of more than 207–fold over the first inhibitor synthesized in the study. The most potent inhibitor displayed at least 1887–fold selectivity for FXa over other coagulation enzymes and a selectivity index of at least 279–fold over the digestive serine proteases. This analog doubled plasma clotting times at 17–20 μM, which are comparable to those of agents being currently studied in clinical trials. Overall, allosteric and orthosteric approaches led to the design of indirect and direct small molecule inhibitors of FXa based on the THIQ scaffold. This work introduces two promising molecules, a tetrasulfated *N*–arylacyl THIQ analog as a heparin mimetic and a neutral THIQ dicarboxamide as a potent, selective, and potentially bioavailable peptidomimetic, for further advanced medicinal chemistry studies.

CHAPTER 1: INTRODUCTION

Blood coagulation is the hallmark of hemostasis. Hemostasis is described as physiologic clotting which prevents excessive blood loss from injured blood vessels. The coagulation cascade maintains a balance between blood flow and blood clotting under physiologic conditions, the dysfunction of which results in hemorrhage or thrombosis.

1.1. The Coagulation Cascade Model—The coagulation process comprises a series of proteolytic reactions working in a cascade fashion. This process can be triggered either by the intrinsic pathway[1,2] or by the extrinsic pathway, both of which converge at factor Xa (FXa) (Figure 1).[3-5]

1.1.1. The Intrinsic Pathway— In this pathway, all clotting factors are present in the blood and are activated when blood comes in contact with activated platelets. Factor XII in plasma is activated to factor XIIa (FXIIa) upon interaction with collagen or other negatively charged surfaces (as in vascular endothelium damage, lipoproteins in hyperlipidemia, or bacteria in infections) with the aid of high molecular–weight kininogen (HMWK). The resulting FXIIa activates factor XI to factor XIa (FXIa) which eventually activates factor IX to factor IXa (FIXa). FIXa combines later with factor VIIIa (FVIIIa) to form the tenase complex in the presence of calcium and phospholipids. This complex subsequently activates factor X to FXa.[3,6,7]

1.1.2. The Extrinsic Pathway— The extrinsic pathway is activated in an injury without direct contact with nonphysiological surfaces, by endothelium damage, or by hypoxia resulting from reduced blood flow.[7] This pathway is triggered when tissue factor (TF) of the extravascular system comes in contact with factor VII in the plasma after injuries to blood vessels. TF activates factor VII to factor VIIa (FVIIa) forming a TF–FVIIa complex which subsequently activates factor X to FXa.[3,6,7]

1.1.3. The Common Pathway— Both intrinsic and extrinsic pathways converge at FXa, the first serine protease in the common pathway leading to clot formation. The resulting FXa, from either pathway, complexes with factor Va (FVa), calcium, and phospholipid to form prothrombinase. Prothrombinase subsequently activates factor II (prothrombin) to factor IIa (FIIa, thrombin) which converts factor I (fibrinogen) to factor Ia (FIa, fibrin) monomers. Factor XIIIa (FXIIIa) which is also activated by thrombin, converts the soluble fibrin to cross-linked fibrin on the surface of the activated platelets and forms an impermeable hemostatic plug. Thrombin also provides positive feedback to the cascade by activating factor XI, factor VIII in the intrinsic pathway, and factor V in the common pathway. This ensures the efficient generation of a burst of thrombin and hence fibrin.[3,6,7]

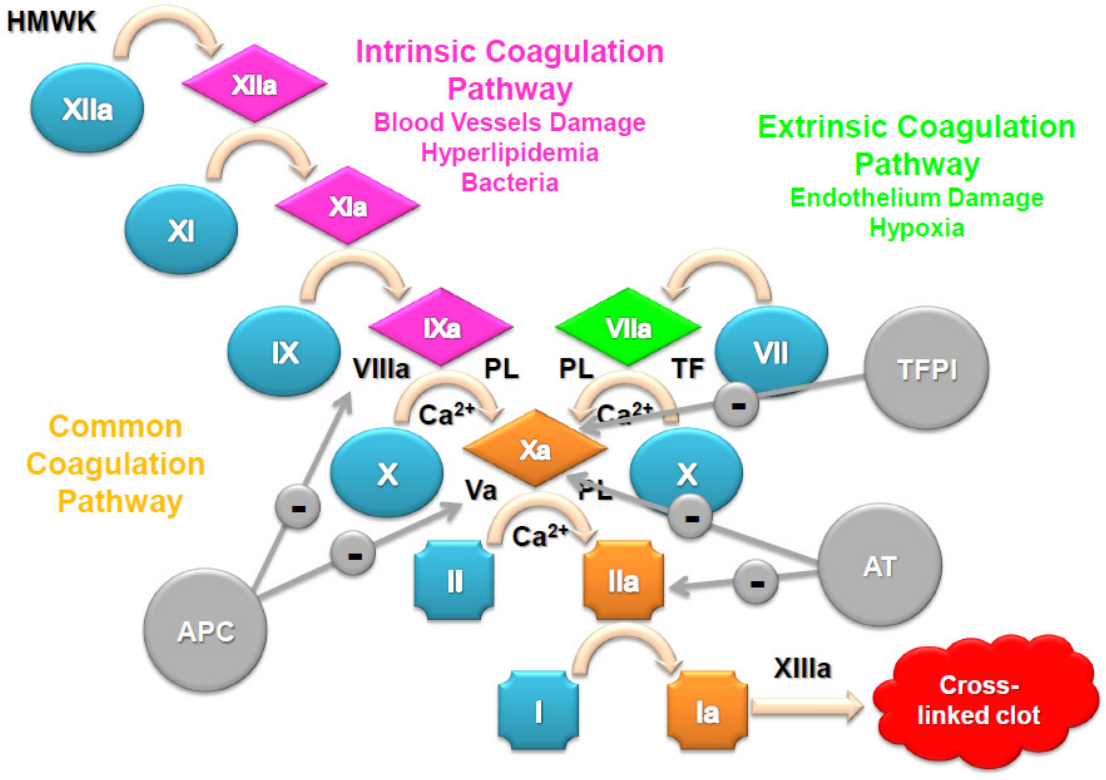

Figure 1. The coagulation cascade: procoagulant proteins and regulatory natural anticoagulants. **APC—** Activated Protein C**, AT—** Antithrombin, **HMWK**— High molecular weight kininogen, **PL**— Phospholipids, **TF**— Tissue factor, **TFPI—** Tissue Factor Pathway Inhibitor.

1.2. Physiologic Regulators of Coagulation— Excessive clotting is certainly detrimental and should be physiologically avoided. At least three anticoagulant proteins exist naturally in our body to regulate the procoagulant activity of coagulation proteins. These proteins include antithrombin (AT),[8] activated protein C (APC),[9] and tissue factor pathway inhibitor (TFPI).[10] The former two anticoagulants target the process of amplification and propagation, while the latter anticoagulant inhibits the initiation steps of coagulation (Figure 1). AT belongs to the serpin (**ser**ine **p**rotease **in**hibitor) family. AT is considered to be the major inhibitor of thrombin, FXa, and FIXa.[8, 11] AT also seems to inhibit FVIIa[12] and FXIa.[13] However, AT is an intrinsically poor anticoagulant and needs heparin, a highly sulfated glycosaminoglycan (GAG), to enhance its inhibitory activity toward the serine proteases of the coagulation about 300–4,000-fold.[14]APC inhibits both FVa and FVIIIa.[9] APC physiologically forms upon activation of protein C by the thrombin–thrombomodulin complex. Lastly, TFPI inhibits only FXa.[10]

1.3. Thrombotic Diseases and Current Therapeutic Options—

1.3.1. Thrombotic Diseases— Dysfunction of the coagulation process may lead either to hemorrhage (haemophilia) or clotting disorders (thrombosis). Thrombosis is the underlying cause of several cardiovascular diseases. Thrombi could form in blood arteries leading to acute myocardial infarction or ischemic stroke. Formation of thrombi in the venous circulation may result in deep vein thrombosis which can lead to life–threatening pulmonary embolism. The morbidity and mortality rates associated with thrombotic diseases are vast. For example, venous thromboembolism afflicts annually up to 600,000 individuals in the US and is implicated in at least 100,000 deaths.[15] The blood clotting disorders are the second most frequent cause of death in cancer patients with a mortality rate of about 15–20% of hospitalized cancer patients.[16]

1.3.2. Current Therapeutic Options— Given the overwhelming impact of thrombotic diseases, developing therapies that prevent and treat these diseases has received a great deal of attention and is still in high demand. Therapies which are used to prevent and/or treat thrombotic diseases belong primarily to three different mechanistic classes including fibrinolytic agents, antiplatelet agents, and more importantly anticoagulants.[17]

1.3.3. Anticoagulants— Anticoagulants are the mainstay for prevention and treatment of all thrombotic diseases. They stop pathological clot formation by inhibiting directly or indirectly one or more procoagulant enzymes. Practically, only thrombin and FXa, the two serine proteases of the common pathway, have been successfully targeted by inhibition for anticoagulant activity.[6,7,17]

Structurally, clinically approved anticoagulants comprise a wide variety of compounds that are either small molecules or macromolecules. They include saccharides such as heparin, low molecular weight heparins (LMWHs), and fondaparinux. Heparin and LMWHs are particularly highly heterogeneous and polydisperse preparations of a mixture of chemical entities while fondaparinux is homogenous synthetic pentasaccharide.[7,14,17] Clinically available anticoagulants also include coumarins such as warfarin, peptides such as bivalirudin, and peptiomimetics such as argatroban, dabigatran etexilate and rivaroxaban.[17] All of these anticoagulants are highly homogenous preparations of a single chemical entity (Figure 2).

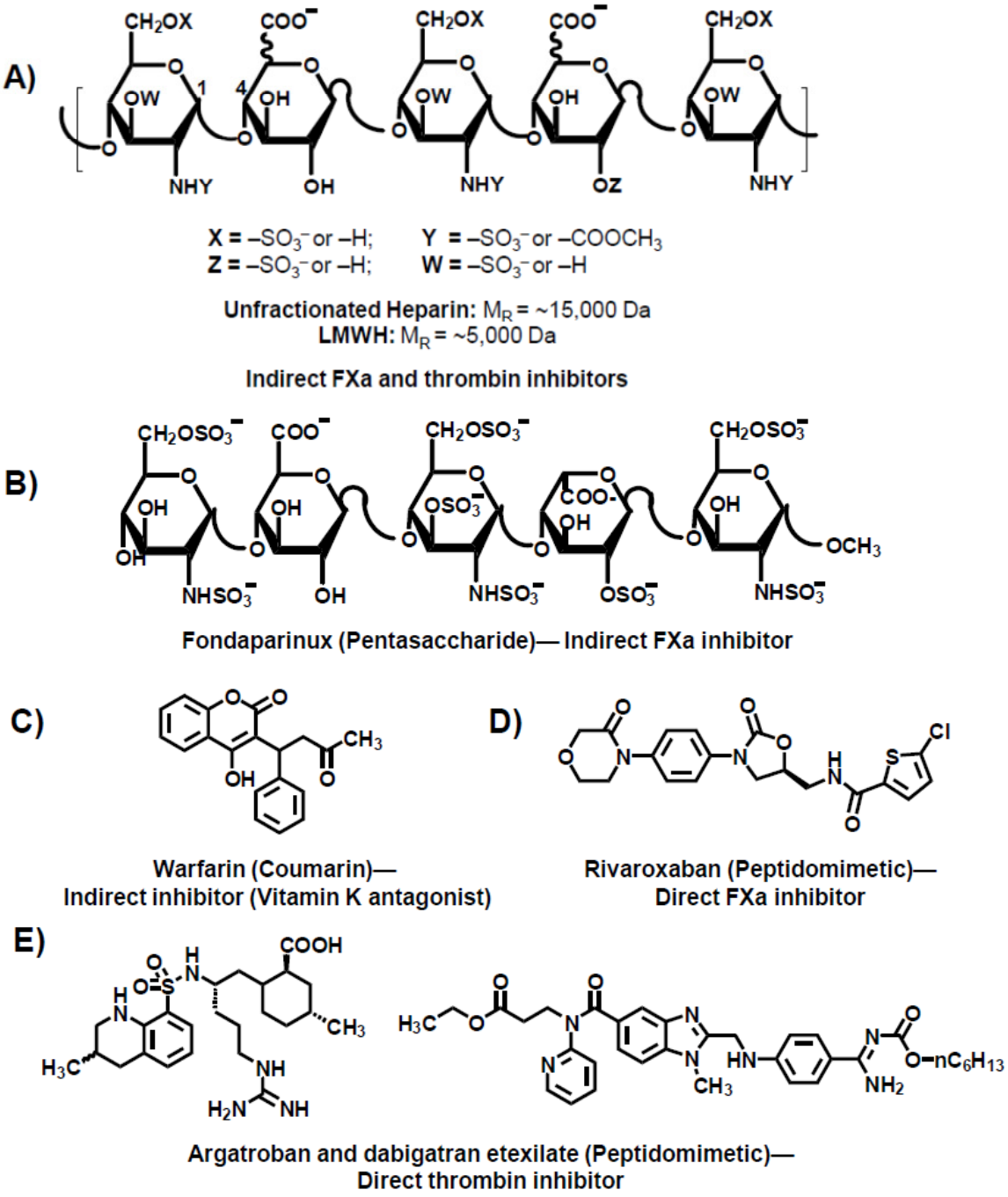

Figure 2. Representative examples of clinically available anticoagulants.

Mechanistically, the intended inhibition could be achieved by direct or indirect inhibition of the targeted enzyme. Direct enzyme inhibitors may compete with the endogenous substrate;

therefore they can be competitive active site inhibitors. They may also disrupt the catalytic triad of the procoagulant proteases by inducing nonproductive conformational change through binding to an allosteric site; therefore they can be un– or non– competitive inhibitors. Hirudin, argatroban, and dabigataran etexilate are examples of direct thrombin inhibitors, whereas rivaroxaban is the only approved direct FXa inhibitor.[6,7,17] The catalytic activity of the procoagulant serine proteases can be also indirectly abolished by activating natural anticoagulant proteins such as AT. The activated natural anticoagulant will act as inhibitory substrate for the coagulation procoagulant enzymes. Unfractionated heparin, LMWHs, and fondaparinux pentasaccharide are the most common AT activators in the clinic, where they are prescribed to promote the indirect inhibition of FXa and/or thrombin. Indirect anticoagulants also include those molecules that adversely affect the biosynthesis of coagulation factors. Warfarin, the prototypic vitamin K antagonist, inhibits the post–translational process necessary for the biosynthesis of fully functional coagulation enzymes.[7]

The core of this work is to design direct and indirect FXa inhibitors as anticoagulants. Accordingly, the following sections will focus on relevant observations that assess the superiority of FXa as promising drug target for anticoagulant activity, structural and mechanistic details about AT and AT–based indirect anticoagulants, structural and mechanistic studies related to FXa, and the current status of direct inhibitors.

1.4. Factor Xa or Thrombin: Which is Better as an Anticoagulant Target— It is generally understood that the more downstream a procoagulant protease in the coagulation cascade is being inhibited, the better anticoagulant efficacy the inhibitor can achieve. In contrast, the more upstream a procoagulant is being inhibited, the less likelihood of bleeding risk the inhibitor causes. Therefore, FXa inhibitors are likely to possess more anticoagulant efficacy

than inhibitors of FVIIa, FIXa, FXIa, and FXIIa and leads to less bleeding complications relative to thrombin inhibitors. Several lines of evidence support the superiority of FXa as more effective and safer drug target as follows:

1) FXa is more thrombogenic than thrombin[18] and activation of one molecule of FX results in the generation of 1000 molecules of thrombin due to the amplification nature of the coagulation cascade.[19] This implies that a lower dose of FXa inhibitor is needed to effect anticoagulation relative to the needed dose of thrombin inhibitor to effect the same response.

2) Fondaparinux, indirect FXa inhibitor, has a significant antithrombotic potential and safety compared with enoxaparin, a LMWH that has both anti-thrombin and anti-FXa activity. In extensive orthopedic trials of venous thromboembolism prophylaxis, fondaparinux showed a 55% reduction in venous thromboembolism compared with enoxaparin.[20,21] In patients with cardiac disease, fondaparinux and enoxaparin showed equivalent efficacy in myocardial infarction and refractory ischemia, but fondaparinux showed a significant reduction in major bleeding compared with the LMWH. Therefore, fondaparinux has provided strong clinical proof supporting the concept that specific FXa inhibition provides more effective and safer therapy.[20,21]

3) Compared with thrombin, FXa is known to have limited number of functions besides activating prothrombin to thrombin via the action of the prothrombinase complex. Thrombin has a range of important activities within and outside the coagulation process, the inhibition of which might influence the efficacy and safety of specific thrombin inhibitors.[22,23]

4) FXa inhibitors are generally associated with less rebound hypercoagulation, which is more common with unfractionated heparin[24,25] and direct thrombin inhibitors.[25]

1.5. Validating Factor Xa as Drug Target — The viability of FXa inhibition was first tested in 1987. The first FXa inhibitor, the naturally occurring compound antistasin, was isolated

from the salivary glands of the Mexican leech *Haementeria officinalis.*[26,27] Antistasin is a 119 amino–acid polypeptide. Enzyme kinetic studies revealed that it is a slow, tight–binding, potent FXa inhibitor with an average *K*i of 0.45 nM.[28] Another naturally occurring FXa inhibitor is a single–chain, 60 amino–acid peptide known as the tick anticoagulant peptide (TAP). TAP was isolated in 1990 from extracts of the soft tick *Ornithodoros moubata.* Similar to antistasin, TAP is a slow, tight–binding inhibitor of FXa with *K*i of ~0.6 nM.[29]

These two natural FXa inhibitors which have >50000–fold selectivity for FXa over other related clotting serine proteases were exploited to guide the efforts to understand the physiologic role of FXa in hemostasis and thrombosis, and to validate FXa as a viable drug target for new effective anticoagulants.[30-34] The antithrombotic effects of these compounds were compared with those of direct thrombin inhibitors (hirudins) and of indirect thrombin and FXa inhibitors (unfractionated heparin and LMWHs) in animal models of thrombosis. The studies concluded that direct FXa inhibitors could be a more effective approach to anticoagulation, and might also offer a wider therapeutic window.[30-34] In fact, FXa is now being targeted by two clinically approved anticoagulants: fondaparinux (saccharide indirect FXa inhibitor) and rivaroxaban (peptiomimetic direct FXa inhibitor).

1.6. Antithrombin and Antithrombin–Based Anticoagulants —Clinically used anticoagulants are generally direct or indirect inhibitors of coagulation–related enzymes. The widely used anticoagulants, heparins, are primarily indirect inhibitors of thrombin and FXa. Unfractionated heparin and LMWHs are AT activators for the accelerated inhibition of thrombin and FXa, whereas the pentasaccharide fondaparinux is an allosteric activator of the inhibitory activity of AT only toward FXa. Non-saccharide AT allosteric activators were also designed as anticoagulants by Desai and co–workers for the accelerated inhibition of FXa.

1.6.1. Antithrombin and the Kinetics of Proteases Inhibition— AT is a plasma glycoprotein belonging to the serpin superfamily.[35] It is a major regulator of blood clotting which inactivates a number of serine proteases in the coagulation cascade, especially thrombin and FXa.[36] Although the rates of AT inhibition of these enzymes are slow under physiological conditions, AT interaction with cell–surface polysaccharide species, such as heparan sulfate, accelerates the inactivation of the procoagulant proteases several fold.[37]

Several crystal structures of AT are available in which the serpin is present in three different forms, namely, intact (uncleaved, native), active, or cleaved inactive forms. The structures of intact, uncleaved free AT reveals 9 α–helices surrounding 3 β-sheets.[38-40] In this form, several structural features are important:[14,35]

1) A dominant five–stranded β-sheet A, approximately in the center of the serpin.

2) A reactive center loop (RCL) of 15 residues containing the reactive bond R393–S394 (P1–P1′) at the top of the serpin.

3) The partial insertion of the two residues G379–S380 at the *N*-terminal end of the RCL as a short β-strand between strands 3 and 4 of β–sheet A in AT. This partially inserted RCL undergoes major changes during the process of protease inhibition.

The structure of AT cleaved at the reactive bond is very similar to intact AT except for the complete insertion of RCL as a new strand in β–sheet A. This structural change results in the movement of the P1 residue in the RCL from the original side to the opposite side of AT. This dramatic conformational change following cleavage of the P1-P1′ bond in the RCL by the target enzyme is critical for the disruption of the catalytic triad of the protease, thereby resulting in the inactivation of the enzyme.[41-44]

The mechanism of AT–mediated inhibition of thrombin and FXa is known as the serpin 'mousetrap' mechanism in which AT acts as bait to trap the target enzyme (E) in an equimolar, covalent, inactive complex (E*–AT*). The RCL initially interacts with the active site of the protease as in a normal substrate reaction to form the Michaelis–Menten complex (E:AT). This is rapidly followed by cleavage of the scissile bond P1-P1′ in the RCL to form an acyl–enzyme intermediate (E-AT) that undergoes a massive rearrangement to disrupt the enzyme's catalytic triad resulting in the protease inhibition (E*-AT*). The efficacy of the inhibition is occasionally diminished by the substrate pathway; however, the contribution of this pathway is negligible under normal experimental conditions (Figure 3).[14,42-45]

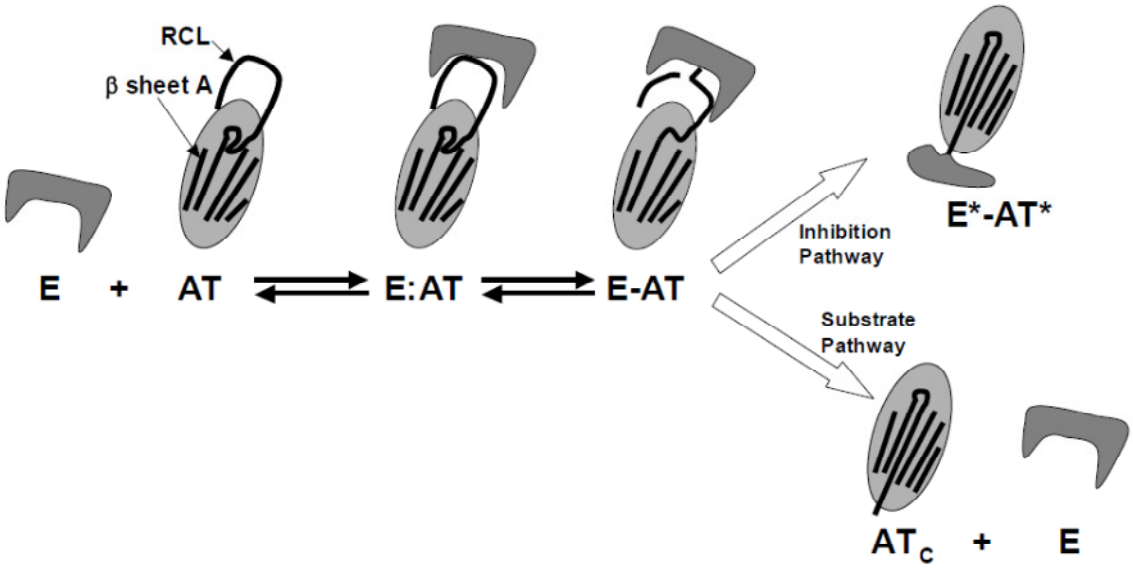

Figure 3. Antithrombin–mediated mousetrap inhibition of coagulation proteins. **AT**—Antithrombin, **E:AT**—Micahelis–Menten Complex, **E–AT**— Acyl–Enzyme Intermediate, **E*–AT***—Antithrombin–Enzyme Complex, **AT$_C$**— Cleaved Antithrombin, **RCL**—Reactive Center Loop. The figure is adapted from reference 7.

Enzyme kinetic studies revealed that the AT–mediated inhibition rates of thrombin and FXa are significantly lower than those of most serpins that inhibit their target serine proteases with a second–order rate constant limited only by diffusion.[14] At pH 7.4 and 25 °C, uncatalyzed *in vitro* thrombin inhibition rates are in the range of 7–11 × 10^3 $M^{-1}s^{-1}$,[46-48] while those for FXa

are in the range of 2–3 × 10^3 $M^{-1}s^{-1}$.[14] The slow rates of thrombin and FXa inhibition are dramatically increased in the presence of heparins. The second–order rate constant for thrombin inhibition by AT–heparin complex is in the range of 1–4 ×10^7 $M^{-1}s^{-1}$ representing an acceleration of more than 2,000–fold. Likewise, the second–order rate constant for FXa inhibition by AT–heparin complex reaches 1.5 ×10^6 $M^{-1}s^{-1}$ giving rise to an increase of some 600–fold.[49-52] Physiologically, the acceleration in FXa inhibition may reach 2,400–fold due to calcium ions.[53] This enhancement in inhibition of thrombin and FXa explains the clinical use of heparin as an anticoagulant.

No more than 33% of heparin chains bind AT with high affinity. These high affinity chains contain a specific sequence of five residues that contribute nearly 95% of AT binding energy. The five–residue sequence is called heparin pentasaccharide DEFGH. This variant selectively inactivates FXa as it accelerates AT inhibition of FXa about 300–fold, while it accelerates AT inhibition of thrombin only about 1.7–fold.[52]

1.6.2. Mechanism of Heparin Activation of Antithrombin — There are two different mechanisms for heparin–activated AT inhibition of FXa and thrombin. In the case of FXa, the mechanism is known as the two–step, induced fit mechanism or the conformation activation mechanism. In this mechanism, high–affinity heparin, or pentasaccharide DEFGH, binds to the HBS on AT resulting in a conformational change that travels to the RCL. The resulting conformational change expels the partially inserted RCL residues and thus exposes a new exosite in AT. The exposed RCL in heparin-AT complex is better recognized by FXa resulting in ~300–600–fold accelerated cleavage of the amide scissile bond and rapid formation of the covalently inhibited complex (E*-AT*) (Figures 3 and 4).[45,51, 52, 54,55]

In contrast, the mechanism and the heparin structural requirements for the AT–mediated inhibition of thrombin are different. The predominant effect of heparin in accelerating thrombin inhibition arises from a bridging mechanism. Tight binding of AT to the DEFGH sequence in full length heparin is followed by the binding of thrombin to the same chain to form an AT–heparin–thrombin ternary complex. Thrombin then diffuses along the polyanionic chain to encounter the inhibitor resulting in at least 2,000-fold acceleration in inhibition under physiological conditions.[7] A saccharide length of about 18 residues is needed to simultaneously hold thrombin and AT for the accelerated inhibition.[56,57] Recent investigations suggest that such a template mechanism may also play an important role in vivo for AT inhibition of FXa. In the presence of physiological concentrations of calcium ion, full-length heparin was found to accelerate the inhibition of FXa about 40-fold suggesting that longer chains bind to an exosite on the FXa enzyme that is only exposed in presence of calcium ion (Figure 4).[53]

It is important to note that the HBS on AT is located approximately 20 Å away from the RCL and is primarily two binding domains. The two domains are pentasaccharide–binding site (PBS) and the extended heparin binding site (EHBS) (Figure 5). The former domain is formed by charged residues of helices A and D, and the polypeptide N-terminus. The crystal structure and the mutagenesis studies of AT–pentasaccharide complex show that residues R47, K114, K125, and R129 in this region interact with DEFGH.[58-63] In addition to interacting with PBS, full-length heparin binds to EHBS, an extended region formed by residues R132, K133, and R136 at the C–terminal end of helix D.[64] The interaction of DEFGH (or full-length heparin) with PBS results in transmission of binding energy for conformational change in the RCL, suggesting that heparin activation of AT is an allosteric phenomenon.[58,65]

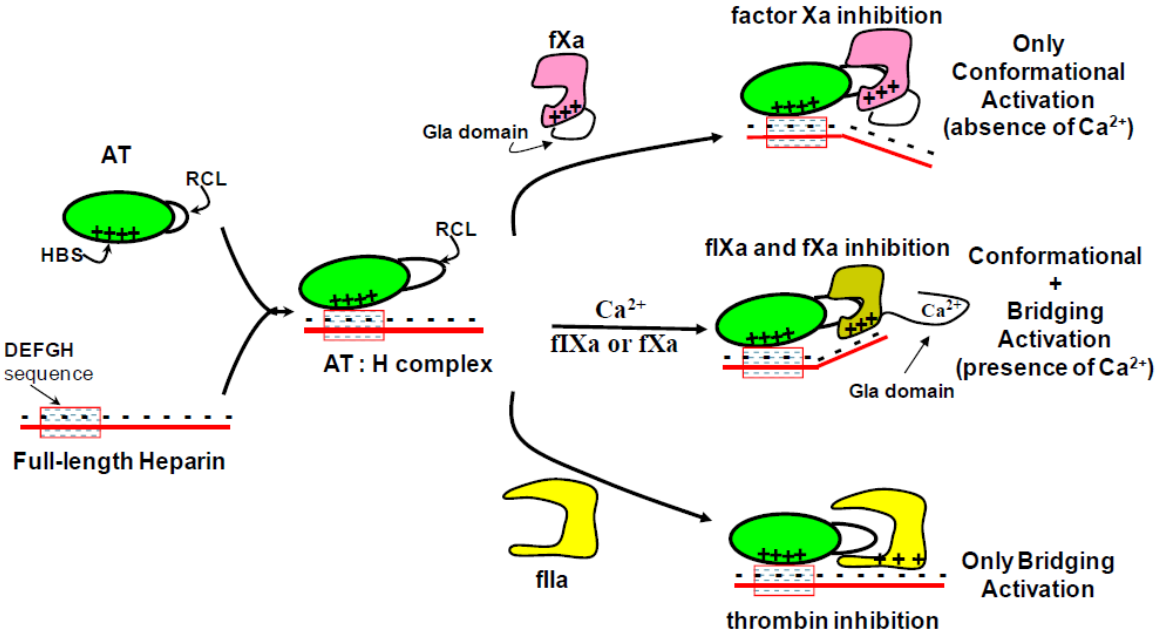

Figure 4. Antithrombin–mediated heparin indirect inhibition of coagulation proteases. **AT—** Antithrombin, **HBS—** Heparin Binding Site, **RCL—** Reactive Center Loop, **H—** Heparin. This figure is adapted from reference 7.

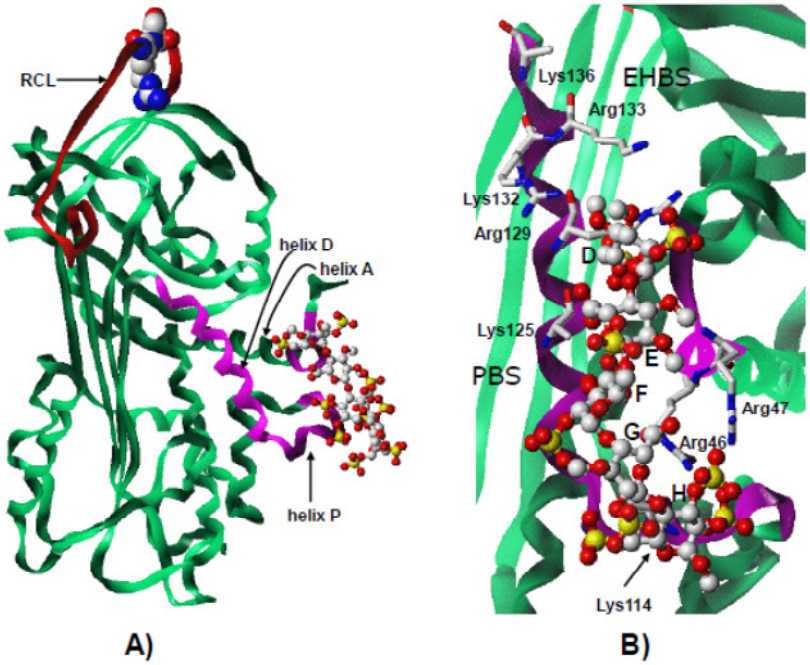

Figure 5. Structure of antithrombin–pentasaccharide DEFGH complex. A) Heparin binding site and RCL. B) Close-up view of the interacting amino acids of PBS with DEFGH and the non–interacting amino acids of EHBS. This figure is adapted from reference 7.

1.6.3. Classes of Antithrombin–Based Anticoagulants—

1.6.3.1. Heparin and Low Molecular Weight Heparins— Heparin, glycosaminoglycan (GAG), is a heterogenous and polydisperse mixture of highly negatively charged linear polysaccharide chains with an average weight of ~14,000. Heparin is a (1—>4) linked copolymer of glucosamine and uronic acid residues that are variously sulfated and acetylated.[14] Heparin could be of high affinity or low affinity to its physiological target, AT. The high–affinity heparin is rich in the pentasaccharide DEFGH sequence and binds to plasma AT with sub–nanomolar affinity at physiological pH resulting in the anticoagulant activity. Such binding is promoted by ionic (40%) and nonionic (60%) interactions between the sulfate and carboxylate groups of DEFGH and positively charged lysines and arginines in the PBS.[52] Low–affinity heparin has less repetition of the DEFGH sequence and binds AT with nearly 1,000-fold lower affinity resulting in much less AT–assisted inhibition acceleration.[66]

The mid–1990s witnessed the discovery of LMWHs which were developed to address the many complications accompanying heparin therapy.[67-69] LMWHs are 1/3rd in length as compared to full length heparin and are commercially produced from heparin through chemical[14] or enzymatic depolymerization.[70-72] Although chemically and mechanistically similar to heparin, the binding affinity of LMWHs for AT significantly varies. Their anti-FXa activity and thrombin inhibition depends on the fraction of DEFGH sequences present in each preparation and the proportion of high–affinity chains that have length greater than 18 saccharides, respectively.[73,74] Established advantages of LMWHs over heparin are the greater bioavailability, better pharmacokinetics, reduced thrombocytopenia, and more predictable dose response, which allows for fixed doses to be administered without laboratory monitoring.[75,76] Nevertheless, LMWHs are still associated with a high risk of bleeding.[76-79]

1.6.3.2. Heparin Pentasaccharide DEFGH — The heparin pentasaccharide sequence DEFGH can be chemically dissected into two chemical domains; a trisaccharide DEF and a disaccharide GH domain. The GH sequence consists of α–L–iduronic acid unit sulfated at the 2–position and β–D–glucosamine unit sulfated at the 2– and 6–positions. The D unit in the trisaccharide DEF is identical to the H unit whereas the E residue is the unsulfated β–D–glucouronic acid. A structural feature that characterizes the DEFGH sequence is the central β–D–glucosamine residue F consisting of three sulfates at the 2–, 3–, and 6–positions (Figure 2). [14] Mechanistically, the heparin pentasaccharide DEFGH is a selective anti-FXa molecule. Accelerated inhibition of FXa by DEFGH is an indirect mechanism and is achieved by activating AT through the two–step, induced–fit, allosteric mechanism depicted in figure 4.[7] The two domains in DEFGH differently contribute to the conformational activation of AT. [52,80,81]

Biochemical studies with the truncated variants, trisaccharide DEF and tetrasaccharide EFGH″ (1–OCH_3 and 3–OSO_3^- as opposed to 1–OH and 3–OH in DEFGH) indicate that the DEF sequence is critical for both the initial recognition of the heparin–binding site and conformational activation processes in AT.[82,83] In addition, the efficient conformational activation of AT to achieve ~300-fold FXa inhibition acceleration can be achieved with trisaccharide DEF except that the affinity of DEF for AT is much weaker (K_D ~66 μM) under physiological conditions.[83] Therefore, it seems that the disaccharide unit GH of the pentasaccharide only enhances the affinity of the pentasaccharide for the conformationally activated inhibitor.[81]

Clinically, heparin pentasaccharide DEFGH is more effective than a LMWH in preventing venous thromboembolism and was equally safe.[84,85] Structurally, DEFGH is relatively decorated with limited number of negative charges, thus it shows reduced non–specific

interactions and improved bioavailability in comparison to the polymeric heparins.[86-89] Synthetically, the heparin pentasaccharide was initially assembled in about 40 steps, yet the reported synthetic protocol helped in establishing the structure–activity relationship (SAR).[90,91] Furthermore, crystal structure of the pentasaccharide–AT complex as well as as enzyme kinetics using the plasma as well as the mutated AT shows that each of the sulfate and carboxylate groups interacts with either one or more lysine or arginine residues in the PBS (Figure 6).[81] Following are the important conclusions of these studies (Figure 7): [14, 91-96]

1) *N*–acetylation of the non–reducing end glucosamine residue D results in formation of D′EFGH which has about 50% anti–FXa activity of the *N*–sulfated pentasaccharide DEFGH.[91]

2) Four sulfate groups, at the 6–position of residue D, 3– and 2–positions of residue F, and 2–position of residue H, are extremely critical for high–affinity binding to AT. For example, removing 3-OSO_3^- of residue F resulted in an approximately 3×10^6–fold loss in affinity.[91,92]

3) The carboxylate groups of uronic acid residues are also important as demonstrated by pentasaccharides DE′FGH and DEFG′H that exhibit less than 5% of the activity of the reference DEFGH.[14]

4) Replacement of $NHSO_3^-$ group in all three glucosamine residues with OSO_3^- and introduction of methyl ethers at the free hydroxyl groups increased FXa inhibitory activity ~200%. The new pentasaccharide (DEFGH–NGA) contains glucose residues instead of glucosamines, which made the total synthesis much easier. This pentasaccharide retains the same negatively charged groups of the natural pentasaccharide and hence is likely to retain the conformational preference and flexibility of the parent molecule.[93]

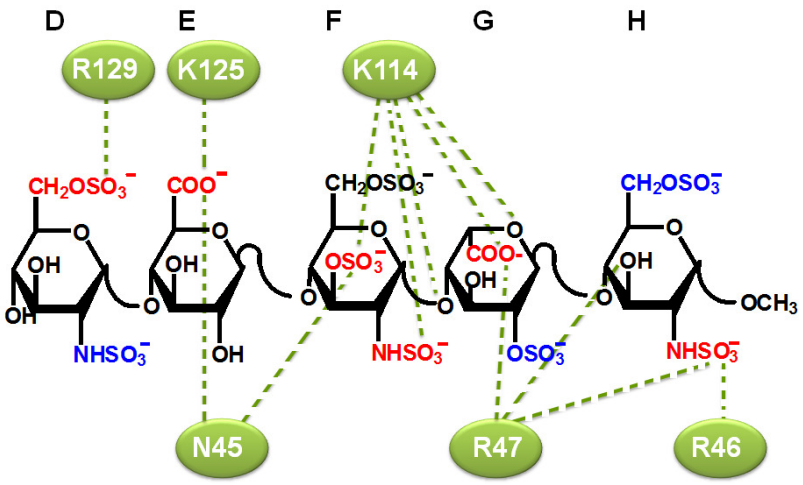

Figure 6. The antithrombin– pentasaccharide interactions. Highlighted amino acids are of PBS. Functional groups in red are essential for interaction with AT while functional groups in blue are needed as optimal structural features.

5) Replacing the sulfate group on the D residue of DEFGH–NAG with a methoxy group led to the discovery of idraparinux, which exhibits about 269% of the activity of the reference DEFGH. Idraparinux can be synthesized from glucose in only 25 steps. It binds to AT with approximately 50–fold higher affinity and has at least a 10–fold longer half life than fondaparinux. Although an injection of idraparinux once–a–week is enough to achieve and maintain the required clinical blood level in patients, idraparinux has a substantial higher rate of major bleeding. Clinical trials had to be stopped because the heparin antidote was not effective with bleeding caused by idraparinux. This led to the development of biotinylated idraparinux that was as effective as idraparinux in animal models of thrombosis, and avidin injection resulted in complete neutralization of its anticoagulant activity.[94,95]

6) A C-pentasaccharide consisting of a carbon (CH_2)–based interglycosidic bond between residues D and E shows FXa inhibitory activity approximately 34% better than DEFGH.[96]

A)

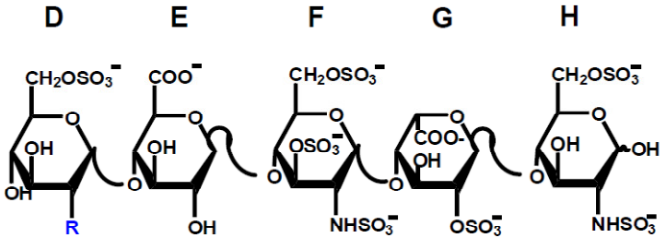

Derivative	R	Anti–FXa activity
DEFGH	-$NHSO_3^-$	~600
D'EFGH	-$NHCOCH_3$	~300

B)

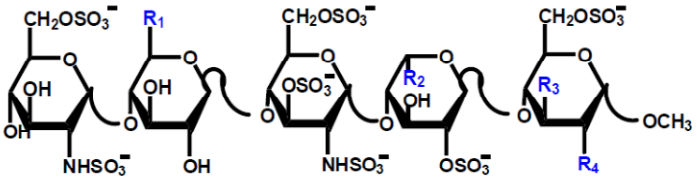

	R_1	R_2	R_3	R_4	Anti–FXa activity
Fondaparinux	-COO^-	-COO^-	-OH	-$NHSO_3^-$	700
DE'FGH	-$COOCH_3$	-COO^-	-OH	-$NHSO_3^-$	35
DEFG'H	-COO^-	-H	-OH	-$NHSO_3^-$	~0
DEFGH''	-COO^-	-COO^-	-OSO_3^-	-OSO_3^-	1250

C)

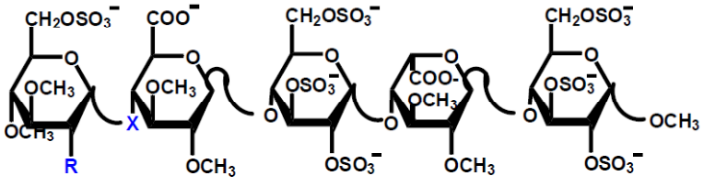

Derivative	R	X	Anti–FXa activity
Idraparinux	-OCH_3	-O-	1611
Biotinylated Idraparinux	Biotin amide	-O-	1611
DEFGH–NGA	-OSO_3^-	-O-	1318
C–DEFGH	-OSO_3^-	-C-	880

Figure 7. Pentasaccharide derivatives synthesized to establish structure–activity relationship. Anti-factor Xa activity is reported as U/mg.

1.6.3.3. Nonsaccharide, Aromatic, and Allsoteric Activators of Antithrombin—

Unfractionated heparin and LMWHs indirectly inhibit FXa by the induced fit allosteric mechanism that results in an acceleration level of ~600–fold for the AT–mediated inhibition. Heparins occupy the entire heparin-binding site that consists of PBS as well as EHBS. In contrast, the specific sequence pentasaccharide DEFGH binds only to the PBS and activates AT for the ~300–fold accelerated inhibition of FXa by the same mechanism. Detailed SAR studies show that several anionic groups of DEFGH are critical for its high–affinity interaction with AT. Nevertheless, studies with truncated variants indicate that DEF is the minimum structure that retains the functional role of heparin represented by the allosteric activation, although with significant loss of affinity under physiological conditions.

To design novel anticoagulants based on the allosteric activation of AT, various attempts have been made. Yet, all of these attempts have recruited a saccharide scaffold as a mimic of heparin.[97-105] Comparative studies with a number of scaffolds such as fucoidan,[97,98] curdlan sulfate,[99] chitosan,[100] galactomannan,[101] and others suggest that the heparin scaffold is uniquely tuned to activate AT. In fact, all newer molecules designed to potently bind AT have been derivatives of DEFGH.[104,105] Implied in such designs is the assumption that a saccharide scaffold was essential to induce AT activation. The assumption was made because of the remarkable loss in accelerated inhibition following a saccharide ring disruption in the pentasaccharide framework. However, a major concern with the saccharide–based approach is the difficulty of synthesis. Accordingly, the Desai group challenged this assumption by designing non–saccharide allosteric activators of AT for the accelerated inhibition of FXa.[106-110] The non–saccharide, aromatic mimetics of heparin are likely to provide several advantages over the saccharide

skeleton including greater non–ionic binding energy in AT recognition, enhanced hydrophobicity for possible oral delivery, improved synthetic accessibility, and higher specificity of action in comparison to heparin's several activities.[106,110,111]

Based on the interaction of DEF with the PBS of AT, two generations of non-saccharide, aromatic allosteric activators of AT were designed. The molecules of both generations were assessed biochemically under similar physiologic conditions to determine their affinity (K_D) by fluorescence spectroscopy and their AT acceleration potential by UV-Vis spectroscopy.[106-110]

The first generation utilized protein–based approach in which HINT–assisted molecular modeling studies guided the design of sulfated flavonoid–based scaffolds.[106] In this generation, (–)-epicatechin sulfate (ECS) was initially designed and was found to interact with AT with an affinity comparable to DEF.[106,107, 109] ECS accelerated the inhibition of FXa ~10–fold. Other molecules were designed in a similar fashion, however their acceleration potentials did not increase beyond ~20–fold in comparison to the ~300–fold known for DEF (Figure 8).[106-109]

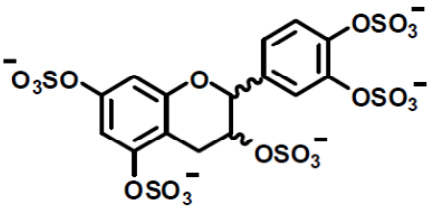

ECS: (2S,3S)
(+)CS: (2S,3R)

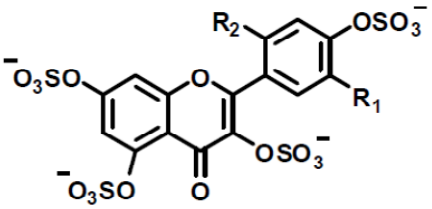

MoS: R_1 = H, R_2 = $-OSO_3^-$
QS: R_1 = $-OSO_3^-$, R_2 = H

Flavonoid–based AT activator	K_D (μM)	AT acceleration
ECS	10.7 ± 1.1	10.4
(+)CS	3.5 ± 0.5	20.8
MoS	1.8 ± 0.4	21.8
QS	17 ± 3.9	17.5

Figure 8. The affinity and the acceleration potential of flavonoid–based allosteric antithrombin activators.

To improve the design concept of non–saccharide allosteric AT activators, a pharmacophore–based approach was later exploited to design the second generation of AT activators based on the tetrahydroisoquinoline (THIQ) architecture.[110] Structure–activity relationship studies of DEF show that the sulfate groups at the 6–position on residue D, the 3–position and the 2–position on residue F as well as the 6–carboxylate group of residue E are critical for conformational activation of AT. Therefore, the pharmacophore was extracted and the four critical groups were connected in three–dimensional space leading to a blueprint of a potential AT activator. The blueprint was transformed into a potential organic activator by introducing rigidity and simplifying the structure for rapid synthesis. Several scaffolds were modeled and their three–dimensional similarities with the extracted pharmacophore were assessed resulting in THIQ being as the best scaffold candidate to be decorated with the essential sulfate and carboxylate groups. Accordingly, four THIQ–based potential AT activators were synthesized and biochemically evaluated (Figure 9).[110]

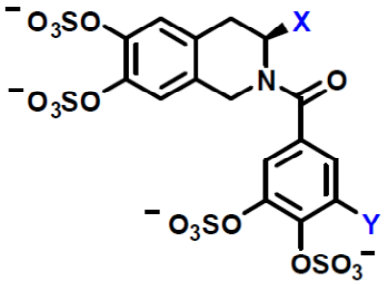

THIQ–based AT activator	X	Y	K_D (μM)	AT acceleration
IAS5	$–COO^-$	$–OSO_3^-$	320 ± 10	30
IAS4	$–COO^-$	–H	>1000	2.3
IES4	$–COOC_2H_5$	–H	330 ± 20	4.7
IES5	$–COOC_2H_5$	$–OSO_3^-$	805 ± 70	2.7

Figure 9. The affinity and the acceleration potential of THIQ–based allosteric antithrombin activators.

The best molecule identified in this generation was IAS5 which exhibited a K_D of 320 μM. More importantly, the acceleration in AT inhibition of FXa induced by IAS5 was found to be ~30–fold. Overall, results listed in figure 9 suggest that possibly all sulfate and carboxylate groups of IAS5 are important for the accelerated FXa inhibition by the activated AT as even a unit change in functional group modification appears to be not tolerated well.[110] In comparison to the first generation flavonoid–based activators, IAS5 was found to be ~1.5– to 3–fold better at AT acceleration, suggesting reasonable improvement in design. Detailed competitive binding and molecular modeling studies have indicated that both designed small molecules, flavonoid–based and THIQ–based molecules, prefer to bind in EHBS rather than the PBS to which DEFGH bind which explains their weaker acceleration potential.[106-110]

Far from the above novel approaches for designing non–saccharide, aromatic, and allosteric AT activators for the accelerated inhibition of FXa, their syntheses are challenging because of sulfation which typically leads to or is associated with the following consequences:[112] 1) nearly all sulfated molecules are water soluble, which makes them difficult to isolate in highly pure form; 2) the presence of inorganic salts, the proportion of which is usually higher at small synthetic scales; 3) aromatic sulfates are relatively unstable under acidic conditions and high temperatures; 4) the lack of maneuverability following introduction of sulfate group as only few functional group transformations can be successfully performed in the presence of a sulfate group. This essentially forces the design of the synthetic scheme to include sulfation as the final step; 5) the above complications increase geometrically for a poly–sulfated aromatic scaffold; 6) although a synthetic approach for a mono–sulfated scaffold should be easy to extend to a poly–sulfated scaffold, polysulfation is practically challenging. The major challenge is driving the reaction to completion to sulfate all available reactive functional groups. As the number of these

groups increases on a small scaffold, sulfation becomes progressively more difficult because of high anionic crowding, resulting in numerous partially sulfated side–products; and 7) lack of sulfation regioselectivity is a dominant issue with polyfunctional substrates.

Various synthetic protocols are available to effect sulfation. The flavonoids–based AT activators were mainly synthesized by a protection/deprotection strategy using trichloroethyl chlorosulfate as sulfate group donor.[112] For THIQ–based AT activators, a high yielding microwave–assisted sulfation protocol was developed. The latter protocol has certainly helped in addressing many of the difficulties associated with sulfation reaction.[113]

1.7. Factor Xa and Factor Xa Active Site Inhibitors as Anticoagulants —

1.7.1. Factor Xa: Function— Biologically, FXa plays a critical role in the common pathway of the coagulation cascade. Together with FVa, calcium ions, and phospholipid surface, FXa forms the prothrombinase complex that is responsible for the conversion of prothrombin to thrombin. This eventually leads to clot formation and wound closure.[114-115]Deficiency of FXa may disturb hemostasis resulting in severe bleeding tendencies.[116] Yet, this severe bleeding risk is only possible when FXa activity drops to less than 1% of its normal activity. Therefore, it seems that FXa activity can be suppressed without significantly affecting the hemostasis and thus with relatively minimal risk of bleeding, a highly desirable property for an ideal anticoagulant.[116]

1.7.2. Factor Xa: Structure— FXa structurally belongs to the family of trypsin–like serine proteases, which are involved in many physiological functions. Considering the desired safety profile for any medicine, a designed FXa inhibitor should be selective against all other serine proteases particularly thrombin and trypsin. Inhibiting thrombin activity along with that of FXa may cause life–threatening bleeding. Trypsin is a digestive enzyme and although its

inhibition consequences have not been thoroughly studied, orally active FXa inhibitor should be selective against trypsin.

The FXa structure was first determined by X–ray crystallography in 1993.[117] FXa consists of a 254 amino acids–containing heavy chain and a 142 amino acids–containing light chain. The heavy chain contains the trypsin–like serine protease domain, whereas the light chain is built up of a glutamate-rich domain and two epidermal growth factor–like domains. FXa is formed from the precursor protein FX following cleavage of a 52 amino acid activation peptide by FIXa or FVIIa.[6,7,17,118]

The catalytic domain of FXa consists of two similar antiparallel β-barrel folds that together form the catalytic triad of H57, D102, and S195 and substrate binding site. The FXa binding site is defined by the S1 and S4 subsites and surrounding residues. S1 is a deep, largely hydrophobic cleft at the bottom of which lies the D189 and Y228 side chains. S4 is a strongly hydrophobic pocket defined by the side chains of Y99, F174, and W215. The most potent ligands reported in the literature engage both sites (Figure 10).[6,7,17,118]

Despite the fact that FXa shares high sequence and spatial similarity with other serine proteases particularly trypsin and thrombin, structural differences do exist among them and thus provide the fundamental structural basis to design selective FXa inhibitors. Substrate specificities of both FXa and thrombin are trypsin–like, yet they are more restricted than trypsin. The active site of FXa is more open (groove–like) compared to the narrow and deep active site of thrombin (canyon–like). Both the proteases prefer arginine–like residues at P1 of the substrate or inhibitors in order to interact by ionic and hydrogen bonds with D189 at the base of S1 pocket. Table 1 shows the structural comparison for the four subsites of active sites in FXa and thrombin, which have been exploited to design selective FXa inhibitors.[6,7,17,118]

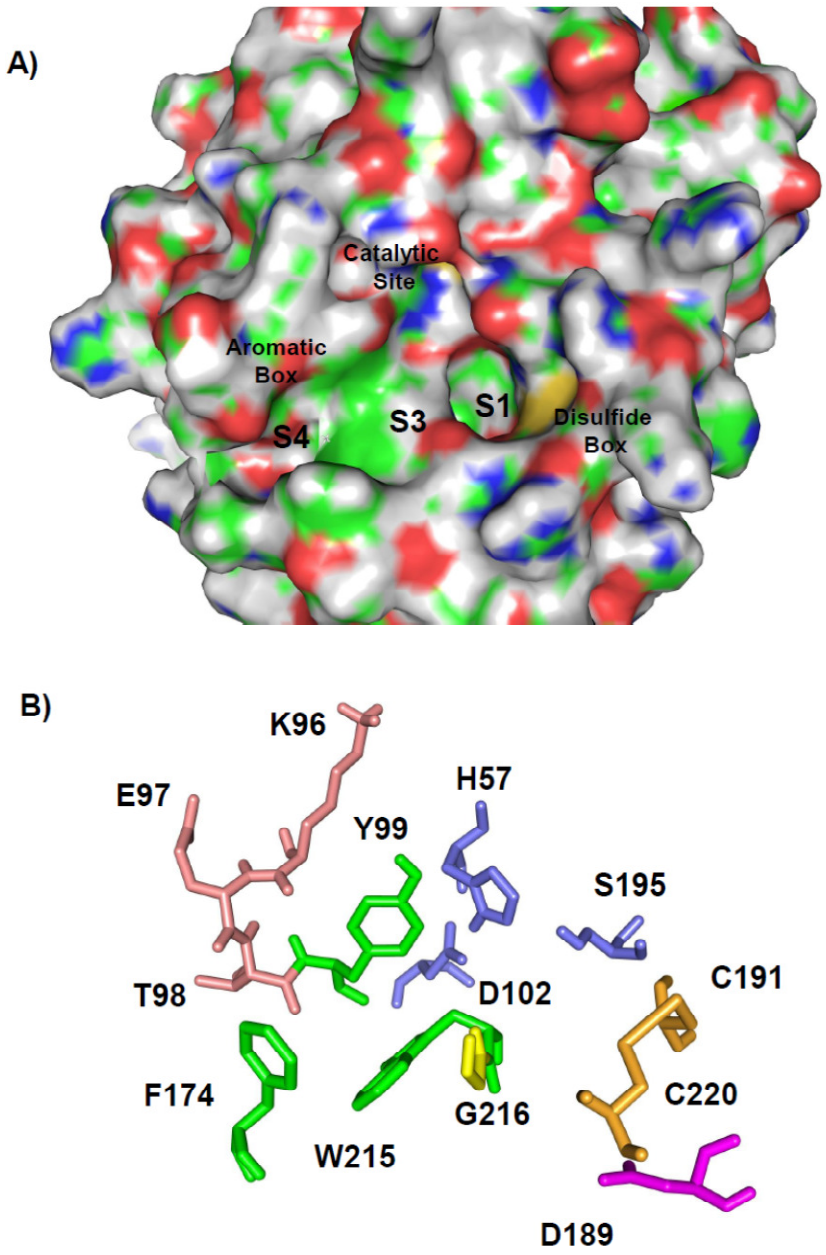

Figure 10. A) A top view of Connolly surface of the factor Xa binding site (PDB ID: 2P16). Carbon is in green, oxygen is in red, nitrogen is in blue, hydrogen is in white, and sulfur is in yellow. B) A close up view of the factor Xa binding site. The S4/aromatic box is in green, the cationic hole is highlighted in pink, the blue color is for the catalytic triad, the S1 pocket is in magenta, the disulfide box is in orange, and the S3 is indicated by yellow. This figure is adapted from reference 17.

Table 1. Structural comparison between the subsites of factor Xa and thrombin.

Subsite	Factor Xa	Thrombin
S1	D189 at the base preferring arginine–like P1 (I227 and Q192)	D189 at the base preferring arginine–like P1 (F227 and E192)
S2	Obstructed by Y99 side chain Binds to small residues such as glycine in P2	Created by W60D, Y60A, H57, W215, L99 Binds to large lipophilic residues such valine and proline in P2
S3	Flat surface having S172 shielded by the larger F174	Flat surface having exposed T172
S4	Aromatic hydrophobic pocket of Y99, W215, F174 Cation carbonyls of L96, E97, T98 (More open pocket)	Aliphatic hydrophobic pocket of N98, L99, I174,W215 (Less open pocket)

1.7.3. Active Site Factor Xa Inhibitors: Chemical Classes— Several chemical scaffolds were considered to develop reversible, synthetic, potent and selective active site FXa inhibitors. Considering the chemical anatomy of all FXa inhibitors developed thus far, their structures can be dissected into three chemical domains: a bifunctional core structure, which is decorated by two chemical arms that fit into subsites S1 and S4. All promising FXa inhibitors adopt L– or V–shaped conformations. Active site FXa inhibitor discovery and development has undergone three primary phases as follows (Figure 11):

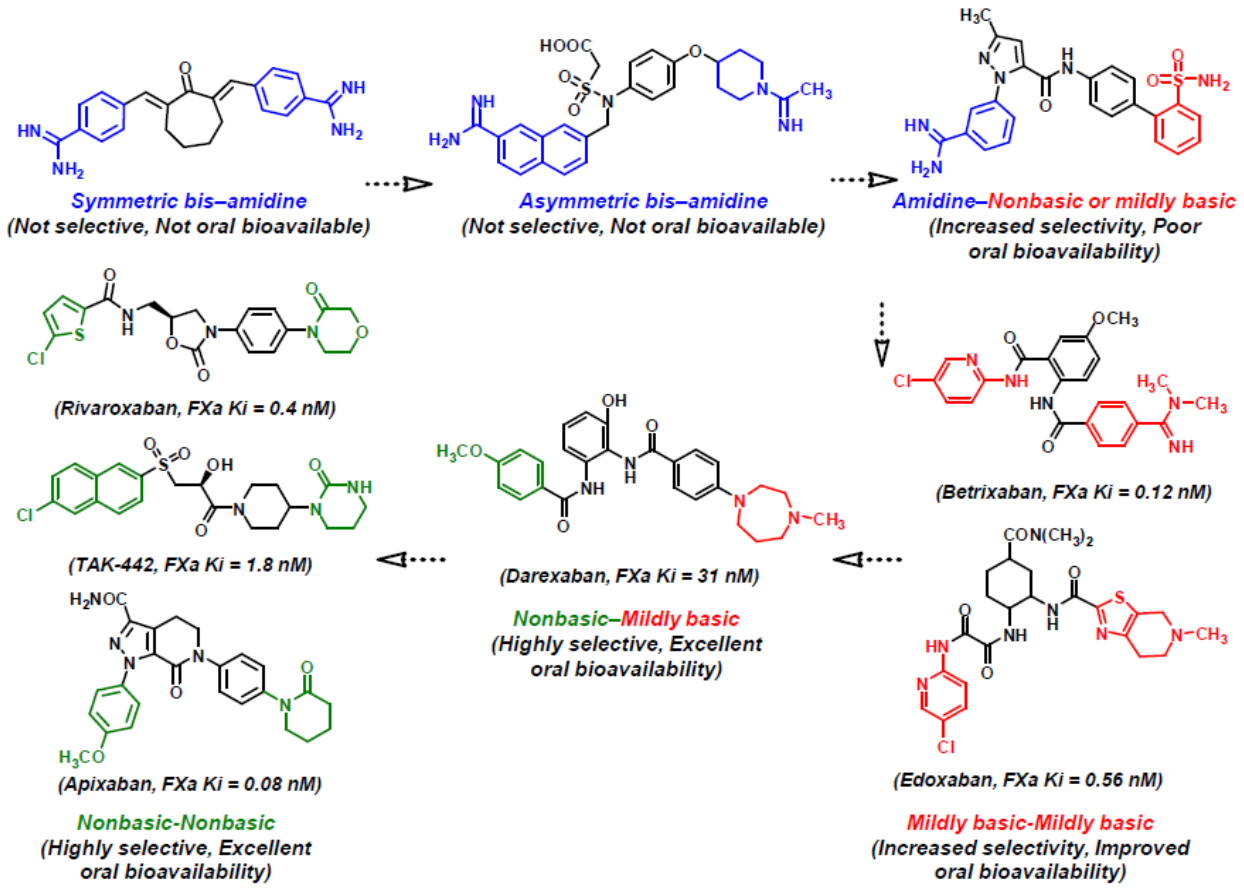

Figure 11. Evolution of reversible active site factor Xa inhibitors. Functional groups in blue are highly basic, functional groups in red are mildly basic, whereas those in green are nonbasic, lipophilic functional groups.

1) Highly basic scaffolds—The early discovery efforts were concentrated on symmetric *bis*–benzamidines which resulted from programs launched earlier to develop potent and selective thrombin inhibitors. The resulting FXa inhibitors were generally moderately potent and were not selective against other serine proteases in the coagulation cascade and digestive system. It was later discovered that desymmetrization of the scaffold improved potency and selectivity against other serine proteases. However, all FXa inhibitors developed in this stage suffered from poor oral bioavailability. [6,7,17,118]

2) Mildly basic scaffolds— In this phase, one of the highly basic benzamidine/amidine moieties on the scaffold (P1 or P4) was replaced with a mildly basic to nonbasic functional group such as pyridine–containing or sulfonamide–substituted aromatic scaffolds in order to improve the oral bioavailability. This led to improved bioavailability and selectivity and resulted in relatively diminished FXa inhibition in some cases. [6,7,17,118]

3) Nonbasic lipophilic scaffolds— The remaining basic benzamidine/amidine on the scaffold was replaced by another mildly basic to nonbasic functional group. This led to the discovery of several highly potent, highly selective, and orally bioavailable direct FXa inhibitors. [6,7,17,118] Optimization of pharmacokinetic measures of molecules belonging to this class has been accomplished resulting in promising drug candidates, which have been advanced into clinical development such as apixaban,[119] betrixaban,[120] eribaxaban,[121] edoxaban,[122] LY517717,[118] darexaban,[123] and TAK-442.[124] Of these, rivaroxaban was approved in 2011 in US.[125] The anatomy of this class of FXa inhibitors is depicted in figure 12.

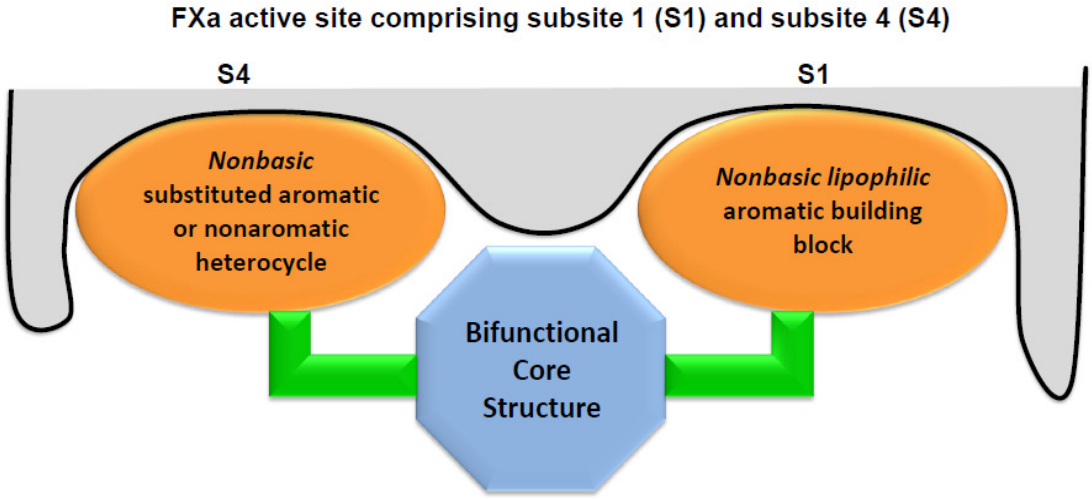

Figure 12. Chemical anatomy of the most promising orally bioavailble active site factor Xa inihibitors having three chemical domains. Describtion of the optimal features of the chemical arms is included. The chemical space of the bifunctional core structure involves either flexible or rigid scaffolds**.**

1.7.4. Oral Active Site Factor Xa Inhibitors — In this section, oral direct FXa inhibitors which have demonstrated high potency, remarkable selectivity, and good pharmacokinetic profile will be detailed. The P1 and P4 moities are highlighted. All of the following FXa inhibitors are at different stages of clinical trials, except for rivaroxaban, which was approved by FDA in 2011 as the first oral direct FXa inhibitor to be used to reduce the risk of stroke and systemic embolism and in the prophylaxis of deep vein thrombosis.[114]

A) Rivaroxaban — Rivaroxaban is the first potent, selective, orally bioavailble direct FXa inhibitor. It has oxazolidinone as the bifunctional core structure, chlorothienyl unit as P1 group, and morpholinone moiety as P4 residue. X–ray crystallography studies revealed that rivaroxaban forms two hydrogen bonds to G219: a strong hydrogen bond from the carbonyl oxygen of the oxazolidinone core and a weaker one from the amino group of the chlorothiophenecarboxamide. The two hydrogen bonds and the *(S)*–oxazolidinone core guarantee the L-shape needed for FXa binding. The oxazolidinone core and the aryl ring are coplanar.[125]

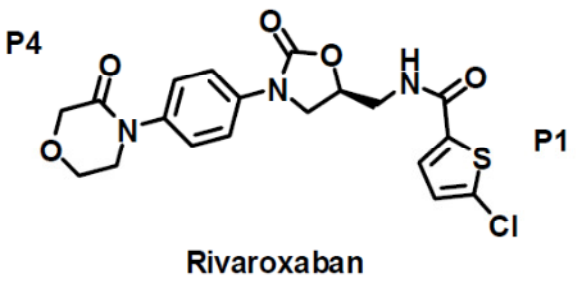

Rivaroxaban

In the S1 pocket, the key interaction of rivaroxaban with FXa involves the chlorothiophene moiety as its chlorine substituent interacts with the aromatic ring of Y228 located at the bottom of the S1 pocket. In the S4 pocket, the nonpolar aryl ring extends across the face of W215, and the morpholinone moiety is sandwiched between Y99 and F174. The carbonyl group of the morpholinone does not interact directly with FXa, however it is essential to bring the morpholinone ring into a perpendicular arrangement to the aryl ring, and thus increasing the

aromatic ring stacking and edge–to–face interaction. This interaction also displaces a molecule of water providing a further entropic binding contribution.[125]

Rivaroxaban has a K_i of 0.4 nM. Concentrations of 0.23 μM and 0.69 μM are needed to double the clotting times PT and aPTT, respectively. It exhibits >10,000–fold greater selectivity for FXa over other serine proteases. Due to the lack of the arginine–like moieties and the presence of chlorothiophene group, rivaroxaban demonstrates high oral bioavailability of 57–66% (rat) and 60–80% (dog).[118,126]

B) Apixaban — Apixaban is another nonbasic FXa inhibitor having 7-oxo-4,5,6,7-tetrahydro-*1H*-pyrazolo[3,4-c]pyridine-3-carboxamide as the bifunctional core structure, *p*–methoxyphenyl unit as P1 group, and piperidinone moiety as P4 residue.

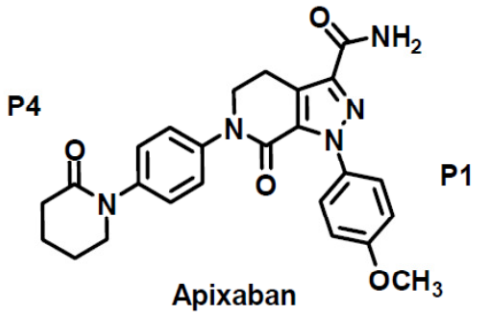

Apixaban

The X–ray structure analysis of this inhibitor shows that in the S1 pocket the *p*-methoxy group displaces an unfavorably bound water molecule. The pyrazole N_2 nitrogen atom interacts with the backbone of N192 and the carbonyl oxygen atom of the carboxamide interacts with the NH unit of G216. The orientation of the lactam phenyl residue in the S4 pocket indicates an edge-to-face interaction with W215.[119]

Apixaban has a K_i of 0.08 nM and 3.8 μM and 5.1 μM concentrations are needed to double the clotting times PT and aPTT, respectively. It is selective for FXa and inhibits thrombin and trypsin, with *Ki* values of about 3 μM and >15 μM, respectively. Apixaban exhibits high oral bioavailability of 51% (chimpanzee), 88% (dog), and 34% (rat) due to the lack of the arginine–like moieties.[118,126]

C) Betrixaban — Betrixaban is oral bioavailable, potent and selective competitive FXa inhibitor. It exhibits >86,000–fold greater selectivity for FXa over other related proteases. Betrixaban adopts the same binding modes of rivaroxaban and apixaban. Particularly, the core structure of *m*–methoxy anthanilamide holds *p*–chloropyridine–amine to fit into the S1 pocket while *N,N*–dimethylamidine to interact with the S4 pocket. The chlorine of the former group interacts with Y228 and the amide NH hydrogen bonds with G218. The dimethylamidine group forms cation–π interaction in the lipophilic S4 pocket. Suprisingly, betrixaban has good oral bioavailability although the amidine group is protonated under physiological conditions. Biologically, betrixaban has a K_i of 0.12 nM. It doubles the clotting times of PT at plasma concentration of 0.4 μM. Betrixaban has oral bioavailability of 23.8 % (rat), 51.6% (dog), and 58.7% (monkey).[118,120,126]

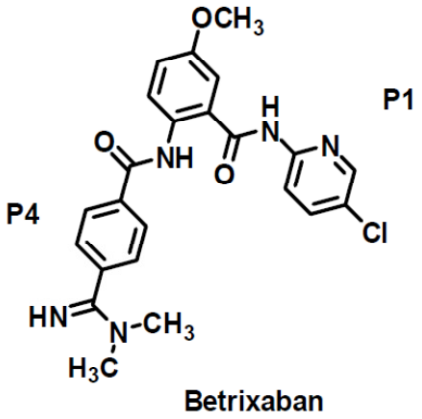

Betrixaban

D) Darexaban — Darexaban was developed using anthranilamide as core structure. Darexaban has high affinity for human FXa with a K_i of 31 nM and relatively low affinity for other serine proteases such as thrombin, trypsin, kallikrein and plasmin with K_i*'s* of at least 10 μM. PT clotting time is doubled by 1.2 μM of darexaban.[118,126]

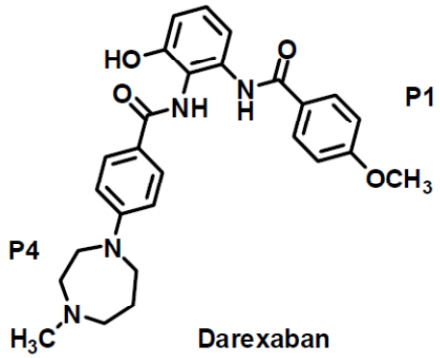

Darexaban

The structure of darexaban was only disclosed recently after studying its metabolic profile. It was concluded that this molecule undergoes Phase II metabolic glucuronidation at the phenolic group resulting in more potent metabolite.[123]

Molecular modeling studies indicated that *p*-methoxyphenyl moiety deeply occupies the S1 pocket, while the 1,4-diazepane moiety fits into the S4 pocket. It was further suggested that the backbone carbonyl group of G216 and the backbone NH group of G218 hydrogen bond to the NH group of the amide bond linked to the methoxyphenyl moiety and the carbonyl group of the amide bond connected to the 4-(1,4-diazepane) benzene, respectively. This binding mode guarantees the preferred L–conformation, with the hydroxy group of the central benzene facing out toward the solvent. Therefore, glucuronidation of darexaban takes place without colliding with any residual portions of FXa, and the glucuronic acid moiety is exposed to the solvent, thereby stabilizing the moiety by hydration. Furthermore, the binding mode indicated that the carboxyl group of the glucuronic acid moiety interacts with R143 and K147.[123]

E) TAK–442 — TAK-442 is in clinical development for the treatment of thromboembolic diseases. The X–ray structure of the complex with human FXa confirmed that the 6–chloronaphthyl group occupies the S1 substrate binding pocket in which the chlorine atom has a hydrophobic interaction with Y228. The sulfonyl oxygen atom is involved in a hydrogen bond with N192. In addition, hydrogen bonds between the oxygen atoms of the amide carbonyl group and the hydroxy group and the backbone NH units of G219 and G216, respectively, were observed. The cyclic urea interacts with the aromatic amino acids of the S4 pocket whereas the carbonyl group forms a water–mediated contact with the amide oxygen atom of K96.[124] Lastly TAK–442 is potent FXa inhibitor as it inhibits FXa with a K_i of 1.8 nM and doubles the clotting time aPTT at 0.59 μM.[118,126]

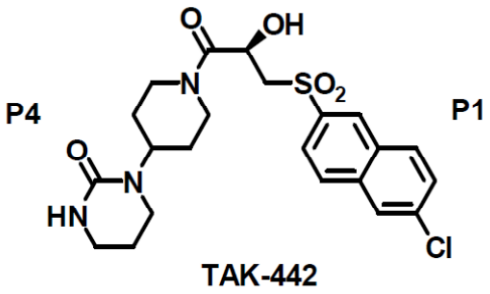

TAK-442

CHAPTER 2: DRAWBACKS OF THE CURRENT ANTICOAGULANTS AND SPECIFIC AIMS OF THE CURRENT WORK

2.1. Drawbacks of Indirect Anticoagulants: Heparins and Coumarins—Heparins and coumarins are essentially irreversible indirect inhibitiors of the coagulation enzymes. The drawbacks of heparins stem from their enormous structural heterogeneity and polydispersity in addition to the redundant number of sulfate groups. Drawbacks associated with warfarin relate to its essentially non–specific mechanism as it eventually inhibits several clotting factors. Heparins and warfarin cause several adverse effects and fatal outcomes as follows:

1) Significant bleeding is the major risk imposed not only by heparins and warfarin but also by all current anticoagulants. The anticoagulant class was ranked first in two consecutive years of 2003 and 2004 with respect to the total deaths from drugs causing adverse effects in therapeutic use.[7] From 1990 through 2000, warfarin was ranked in the top 10 for most number of serious and adverse event reports received by the FDA.[127] Unfractionated heparin, LMWHs, and fondaparinux also exhibit bleeding complications, although the last two variants were developed to address the bleeding risk of the unfractionated form.[128-133] Although the action of the polymeric heparins can be terminated by protamine, yet fondaparinux does not have an effective antidote to reverse excessive bleeding. [134,135]

2) Because warfarin targets the liver which is the main physiologic machinery for the metabolic and detoxification processes of most drugs and food ingredients, warfarin suffers from several drug–drug or drug–food interactions which result in excessive or inadequate anticoagulation and sometimes excessive bleeding.[136-141]Another implication of warfarin mechanism is the well–reported narrow therapeutic window.[7]

3) Heparins and warfarin also suffer from significant intra– and inter–patient response variability which requires frequent laboratory monitoring. The inconsistent response with heparin is due to differences in the bioavailability and from heparin binding to proteins in the plasma and on cells, which are elevated in very ill patients. In addition, heparins do not inhibit clot–bound thrombin.[142-144] The variations in patient response to warfarin are likely to be because of genetic polymorphism.[145,146]

4) Heparin–induced thrombocytopenia is a lethal complication affecting 2.6% of patients taking heparin or LMWHs.[147,148] It refers to a significant drop in platelet count between 4 and 14 days after the initiation of therapy as a result of heparin–induced platelet activation.[149]

5) The high risk for heparin to be contaminated with other glycosaminoglycans is very serious drawback**.** Several severe allergic reactions following the use of unfractionated heparin were reported in 2007 in the US. The reactions resulted in at least 8 deaths. Investigations determined that heparin was contaminated up to 30% by oversulfated chondroitin sulfate. [150,151]

6) Other limitations of heparins include the development of osteoporosis in patients receiving high dose therapy for more than six months[152] and the poor oral bioavailability.[7]

2.2. Drawbacks of Direct Anticoagulants — Direct inhibition of coagulation enzymes has been suggested to offer several advantages over the indirect inhibitors. Available direct inhibitors are thrombin inhibitors, FXa inihibtors, or dual thrombin and FXa inhibitors. Direct inhibitors are generally reversible inhibitors that are capable of inhibiting both the free forms of clotting enzymes and the clot–bound enzymes. Several direct inhibitors are neutral molecules, thus they offer the advantage of having better oral bioavailbility. Furthermore, direct anticoagulants possess more selectivity toward their corresponding targets, and therefore they have relatively limited off–target events. For example, none of the direct anticoagulants is

associated with the life–threatening thrombocytopenia or osteoporosis. Finally, patients receiving such anticoagulants are expected to show consistent clinical profiles over the time course of therapy. Accordingly, administration of direct inhibitors of clotting enzymes as anticoagulants does not demand laborious and expensive laboratory monitoring. Despite all of these advantages, direct anticoagulants are still associated with some deleterious events as follows:

1) All direct thrombin inhibitors such as hirudin, bivalirudin and argatroban are associated with significant bleeding episodes.[7] Particularly, hirudin and its recombinant variants lack an effective antidote, thus limiting their use to patients refractory to heparins or patients with high susceptibility to thrombocytopenia.[153,154]

2) Because hirudins are foreign peptides, they are potentially immunogenic and may cause life-threatening complications.[155]

3) Hirudins are extremely potent. The thrombin K_i values are 20, 60 and 200 fM for hirudin, lepirudin and desirudin, respectively,[156,157] which makes these peptides essentially irreversible and likely to possess narrow therapeutic windows. Bivalirudin was later rationally designed to address some of the hirudins complications. It binds thrombin with a K_i of 1–2 nM, has more predictable anticoagulant response, and lower immunogenicity, yet it has short duration of action (plasma half life 25 min).[7]

4) Other inhibitor–specific drawbacks include the hepatotoxicity of ximelagatran,[158] mast cell degranulation and histamine-release[159,160] as well as poor bioavailability of cationic and peptidic direct inhibitors, and lastly the short duration of action of argatroban, which is approved for use in patients at high risk for thrombocytopenia (plasma half life 24 min).[7]

2.3. Ideal Characteristics of Anticoagulants — According to several reports in literature, the hypothetical "ideal" anticoagulants should:[6,7,17,114,118] 1) be administered orally; 2) have rapid

onset of action and several hours of duration of action; 3) have wide therapeutic window; 4) have little or no inter–individual variability; 5) have little or no interaction with food and other drugs; and 6) have predictable pharmacokinetic and pharmacodynamic characteristics.

Other characteristics include no requirement of dose adjustment or coagulation monitoring, high efficacy with respect to reduced thromboembolic incidents, availability of antidote, and good safety profile especially with regard to the bleeding risk.

2.4. Specific Aims of the Current Work — Despite the significant improvements offered by the recently approved oral anticoagulants such as dabigatran etexilate (oral thrombin inhibitor that was first approved in October 2010 in US), and rivaroxaban (oral FXa inhibitor that was first approved in July 2011 in US), contrasting the profile of ideal anticoagulants with that of the clinically approved ones reveals an unmet need for new anticoagulants.

For example, on December 2011, the FDA initiated an investigation into serious bleeding events associated with dabigatran etexilate stating that the "FDA is working to determine whether the reports of bleeding in patients taking Pradaxa (dabigatran etexilate) are occurring more commonly than would be expected, based on observations in the large clinical trial that supported the approval of Pradaxa [RE-LY trial]."[161] In November 2011, Boehringer Ingelheim confirmed 260 fatal bleeding events worldwide between March 2008 and October 2011 because of Pradaxa.[215]

Furthermore, the efficacy and safety of the new anticoagulants is yet to be established in high risk populations such as cancer patients, pregnant and lactating women, and patients with hepatic diseases. The cerebrovascular bleeding is fast becoming a real concern, especially with the oral anticoagulants where mortality rate rises to 67%.[162]

Therefore, with such high demand for new anticoagulants, the current work deals with two specific aims (Figure 13):

1) Design, synthesis, and biochemical evaluation of sulfated, nonsaccharide, allosteric activators of antithrombin based on the 1,2,3,4-tetrahydroisoquinoline-3-carboxylic acid (THIQ3CA) scaffold. These activators are expected to serve as indirect FXa inhibitors. This aim will be discussed in Chapters 3, 4, and 6.

2) Design, synthesis and biochemical characterization of direct FXa inhibitors based on the 1,2,3,4-tetrahydroisoquinoline (THIQ) dicarboxamides. This aim will be discussed in Chapters 5 and 6.

The first goal is of particular interest as it tends to establish a synthetic library of sulfated small molecules. Although the library is supposed to serve the stated objective, however establishing such a library demands optimizing or developing techniques to deal with sulfated compounds at several levels including synthesis, isolation, identification, and characterization. Furthermore, as the synthesized compounds carry the unique structural characteristic of being sulfated, they are elected to be potential heparin functional mimetics. In fact, the executed compounds of the chemical library will be added to a larger library of sulfated compounds for screening against other proteins interacting with heparin. This should help in addressing questions at a fundamental level regarding heparin–protein interactions. Finally, in lieu of appropriate computational tools to model such interactions, the biological profile of the synthesized compounds should help to validate, optimize, or develop new computational tools in order to eventually help in designing potent and selective heparin functional mimetics with high level of confidence and for the vast biological activities of heparin.

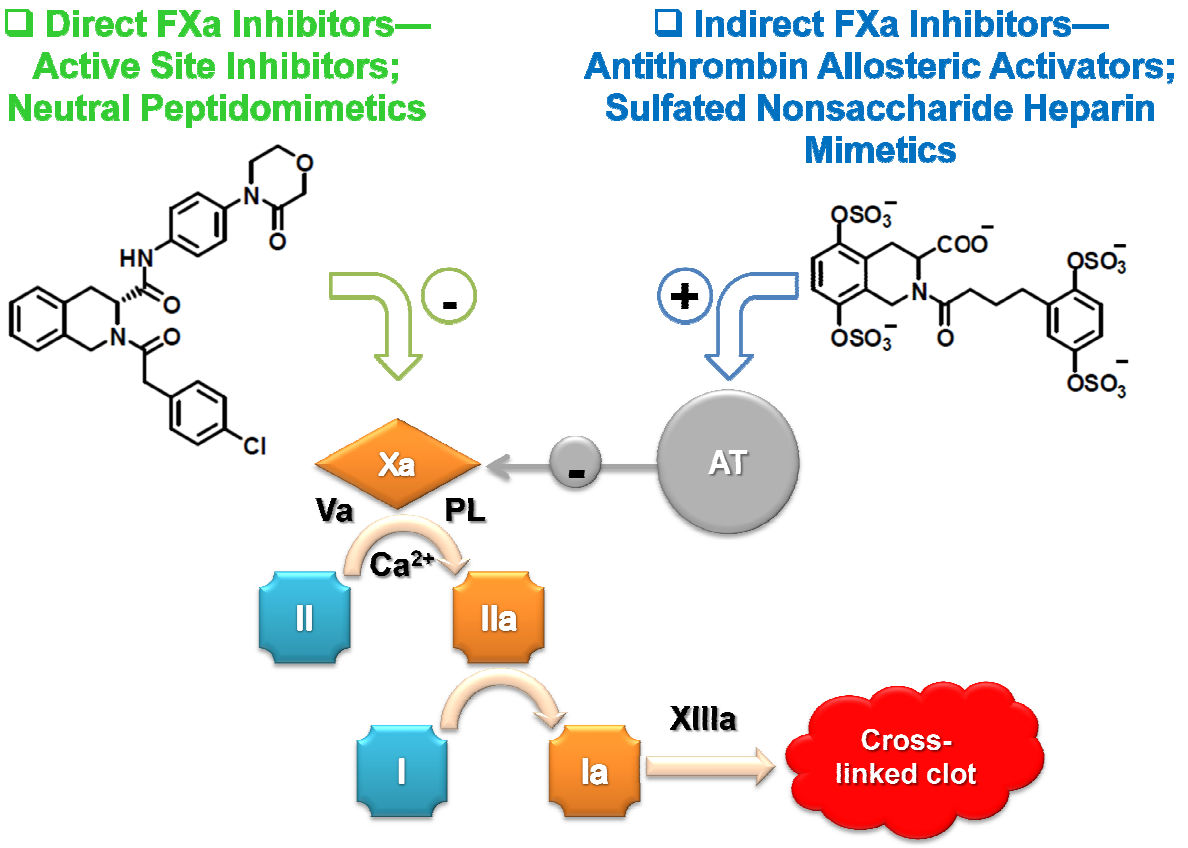

Figure 13. Outline of the specific aims of the current work.

CHAPTER 3: SYNTHESIS OF ELECTRONICALLY RICH *N*-SUBSTITUTED, 1,2,3,4–TETRAHYDROISOQUINOLINE-3–CARBOXYLIC ACID ESTERS: PRECURSORS OF ANTITHROMBIN ACTIVATORS

3.1. Introduction— Nitrogen heterocycles are key building blocks for a large number of medicinally–relevant molecules and serve as fundamental scaffolds for discovering drugs. The 1,2,3,4–tetrahydroisoquinoline (THIQ) scaffold is an especially useful nitrogen heterocycle due to its ability to quickly enhance structural diversity of a potential library. An interesting variant of the THIQ scaffold is the 1,2,3,4–tetrahydroisoquinoline–3–carboxylic acid (THIQ3CA) structure, which has been utilized in the design of several pharmacologically relevant molecules.[163-166]Desai and co–workers have exploited the THIQ3CA scaffold in the rational design of non–saccharide activators of AT.[110]

Several methods are available for synthesis of the THIQ3CA analogs.[167-175] The Pictet-Spengler[167] and Bischler–Napieralski[168] reactions, which rely on cyclization of β-arylethylamine derivatives in presence of a protic or Lewis acid,[176-187] are among most common protocols for this purpose. Several other methods have also been developed including cycloaddition and enyne metathesis reactions for the synthesis of 1,2–dihydroisoquinoline–3–carboxylic acids[169] and 5,6–, 6,7–, or 7,8–functionalized THIQ3CA esters.[170,171]

An interesting method to synthesize THIQ3CA analogs has been to utilize α,α'–dibromo-*O*-xylenes as dielectrophiles in reaction with a glycine equivalent. The glycine equivalents studied to date include (2*S*)–2–isopropyl–3,6–dimethoxy–5–methyl–2,5–dihydropyrazine **(a)**,[188] *(R)*–di–*tert*–butyl 2–*tert*–butyl–4–oxoimidazolidine–1,3–dicarboxylate **(b)**,[189] diethyl acetamidomalonate **(c)**,[190] ethyl acetamidocyano–acetate **(d)**,[191] ethyl 2–(benzylidene amino)acetate **(e)**,[192] (*6R*)–6–isopropyl–3–methyl–5–phenyl–3,6–dihydro–2H–1,4–oxazin–2–one

(f),[193] and 1,4–diacetyl piperazine-2,5-dione **(g)** (Figure 14).[194] An alternative to using dibromo-*O*-xylenes as electrophiles in the reaction with glycine donors is α-methyl benzyl bromide, which when reacted with (*2S,5S*)–1–benzoyl–2-*tert*–butyl-3,5-dimethyl–imidazolidin–4–one **(h)** (Figure 14) afforded α,β–dimethyl THIQ3CA after Pictet-Spengler cyclization.[195] At a fundamental level, the glycine equivalents in these reactions undergo base-mediated, simultaneous or sequential *C*– and *N*– alkylation to afford racemic or enantiomerically pure products. If alkylation is sequential, then *N*–alkylation can be achieved by acid–mediated hydrolytic cyclization.[188,193]

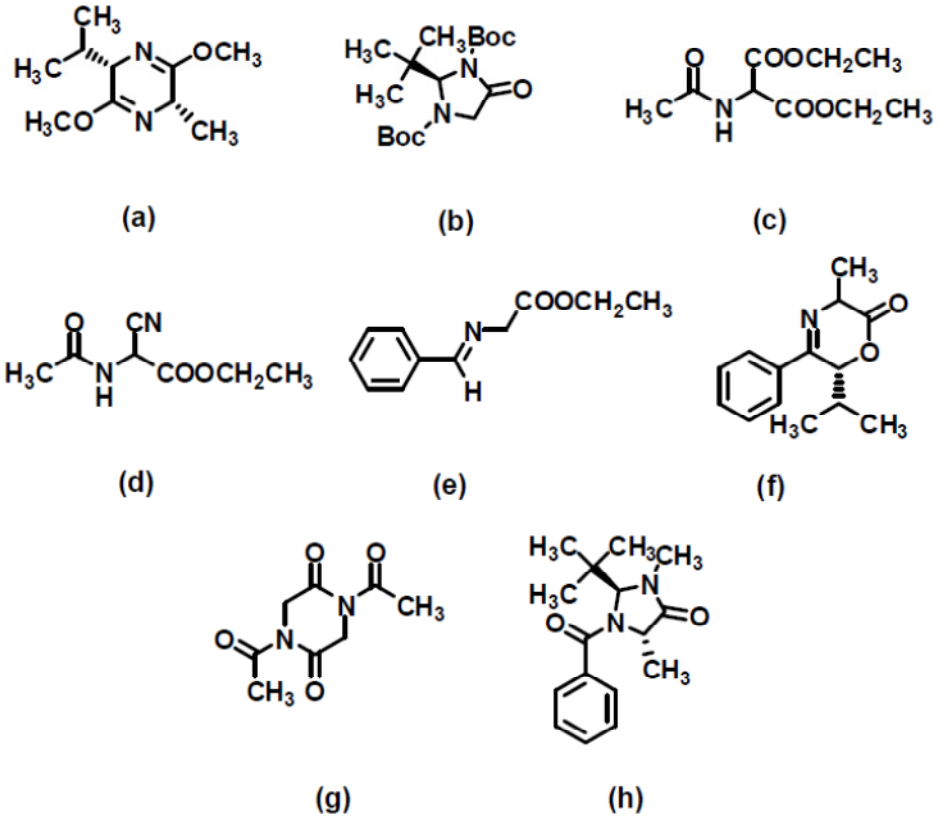

Figure 14. Glycine equivalents reported in literature for the synthesis of THIQ.

We have been interested in developing a THIQ3CA–based library to gain insight into the mechanism of AT activation by non-saccharide mimetics of heparin.[106-110] The unique highly sulfated nature of the parent biomolecule, heparin, dictates that the THIQ3CA scaffold contain multiple hydroxyls for sulfation in the last step.[112] Unfortunately, appropriate polyphenolic THIQ3CA precursors are either not available commercially or their purported synthesis based on literature reports fails to yield product in high yields and purity. More specifically, the starting materials (dimethoxy–β–arylethylamines) for the synthesis of 5,6–dimethoxy–, 5,8–dimethoxy–, and 6,7–dimethoxy–THIQ3CA esters using Pictet-Spengler and Bischler–Napieralski reactions are not available. The glycine equivalents approach is also not feasible for our targeted THIQ3CA derivatives because of the lack of availability of appropriate α,α'–dibromo-*O*–xylenes. In fact, a survey of literature shows that each THIQ3CA derivative synthesized to date through the glycine equivalent approach has not carried any functionalization on the aromatic ring of THIQ3CA.[188,189,193,195] An added problem has been that these reactions require extended reflux in strong bases[191,192,195] and/or concentrated mineral acids.[188,189,191,193,195] Such strong conditions severely limit the nature of protecting groups that can be used in the synthesis of polyphenolic THIQ3CAs. Finally although useful, the cyclo–addition approaches have been developed primarily for unsubstituted or minimally substituted THIQ3CA esters and are long winding.[169-171] Thus, we realized that developing a facile, concise, high yielding synthesis to THIQ3CA analogs containing phenolic groups placed at varying positions was necessary for exploring a library of such molecules as anticoagulants.

3.2. Results and Discussion—

3.2.1. Glycine Donor based Approach to Synthesize Electronically Rich THIQ3CA Esters— A quick retro-synthetic analysis of the THIQ3CA core suggested that the structure

could be built using three building blocks – a benzaldehyde, formaldehyde, and a glycine equivalent moiety (**1**–**3**) (Figure 15). While the benzaldehyde block is available with many different electronically rich substituents, which provides a facile entry to the desired THIQ3CA esters, the glycine block has stringent requirements. One of the requirements is that the glycine unit should possess a more nucleophilic α–carbon than its amine and carboxylic acid groups. This is satisfied by imidazolidine-2,4-dione **1**, commonly refered to as hydantoin (Scheme 1). To test its applicability, we utilized 2,3–dimethoxy and 2,5–dimethoxy benzaldehydes (**4** and **5**) that should yield 5,6–dimethoxy– and 5,8–dimethoxy–THIQ3CA derivatives, which are not readily accessible through other competing approaches and form key scaffold of our novel anticoagulants.[110]

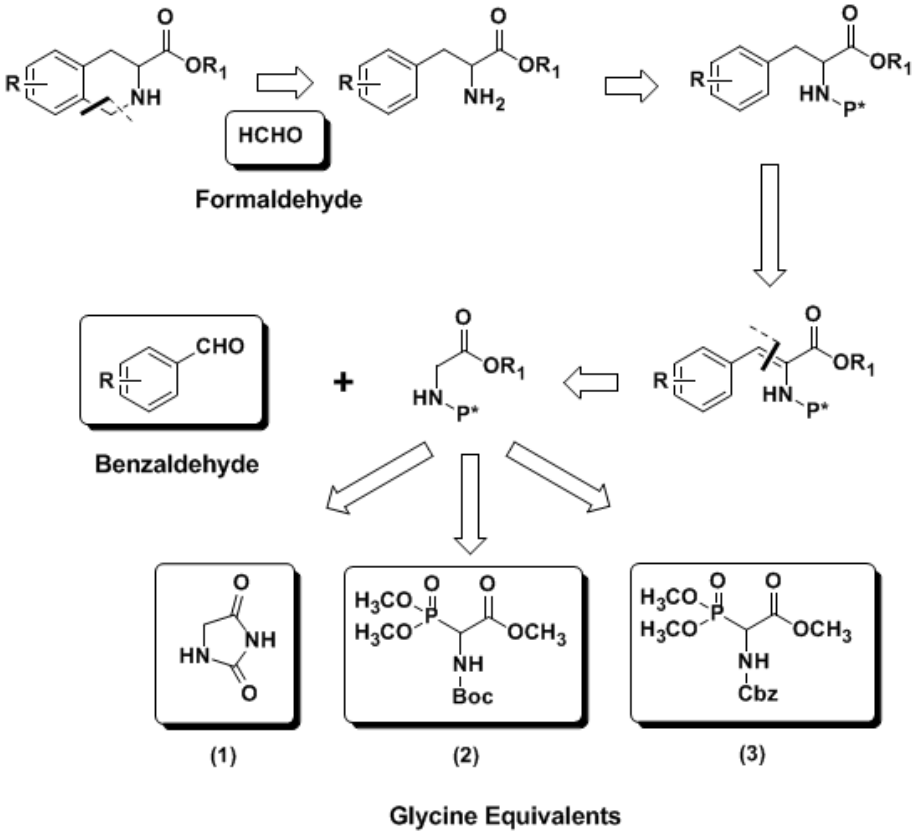

Figure 15. Retrosysnthetic analysis for THIQ3CA scaffold based on new glycine equivalents. This figure is adapted from reference 268.

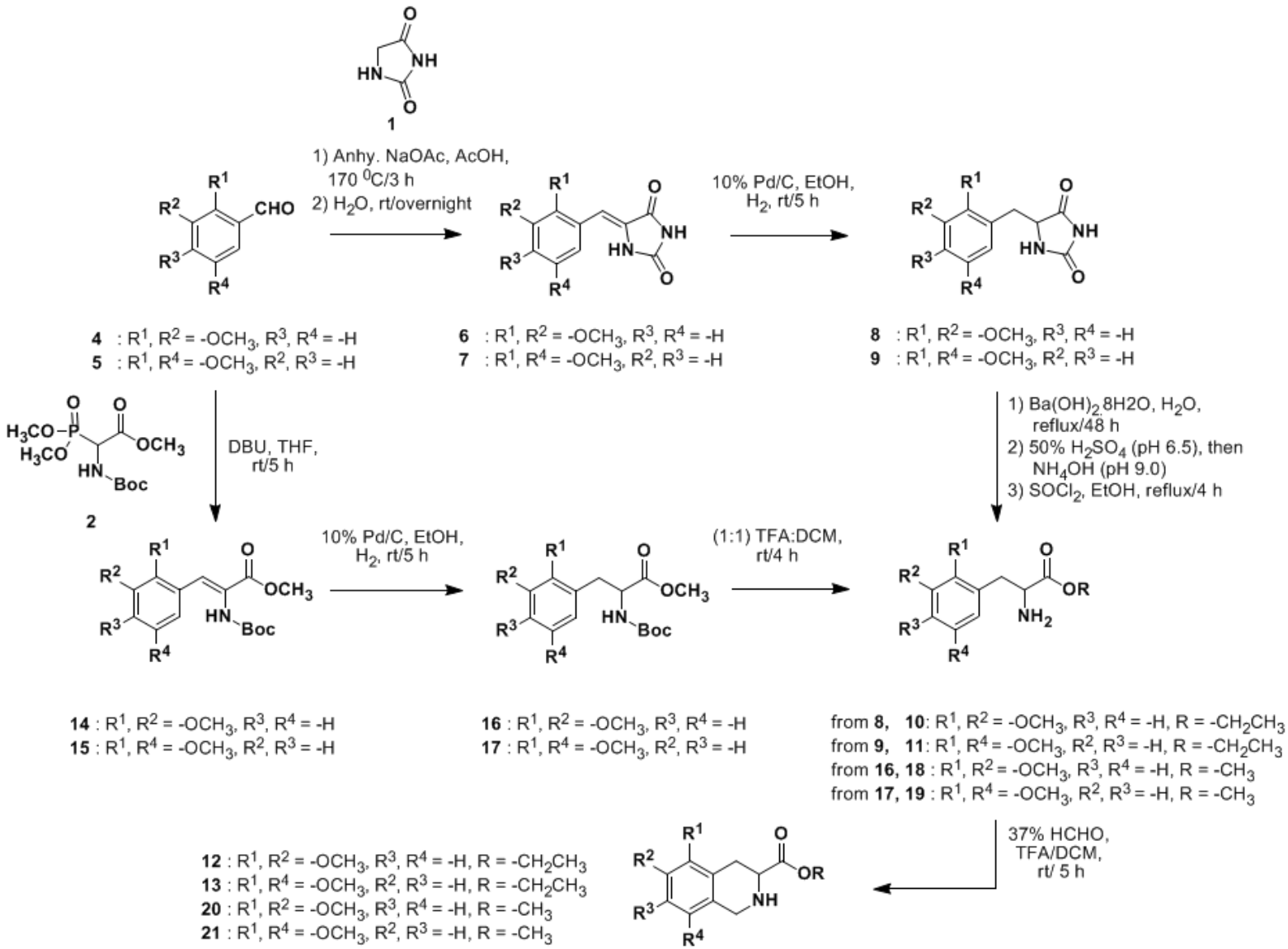

Scheme 1. Synthesis of 5,6– and 5,8– dimethoxy THIQ3CA esters using **1** and **2** as glycine equivalent. Adapted from reference 268.

Reaction of benzaldehyde **4** with **1** at 170 ^{O}C gave intermediate **6**, which was hydrogenated to imidazolidine-2,4-dione **8** (Scheme 1). The hydantoin moiety of **8** was hydrolyzed and the resulting crude acid was esterified through sequential treatments with $SOCl_2$ and ethanol to afford 2,3-dimethoxy phenylalanine ethyl ester **10**. Pictet–Spengler cyclization of **10** under acidic conditions with aqueous formaldehyde resulted in 5,6-dimethoxy-THIQ3CA ethyl ester **12**. 5,8-Dimethoxy derivative **13** was also synthesized using the same protocol.

Although useful, the above protocol was not as high yielding and efficient as desired. Two other glycine equivalents, namely (±)-Boc-α-phosphonoglycine trimethyl ester **2** (Scheme 1) and (±)-Z-*α*-phosphonoglycine trimethyl ester **3** (Scheme 2), were studied to improve yield and enhance feasibility. It is known that the α-proton of trimethylphosphonate is considerably acidic and formation of a strong O-P bond in the by-product dimethyl phosphate drives the addition–elimination reaction.[196] Thus, we reasoned that glycine donors **2** and **3** may allow the use of milder conditions to effect similar transformations than those used for hydantion **1**. A further advantage is likely to arise from the use of **2** and **3** was the easier purification of products because the by–product was known to be water soluble. In contrast, the hydantoin adduct required hot methanol for solubilization. The reaction was also expected to yield a predominantly *Z*-product[197] and thus, these glycine donors offered an excellent opportunity for the synthesis of THIQ3CA esters.[198]

Trimethyl phosphonate **2** was first treated with 1,8-diazabicyclo[5.4.0]undec-7-ene (DBU) at 0 ^{o}C in THF and then with either benzalaldehyde **4** or **5** in a dropwise manner to yield the corresponding benzylidene **14** or **15**, respectively, in yields of 77–85%. Catalytic hydrogenation and acidification with equi-volume mixture of TFA and CH_2Cl_2 gave the α-amino-β-aryl methyl acrylate **18** or **19** in 80–86% yield. Lastly, Pictet–Spengler cyclization using

the condition of 37% HCHO/TFA in CH_2Cl_2 at RT afforded the corresponding THIQ3CA methyl esters **20** and **21** within 5 h and high yields of 70–80%.

3.2.2. Further Improvement in the Glycine Donor Approach— Analysis of the approach described in Scheme 1 led to the realization that a significant improvement in the overall efficiency of the process would be realized if alkene reduction and deprotection steps can be achieved in one step. Thus, benzyloxycarbonyl (Cbz) derivatized α–phosphonoglycine trimethyl ester **3** was treated with either benzaldehyde **4**, **5**, or **22** to yield benzylidenes **23**–**25** in 77-85% yield (Scheme 2). The planned simultaneous reduction and deprotection strategy was employed on benzylidene **23** using catalytic hydrogenation (50 psi H_2 (g) and 10% $Pd(OH)_2$ on charcoal in equivolume mixture of CH_3OH and *t*-butanol) to give the desired α-amino-β-aryl amino methyl esters **18**, **19**, and **26** in good yields (73-76%, Scheme 2). Pictet–Spengler cyclization with formaldehyde under acidic conditions afforded the corresponding THIQ3CA methyl esters **20**, **21**, and **27** in high yields.

Overall, using hydantoin **1** as glycine donor led to two THIQ3CA ethyl esters **12** and **13** in six steps, while using phosphonoglycine trimethyl ester **2** as a glycine donor gave two di–activated THIQ3CA methyl esters **20** and **21** in four steps. An alternative strategy involved the glycine donor **3**, which utilized three mild and efficient steps for the synthesis of THIQ3CA methyl esters **20**, **21**, and **27**. The hydantoin-based approach afforded THIQ3CA ethyl esters in 21–30% overall yields, while the phosphonoglycine trimethyl esters **2** and **3** led to yields of 43–58% and 40–52%, respectively. Finally, the Horner–Wadsworth–Emmons/Pictet–Spengler approach for synthesis of activated THIQ3CA esters is mild, concise, and high yielding.

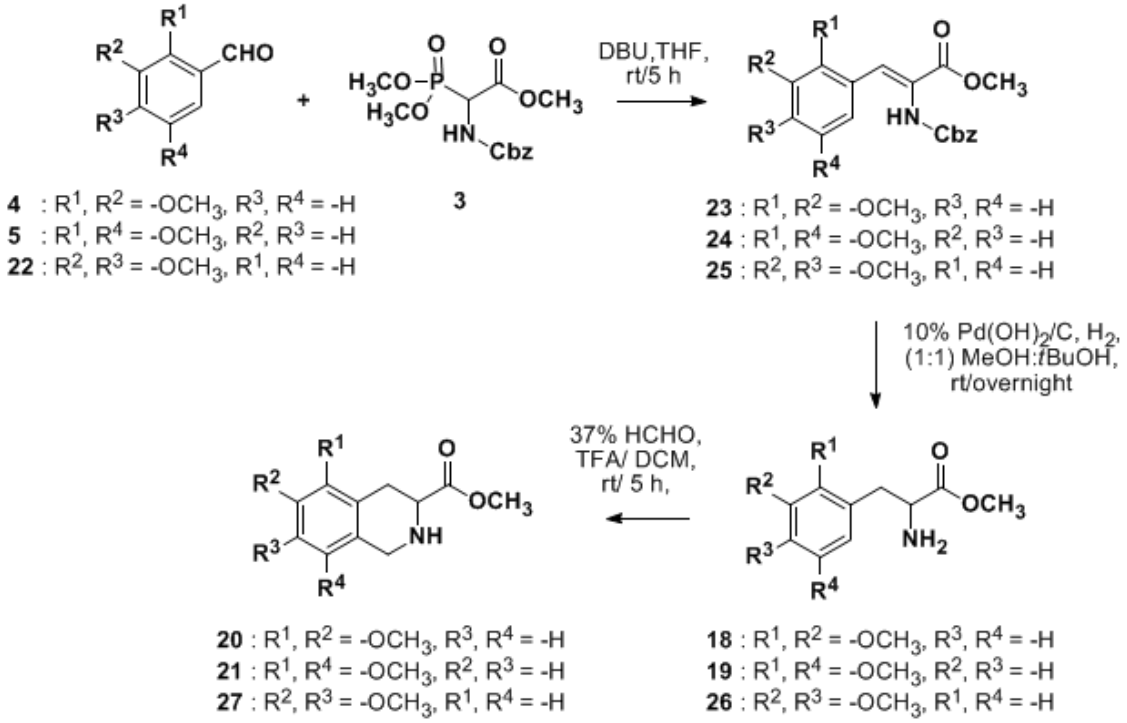

Scheme 2. Synthesis of 5,6– , 5,8–, and 6,7– dimethoxy THIQ3CA esters using (±)-Z-*α*-Phosphonoglycine trimethyl ester **3**, as glycine equivalent. Adapted from reference 268.

3.2.3. Synthesis of Advanced *N*-Arylacyl, *N*-Arylalkyl, and *Bis*-THIQ3CA Analogs— The synthetic protocol developed above (Scheme 2) appeared very attractive for preparing a library of electronically rich THIQ3CA derivatives. In particular, (±)-*Z*-*α*-phosphonoglycine trimethyl ester **3** was especially useful as several novel THIQ3CA–based compounds could be synthesized in near quantitative yields. These include the *N*-arylacyl THIQ3CA esters **30**-**35** and **38**-**42**; the *N*-arylalkyl THIQ3CA ester **43** and the *bis*-THIQ3CA esters **44** and **45** (Scheme 3).

The *N*–benzoyl and *N*–acetyl THIQ3CA esters **30**-**35** were synthesized by direct *N*-acylation using benzoyl or phenyl acetyl chloride in the presence of triethylamine. The *N*–propanoyl and *N*–butanoyl THIQ3CA esters **38**-**42** were prepared using EDCI–mediated coupling reactions with appropriate propioinc or butanoic acids in presence of DMAP at RT.

The synthesis of *N*-alkylated derivatives was somewhat more challenging than that described above for *N*-acylated derivatives. Several bases (K_2CO_3, Cs_2CO_3, Et_3N, and DIPEA), solvent systems (CH_3CN, DMF and their mixtures), and heating methods (conventional refluxing and microwave) were screened to identify high yielding conditions for *N*-*p*-methoxybenzyl THIQ3CA methyl ester **43**. A 92% yield of **43** was obtained following microwave-assisted heating of 1 equivalent of THIQ3CA methyl ester **27**, 2.5 equivalents of DIPEA, 1.1 equivalents of *p*-methoxy benzyl chloride in CH_3CN at 150 ºC for 30 min. Combining these optimized conditions with search for best xylene-based electrophile (α,α'–dichloro or dibromo– *m*– and *p*–xylenes) led to a high yielding synthesis of *bis*-THIQ3CA derivatives **44** and **45**. The best dimerization yield (62–66%) was obtained by refluxing two equivalents of THIQ3CA **28** with one equivalent of a xylene derivative in presence of 4 equivalents of Cs_2CO_3 in equivolume mixture of DMF and CH_3CN.

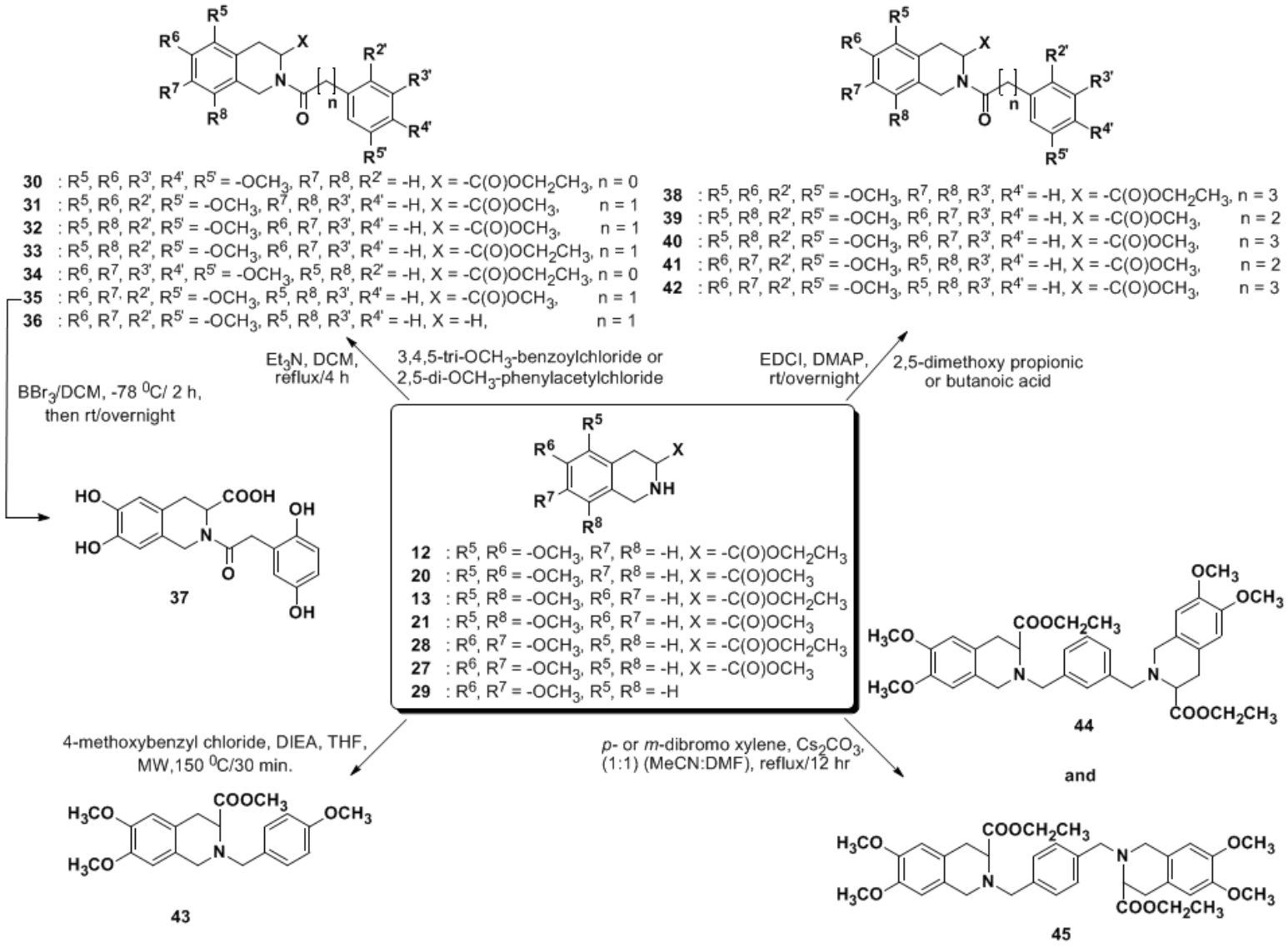

Scheme 3. Synthesis of *N*-substituted THIQ3CA-based library. The scheme is adapted from reference 268.

Overall, a small library of 14 THIQ3CA esters was synthesized using a combination of Horner–Wadsworth–Emmons/Pictet–Spengler reactions (Schemes 2 and 3) in near quantitative yields. These derivatives vary at different structural levels including the substitution pattern of THIQ3CA (5,6–; 5,8–; or 6,7–disubstituted moiety); the type of ester at position–2 (methyl or ethyl ester); the length of the linker (benzyl, benzoyl, acetyl, propanoyl, or butanoyl); and the type of the linker (amide as in *N*-arylacyl THIQ3CA or amine as in *N*-arylalkyl THIQ3CA); and lastly the number and pattern of substituents on the aryl moiety (4–substituted; 2,5–disubstituted; or 3,4,5–trisubstituted moieties). The library of electronically rich THIQ3CA ester analogs, and their chemically modified forms including deprotected poly-phenolic or poly-sulfated derivatives, is likely to be useful in mapping protein binding site(s) so as to deduce optimal binding and/or selectivity properties.

From the perspective of chemical synthesis, several points are noteworthy regarding synthesis using (±)–Z–*α*–phosphonoglycine trimethyl ester **3**. First, this approach can be further exploited in synthesis of many unnatural α-amino acids and their corresponding cyclic rigid forms. Second, the Pictet–Spengler reaction is highly amenable to microwave conditions, which greatly expedites the construction of a library. Third, it is possible to control chirality at the 3-position to afford enantiomerically pure THIQ3CA using rhodium (I) or ruthenium (II)–catalyzed asymmetric hydrogenation.[199,200] These advantages are expected to further enhance the applicability of the THIQ3CA library for drug discovery purposes.

3.2.4. NMR Studies on *N*-Arylacyl THIQ3CA esters— A ^{1}H NMR spectrum is thought of as a classic reflection of the purity of a new compound. The *N*–arylacyl THIQ3CA esters synthesized in this work were highly pure entities as indicated by RP-HPLC and uPLC-MS analysis, however, each molecule demonstrated complex ^{1}H NMR and ^{13}C NMR spectra, which

could not be analyzed on the basis of a single conformational entity composition. We reasoned that the complexity of NMR spectra arises from the –N–C(O)– bond at position–2, which was likely to exhibit partial double-bond character with *cis*- and *trans*-isomers. It was likely that the energy barrier for rotation around the amide bond was large resulting in geometrically and magnetically nonequivalent *N*-substituents. This phenomenon of rotational isomerism has been observed earlier for non-carboxylated THIQ derivatives.[201-206] Considering the medicinal importance of the carboxylated THIQ derivatives being studied, we decided to investigate this phenomenon in detail so as to aid development of appropriate computational protocols for the interaction of THIQ3CA with proteins. Derivatives **32** and **35** were chosen as representative THIQ3CA analogs.

For molecule **35**, two sets of nine ^{1}H signals were observed at room temperature in $CDCl_3$ (Figure 16, Table 2). The relative proportion of the two pairs of peaks was essentially identical across all seven signals and was approximately 75:25. Likewise, **32** displayed two sets of seven ^{1}H signals (Table 3). In addition, the number of ^{13}C signals for both **32** and **35** were double the number of carbons, although the frequencies for some atoms could not be measured accurately due to lower resolution. These observations suggested the possibility of two conformational isomers.

Table 2. ^{1}H NMR-$CDCl_3$ parameters for set of signals that reveal the rotational isomerism in derivative **35**.

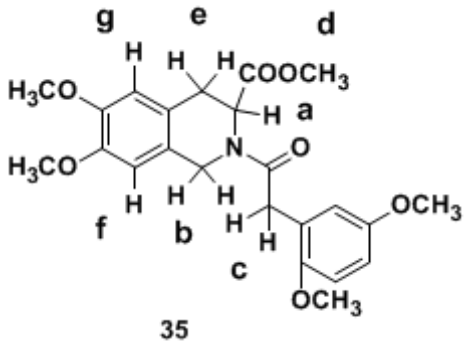

35

Protons	Chemical Shift (δ)	Splitting	Integration
H_a, Position-3	5.51-5.49 & 4.94-4.92	dd & dd	1
H_b, Position-1	4.91-4.60	dd	1
H_b, Position-1	4.52-4.30	dd	1
H_c, Methylene linker	3.76	broad s	2
H_d, Methyl ester	3.67-3.3.66	d	3
H_e, Position-4	3.14-3.00	dt	1
H_e, Position-4	3.02-2.96 & 2.89-2.84	dd & dd	1
H_f, Position-8	6.49-6.40	d	1
H_g, Position-5	6.56-6.53	d	1

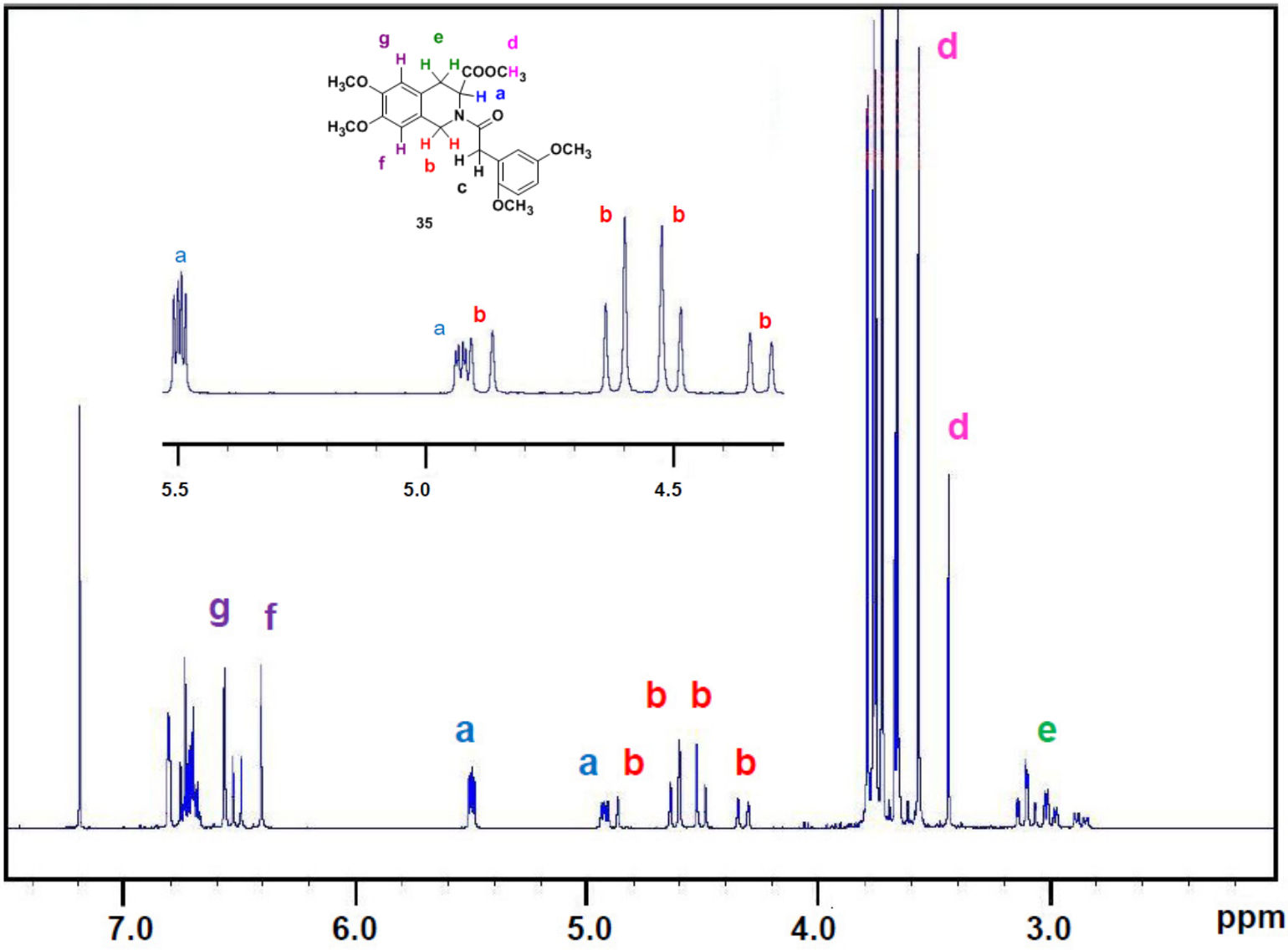

Figure 16. [1]H NMR spectrum of THIQ3CA analog **35** in $CDCl_3$ showing duplicity of signals at ambient temperature. Inset shows 6.0-4.0 δ region, assignable to '*a*' and '*b*' protons, for better clarity. The figure is adapted from reference 268.

Table 3. ^{1}H NMR-$CDCl_3$ parameters for set of signals that reveal the rotational isomerism in derivative **32**.

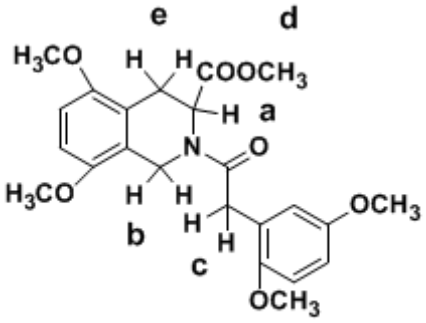

32

Protons	Chemical Shift (δ)	Splitting	Integration
H_a, Position-3	5.64-5.62 & 4.96-4.94	dd & dd	1
H_b, Position-1	5.02-4.78	dd	1
H_b, Position-1	4.41-4.14	dd	1
H_c, Methylene linker	3.79-3.73	d	2
H_d, Methyl ester	3.54-3.43	d	3
H_e, Position-4	3.42-3.37	m	1
H_e, Position-4	2.78-2.72 & 2.55-2.49	dd & dd	1

To understand whether polarity of solvent affects conformational preferences, the ^{1}H NMR spectrum of **32** was studied in C_6D_6, $CDCl_3$, CD_3CN, and DMSO-*d_6* at ambient temperature. The effect was studied by monitoring H_a, H_d, and H_e signals (Figure 17). For proton H_e the splitting pattern changed dramatically as the solvent polarity increased. The two doublet of doublets in C_6D_6 and $CDCl_3$ merged into an unresolved multiplet in CD_3CN, and gave one doublet of doublet in DMSO-*d_6* (Figure 17A). Protons H_a and H_d belonging to carbon-3 and

methyl ester group, respectively, displayed a gradual loss of intensity as the signal spread due to increase in solvent polarity. Whereas the signal spread was 375.7 Hz for H_a in C_6D_6, it decreased to 62.0 Hz in DMSO-d_6 (Figure 17C, see Table 4). Likewise, the spread decreased from 42.6 Hz (C_6D_6) to 9.7 Hz (DMSO-d_6) for H_d (Figure 17B, Table 4). This likely indicates that the two conformers tend to coalesce with increasing solvent polarity which favorably stablizes the oppositely charged double bond charcter of position–3 amide bond.

Table 4. The change in Δδ for protons H_a and H_d of the two detected conformers of THIQ3CA derivative **32** in different solvents.

Solvents	Ha Δδ (Hz)	Hd Δδ (Hz)
C_6D_6	374.68	42.64
$CDCl_3$	269.22	46.76
CD_3CN	151.98	19.24
DMSO-d_6	61.98	9.68

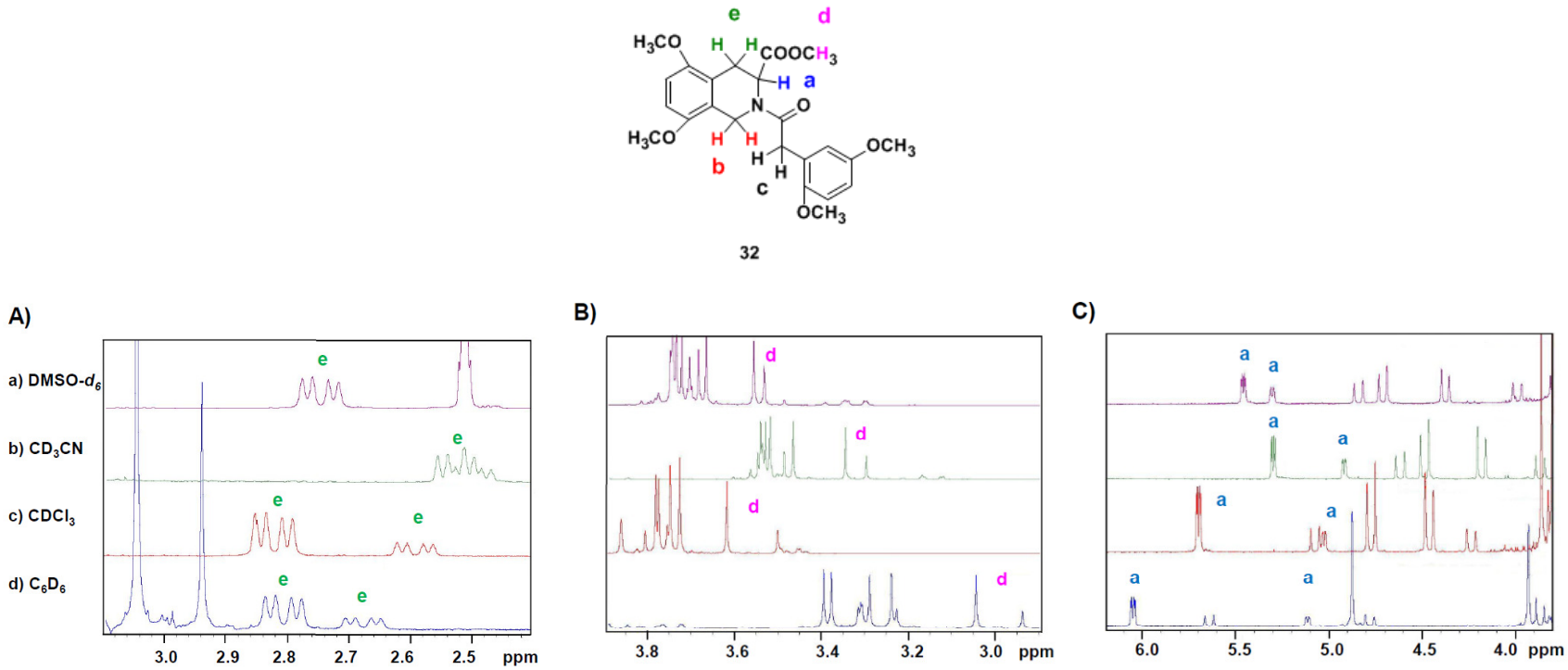

Figure 17. Solvent-dependent changes in the conformational isomerism of **32**. A) 3.1-2.4 δ; B) 3.9-2.8 δ; and C) 6.2-3.8 δ.The figure is adapted from reference 268.

The influence of temperature on the conformational distribution of THIQ3CA analog **32** was studied by measuring spectral changes in DMSO-d_6 over the range of 293 – 373 K. Figure 18 shows that the signal spread (Δδ) between the signals of H_a (position-3 proton) and H_b (position-1 protons) gradually decreases as the temperature increases. Both signals retain distinct resonance positions until 353 K and then start to coalesce on the NMR time scale. Measurements at 373 K for both H_a and H_b show that the two conformers have lost their distinction and exhibit a rapidly equilibrating species. Likewise, two singlets at 3.54 and 3.49 δ corresponding to H_d merge as one singlet 3.57 δ and the two doublet of doublet at 2.78-2.72 δ and 2.55-2.49 δ corresponding to H_e also coalesce as one doublet at 2.82-2.78 δ (not shown). At ambient temperature, the ratio of the major to minor conformer was approximately 3 to 1, which equalized over the range of 353 – 373 K.

The variable temperature results can be used to analyze the free energy of activation of the dynamic inter-conversion between the conformers. The Eyring equation based on detailed line-shape analysis is the most accurate method, although several other methods have been reported.[206-208] Two approximations have been particularly useful including equations 1 and 2 that afford reliable estimates of the free energy of interconversion (ΔG^{++}) in conjunction with the rate constant (k_c) at the coalescence temperature (T_C).[207,208] In these equations, a is constant with a value of 0.004575 kcal/mol, T is the temperature in Kelvin (K), and Δν is the maximum peak separation in Hz. This approach has been shown to give reliable estimates for both coalescing singlets and doublets with different intensities as long as $\Delta\nu > 4$ Hz.

$$\Delta G^{++} = aT(9.972 + \log(\frac{T_C}{\Delta v})) \qquad (1)$$

$$k_c = \frac{\pi\Delta v}{\sqrt{2}} \qquad (2)$$

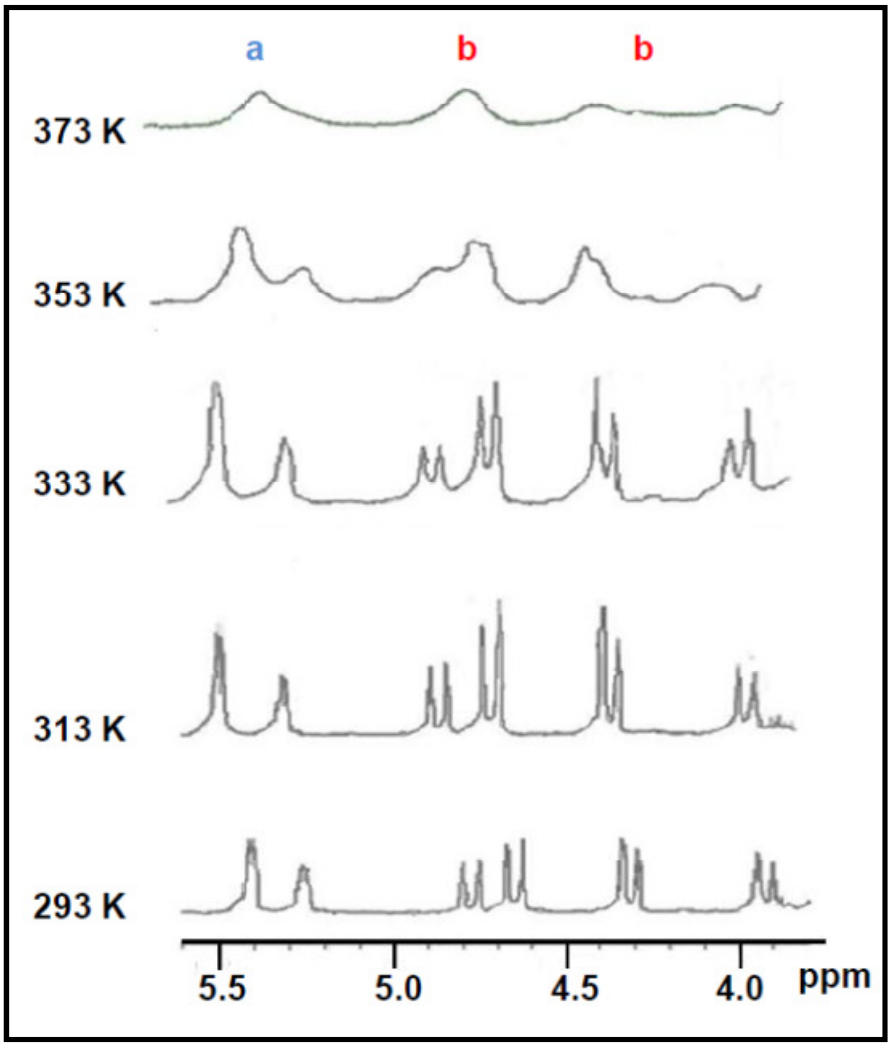

Figure 18. Temperature effect on the conformational isomerism of **32** in DMSO–d_6. The entire ^{1}H NMR spectrum of **32** was recorded but only the 5.6-3.8 δ range is shown for enhanced clarity. ^{1}H NMR spectra at 293, 313, 333 and 353 K were recorded on a Varian 300 MHz instrument, while the spectrum at 373 K was recorded on a Bruker 400 MHz. The figure is adapted from reference 268.

Using this approach, evaluation of the two singlets at 3.56 and 3.53 δ, belonging to the methyl ester proton H_d, resulted in values of 16.7 ± 1.0 kcal/mol and 15.5 ± 1.9 Hz for ΔG^{++} and k_c at 353 K, respectively. This value is significantly higher than a value of 7.8 kcal/mol and 15 kcal/mol for *N*-acetyl-1-benzyl and *N*-acetyl-1,3-dimethyl THIQ derivatives and comparable to the activation energy range of 17.7 – 20.1 measured for *N*-acetyl-1-alkylidene THIQ (Figure 19).[202-204]

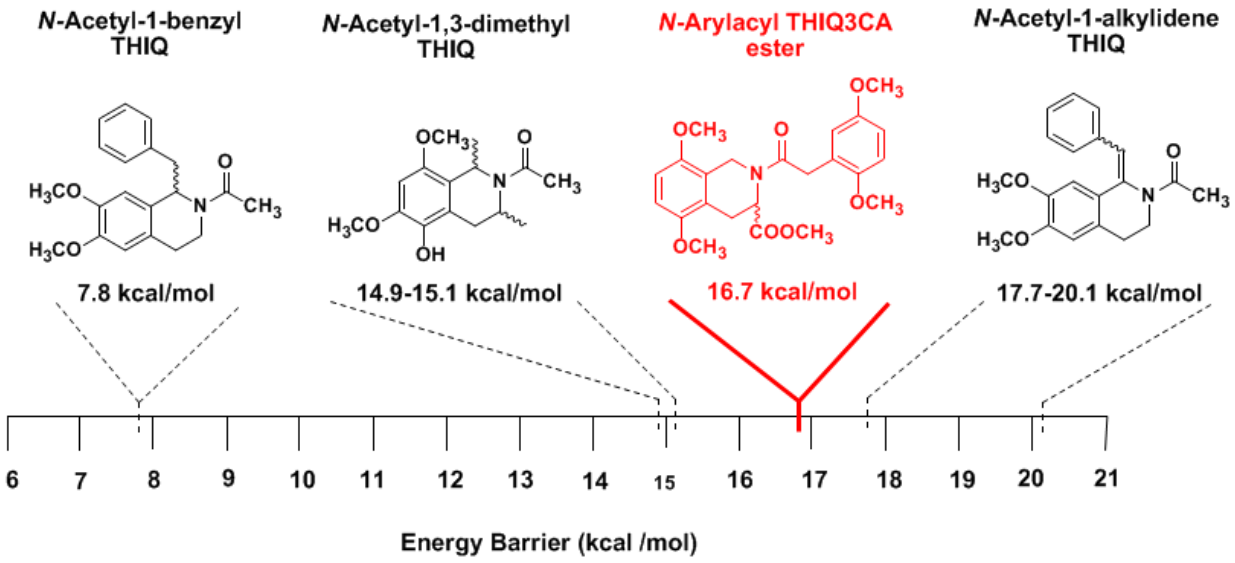

Figure 19. THIQ derivatives display a wide range of energy barriers for conformational transitions. The *N*–arylacyl THIQ3CA esters studied in this work show a distinct high energy barrier of ~17 kca/mol. The figure is adapted from reference 268.

Overall, our work reveals that the duplicity of NMR signals persists for all THIQ3CA derivatives irrespective of groups present on the scaffold as long as the position–2 linker is an amide. Conformational isomerism noted for *N*–arylacyl THIQ3CA analogs arises from rotational restrictions around the amide bond at position–2 with an estimated ΔG^{++} of ~17 kcal/mol. Lastly, we expect that the two corresponding rotational isomers to be equi-energetic with a calculated energy difference of 0.655 kcal/mol ($\Delta G° = -2.3RT\log K_e$, in which $\Delta G°$ is the standard energy

difference; R is the gas constant; T is temperature in Kelvin and K_e is the equilibrium constant, which was found to be 0.33 based on the NMR study).

3.3. Conclusion—In this work, we describe multiple strategies that yield THIQ3CAs containing multiple electron rich methoxy substituents. The work leads to a major conclusion that highly substituted, electron rich THIQ3CA analogs can be synthesized in three, mild, and high yielding steps based on Horner–Wadsworth–Emmons and Pictet–Spengler reactions. Interestingly, NMR studies indicate that the *N*–arylacyl–THIQ3CA derivatives display two equi-energetic, conformational isomers that are separated by a high kinetic barrier of ~17 kcal/mol. This phenomenon is of major significance for structure-based drug design considering that such efforts typically utilize only one of the rotamers.

3.4. Experimental Section—

3.4.1. Chemicals and Reagents— Anhydrous CH_2Cl_2, THF, CH_3CN, DMF, and toluene were purchased from Sigma-Aldrich (Milwaukee, WI) or Fisher Scientific (Pittsburgh, PA) and used as such. All other solvents were of reagent gradient and used as supplied. Other chemical reagents were purchased either from Sigma-Aldrich, Fisher Scientific, or Alfa-Aesar (Ward Hill, MA). Analytical TLC was performed using UNIPLATE^{TM} silica gel GHLF 250 μm pre-coated plates (ANALTECH, Newark, DE). TLC was visualized using light of 254 nm. Chemical reactions sensitive to air or moisture were carried out under nitrogen atmosphere in oven-dried glassware. All reagent solutions unless otherwise noted were handled under an inert nitrogen atmosphere using syringe techniques. Each chemical reaction was optimized to afford a yield of more than 65%.

3.4.2. Purification of Reaction Products— Flash chromatography was performed using Combiflash RF from Teledyne Isco (Lincoln, NE) and disposable normal silica cartridges of 30–

70 μ particle size, 230–400 mesh size and 60 Å pore size. The normal phase silica content of cartridges were 4–24 gms (for purification of 250–1000 mg crude samples). Mobile linear gradients utilized either EtOAc or CH_3OH in hexanes or CH_2Cl_2, respectively. The flow rate of the mobile phase was in the range of 18 to 35 ml/min based on the size of the silica cartridge.

3.4.3. NMR Studies— The ^1H and ^{13}C NMR spectra were recorded on Bruker 400 MHz spectrometer (unless otherwise noted) in $CDCl_3$, DMSO-d_6, CD_3OD, C_6D_6 or CD_3COCD_3. Signals, in part per million (ppm), are either relative to the internal standard (tetramethyl silane, TMS) or to the residual peak of the solvent. The NMR data are being reported as: chemical shift (ppm), multiplicity of signal (s = singlet, d = doublet, t = triplet, q = quartet, dd = doublet of doublet, m = multiplet, br = broad), coupling constants (Hz), and integration.

^1H and ^{13}C NMR spectra of compounds were measured using 5 – 35 mg sample dissolved in 0.6 mL of solvent. For ^1H NMR spectrum, 16 scans were recorded with a spectral width of 8223.685 Hz, a FID resolution of 0.125 Hz, relaxation delay of 1 s, and acquisition time of 4 s, while the ^{13}C spectra were recorded using 1024 – 10240 scans with a spectral width of 24038.461 Hz, FID resolution of 0.367 Hz, acquisition time of 1.5 s, and a relaxation delay of 2 s. Variable temperature NMR studies were performed on a Varian 300 MHz in the range of 293–353 K and on a Bruker 400 MHz at temperatures up to 373 K.

3.4.4. Mass Spectrometric Characterization— The ESI MS characterization of all THIQ3CA derivatives was performed using a Waters Acquity TDQ mass spectrometer in positive ion mode. Samples, dissolved in methanol, were infused at a rate of 20 μL/min and mass scans were collected in the range of 200 – 700 amu with a scan time of 1 s. The capillary and cone voltages were varied between 3 – 4 kV and 38 – 103 V, respectively. The extractor voltage was set to 3 V, the Rf lens voltage was 0.1 V, the source block temperature was 150 ºC, and

desolvation temperature was set to about 250 ºC. Ionization conditions were optimized for each compound to maximize ionization of the parent ion.

3.4.5. General Synthetic Procedures and Spectral Characterization Data—

General Procedure for Preparation of Benzylidene Imidazoline-2,4-dione Derivatives 6 and 7. Hydantoin **1** (5.0 gm, 50.0 mmol), anhydrous sodium acetate (8.2 gm, 100.0 mmol) and aldehyde (**4** or **5**) (7.5 gm, 45.0 mmol) were successively added in a solution of glacial acetic acid (15 mL) and acetic anhydride (2 mL). The mixture was stirred at 170 °C under nitrogen atmosphere for 3 h. Upon cooling to 110 °C, water (100 mL) was added drop-wise and the mixture left for stirring overnight at RT. The orange precipitate of the desired compound was filtered off and then washed with water to remove acetic acid, the unreacted hydantoin, and sodium acetate. The orange solid was then purified by flash chromatography using mobile phase gradient of 40% to 100% (EtOAc: hexanes) to afford benzylidene imidazoline-2,4-dione derivative **6** or **7** as yellow to white solid in 65-72% yield.

5-(2,3-dimethoxybenzylidene)imidazolidine-2,4-dione (6). ^{1}H NMR (DMSO-d_6, 400 MHz): δ = 11.24 (br, 1H, NH), 10.39 (s, br, 1 H, NH), 7.25 (d, ^{1}J = 6.9 Hz, 1 H, Ar), 7.08 (t, ^{1}J = 8.0 Hz, 1H, Ar), 7.03 (d, ^{1}J = 7.2, 1 H, Ar), 6.62 (s, 1 H, CH), 3.81 (s, 3 H, CH_3), 3.74 (s, 3H, CH_3). ^{13}C NMR (DMSO-d_6, 100 MHz): δ = 165.5, 155.5, 152.4, 147.1, 128.7, 126.7, 124.2, 113.3, 102.3, 60.6, 55.7. MS (ESI) calculated for $C_{12}H_{12}N_2O_4$, $[M+H]^+$, *m/z* 249.09, found for $[M+Na]^+$, *m/z* 271.20.

5-(2,5-dimethoxybenzylidene)imidazolidine-2,4-dione (7). ^{1}H NMR (DMSO-d_6, 400 MHz): δ = 7.12 (d, ^{1}J= 2.9 Hz, 1 H, Ar), 6.96 (d, ^{1}J = 9.0 Hz, 1 H, Ar), 6.88-6.85 (dd, ^{1}J= 3.0 Hz, ^{2}J = 9.0 Hz, 1 H, Ar), 6.55 (s, 1H, CH), 3.78 (s, 3H, CH_3), 3.77 (s, 3H, CH_3). ^{13}C NMR (DMSO-d_6, 100 MHz): δ =166.8, 157.1, 153.0, 151.4, 129.4, 122.6, 115.1, 114.1, 112.1, 101.8,

56.0, 55.5. MS (ESI) calculated for $C_{12}H_{12}N_2O_4$, $[M+H]^+$, *m/z* 249.09, found for $[M+Na]^+$, *m/z* 271.23.

General Procedure for Preparation of Benzyl Imidazoline-2,4-dione Derivatives 8 and 9. Benzylidene imidazolidine-2,4-dione derivative (**6** or **7**) (7.3 gm, 29.5 mmol) was dissolved in hot ethanol (100 mL) followed by addition of 10% Pd/C (0.73 gm) after cooling. H_2 gas was then pumped into the reaction vessel to achieve 50 psi at RT. After stirring the mixture for 5 h, the catalyst was filtered on Celite, which was washed using a 1:1 mixture of EtOAc and CH_3OH. The organic filtrate was concentrated *in vacuo* to afford the corresponding reduced product (**8** or **9**) in ~100% yield which was used without any further purification.

5-(2,3-Dimethoxybenzyl)imidazolidine-2,4-dione (8). ^{1}H NMR (DMSO-d_6, 400 MHz): δ = 10.58 (s, 1 H, NH), 7.76 (s, 1 H, NH), 7.00-6.94 (dd, ^1J = 8.0 Hz, ^2J = 15.6, 1 H, Ar), 6.94-6.91 (dd, ^1J = 1.6 Hz, ^2J = 8.2 Hz, 1 H, Ar), 6.81-6.79 (dd, ^1J = 1.6 Hz, ^2J = 7.4 Hz, 1 H, Ar), 4.26 (t, ^1J= 6.5 Hz, 1 H, CH), 3.79 (s, 3H, CH_3), 3.73 (s, 3H, CH_3), 3.09-3.04 (dd, ^1J = 4.9 Hz, ^2J = 13.9 Hz, 1 H, CH), 2.81-2.76 (dd, ^1J = 7.5 Hz, ^2J = 13.9 Hz, 1 H, CH). ^{13}C NMR (DMSO-d_6, 100 MHz): δ = 175.4, 157.3, 152.2, 147.1, 129.7, 122.4, 111.6, 60.0, 58.0, 55.5, 31.5. MS (ESI) calculated for $C_{12}H_{14}N_2O_4$, $[M+H]^+$, *m/z* 251.10, found for $[M+Na]^+$, *m/z* 273.24.

5-(2,5-Dimethoxybenzyl)imidazolidine-2,4-dione (9). ^{1}H NMR (DMSO-d_6, 400 MHz): δ = 10.60 (s, 1 H, NH), 7.75 (s, 1 H, NH), 6.87 (d, ^1J= 8.6 Hz, 1 H, Ar), 6.78 (d, ^1J = 3.0 Hz, 1 H, Ar), 6.76-6.74 (m, 1 H, Ar), 4.26-4.22 (dd, ^1J= 5.1 Hz, ^2J = 7.2 Hz, 1 H, CH), 3.71 (s, 3H, CH_3), 3.68 (s, 3H, CH_3), 3.08-3.03 (dd, ^1J = 4.8 Hz, ^2J = 13.8 Hz, 1 H, CH), 2.72-2.67 (dd, ^1J = 7.6 Hz, ^2J = 13.8 Hz, 1 H, CH). ^{13}C NMR (DMSO-d_6, 100 MHz): δ =175.5, 157.4, 152.7, 151.5, 125.4, 117.1, 112.2, 111.5, 57.4, 55.8, 55.2, 32.2. MS (ESI) calculated for $C_{12}H_{14}N_2O_4$, $[M+H]^+$, *m/z* 251.10, found for $[M+Na]^+$, *m/z* 273.24.

General Procedure for Preparation of Dimethoxy Phenylalanine Ethyl Esters 10 and 11. A mixture of the benzyl imidazolidine-2,4-dione (**8** or **9**) (7.0 gm, 28.0 mmol), barium hydroxide (14.4 gm, 84.0 mmol) and water (150 mL) was refluxed for 48 h, then filtered hot and the residue washed with hot water. Following cooling, the filtrate was acidified to pH 6.5 with 50% H_2SO_4. The resulting $BaSO_4$ precipitate was filtered and the pH of the aqueous filtrate adjusted to 9.0 using NH_4OH. The aqueous filtrate was then concentrated, suspended in ethanol (100 mL), treated with thionyl chloride (20 mL of 2.0 M solution in CH_2Cl_2) at 0 $^{\circ}$C, and then mixture refluxed for 4 h. Following neutralization with saturated $NaHCO_3$ solution, the reaction mixture was partitioned between EtOAc and water, and a crude product obtained from the EtOAc layer. Flash chromatography using 70% (EtOAc: hexanes) as the mobile phase was used to yield derivative **10** or **11** as white solid in 43-51% yield.

Ethyl 2,3-dimethoxy phenylalanine (10). ^{1}H NMR ($CDCl_3$, 400 MHz): δ = 6.91 (t, ^1J = 7.9 Hz, 1 H, Ar), 6.75-6.73 (dd, ^1J = 1.4 Hz, ^2J = 8.2 Hz, 1 H, Ar), 6.70-6.68 (dd, ^1J = 1.4 Hz, ^2J = 7.6 Hz, 1 H, Ar) 4.10-4.04 (q, ^1J = 7.2 Hz, 2 H, CH_2), 3.78 (s, 3 H, CH_3), 3.76 (s, 3 H, CH_3), 3.73-3.67 (m, 1 H, CH), 3.03-2.99 (dd, ^1J = 5.6 Hz, ^2J = 13.3 Hz, 1 H, CH), 2.83-2.78 (dd, ^1J = 8.3 Hz, ^2J = 13.3 Hz, 1 H, CH), 1.15 (t, ^1J= 7.1 Hz, 3 H, CH_3). ^{13}C NMR ($CDCl_3$, 100 MHz): δ =175.1, 152.8, 147.7, 131.2, 123.8, 122.8, 111.3, 60.8, 60.5, 55.7, 55.1, 35.8, 14.1. MS (ESI) calculated for $C_{13}H_{19}NO_4$, $[M+H]^+$, *m/z* 254.14, found for $[M+H]^+$, *m/z* 254.30.

Ethyl 2,5-dimethoxy phenylalanine (11). ^{1}H NMR ($CDCl_3$, 400 MHz): 6.79-6.76 (m, 1 H, Ar), 6.74 (d, ^1J = 3.0 Hz, 1 H, Ar), 6.72 (d, ^1J = 1.8 Hz, 1 H, Ar), 4.18-4.11 (q, ^1J = 7.2 Hz, 2H, CH_2), 3.80-3.78 (m, 1H, CH), 3.77 (s, 3H, CH_3), 3.74 (s, 3 H, CH_3), 3.09-3.03 (dd, ^1J = 6.0 Hz, ^2J = 12.2 Hz, 1 H, CH), 2.86-2.79 (dd, ^1J = 9.0 Hz, ^2J = 12.1 Hz, 1H, CH), 1.15 (t, ^1J = 7.2 Hz, 3 H, CH_3). ^{13}C NMR ($CDCl_3$, 100 MHz): δ =173.1, 153.5, 151.9, 125.9, 117.4, 112.7, 111.5,

61.2, 56.0, 55.7, 53.8, 33.1, 14.1. MS (ESI) calculated for $C_{13}H_{19}NO_4$, $[M+H]^+$, *m/z* 254.14, found for $[M+H]^+$, *m/z* 254.30.

General Procedure for Pictet–Spengler Reaction to Synthesize 12, 13, 20, 21 and 27. A solution of substituted phenylalanine methyl (**18**, **19**, or **26**) (0.6 gm, 2.5 mmol) or ethyl ester (**10** or **11**) (0.5 gm, 2.0 mmol) in CH_2Cl_2 (10 mL) was treated with formaldehyde (37% aq. solution, 0.2-0.25 mL, 2.5-3.0 mmol) at RT. Trifluoro-acetic acid (TFA, 3.7-4.6 gm, 2.5-3.0 mL, 10.0-12.5 mmol) was then slowly added over 15 min and the reaction mixture was stirred for 5 h following which it was diluted with CH_2Cl_2 (15 mL) and neutralized with saturated $NaHCO_3$ solution (20 mL). The organic extracts of the aqueous solution were combined, the solvent evaporated under reduced pressure, and the crude mixture was separated by flash chromatography using the mobile phase of 50% (EtOAc: hexanes) to give the desired THIQ3CA ethyl ester (**12** or **13**) or methyl ester (**20**, **21** or **27**) as yellow oil in 70-82% yield.

Ethyl 5,6-dimethoxy-1,2,3,4-tetrahydroisoquinoline-3-carboxylate (12). ^{1}H NMR ($CDCl_3$, 400 MHz): δ = 6.73 (s, 2H, Ar), 4.10-3.80 (m, 5 H, CH, 2 × CH_2), 3.80 (s, 3 H, CH_3), 3.79 (s, 3 H, CH_3), 3.26 (d, ^1J = 16.8 Hz, 1 H, CH), 3.04-2.94 (dd, ^1J= 6.3 Hz, ^2J = 17.1 Hz, 1 H, CH), 1.15 (t, ^1J = 7.2 Hz, 3 H, CH_3). ^{13}C NMR ($CDCl_3$, 100 MHz): δ = 173.2, 150.5, 146.5, 127.5, 127.0, 121.7, 109.7, 61.1, 55.7, 55.5, 55.3, 42.8, 26.2, 14.1. MS (ESI) calculated for $C_{14}H_{19}NO_4$, $[M+H]^+$, *m/z* 266.14, found for $[M+H]^+$, *m/z* 266.28.

Ethyl 5,8-dimethoxy-1,2,3,4-tetrahydroisoquinoline-3-carboxylate (13). ^{1}H NMR ($CDCl_3$, 400 MHz): δ = 6.58 (d, ^1J = 8.9 Hz, 1 H, Ar), 6.55 (d, ^1J = 8.9 Hz, 1 H, Ar), 4.20-4.18 (dd, ^1J = 2.3 Hz, ^2J = 7.2 Hz, 1 H, CH), 4.16-4.14 (dd, ^1J = 2.2 Hz, ^2J = 7.2 Hz, 1 H, CH), 4.13 (d, ^1J = 14.2 H, 1 H, CH), 3.80 (d, ^1J = 17.0 Hz, 1 H, CH), 3.71 (s, 3 H, CH_3), 3.69 (s, 3 H, CH_3), 3.59-3.55 (dd, ^1J = 4.6 Hz, ^2J = 10.4 Hz, 1 H, CH), 3.07-3.01 (ddd, ^1J = 1.0 Hz, ^2J = 4.5 Hz, ^3J

=17.1 Hz, 1 H, CH), 2.64-2.57 (dd, ^1J = 10.4 Hz, ^2J = 17.1 Hz, 1 H, CH), 1.24 (t, ^1J = 7.2 Hz, 3 H, CH_3). ^{13}C NMR ($CDCl_3$, 400 MHz): δ = 173.1, 151.2, 150.0, 124.9, 123.6, 107.4, 107.1, 61.1, 55.7, 55.5, 55.3, 42.8, 26.2, 14.1. MS (ESI) calculated for $C_{14}H_{19}NO_4$, $[M+H]^+$, *m/z* 266.14, found for $[M+H]^+$, *m/z* 266.28 .

Methyl 5,6-dimethoxy-1,2,3,4-tetrahydroisoquinoline-3-carboxylate (20). ^{1}H NMR ($CDCl_3$, 400 MHz): δ = 6.68 (s, 2H, Ar), 3.97-3.78 (m, 3H, CH, CH_2), 3.75 (s, 3H, CH_3), 3.73 (s, 3H, CH_3), 3.47, (s, 3 H, CH_3), 3.22-312 (dd, ^1J = 4.3 Hz, ^2J = 17.4 Hz, 1H, CH), 2.97-2.91 (dd, ^1J = 9.2 Hz, ^2J = 16.4 Hz, 1H, CH). ^{13}C NMR ($CDCl_3$, 100 MHz): δ = 173.2, 150.5, 146.5, 127.5, 127.0, 121.7, 110.7, 60.1, 56.9, 55.8, 51.3, 49.3, 25.8. MS (ESI) calculated for $C_{13}H_{17}NO_4$, $[M+H]^+$, *m/z* 252.12, found for $[M+H]^+$, *m/z* 252.26.

Methyl 5,8-dimethoxy-1,2,3,4-tetrahydroisoquinoline-3-carboxylat (21). ^{1}H NMR ($CDCl_3$, 400 MHz): δ = 6.53 (d, ^1J = 3.1 Hz, 1 H, Ar), 6.52 (d, ^1J = 2.9 Hz, 1 H, Ar), 3.94-3.87 (m, 2H, CH_2), 3.86-3.81 (dd, ^1J = 7.8 Hz, ^2J = 16.4 Hz, 1 H, CH), 3.69 (s, 3H, CH_3), 3.67 (s, 3H, CH_3), 3.46 (s, 3H, CH_3), 3.12-3.13.06 (dd, ^1J = 3.9 Hz, ^2J = 17.2 Hz,1H, CH), 2.86-2.79 (dd, ^1J = 10.2 Hz, ^2J = 17.4 Hz, 1H, CH). ^{13}C NMR ($CDCl_3$, 100 MHz): δ = 173.5, 151.2, 150.2, 124.7, 123.2, 107.1, 106.8, 60.1, 56.4, 55.7, 51.2, 45.6, 25.0. MS (ESI) calculated for $C_{13}H_{17}NO_4$, $[M+H]^+$, *m/z* 252.12, found for $[M+H]^+$ *m/z* 252.14.

Methyl 6,7-dimethoxy-1,2,3,4-tetrahydroisoquinoline-3-carboxylate (27). ^{1}H NMR ($CDCl_3$,400 MHz): δ = 6.52 (s, 1 H, Ar), 6.46 (s, 1 H, Ar), 4.08-3.98 (dd, ^1J = 15.8 Hz, ^2J= 25.6 Hz, 2 H, CH_2), 3.73-3.79 (m, 1 H, CH), 3.78 (s, 3 H, CH_3), 3.77 (s, 3 H, CH_3), 3.72 (s, 3 H, CH_3), 3.00-2.95 (dd, ^1J= 4.8 Hz, ^2J = 16.1 Hz, 1 H, CH), 2.91-2.84 (dd, ^1J = 9.7 Hz, ^2J= 16.0 Hz, 1 H, CH). ^{13}C NMR ($CDCl_3$, 100 MHz): δ = 172.7, 147.8, 125.5, 124.4, 111.7, 108.9, 55.9,

55.6, 52.3, 46.4, 30.6. MS (ESI) calculated for $C_{13}H_{17}NO_4$, $[M+H]^+$, *m/z* 252.12, found for $[M+Na]^+$, *m/z* 274.19.

General procedure for Horner–Wadsworth–Emmons Reaction for Synthesis of 14, 15, 23, 24 and 25. To a solution of (±)-Boc-α-phosphono glycine trimethyl ester **2** (2.0 gm, 6.7 mmol) or (±)-Z-*α*-phosphonoglycine trimethyl ester **3** (2.0 gm, 6.0 mmol) in dry THF (3 mL) was added DBU (0.91-1.0 gm, 6.0-6.7 mmol) and the mixture stirred for 30 min at 0 °C. A solution of either 2,3-dimethoxy benzaldehyde **4**, 2,5-dimethoxy benzaldehyde **5**, or 3,4-dimethoxybenzaldehyde **22** (0.83-0.93 gm, 5.0-5.6 mmol) in dry THF (3 mL) was then added slowly. The reaction mixture was allowed to warm to RT, stirred for 5 h and the solvent evaporated under reduced pressure. The residue was taken up in EtOAc (50 mL) and following routine organic extraction and evaporation procedures a crude product was obtained. The crude product was then purified by flash chromatography using 30% (EtOAc: hexanes) as eluent to give **14**, **15**, or **23**-**25** as white to yellow solid in 77-85% yield.

Methyl-2-(*tert*-butoxycarbonylamino)-3-(2,3-dimethoxyphenyl)acrylate (14). ^{1}H NMR ($CDCl_3$, 400 MHz): δ = 7.12 (s, 1 H, Ar), 7.06 (d, ^1J = 4.3 Hz, 2 H, Ar), 6.91-6.89 (dd, ^1J = 0.7 Hz, ^2J = 4.8 Hz, 1H, CH), 3.88 (s, 3H, CH_3), 3.86 (s, 3H, CH_3), 3.80 (s, 3H, CH_3), 1.40 (s, 9H, 3 × CH_3). ^{13}C NMR ($CDCl_3$, 100 MHz): δ = 166.2, 153.0, 152.9, 147.0, 128.3, 127.6, 124.2, 121.9, 121.7, 112.7, 80.7, 61.4, 55.9, 52.5, 28.1. MS (ESI) calculated for $C_{17}H_{23}NO_6$, $[M+H]^+$, *m/z* 338.16, found for $[M+H]^+$, *m/z* 338.32.

Methyl-2-(*tert*-butoxycarbonylamino)-3-(2,5-dimethoxyphenyl)acrylate (15). ^{1}H NMR ($CDCl_3$, 400 MHz): δ = 7.21 (s, 1H, Ar), 7.01 (s, 1 H, Ar), 6.78 (t, ^1J = 0.9 Hz, 1 H, CH), 3.78 (s, 3H, CH_3), 3.76 (s, 3H, CH_3), 3.68 (s, 3H, CH_3), 1.32 (s, 9 H, 3 × CH_3). ^{13}C NMR ($CDCl_3$, 100 MHz): δ = 166.1, 153.4, 152.8, 151.5, 126.1, 123.8, 123.5, 116.1, 114.5, 112.6,

80.7, 56.5, 55.7, 52.4, 28.3. MS (ESI) calculated for $C_{17}H_{23}NO_6$, $[M+H]^+$, *m/z* 338.16, found for $[M+Na]^+$, *m/z* 360.18.

Methyl-2-(benzyloxycarbonylamino)-3-(2,3-dimethoxyphenyl)acrylate (23). ^{1}H NMR ($CDCl_3$, 400 MHz): δ = 7.32-7.28 (m, 5H, Ar), 7.18 (s, 1 H, Ar), 6.96-6.93 (m, 2 H, Ar), 6.83-6.81 (m, 1 H, CH), 5.00 (s, 2 H, CH_2), 3.79 (s, 3H, CH_3), 3.73 (s, 3H, CH_3) 3.69 (s, 3H, CH_3). ^{13}C NMR ($CDCl_3$, 100 MHz): δ = 165.7, 153.7, 153.0, 146.9, 136.0, 128.5, 128.3, 128.2, 128.0, 127.0, 124.3, 123.7, 121.6, 112.9, 67.3, 61.5, 55.8, 52.6. MS (ESI) calculated for $C_{20}H_{21}NO_6$, $[M+H]^+$, *m/z* 372.14, found for $[M+H]^+$, *m/z* 372.28.

Methyl-2-(benzyloxycarbonylamino)-3-(2,5-dimethoxyphenyl)acrylate (24). ^{1}H NMR ($CDCl_3$, 400 MHz): δ = 7.34-7.30 (m, 5H, Ar), 6.99 (d, ^1J= 2.0 Hz, 1 H, Ar), 6.84 (d, ^1J = 2.4 Hz, 2 H, Ar), 6.77-6.73 (m, 1H, CH), 5.08 (s, 2H, CH_2), 3.73 (s, 6 H, 2 × CH_3), 3.59 (s, 3H, CH_3). ^{13}C NMR ($CDCl_3$, 100 MHz): δ =165.7, 153.5, 152.8, 151.4, 136.0, 128.6, 128.4, 128.2, 125.8, 125.0, 123.4, 116.4, 114.4, 112.9, 67.3, 56.6, 55.6, 52.5. MS (ESI) calculated for $C_{20}H_{21}NO_6$, $[M+H]^+$, *m/z* 372.14, found for $[M+H]^+$, *m/z* 372.32.

Methyl-2-(benzyloxycarbonylamino)-3-(3,4-dimethoxyphenyl)acrylate (25). ^{1}H NMR (400 MHz, $CDCl_3$): δ = 7.36 (s, 1 H, Ar), 7.35-7.30 (m, 4 H, Ar), 7.13-7.11 (m, 2 H, Ar), 6.90-6.85 (m, 1 H, Ar), 6.82 (d, ^1J = 8.9 Hz, 1 H, CH), 6.26 (br, s, 1 H, NH), 5.13 (s, 2 H, CH_2), 3.90 (s, 3 H, CH_3), 3.81 (s, 3 H, CH_3), 3.71 (s, 1 H, CH_3). ^{13}C NMR ($CDCl_3$, 100 MHz): δ = 165.9, 150.4, 148.8, 136.0, 133.0, 130.0, 128.5, 128.3, 126.4, 124.2, 124.2, 122.1, 114.2, 112.2, 110.9, 67.5, 55.9, 55.6, 52.6. MS (ESI) calculated for $C_{20}H_{21}NO_6$, $[M+H]^+$, *m/z* 372.14, found for $[M+H]^+$, *m/z* 372.28.

General Procedure for Catalytic Hydrogenation of *N*-Boc and *N*-Cbz Protected α-Amino-β-aryl methyl acrylates. Method A: Methyl acrylate (**14** or **15**) (0.5 gm, 1.5 mmol) and

10% Pd/C (0.05 gm) were mixed in ethanol (15 mL) and H_2 gas pumped into the reaction mixture at RT. After stirring the solution 5 h, the catalyst was filtered on Celite and the organic filtrate concentrated *in vacuo* to afford the reduced product (**16** or **17**) as white solid in ~100% yield. **Method B**: *N*-Cbz protected methyl acrylate **23**, **24**, or **25** (0.5 gm, 1.3 mmol) and 10% $Pd(OH)_2$ (0.05 gm) on activated charcoal were mixed in CH_3OH:*t*-butanol (1:1) mixture (10 mL) and H_2 gas pumped into the mixture at RT. After stirring overnight, the catalyst was filtered on Celite, the organic filtrate concentrated *in vacuo*, and the residue purified by flash chromatography using 70% (EtOAc: hexanes) as mobile phase to afford the corresponding dimethoxy β-aryl-α-amino methyl ester **18** (oil), **19** (oil), or **26** as a yellow solid in 73-76% yield.

Methyl 2-(*tert*-butoxycarbonylamino)-3-(2,3-dimethoxyphenyl)propanoate (16). ^{1}H NMR ($CDCl_3$, 400 MHz): δ = 7.00 (t, ^1J = 1.5 Hz, 1H, Ar), 6.82 (d, ^1J= 8.2 Hz, 1 H, Ar), 6.73 (d, ^1J= 7.6, 1 H, Ar), 5.32 (d, ^1J= 7.0 Hz, 1 H, NH), 4.48-4.43 (dd, ^1J= 6.8 Hz, ^2J= 13.2 Hz, 1 H, CH), 3.86 (s, 3H, CH_3), 3.84 (s, 3H, CH_3), 3.71 (s,3H, CH_3), 3.06-3.04 (m, 2 H, CH_2), 1.39 (s, 9H, 3 × CH_3). ^{13}C NMR ($CDCl_3$, 100 MHz): δ = 172.8, 155.4, 152.7, 147.5, 130.1, 124.0, 122.7, 111.6, 79.6, 60.6, 55.7, 54.7, 52.2, 32.4, 28.3. MS (ESI) calculated for $C_{17}H_{25}NO_6$, $[M+H]^+$, *m/z* 340.18, found for $[M+Na]^+$, *m/z* 361.82.

Methyl 2-(*tert*-butoxycarbonylamino)-3-(2,5-dimethoxyphenyl)propanoate (17). ^{1}H NMR ($CDCl_3$, 400 MHz): δ = 6.70-6.68 (m, 2H, Ar), 6.61 (d, ^1J= 2.8 Hz, 1 H, Ar), 5.19 (d, ^1J= 7.1 Hz, 1 H, NH), 4.45-4.39 (dd, ^1J= 13.2 Hz, ^2J= 7.0 Hz, 1 H, CH), 3.71 (s, 3H, CH_3), 3.67 (s, 3H, CH_3), 3.64 (s, 3H, CH_3), 2.96 (t, ^1J= 4.8 Hz, 2H, CH_2), 1.31 (s, 9H, 3 × CH_3). ^{13}C NMR ($CDCl_3$, 100 MHz): δ = 172.7, 155.2, 153.5, 151.8, 125.7, 117.2, 112.7, 111.3, 79.5, 55.8, 55.6, 54.1, 52.0, 32.9, 28.2. MS (ESI) calculated for $C_{17}H_{25}NO_6$, $[M+H]^+$, *m/z* 340.18, found for $[M+Na]^+$, *m/z* 361.82.

Methyl 2,3-dimethoxy phenylalanine (18). ^{1}H NMR ($CDCl_3$, 400 MHz): δ = 8.47 (s, br, 2H, NH_2), 7.00 (t, ^{1}J= 8.0 Hz, 1 H, Ar), 6.86-6.84 (dd, ^{1}J= 1.2 Hz, ^{2}J= 8.2 Hz, 1 H, Ar), 6.77-6.75 (dd, ^{1}J= 1.1 Hz, ^{2}J= 7.6 Hz, 1 H, Ar), 4.34-4.31 (dd, ^{1}J= 5.4 Hz, ^{2}J= 7.0 Hz, 1 H, CH), 3.82 (s, 3H, CH_3), 3.81 (s, 3H, CH_3), 3.69 (s, 3H, CH_3), 3.36-3.31 (dd, ^{1}J= 5.2 Hz, ^{1}J= 14.2 Hz, 1 H, CH), 3.23-3.18 (dd, ^{1}J= 5.2 Hz, ^{2}J= 14.2 Hz, 1 H, CH). ^{13}C NMR ($CDCl_3$, 100 MHz): δ = 169.1, 152.7, 147.1, 127.7, 124.7, 123.0, 112.5, 60.7, 55.6, 53.7, 53.0, 31.6. MS (ESI) calculated for $C_{12}H_{17}NO_4$, $[M+H]^+$, *m/z* 240.12, found for $[M+H]^+$, *m/z* 240.24.

Methyl 2,5-dimethoxy phenylalanine (19). ^{1}H NMR ($CDCl_3$, 400 MHz): δ = 6.71 (s, 3H, Ar), 4.28-4.25 (dd, ^{1}J= 8.0 Hz, ^{2}J= 5.0 Hz, 1H, CH), 3.70 (s, 3H, CH_3), 3.66 (s, 3H, CH_3), 3.63 (s, 3H, CH_3), 3.33-3.28 (dd, ^{1}J= 5.0 Hz, ^{2}J= 14.1 Hz, 1 H, CH), 3.03-2.97 (dd, ^{1}J= 8.0 Hz, ^{2}J= 14.1 Hz, 1H, CH). ^{13}C NMR ($CDCl_3$, 100 MHz): δ = 169.5, 153.4, 151.8, 123.0, 117.9, 113.9, 111.7, 55.8, 53.0, 52.8, 32.0. MS (ESI) calculated for $C_{12}H_{17}NO_4$, $[M+H]^+$, *m/z* 240.12, found for $[M+Na]^+$, *m/z* 262.15.

Methyl 3,4-dimethoxy phenylalanine (26). ^{1}H NMR ($CDCl_3$, 400 MHz): δ = 6.73 (d, ^{1}J= 7.8 Hz,1 H, Ar), 6.66 (d, ^{1}J = 7.4 Hz, 1 H, Ar), 6.65 (s, 1 H, Ar), 3.79-3.65 (m, 1 H, CH), 3.79 (s, 3 H, CH_3), 3.78 (s, 3H, CH_3), 3.64 (s, 3H, CH_3), 2.99-2.95 (dd, ^{1}J= 4.8 Hz, ^{2}J= 13.6 Hz, 1H, CH), 2.79-2.74 (dd, ^{1}J= 7.6 Hz, ^{2}J= 13.6 Hz, 1H, CH), 1.86 (br, s, 2 H, NH_2). ^{13}C NMR ($CDCl_3$, 100 MHz): δ = 175.2, 149.0, 148.0, 129.5, 121.4, 112.4, 111.3, 55.9, 55.8, 55.8, 52.0, 40.4. MS (ESI) calculated for $C_{12}H_{17}NO_4$, $[M+H]^+$, *m/z* 240.12, found for $[M+Na]^+$, *m/z* 262.22.

General Procedure for *N*-Boc Deprotection to Synthesize 18 and 19. To a solution of *N*-Boc α–amino–β-aryl ester (**16** or **17**) (0.35 gm, 1.0 mmol) in CH_2Cl_2 (5 mL), trifluoro-acetic acid (TFA, 5 mL) was added drop-wise at 0 ^{0}C, and the mixture was warmed to RT. After stirring for 4 h, the reaction mixture was diluted with CH_2Cl_2 (25 mL) and neutralized by drop-

wise addition of saturated aqueous $NaHCO_3$ (20 mL). The organic layer was separated and following routine extraction, evaporation procedure gave a crude product, which was purified by flash chromatography using 70% (EtOAc: hexanes) to give the desired α–amino–β-aryl ester **18** or **19** as yellow oil in 80-86% yield. The NMR spectra for the corresponding product are presented above.

General Procedure for Step–wise Transesterification of THIQ3CA Methyl Esters to Ethyl Esters. To a stirred solution of dimethoxy THIQ3CA methyl ester (**20**, **21**, or **27**) (0.15 gm, 0.6 mmol) in methanol (25 mL), lithium hydroxide (0.072 gm, 3.0 mmol) was added. The mixture was stirred at RT for 5 h and then concentrated *in vacuo,* and washed with ethanol (3 × 10 mL). Ethanol (20 mL) was then added to the reaction solid residue followed by step-wise addition of thionyl chloride ($SOCl_2$, 10 mL of 2 M in CH_2Cl_2) at 0 ºC. The resulting mixture was refluxed for 4 hours, then cooled to RT and neutralized with saturated $NaHCO_3$ solution. The product was extracted with CH_2Cl_2 (3 × 50 mL) followed by routine extraction and concentration process to give a residue that was purified using 45% (EtOAc: hexanes) as eluent of flash chromatography to give corresponding ethyl ester **12**, **13**, or **28** as yellow oil in 55-72% yield.

Ethyl 6,7-dimethoxy-1,2,3,4-tetrahydroisoquinoline-3-carboxylate (28). ^{1}H NMR ($CDCl_3$, 400 MHz): δ = 6.52 (s, 1 H, Ar), 6.45 (s, 1 H, Ar), 4.18-4.13 (q, ^1J = 7.1 Hz, 2 H, CH_2), 3.96 (s, 2 H, CH_2), 3.80 (s, 3 H, CH_3), 3.79 (s, 3 H, CH_3), 3.63-3.60 (dd, ^1J = 4.7 Hz, ^2J = 10.1 Hz, 1 H, CH), 2.94-2.89 (dd, ^1J = 4.6 Hz, ^2J = 16.0 Hz, 1 H, CH), 2.83-2.77 (dd, ^1J = 10.0 Hz, ^2J = 15.8 Hz, 1 H, CH), 2.19 (br, s , 1 H, NH), 1.23 (t, ^1J = 7.1 Hz, 3 H, CH_3). ^{13}C NMR ($CDCl_3$, 100 MHz): δ =173.1, 147.6, 126.7, 124.9, 111.8, 108.9, 61.0, 55.9, 55.9, 55.9, 47.0, 31.1, 14.2. MS (ESI) calculated for $C_{14}H_{19}NO_4$, $[M+H]^+$, *m/z* 266.14, found for $[M+Na]^+$, *m/z* 288.21.

General Procedure for *N*-arylacylation of 1,2,3,4–tetrahydroisoquinoline–3–carboxylic acid Methyl or Ethyl ester (THIQ3CA Ester) and 1,2,3,4–tetrahydroisoquinoline (THIQ). Method C: To a stirred solution of dimethoxy-1,2,3,4-tetrahydroisoquinoline (**12**, **13**, **20**, **21** or **27-29**) (0.2 gm, 0.8-1.0 mmol) and triethylamine (0.3 gm, 3.0 mmol) in anhydrous CH_2Cl_2 (10 mL) at 0 ºC was added 3,4,5-trimethoxy benzoyl chloride (0.24 gm, 1.05 mmol) or 2,5-dimethoxylphenyl acetyl chloride (0.24 gm, 1.05 mmol). The reaction mixture was allowed to warm to RT, refluxed for 4 h and then diluted with CH_2Cl_2 (15 mL). After routine extraction and concentrations steps, the crude product was purified by flash chromatography utilizing 50% (EtOAc: hexanes) to give the desired *N*-arylacyl THIQ3CA ester (**30**-**35**) or *N*-arylacyl THIQ (**36**) as colorless or yellow oil in 85-92% yield. **Method D:** To a stirred solution of either propionic or butanoic acid (0.3 gm, 1.4 mmol) in anhydrous CH_2Cl_2 (5 mL) was added 1-ethyl-3-(3-dimethylaminopropyl)carbodiimide (EDCI, 0.3 gm, 1.55 mmol) and DMAP (0.17 gm, 1.4 mmol) at RT under nitrogen atmosphere. Dimethoxy-1,2,3,4-tetrahydroisoquinoline (**12**, **21** or **27**) (0.4 gm, 1.5-1.6 mmol) in anhydrous CH_2Cl_2 (5 mL) was then added drop-wise. After stirring overnight, the reaction mixture was partitioned between 2 N HCl solution (20 mL) and CH_2Cl_2 (30 mL), and the organic layer washed with aqueous solution and concentrated to give a crude product. The crude product was purified using 50% (EtOAC: hexanes) as the mobile phase in flash chromatography to give the desired product (**38**-**42**) as colorless or yellow oil in 70–87 % yield.

Ethyl 5,6-dimethoxy-2-(3,4,5-trimethoxybenzoyl)-1,2,3,4-tetrahydroisoquinoline-3-carboxylate (30). ^{1}H NMR ($CDCl_3$, 400 MHz): δ = 6.85-6.68 (m, 2 H, Ar), 6.64-6.60 (m, 2 H, Ar), 5.34-5.32 & 4.78-4.76 (m, 1 H, CH), 5.08-5.04 & 4.50-4.41 (m, 2 H, CH_2), 4.13-3.98 (m, 2 H, CH_2), 3.80-3.74 (m, 15 H, 5 × CH_3), 3.52-3.48 & 3.37-3.33 (d & dd, ^1J = 16.3 Hz & ^1J = 3.6

Hz, ^{2}J = 16.3 Hz, 1 H, CH), 3.16-3.10 & 2.82-2.77 (dd & dd, ^{1}J = 5.9 Hz, ^{2}J = 16.2 Hz & ^{1}J = 4.8 Hz, ^{2}J = 16.6 Hz, 1 H, CH), 1.18 & 1.07 (t & t, ^{1}J = 6.7 Hz & ^{1}J = 8.8 Hz, 3 H, CH_3). ^{13}C NMR ($CDCl_3$, 100 MHz): δ = 171.5, 170.9, 170.5, 153.5, 153.4, 151.5, 151.0, 146.4, 139.4, 131.1, 126.8, 126.0, 125.7, 125.0, 122.0, 121.1, 111.6, 111.0, 104.4, 103.8, 61.6, 61.4, 60.9, 60.6, 60.4, 56.6, 56.3, 55.9, 52.0, 47.4, 42.9, 25.9, 24.7, 14.1. MS (ESI) calculated for $C_{24}H_{29}NO_8$, $[M+H]^+$, *m/z* 460.20, found for $[M+H]^+$, *m/z* 460.40.

Methyl-2-(2-(2,5-dimethoxy phenyl) acetyl)- 5,6-dimethoxy- 1,2,3,4-tetrahydro-isoquinoline-3-carboxylate (31). ^{1}H NMR ($CDCl_3$, 400 MHz): δ = 6.77-6.62 (m, 5 H, Ar), 5.38-5.35 & 4.96-4.94 (dd & dd, ^{1}J = 4.0 Hz, ^{2}J = 6.2 Hz & ^{1}J = 2.5 Hz, ^{2}J = 5.9 Hz, 1 H, CH), 4.85-4.56 (dd, ^{1}J = 17.0 Hz, ^{2}J = 101.0 Hz, 1 H, CH), 4.49-4.34 (dd, ^{1}J = 15.2 Hz, ^{2}J = 43.2 Hz, 1 H, CH), 3.75-3.63 (m, 14 H, CH_2, 4 × CH_3), 3.47 (d, ^{1}J = 52.2 Hz, 3 H, CH_3), 3.48-3.44 & 3.39-3.34 (dd & dd, ^{1}J = 2.5 Hz, ^{2}J = 16.2 Hz & ^{1}J = 4.0 Hz, ^{2}J = 16.3 Hz, 1 H, CH), 2.92-2.86 & 2.67-2.62 (dd & dd, ^{1}J = 6.3 Hz, ^{2}J = 16.3 Hz & ^{1}J = 5.8 Hz, ^{2}J = 16.2 Hz, 1 H, CH). ^{13}C NMR ($CDCl_3$, 100 MHz): δ = 171.4, 171.3, 171.0, 153.7, 151.4, 151.1, 150.9, 150.5, 146.3, 146.0, 126.7, 125.6, 124.2, 123.8, 122.0, 121.4, 115.8, 113.2, 113.0, 111.5, 111.4, 111.0, 60.5, 60.4, 56.0, 55.8, 55.7, 54.5, 52.3, 52.2, 51.5, 45.3, 43.0, 35.2, 35.0, 25.9, 24.9. MS (ESI) calculated for $C_{23}H_{27}NO_7$, $[M+H]^+$, *m/z* 430.19, found for $[M+H]^+$, *m/z* 430.36.

Methyl-2-(2-(2,5-dimethoxy phenyl) acetyl)- 5,8-dimethoxy- 1,2,3,4-tetrahydro-isoquinoline-3-carboxylate (32). ^{1}H NMR ($CDCl_3$, 400 MHz): δ = 6.82-6.79 (dd, ^{1}J = 2.9 Hz, ^{2}J = 12.0 Hz, 1 H, Ar), 6.72 (d, ^{1}J = 8.8 Hz, 1 H, Ar), 6.69-6.66 (dd, ^{1}J = 2.8 Hz, ^{2}J = 8.8 Hz, 1 H, Ar), 6.60-6.54 (m, 2 H, Ar), 5.64-5.62 & 4.96-4.94 (dd & dd, ^{1}J = 2.4 Hz, ^{2}J = 6.8 Hz & ^{1}J = 1.6 Hz, ^{2}J = 6.4 Hz, 1 H, CH), 5.02-4.68 (dd, ^{1}J = 18.8 Hz, ^{2}J = 120.8 Hz, 1 H, CH), 4.41-4.14 (dd, ^{1}J = 17.1 Hz, ^{2}J = 88.1 Hz, 1 H, CH), 3.76 (d, ^{1}J = 23.8 Hz, 2 H, CH_2), 3.71 (s, 3 H, CH_3), 3.70

(s, 3 H, CH_3), 3.67 (s, 3 H, CH_3), 3.65 (s, 3 H, CH_3), 3.48 (d, ^1J = 46.7 Hz, 3 H, CH_3), 3.42-3.36 (m, 1 H, CH), 2.78-2.72 & 2.55-2.49 (dd & dd, ^1J = 6.8 Hz, ^2J = 17.0 Hz & ^1J = 6.5 Hz, ^2J = 16.9 Hz, 1 H, CH). ^{13}C NMR (100 MHz, $CDCl_3$): δ = 171.7, 171.7, 171.5, 171.0, 153.8, 153.6, 151.3, 150.9, 150.6, 150.4, 150.1, 149.6, 124.4, 123.7, 122.3, 121.9, 121.1, 116.0, 115.6, 113.5, 113.0, 111.6, 111.4, 108.1, 107.7, 107.5, 107.4, 56.1, 56.0, 55.8 (× 2), 55.7 (× 3), 55.4, 54.0, 52.4, 52.2, 49.9, 41.2, 39.2, 35.1, 34.9, 25.2, 24.3. MS (ESI) calculated for $C_{23}H_{27}NO_7$, $[M+H]^+$, *m/z* 430.19, found for $[M+Na]^+$, *m/z* 452.30.

Ethyl- 2-(2-(2,5-dimethoxy phenyl) acetyl)- 5,8-dimethoxy- 1,2,3,4-tetrahydro-isoquinoline-3-carboxylate (33). ^{1}H NMR ($CDCl_3$, 400 MHz): δ = 6.84-6.80 (dd, ^1J = 2.8 Hz, ^2J = 14.0 Hz, 1 H, Ar), 6.74-6.72 & 6.60-6.54 (m, 3 H, Ar), 6.69-6.66 (dd, ^1J = 2.9 Hz, ^2J = 8.9 Hz, 1 H, Ar), 5.61-5.59 & 4.94-4.93 (dd & dd, ^1J = 2.1 Hz, ^2J = 6.6 Hz & ^1J = 1.5 Hz, ^2J = 6.4 Hz, 1 H, CH), 5.00-4.68 (dd, ^1J = 18.7 Hz, ^2J = 110.4 Hz, 1 H, CH), 4.44-4.19 (dd, ^1J = 17.1 Hz, ^2J = 81.3 Hz, 1 H, CH), 4.06-3.85 (m, 2 H, CH_2), 3.80-3.58 (m, 12 H, 3 × CH_3), 3.57-3.39 (m, 1 H, CH), 2.77-2.71 & 2.55-2.49 (dd & dd, ^1J = 6.7 Hz, ^2J = 17.0 Hz & ^1J = 6.5 Hz, ^2J = 17.2 Hz, 1 H, CH), 1.06 & 0.98 (t & t, ^1J = 7.1 Hz & ^1J = 7.1 Hz, 3 H, CH_3). ^{13}C NMR ($CDCl_3$, 100 MHz): δ = 171.7, 170.9, 153.8, 153.6, 151.3, 151.0, 150.6, 150.4, 150.2, 149.9, 124.4, 123.7, 123.5, 122.4, 122.0, 121.3,117.2, 116.0, 115.6, 113.5, 113.0, 111.7, 111.4, 108.2, 107.8, 107.6, 61.4, 61.1, 56.2, 56.1, 56.0, 55.9, 55.8, 55.7, 55.7, 55.4, 54.2, 50.1,41.3, 39.3, 35.9, 35.0, 25.3, 24.3, 14.0, 13.9. MS (ESI) calculated for $C_{24}H_{29}NO_7$, $[M+H]^+$, *m/z* 444.20, found for $[M+H]^+$, *m/z* 444.34.

Ethyl 6,7-dimethoxy-2-(3,4,5-trimethoxybenzoyl)-1,2,3,4-tetrahydroisoquinoline-3-carboxylate (34). ^{1}H NMR ($CDCl_3$, 400 MHz): δ = 6.85-6.60 (m, 4 H, Ar), 5.35-5.32 & 4.78-4.75 (m, 1 H, CH), 5.10-5.04 & 4.50-4.40 (m, 2 H, CH_2), 4.13-3.99 (m, 2 H, CH_2), 3.81-3.73 (m,

15 H, 5 × CH_3), 3.52-3.48 & 3.37-3.33 (d & dd, ^1J = 16.3 Hz & ^1J = 3.6 Hz, ^2J = 16.3 Hz, 1 H, CH), 3.16-3.10 & 2.82-2.77 (dd & dd, ^1J = 5.9 Hz, ^2J = 16.2 Hz & ^1J = 4.8 Hz, ^2J = 16.7 Hz, 1 H, CH), 1.17 & 1.06 (t & t, ^1J = 6.7 Hz & ^1J = 8.8 Hz, 3 H, CH_3). ^{13}C NMR ($CDCl_3$, 400 MHz): δ = 171.5, 170.9, 170.5, 153.5, 153.4, 151.5, 151.0, 146.4, 139.4, 131.1, 126.8, 126.0, 125.7, 125.0, 122.0, 121.1, 111.6, 111.0, 104.4, 103.8, 61.6, 61.4, 60.9, 60.6, 60.4, 56.6, 56.3, 55.9, 52.0, 47.4, 42.9, 25.9, 24.7, 14.1. MS (ESI) calculated for $C_{24}H_{29}NO_8$, $[M+H]^+$, *m/z* 460.20, found for $[M+H]^+$, *m/z* 460.34.

Methyl- 2-(2-(2,5-dimethoxy phenyl) acetyl)- 6,7-dimethoxy- 1,2,3,4-tetrahydro-isoquinoline-3-carboxylate (35). ^{1}H NMR ($CDCl_3$, 400 MHz): δ = 6.80 (d, ^1J = 2.6 Hz, 1 H, Ar), 6.74 (d, ^1J = 8.8 Hz, 1 H, Ar), 6.72-6.67 (m, 1 H, Ar), 6.54 (d, ^1J = 14.1 Hz, 1 H, Ar), 6.45 (d, ^1J = 34.9 Hz, 1 H, Ar), 5.51-5.49 & 4.94-4.92 (dd & dd, ^1J = 3.3 Hz, ^2J = 6.0 Hz & ^1J = 2.3 Hz, ^2J = 5.8 Hz, 1 H, CH), 4.91-4.60 (dd, ^1J = 17.2 Hz, ^2J = 108.8 Hz, 1 H, CH), 4.52-4.30 (dd, ^1J = 15.4 Hz, ^2J = 71.5 Hz, 1 H, CH), 3.78-3.66 (m, 14 H, CH_2, 4 × CH_3), 3.50 (d, ^1J = 51.5 Hz, 3 H, CH_3), 3.14-3.06 (dt, ^1J = 3.4 Hz, ^2J = 15.8 Hz, 1 H, CH), 3.02-2.97 & 2.89-2.85 (dd & dd, ^1J = 6.0 Hz, ^2J = 18.8 Hz & ^1J = 5.8 Hz, ^2J = 15.8 Hz, 1 H, CH). ^{13}C NMR ($CDCl_3$, 100 MHz): δ =171.5, 171.4 (×2), 171.2, 153.8, 151.2, 150.6, 148.2, 148.1, 148.0, 147.7, 124.3, 124.2, 123.9, 123.8, 122.8, 115.9, 115.8, 113.3, 112.9, 111.6, 111.4, 111.2, 111.0, 109.3, 109.0, 56.1 (×2), 56.0 (×2), 55.9 (×2), 55.7, 55.0, 52.4, 52.3, 51.3, 45.5, 43.3, 35.3, 35.0, 31.2, 30.3. MS (ESI) calculated for $C_{23}H_{27}NO_7$, $[M+H]^+$, *m/z* 430.19, found for $[M+Na]^+$, *m/z* 452.36.

1-(6,7-dimethoxy-3,4-dihydroisoquinolin-2(1H)-yl)-2-(2,5-dimethoxyphenyl) ethanone (36). ^{1}H NMR ($CDCl_3$, 400 MHz): δ = 6.78-6.64 (m, 5H, Ar), 4.54 (d, ^1J= 48.8 Hz, 2H, CH_2), 3.76 (s, 3H, CH_3), 3.71(s, 3H, CH_3), 3.69 (s, 3H, CH_3), 3.67(s, 3H, CH_3), 3.63-3.60 (m, 3H, CH, CH_2), 3.58-3.54 (m, 1H, CH), 2.78 (t, ^1J = 6.0 Hz, 1 H, CH), 2.64 (t, ^1J = 5.9 Hz, 1

H, CH). ^{13}C NMR ($CDCl_3$, 100 MHz): δ = 170.4, 170.2, 153.7, 151.2, 151.0, 150.9, 150.8, 146.6, 146.2, 129.4, 128.5, 126.7, 126.2, 124.7, 122.0, 121.2, 117.1, 115.8, 112.9 (×2), 111.6 (×2), 111.5, 110.9, 110.7, 60.3, 56.1 (×2), 56.0, 55.9, 55.7, 55.6, 47.2, 43.9, 43.2, 39.7, 35.9, 35.1, 34.8, 23.6, 22.9. MS (ESI) calculated for $C_{21}H_{25}NO_5$, $[M+H]^+$, *m/z* 372.18, found for $[M+Na]^+$, *m/z* 394.33.

Ethyl- 2-(2-(2,5-dimethoxy phenyl) butanoyl)- 5,6-dimethoxy- 1,2,3,4-tetrahydro-isoquinoline-3-carboxylate (38). ^{1}H NMR ($CDCl_3$, 400 MHz): δ = 6.79-5.59 (m, 5 H, Ar), 5.40-5.37 & 4.67-4.65 (dd & dd, ^1J = 3.6 Hz, ^2J = 6.2 Hz & ^1J = 2.8 Hz, ^2J = 5.8 Hz, 1 H, CH), 4.79-4.74 & 4.52-4.48 (dd, ^1J = 16.8 Hz, ^2J = 107.7 Hz, 1 H, CH),4.47-4.35 (dd, ^1J = 15.1 Hz, ^2J = 29.7 Hz, 1 H, CH), 4.05-3.90 (m, 2 H, CH_2), 3.80-3.60 (m, 12 H, 4 × CH_3), 3.54-3.50 & 3.42-3.37 (dd & dd, ^1J = 2.6 Hz, ^2J = 16.1 Hz & ^1J = 3.6 Hz, ^2J = 16.3 Hz, 1 H, CH), 2.86-2.80 (m, 1 H, CH), 2.63-2.55 (m, 2 H, CH_2), 2.43-2.26 (m, 2 H, CH_2), 1.98-1.81 (m, 2 H, CH_2), 1.08 & 1.00 (t & t, ^1J = 7.1 Hz, ^1J = 7.1 Hz, 3 H, CH_3). ^{13}C NMR ($CDCl_3$, 100 MHz): δ = 177.9, 173.1, 171.1, 170.6, 153.5, 153.3, 151.9, 151.6, 151.4, 151.0, 146.4, 146.1, 131.3, 131.0, 129.8, 126.8, 126.3, 126.0, 125.5, 122.0, 121.4, 116.4, 116.3, 111.5, 111.2, 111.0, 61.6, 61.1, 60.6, 60.5, 55.9, 55.8, 55.7 (×2), 54.6, 51.1, 45.0, 42.9, 33.4, 33.1, 29.8, 29.8, 29.5, 26.1, 25.0, 24.9, 24.8, 14.1, 14.0. MS (ESI) calculated for $C_{26}H_{33}NO_7$, $[M+H]^+$, *m/z* 472.23, found for $[M+H]^+$, *m/z* 472.40.

Methyl 2-(3-(2,5-dimethoxyphenyl)propanoyl)-5,8-dimethoxy-1,2,3,4-tetrahydro-isoquinoline-3-carboxylate (39). ^{1}H NMR ($CDCl_3$, 400 MHz): δ = 6.73-6.67 (m, 2 H, Ar), 6.63-6.54 (m, 3 H, Ar), 5.65-5.63 & 4.96-4.94 (dd & dd, ^1J = 2.2 Hz, ^2J = 6.8 Hz & ^1J = 1.6 Hz, ^2J = 6.4 Hz, 1 H, CH), 5.03-4.98 & 4.61-4.56 (dd, ^1J = 18.7 Hz, ^2J = 168.5 Hz, 1 H, CH), 4.43-4.14 (dd, ^1J = 17.1 Hz, ^2J = 98.6 Hz, 1 H, CH), 3.73 (s, 3 H, CH_3), 3.70 (s, 3 H, CH_3), 3.69 (s, 3 H, CH_3), 3.67 (s, 3 H, CH_3), 3.55 (s, 3 H, CH_3), 3.52-3.47 & 3.43-3.38 (dd & dd, ^1J = 1.4 Hz, ^2J =

17.7 Hz & ^{1}J = 2.0 Hz, ^{2}J = 17.1 Hz, 1 H, CH), 2.94-2.85 (m, 2 H, CH_2), 2.78-2.53 (m, 3 H, CH, CH_2). ^{13}C NMR ($CDCl_3$, 100 MHz): δ = 173.2, 172.9, 171.6, 171.1, 153.6, 153.5, 151.8, 151.6, 150.9, 150.6, 150.1, 149.6, 130.7, 130.3, 122.4, 122.3, 121.7, 121.1, 116.5, 116.4, 111.8, 111.5, 111.2, 111.1, 108.1, 107.8, 107.6, 107.3, 55.8, 55.8, 55.7 (×2), 55.4, 55.3, 54.0, 52.6, 52.3, 49.6, 41.0, 38.9, 34.2, 34.1, 27.2, 26.7, 25.3, 24.3. MS (ESI) calculated for $C_{24}H_{29}NO_7$, $[M+H]^+$, *m/z* 444.20, found for $[M+Na]^+$, *m/z* 465.97.

Methyl 2-(4-(2,5-dimethoxyphenyl)butanoyl)-5,8-dimethoxy-1,2,3,4-tetrahydro-isoquinoline-3-carboxylate (40). ^{1}H NMR ($CDCl_3$, 400 MHz): δ = 6.70-6.65 (m, 2 H, Ar), 6.63-6.55 (m, 3 H, Ar), 5.63-5.60 & 4.72 (dd & d, ^{1}J = 2.3 Hz, ^{2}J = 6.8 Hz & ^{1}J = 4.9 Hz, 1 H, CH), 5.02-4.97 & 4.56-4.53 (dd, ^{1}J = 18.7 Hz, ^{1}J = 181.9 Hz, 1 H, CH), 4.44-4.09 (dd, ^{1}J = 17.0 Hz, ^{2}J = 117.8 Hz, 1 H, CH), 3.71 (s, 3 H, CH_3), 3.70 (s, 3 H, CH_3), 3.69 (s, 3 H, CH_3), 3.67 (s, 3 H, CH_3), 3.55 (s, 3 H, CH_3), 3.40-3.37 (dd, ^{1}J = 2.2 Hz, ^{2}J = 17.1 Hz, 1 H, CH), 2.75-2.70 (dd, ^{1}J = 6.8 Hz, ^{2}J = 17.0 Hz,1 H, CH), 2.66-2.53 (m, 2 H, CH_2), 2.51-2.31 (m, 2 H, CH_2), 1.97-1.89 (m, 2 H, CH_2). ^{13}C NMR ($CDCl_3$, 100 MHz): δ = 173.4, 173.0, 171.6, 171.0, 153.5, 151.9 (×2), 150.6, 150.1, 149.6, 131.5, 131.2, 122.5, 122.4, 121.8, 121.1, 116.4, 116.3, 111.5, 111.3, 111.2, 108.2, 107.8, 107.6, 107.4, 55.8, 55.7, 55.4, 53.9, 52.6, 52.3, 49.6, 40.9, 38.8, 33.3, 33.0, 29.9, 29.8, 25.3, 25.1, 24.9, 24.3. MS (ESI) calculated for $C_{25}H_{31}NO_7$, $[M+H]^+$, *m/z* 458.22, found for $[M+Na]^+$, *m/z* 480.40.

Methyl 2-(3-(2,5-dimethoxyphenyl)propanoyl)-6,7-dimethoxy-1,2,3,4-tetrahydro-isoquinoline-3-carboxylate (41). ^{1}H NMR ($CDCl_3$, 400 MHz): δ = 6.72-6.69 (m, 2 H, Ar), 6.67-6.63 (m, 1 H, Ar), 6.54 (d, ^{1}J = 9.4 Hz, 1 H, Ar), 6.45 (s, 1 H, Ar), 5.52-5.50 & 4.87-4.85 (dd & dd, ^{1}J = 3.0 Hz, ^{2}J = 6.1 Hz & ^{1}J = 2.4 Hz, ^{2}J = 5.8 Hz, 1 H, CH), 4.88-4.54 (dd, ^{1}J = 17.0 Hz, ^{2}J = 120.7 Hz, 1 H, CH), 4.53-4.30 (dd, ^{1}J = 17.2 Hz, ^{2}J = 74.0 Hz, 1 H, CH), 3.78-3.67 (m, 12 H, 4

× CH_3), 3.55 (d, ^1J = 8.5 Hz, 3 H,CH_3), 3.78-3.09 (m, 1 H, CH), 2.99-2.84 (m, 3 H, CH, CH_2), 2.70-2.67 (m, 2 H, CH_2).^{13}C NMR ($CDCl_3$,100 MHz): δ = 172.8, 172.7, 171.6, 171.2, 153.6 (×2), 151.8, 151.6, 148.3, 148.1 (×2), 147.8, 130.7, 130.3, 124.5, 124.1, 123.7, 122.9, 116.5 (×2), 111.7, 111.5, 111.3 (×2), 111.2, 111.1, 111.0, 109.4, 108.9, 65.8, 55.9 (×2), 55.8, 55.7, 54.9, 52.6, 52.3, 51.0, 46.9, 45.1, 43.1, 34.2, 30.3, 29.4, 27.1, 26.7, 26.5. MS (ESI) calculated for $C_{24}H_{29}NO_7$, $[M+H]^+$, *m/z* 444.20, found for $[M+Na]^+$, *m/z* 466.04.

Methyl 2-(4-(2,5-dimethoxyphenyl)butanoyl)-6,7-dimethoxy-1,2,3,4-tetrahydro-isoquinoline-3-carboxylate (42). ^{1}H NMR ($CDCl_3$, 400 MHz): δ = 6.71-6.62 (m, 3 H, Ar), 6.55 (d, ^1J = 6.16 Hz, 1 H, Ar), 6.46 (s, 1 H, Ar), 5.52-5.50 & 4.69-4.67 (dd & dd, ^1J = 2.9 Hz, ^2J =5.9 Hz & ^1J = 2.4 Hz, ^2J = 5.6 Hz, 1 H, CH), 4.86-4.82 & 4.48-4.48 (dd, ^1J = 17.0 Hz, ^2J = 136.0 Hz, 1 H, CH), 4.48-4.25 (dd, ^1J = 16.0 Hz, ^2J = 75.8 Hz, 1 H, CH), 3.78 (s, 3 H, CH_3), 3.77 (s, 3 H, H_3), 3.69 (s, 3 H, CH_3), 3.68 (s, 3 H, CH_3), 3.54 (d, ^1J = 3.2 Hz, 3 H, CH_3), 3.17-3.09 (m, 1 H, CH), 3.04-2.93 (m, 1 H, CH), 2.64-2.58 (m, 2 H, CH_2), 2.44-2.40 (m, 2 H, CH_2), 1.97-1.89 (m, 2 H, CH_2). ^{13}C NMR ($CDCl_3$, 100 MHz): δ =173.1, 173.0, 171.6, 171.1, 153.5, 151.9, 151.8, 148.3, 148.1, 147.8, 131.3, 131.2, 124.5, 124.1, 123.6, 122.9, 116.5, 116.4, 111.5, 111.3 (×2), 111.2 (×2), 111.0, 109.4, 109.0, 56.6, 56.0, 55.9 (×2), 55.7, 54.8, 52.6, 52.3, 50.9, 45.2, 43.1, 33.1, 33.0, 31.6, 31.3, 30.9, 30.3, 29.8 (×2), 28.9, 25.0, 24.8. MS (ESI) calculated for $C_{25}H_{31}NO_7$, $[M+H]^+$, *m/z* 458.22, found for $[M+Na]^+$, *m/z* 479.96.

2-(2-(2,5-Dihydroxyphenyl)acetyl)-6,7-dihydroxy-1,2,3,4-tetrahydroisoquinoline-3-carboxylic acid (37). To a stirred solution of THIQ3CA ester **35** (0.45 gm, 1.0 mmol) in anhydrous CH_2Cl_2 (5 mL), BBr_3 (1 M solution in CH_2Cl_2, 0.4 gm, 9 mmol) was added dropwise at -78 ^{0}C under nitrogen atmosphere over 10 min. After 2 h, the reaction mixture was brought to RT and allowed to equilibrate overnight. A mixture of methanol/water (1:1 v/v, 2 mL) was then

added slowly at 0 ^{0}C and vigorously stirred for 10 min to quench the reaction. The reaction mixture was then concentrated and partitioned between EtOAc (25 mL) and saturated solution of NH_4Cl (15 mL), and aqueous layer further washed with EtOAc (2 × 20 mL). The combined organic layer was concentrated *in vacuo* and the crude was purified by 0% to 25% (CH_3OH:CH_2Cl_2) as mobile phase gradient in flash chromatography to yield **37** (75 %) as yellow solid. ^{1}H NMR (acetone-d_6, 400 MHz): δ = 6.65-6.58 (dd, ^1J = 2.9 Hz, ^2J = 25.1 Hz, 1 H, Ar), 6.57-6.55 (dd, ^1J = 3.2 Hz, ^2J = 7.3 Hz, 1 H, Ar), 6.53 (d, ^1J = 14.7 Hz, 2 H, Ar), 6.47-6.44 (dd, ^1J = 2.9 Hz, ^1J = 8.6 Hz, 1 H, Ar), 5.20-5.18 & 5.15-5.13 (dd & dd, ^1J = 3.6 Hz, ^2J = 5.9 Hz & ^1J = 2.6 Hz , ^2J = 5.7 Hz, 1 H, CH), 4.79-3.43 (dd & dd, 2 H , CH_2, and d & d &d, 2 H, CH_2), 3.07-3.02 & 3.01-2.96 (dd & dd, ^1J = 2.5 Hz, ^2J = 15.5 Hz & ^1J = 3.6 Hz, ^2J = 15.6 Hz, 1H, CH), 2.88-2.84 (m, 1 H, CH). ^{13}C NMR (acetone-d_6, 100 MHz): δ = 173.3, 172.2, 151.3, 149.9, 149.5, 145.0, 144.9, 124.7, 124.6, 124.5, 124.0, 123.3, 118.5, 118.0, 117.9, 117.8, 117.7, 115.7, 115.6, 115.5, 115.2, 113.8, 113.7, 56.2, 52.6, 46.5, 43.9, 36.5, 36.1, 31.9, 30.9. MS (ESI) calculated for $C_{18}H_{17}NO_7$, $[M+H]^+$, *m/z* 360.11, found for $[M+Na]^+$, *m/z* 382.24.

Methyl 6,7-dimethoxy-2-(4-methoxybenzyl)-1,2,3,4-tetrahydroisoquinoline-3-carboxylate (43). To a stirred solution of methyl 6,7-dimethoxy-1,2,3,4-tetrahydroisoquinoline-3-carboxylate **27** (0.1 gm, 0.4 mmol) in CH_3CN (2 mL), diisopropylethylamine (DIPEA) (0.15 gm, 1.2 mmol) was slowly added. After 15 min, 4-methoxybenzyl chloride (0.078 gm, 0.5 mmol) was dissolved in CH_3CN (1 mL) and was then added slowly to the reaction mixture. The reaction mixture was heated up in the microwave (CEM Discover) for 20 min at 150 ºC. The reaction mixture was cooled to RT, diluted with EtOAc (10 mL) and organic layer worked up as usual to give a crude product, which was purified using 30 % (EtOAc: hexanes) in flash chromatography to yield **43** (yellow oil, 92%). ^{1}H NMR ($CDCl_3$, 400 MHz): δ = 7.29 (d, ^1J = 8.6

Hz, 2 H, Ar), 6.87 (d, ^{1}J = 8.6 Hz, 2 H, Ar), 6.58 (s, 1 H, Ar), 6.47 (s, 1H, Ar), 3.95 (d, ^{1}J = 15.2 Hz, 1H, CH), 3.85 (d, ^{1}J = 2.2 Hz, 2 H,CH_2), 3.84 (s, 3 H, CH_3), 3.80 (s, 3 H, CH_3), 3.79 (s, 3 H, CH_3), 3.77-3.75 (dd, ^{1}J = 4.1 Hz, ^{2}J = 6.0 Hz, 1 H, CH), 3.72 (d, ^{1}J = 15.8 Hz, 1 H, CH), 3.68 (s, 3 H, CH_3), 3.14-3.09 (dd, ^{1}J = 6.0 Hz, ^{2}J = 16.1 Hz, 1 H, CH), 3.05-3.00 (dd, ^{1}J = 3.8 Hz, ^{2}J = 16.0 Hz, 1 H, CH). ^{13}C NMR ($CDCl_3$, 100 MHz): δ = 173.2, 158.9, 147.5, 130.6, 130.1, 128.6, 126.1, 124.0, 113.8, 111.3, 109.3, 58.9, 58.4, 55.9, 55.8, 55.3, 51.4, 50.6, 30.9. MS (ESI) calculated for $C_{21}H_{25}NO_5$, $[M+H]^+$, *m/z* 372.18, found for $[M+H]^+$, *m/z* 372.32.

General Procedure for Xylene-Based Dimerization of 6,7-Dimethoxy THIQ3CA Ethyl Ester. Ethyl 6,7-dimethoxy-1,2,3,4-tetrahydroisoquinoline-3-carboxylate **28** (0.75 gm, 2.8 mmol) was dissolved in DMF:CH_3CN (1:1 v/v, 8 mL) and stirred with Cs_2CO_3 (2.2 gm, 11.2 mmol). After 15 min, *p*- or *m*- α,α'-dibromo xylene (0.37 gm, 1.4 mmol) in CH_3CN (2 mL) was slowly added to the reaction mixture and then refluxed for 12 h. The reaction mixture was cooled, partitioned between EtOAc (25 mL) and water (25 mL), and the organic layer processed in a routine manner to prepare a crude product, which was purified using 30% (EtOAc: hexanes) in flash chromatography to give the desired xylene-based dimer (**44** or **45**) as yellow oil in 62-66% yield.

Diethyl 2,2'-(1,3-phenylene bis(methylene)) bis(6,7-dimethoxy-1,2,3,4-tetrahydro-isoquinoline-3-carboxylate) (44). ^{1}H NMR ($CDCl_3$, 400 MHz): δ = 7.41 (s, 1 H, Ar), 7.30 (s, 3 H, Ar), 6.58 (s, 2 H, Ar), 6.46 (s, 2 H, Ar), 4.19-4.10 (m, 4 H, 2 × CH_2), 33.99-3.93 (m, 6 H, 2 × CH, 2 × CH_2), 3.84 (s, 6 H, 2 × CH_3), 3.79 (s, 6 H, 2 × CH_3), 3.76-3.72 (m, 4 H, 2 × CH_2), 3.14-3.09 (dd, ^{1}J = 6.0 Hz, ^{2}J = 16.1 Hz, 2 H, 2 × CH), 3.05-3.00 (dd, ^{1}J = 4.0 Hz, ^{2}J = 16.0 Hz, 2 H, 2 × CH), 1.24 (t, ^{1}J= 7.1 Hz, 6 H, 2 × CH_3). ^{13}C NMR ($CDCl_3$, 100 MHz): δ = 172.7, 147.5,

138.9, 129.4, 128.3, 127.8, 126.1, 124.1, 111.3, 109.3, 60.3, 59.2, 59.0, 55.9, 55.8, 50.7, 31.1, 14.4. MS (ESI) calculated for $C_{36}H_{44}N_2O_8$, $[M+H]^+$, *m/z* 633.32, found for $[M+H]^+$, *m/z* 633.16.

Diethyl 2,2'-(1,4-phenylene bis(methylene)) bis(6,7-dimethoxy-1,2,3,4-tetrahydro-isoquinoline-3-carboxylate (45). ^{1}H NMR ($CDCl_3$, 400 MHz): δ = 7.28 (s, 4 H, Ar), 6.52 (s, 2 H, Ar), 6.40 (s, 2 H, Ar), 4.12-4.05 (m, 4 H, 2 × CH_2), 3.85-3.93 (m, 6 H, 2 × CH, 2 × CH_2), 3.77 (s, 6 H, 2 × CH_3), 3.73 (s, 6 H, 2 × CH_3), 3.60-3.70 (m, 4 H, 2 × CH_2), 3.07-3.03 (dd, ^1J = 3.5 Hz, ^2J = 14.9 Hz, 2 H, 2 × CH), 3.00-2.95 (dd, ^1J = 4.1 Hz, ^2J = 16.0 Hz, 2 H, 2 × CH), 1.18 (t, ^1J = 7.1 Hz, 6 H, 2 × CH_3). ^{13}C NMR ($CDCl_3$, 100 MHz): δ = 172.7, 147.5, 138.8, 129.0, 126.0, 124.1, 111.3, 109.2, 60.4, 59.2, 58.7, 55.9, 55.8, 50.7, 30.9, 14.4. MS (ESI) calculated for $C_{36}H_{44}N_2O_8$, $[M+H]^+$, *m/z* 633.32, found for $[M+H]^+$, *m/z* 633.23.

CHAPTER 4: DESIGNING NONSACCHARIDE, ALLOSTERIC ACTIVATORS OF ANTITHROMBIN FOR ACCELERATED INHIBITION OF FACTOR Xa

4.1. Fundamental Hypothesis—Clinically used heparins are highly complex molecules known to be associated with multiple complications.[209,210] Structurally, heparin–based anticoagulant therapy has remained essentially unchanged since its introduction in the 1930s. A synthetic version of DEFGH, called fondaparinux, is arguably the best anticoagulant with regard to such complications[211,212] but its synthesis is complex and expensive, while it suffers, like heparins, from bleeding episodes.[211-216] Accordingly, numerous attempts have been made to discover molecules that activate AT to overcome the drawbacks of heparins. A fundamental tenet of these efforts has been the assumed requirement of a saccharide scaffold.[97-105]

To address the many drawbacks of the heparin–based AT activators, Desai hypothesized that replacing the saccharide skeleton with an aromatic scaffold to have eventually non–saccharide, aromatic, allosteric AT activators acting as heparin functional mimetics for the accelerated inhibition of FXa should be possible. Such non–saccharide mimetics of heparin are likely to offer significant advantages, such as superior non-ionic binding energy in AT recognition,[107] greater hydrophobicity for possible oral bioavailability,[111,217,218] better synthetic accessibility, and narrower specificity of function in comparison to heparin's multitude of activities.

Two independent approaches had been used earlier by Desai and co–workers for designing AT activators that are radically different from the DEFGH–based saccharide molecules.[106,110] These approaches led to the identification of IAS5, a molecule that displayed AT activation of nearly 30-fold.[110]

4.2. Updated Hypothesis: Design Goals and Design Elements for Non-Heparin Antithrombin Activators—

The success with IAS5 indicated a strong possibility of uncovering potent, ease-to-synthesize, small, aromatic AT activators through a rational approach. Figure 20 describes two possible mechanisms of AT activation. The induced fit mechanism is followed by nearly all heparins (including DEFGH and DEF),[219] whereas the pre-equilibrium mechanism has been documented for oligosaccharides that lack the critical PBS recognition element (EFGH″ and 3-O-Desulfonated DEFGH).[83,92] The induced fit mechanism requires that the potential ligand recognize both the native (AT) as well as the activated state (AT*), while the pre-equilibrium mechanism primarily involves ligand recognition of AT*.

Despite considerable effort, the exact mechanism of how the activating conformational change is brought about through the induced fit process remains unclear. In addition, no principles have been elucidated for designing highly sulfated nonsaccharide molecules that allosterically activate a protein such as AT. The major difficulty in designing such allosteric activators is that the binding site is shallow and highly surface exposed, which tends to not subscribe to a high affinity interaction. In addition, the two–step, induced fit allosteric AT activation requires that the binding energy is transmitted to the main body of the protein to induce activation.

Thus design-wise, activators that utilize the pre-equilibrium pathway are expected to be easier to design as this pathway involves preferential recognition of only one AT form. Yet, an apparent limitation of the pre-equilibrium pathway could be inefficient activation because of the limiting rate of intrinsic conversion of AT to the AT* form. This implies that a key goal of the design strategy should be AT activation, which is reflected by acceleration in the AT inhibition of FXa brought about by the designed activator. A secondary goal of the design strategy could be

the affinity of the activator for AT. However, considering that the HBS of AT is a shallow, surface exposed region consisting primarily of amino acids involved in Coulomb-type interactions (Arg and Lys), high affinity as a 'driver' of design could take lesser importance at this early stage of non-heparin, organic activator design.

IAS5 was found to bind in the EHBS and induce accelerated inhibition of FXa.[110] This suggested that the non-saccharide AT activators most probably utilized the pre-equilibrium mechanism. The fact that the pharmacophore-based design, IAS_5, could achieve about 30-fold acceleration in the inhibition of FXa suggested a strong potential of the pre-equilibrium mechanism. Thus, we have hypothesized that extending the linker between the bicyclic and monocyclic parts of IAS5 followed by number and position optimization for the sulfate groups should result in improved profile for IAS5 and should help in establishing the pre-equilibrium pathway as reliable mechanism to design clinically relevant non-saccharide AT allosteric activators.

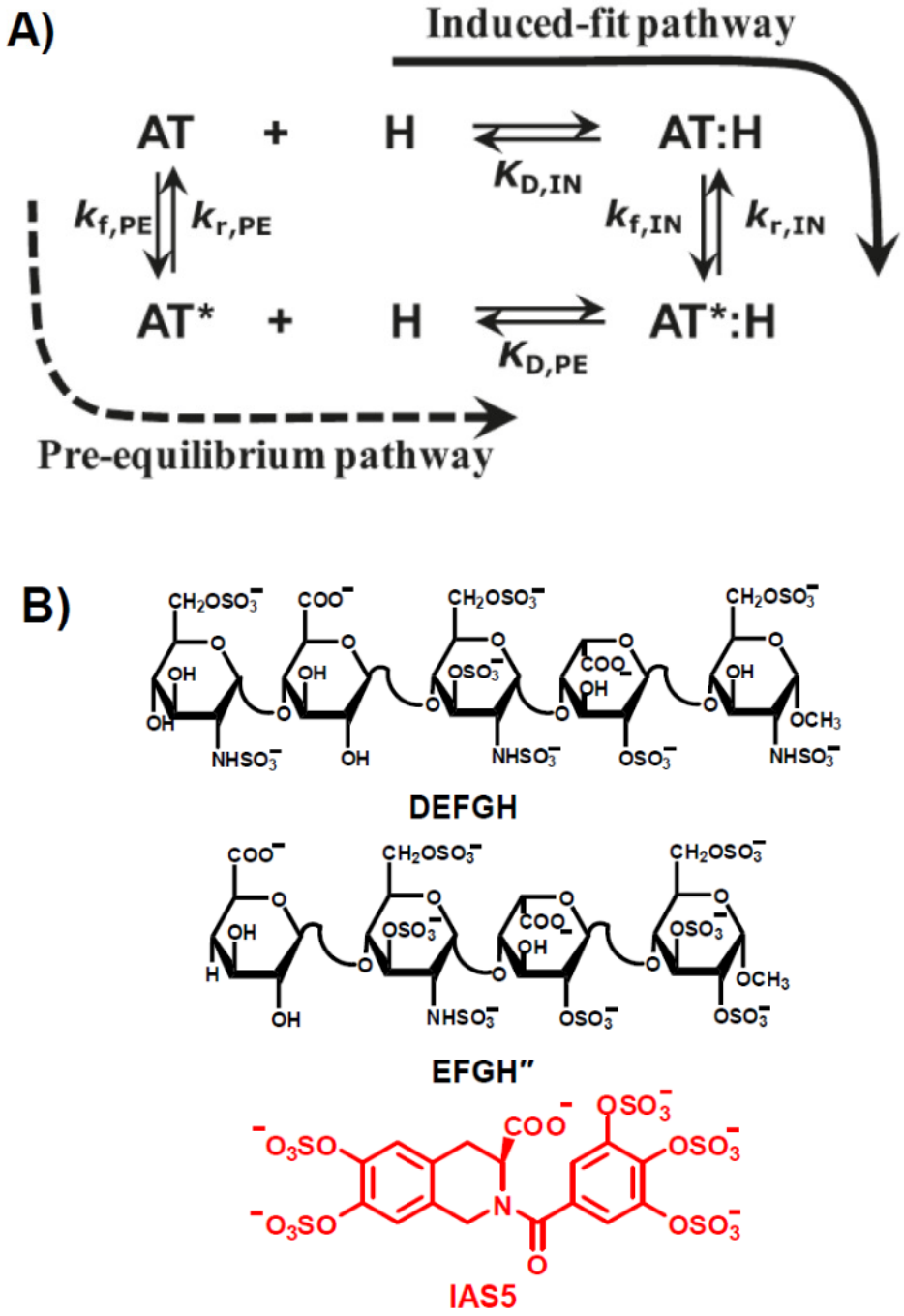

Figure 20. A) Multistep mechanism of heparin activation of antithrombin . AT = native antithrombin; AT* = conformationally altered antithrombin; H = heparin; $K_{D,IN}$ and $K_{D,PE}$ refer to equilibrium dissociation constants of the first and last step of the induced-fit (IF) and pre-equilibrium (PE) pathways, respectively. k_f and k_r refer to forward and reverse rate constants in the two pathways. See text for additional details. B) Structures of DEFGH (heparin pentasaccharide activator), which is known to activate AT through the induced-fit mechanism, EFGH″ (tetrasacharide activator), and IAS5 (non-saccharide aromatic activator), which are thought to activate AT through the pre-equilibrium mechanism. Adapted from reference 231.

4.3. Results and Discussion—

4.3.1. Design of Pre–Equilibrium Pathway Targeting Potential Antithrombin Activators—

To improve upon the AT activation potential achieved with IAS_5 by targeting the pre-equilibrium pathway of AT-mediated inhibition of FXa, a focused library of IAS_5-related THIQ derivatives was generated *in silico*. Combinations of five major structural variations were considered in developing the library. These included the positions of two sulfate groups on the bicyclic THIQ moiety (3 possibilities: 6,7-; 5,8-; and 5,6-); the presence or absence of carboxylic group at 3-position (2 possibilities: $–COO^-$ and –H); the stereochemistry of carboxylate group at the 3-position (2 possibilities: *R* and *S*); the amide linker extension (2 possibilities:1-atom (-CO-) or 2-atom ($-CH_2-CO-$)); and finally the positions of either two or three sulfate groups on the monocyclic part (5 possibilities: 2,3-; 2,4-; 2,5-; 2,3,4-; and 3,4,5- sulfates).

The ninety designed, potential sulfated activators were docked onto the EHBS of AT* (activated AT) using GOLD and scored using GOLD as well as HINT, as described earlier in literature.[106,107,220-222] This is the first study in which two scoring functions are simultaneously utilized to design nonsaccharide AT allosterc activators. GOLD better quantifies the polar interactions particularly the electrostatic as well as the hydrogen bonds of the activators's sulfate/carboxylate interaction with AT's lysine/arginine, thus GOLD allegedly better predicts the enthalpic component of the binding energy. In contrast, HINT better quantifies the entropic component of the binding energy which is expected to play a significant role in the highly charged and hydrated interacting groups under physiologic conditions.

In silico docking and scoring of highly sulfated molecules, e.g., those containing more than a couple of sulfate groups, onto proteins is still a growing area of algorithm design. There is no single algorithm that predicts binding site and geometry with high fidelity. Previously, the

Desai group designed a combinatorial virtual library screening strategy to improve the predictability of complex geometry, however this strategy is finely tuned for heparin-like saccharide sequences, which display reduced flexibility around typical inter-glycosidic torsions.[220,223] Highly sulfated small organic molecules that exhibit significant backbone flexibility pose special challenges because of the phenomenally large conformational search space. The molecules tend to adopt multiple binding modes, which makes ranking less than straightforward. Hence, scoring with two functions, GOLD and HINT, was utilized.

The GOLD and HINT scores of our reference activator IAS_5 bound in the EHBS of AT* were 83.3 and 2200, respectively. The activator was found to interact with R129, R132, and K136 of EHBS, which corroborates competitive studies performed earlier.[224] Analysis of the library docking results highlighted two molecules as potentially interesting, 67A225 and 58A225 (Figures 21; chemical structures are in scheme 5. The *S* isomers of 67A225 and 58A225 demonstrated GOLD scores of 83.9 and 93.0, and HINT scores of 2711 and 2772, respectively, while the *R* enantiomers had scores of 98.9 and 94.3 (GOLD) and 2200 and 2562 (HINT), respectively. This suggested that these designs may be potentially better at recognizing AT. The combinatorial library screen also indicated that 2,5–disulfated unicyclic ring was favored over four other possibilities and that both *R* and *S* enantiomers were likely to activate AT. Specifically, (*R*)–58A225 docking pose is reaching out to K125, which is a critical amino acid residue in the PBS.

Molecules 67A225 and 58A225 were interesting from another angle too. These possess only four sulfate groups as opposed to five present in IAS_5. This aided our ultimate goal of designing activators with the minimum number of sulfate groups (probably three) on a small scaffold so as to eliminate non-specific interactions arising from redundant negative charges.

Reduced polyanionic character coupled with greater hydrophobicity of the scaffold may enhance oral bioavailability, a feature that non-saccharide heparin mimetics are likely to possess. Thus, we decided to develop a small group of molecules around the 67A225 and 58A225 structures to identify optimal sulfate positions on the THIQ moiety and study the effect of 3-carboxylic acid and unicyclic – bicyclic linker length on AT activation.

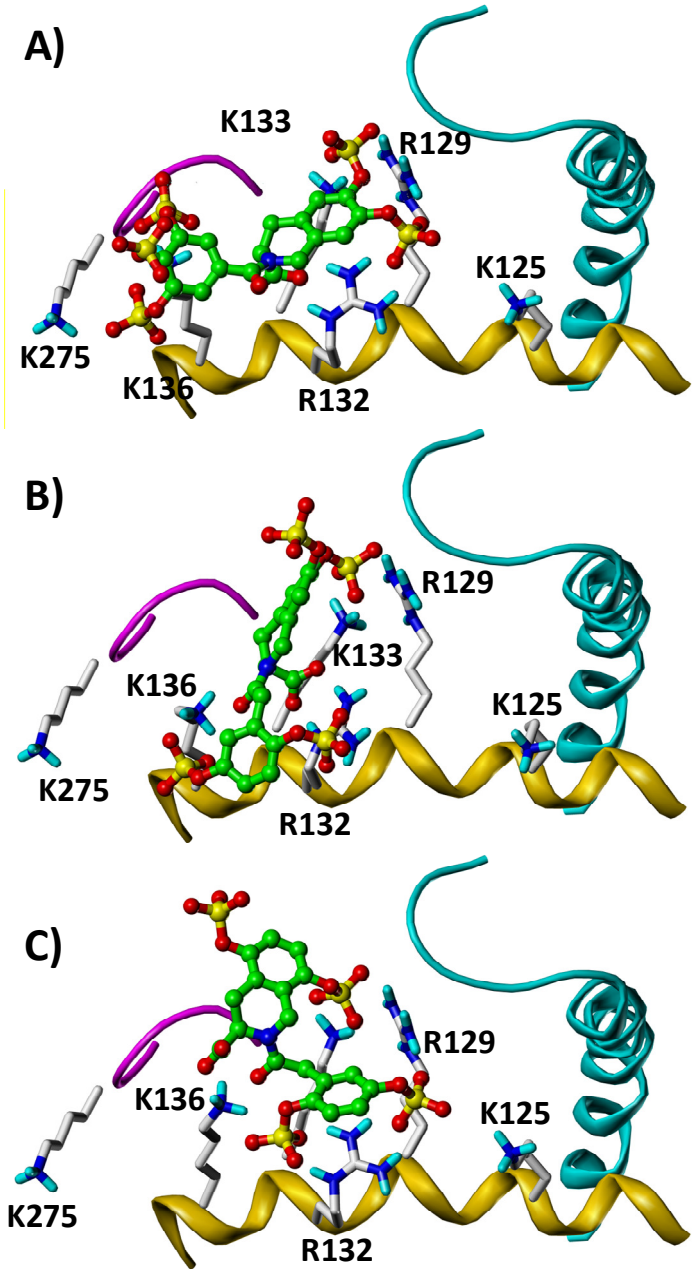

Figure 21. Computational screening of a library of ninety potential sulfated activators docked onto the extended heparin binding site of the activated form of AT using GOLD. Starting with IAS_5, our 2nd generation molecule showing 30-fold AT activation, a focused library considering structural variations on the positions of sulfate groups on the bicyclic and unicyclic rings, the presence or absence of carboxylic group at the 3-position, the stereochemistry at position 3, and the type of linker was built. Molecules showing high promise included 67A225 and 58A225 in both enantiomeric (*R* and *S*) forms. Shown here are three representative molecules. A) (*S*)-IAS5, B) (*S*)-67A225, and C) (*R*)-58A225. Adapted from reference 231.

4.3.2. Synthesis of Non-Saccharide, Sulfated *N*-Arylacyl THIQ Derivatives—The THIQ3CA scaffold was constructed from three components, formaldehyde, substituted benzaldehyde, and glycine moiety donor in four steps (Scheme 5). In our synthetic design, *N*-Boc-α-phosphonoglycine trimethylester served as the glycine donor. Briefly, the Horner–Wadsworth–Emmons reaction of the glycine donor and the desired dimethoxy benzaldehyde **9** or **10** afforded the corresponding benzylidene in excellent yields. This was followed by catalytic hydrogenation using palladized charcoal, *N*-Boc de-protection using acidic conditions, and Pictet-Spengler cyclization with formaldehyde to give THIQ3CA methyl esters **13** and **14** in approximately 55% overall yield. Non-carboxylated THIQ derivative **2** was obtained through direct application of Pictet-Spengler reaction on the corresponding substituted phenethylamine while 6,7-dimethoxy THIQ, **1**, is commercially available (Scheme 4).

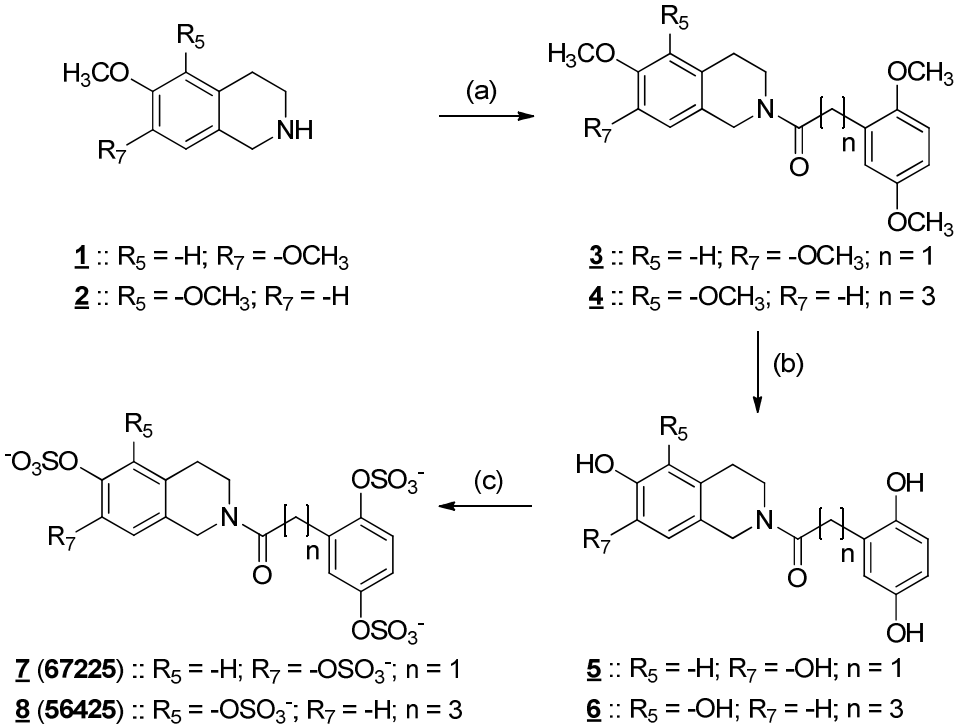

Scheme 4. (a) 2,5-dimethoxyphenyl acetic (n = 1) or butanoic acid (n = 3), EDCI, DMAP, rt/overnight, 70-95%, (b) BBr_3/CH_2Cl_2, -78 ^{0}C/ 2 h, then rt/overnight, 65-85%, (c) SO_3:NMe_3/ (1:1) DMF:CH_3CN, 80 ^{0}C/5 h, followed by Na^+ exchange 45-75%. Adapted from reference 231.

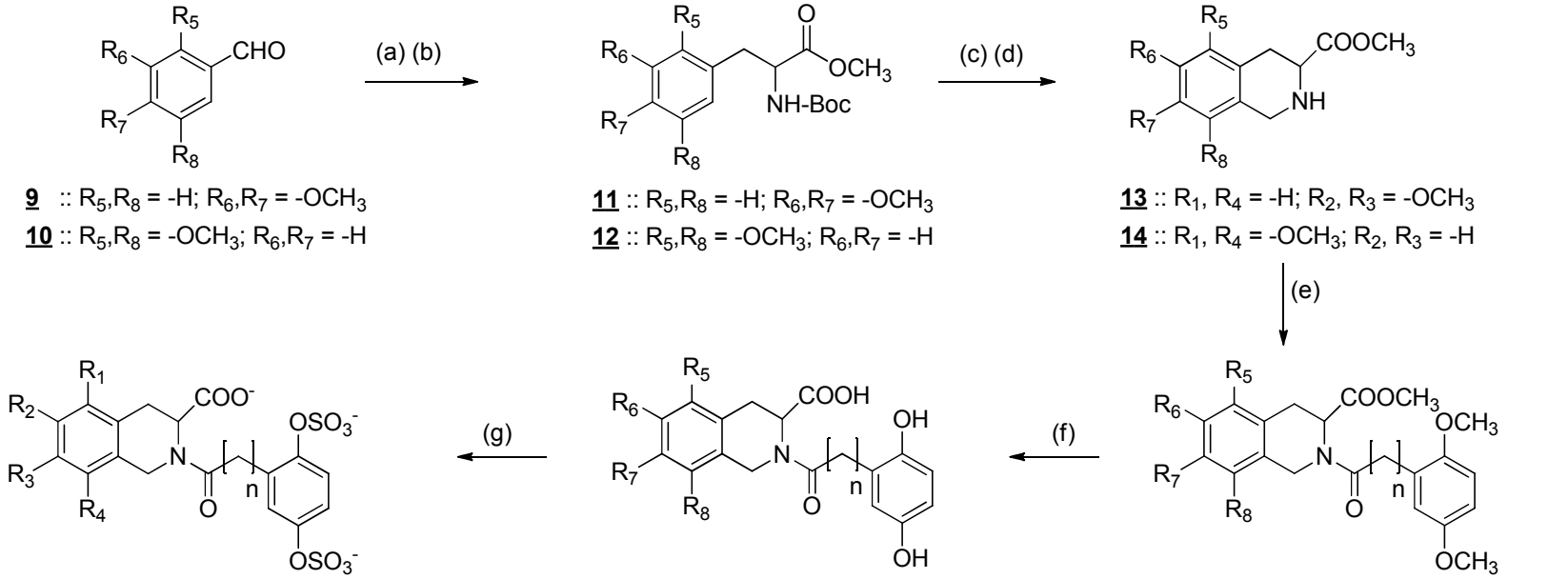

Scheme 5. (a) (±)-Boc-α-phosphonoglycine trimethylester, DBU/THF, rt/overnight, 77-85%, (b) H_2/Pd/Ethanol, rt/5 h, 100%, (c) (1:1) TFA:CH_2Cl_2, rt/4 h, 85%, (d) 37% HCHO/TFA/ CH_2Cl_2, rt/ 5 h, 70-80%, (e) 2,5-dimethoxyphenyl acetic (n = 1), propionic (n = 2), or butanoic acid (n = 3), EDCI, DMAP, rt/overnight, 70-95%, (f) BBr_3/CH_2Cl_2, -78 ^{0}C/ 2 h, then rt/overnight, 65-85%, (g) SO_3:NMe_3/(1:1) DMF:CH_3CN, 80 ^{0}C/5 h, followed by Na^+ exchange 45-75%. Adapted from reference 231.

The THIQ3CA esters were then elaborated to the bicyclic – unicyclic structures with variable linkers by coupling with appropriately substituted arylalkyl carboxylic acids. Thus, coupling with 2-(2,5-dimethoxy phenyl)acetic acid afforded the *N*-arylacylated THIQ3CA esters with a 2-atom linker (**15a**, **16a**), whereas 3-atom (**15b**, **16b**) and 4-atom linker structures (**15c**, **16c**) were prepared using propionic and butanoic acid derivatives, respectively. The methoxyl protecting groups of the coupled *N*-arylacylated THIQ3CA esters were then removed using BBr_3 in CH_2Cl_2, which also led to the concomitant hydrolysis of the carboxylic ester, to yield the per-phenolic *N*-arylacyl THIQ3CAs (**17a-17c**, **18a-18c**). Likewise, the non-carboxylated THIQ derivatives, **3** and **4**, as well as the corresponding per-phenolic THIQs, **5** and **6**, were generated in a similar manner. Overall, the synthesis of the per-phenolic precursors of AT activators from the THIQ scaffold was achieved in 65-85% yield. To the best of our knowledge, these THIQ derivatives have not been reported in the literature and these high yields appear to be the best achieved so far for this class of molecules.

The conversion of per-phenolic precursors, such as **17a-17c** and **18a-18c**, to their per-sulfated derivatives is known to be a challenging.[112] We have earlier developed a base-mediated, microwave-assisted per-sulfation protocol,[113] however, this method resulted in partially sulfated compounds as well as degradation products as demonstrated by CE analysis. We inferred that the free carboxylic group of **17a-17c** and **18a-18c** interferes with base-mediated persulfation and hence explored neutral conditions without microwave heating. Refluxing the per-phenolic precursors in a 1:1 mixture of CH_3CN: DMF with $Me_3N{:}SO_3$ complex for 5 hours gave significantly improved yields (41-75%) of the per-sulfated products (**7**, **8**, **19a-19c**, **20a-20c**) (Schemes 4 and 5). It is worth mentioning here that per-sulfation of at least twelve per-phenolic THIQs was attempted, however, only eight compounds could be successfully isolated. Derivatives

with 5,6-di-sulfate and 3-carboxylate groups proved to be the most difficult perhaps because of limited access to the 5-position.

4.3.3. Affinity of Sulfated *N*-Arylacyl THIQ Activators for Antithrombin— The binding affinity of heparins for plasma AT is typically measured through the 30 – 40% increase in intrinsic tryptophan fluorescence as a function of the concentration of the activator.[52,83,219] However, this technique did not work with the first generation non-saccharide activators because of insufficient signal.[106,107] Later work with second generation molecules demonstrated a significantly different signal in comparison to the heparins. For IAS_5–based activators, the intrinsic fluorescence decreased and reached a plateau at high ligand concentrations.[110] We used this approach to measure the K_D for AT interaction with the per-sulfated activators (**7**, **8**, **19a-19c**, **20a-20c**) in 20 mM sodium phosphate buffer at pH 6.0. Increasing concentrations of the synthesized per-sulfated derivatives gave a saturable decrease in intrinsic fluorescence of AT (Figure 22). The maximal change in fluorescence (ΔF_{MAX}) was found to be in the range of 25 – 100%, which provided excellent signal for K_D measurement. For each per-sulfated derivative, the observed fluorescence decrease was fitted by the standard quadratic binding equation 5 to calculate the K_D of AT – activator complex (Table 5).

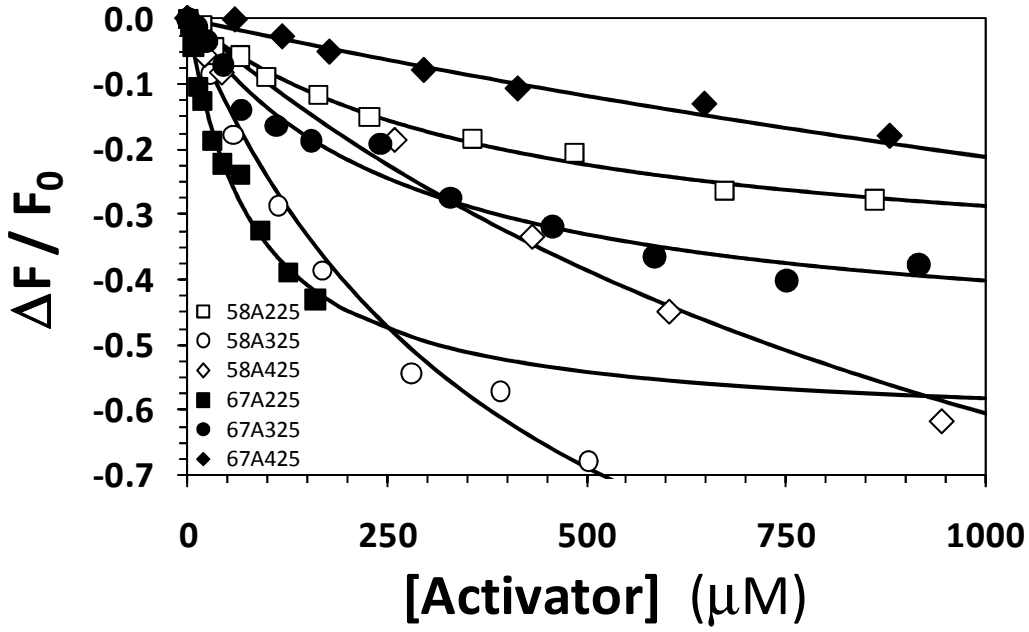

Figure 22. Spectrofluorimetric measurement of the antithrombin affinity of sulfated *N*-arylacyl-tetrahydroisoquinoline activators at pH 6.0, *I* 0.05, 25 °C. The binding of the activators (o = **20b** (58A325); □ = **20a** (58A225); ◇ = **20c** (58A425), ◆ = **19c** (67A425); ● = **19b** (67A325); ■ = **19a** (67A225)) to AT resulted in a saturable decrease in intrinsic tryptophan fluorescence at 340 nm (λ_{EX} = 280 nm), which was fitted to the quadratic binding equation 5 to calculate the observed K_D. Solid lines represent the non-linear regressional fit. The figure is adapted from reference 231.

Table 5. AT affinity of sulfated THIQActivators.[a]

Activator	K_D (μM)	ΔF_{MAX} (%)
58A225	394 ± 46	-40 ± 2
58A325	420 ± 38	-127 ± 8
58A425	1322 ± 237[b]	-140 ± 14
67A225	81 ± 14	-63 ± 5
67A325	273 ± 49	-51 ± 4
67A425	3883 ± 1325	-104 ± 26
67225	753 ± 478	-38 ± 14
56425	1123 ± 191	-24 ± 2
IAS_5[c]	320 ± 10	-130 ± 20
ECS[d]	10.5 ± 1.2	na[e]

[a]Affinity was measured using the decrease in intrinsic tryptophan fluorescence as a function of activator concentration in 20 mM sodium phosphate buffer, pH 6.0, containing 25 mM sodium chloride, 0.1 mM EDTA, and 0.1% PEG 8000 at 25 ^{O}C. See Experimental Procedures for additional details.[b]Error represents ±1 S. E. [c]Taken from ref. 110. [d]Taken from ref. 106 and corresponds to results measured in 20 mM sodium phosphate buffer, pH 6.0, containing 0.1 mM EDTA and 0.1% PEG8000. [e]not applicable.

Overall, the AT affinity of the THIQ-based focused library was found to be mediocre to poor (80 – 3900 μM) in comparison to DEFGH (~0.001 μM).[219] This is not too surprising considering that the DEFGH sequence has been optimized by nature through millions of years of evolution and heparin seems to have been designed specifically for recognizing AT. With regard to the first and second generation activators (2–300 μM), the measured affinity of activators studied in this work is less than expected.[110,106] An important reason for this weaker affinity is that ECS and IAS_5 (Figure 20) relied on a much smaller scaffold, which increases the sulfate charge density with a concomitant rise in the Coulombic forces of attraction.[112]

Despite the relatively weak interaction with AT, the affinities demonstrate a strong structural dependence. For the 5,8–series containing the carboxylic acid group, the AT binding affinity ranged from 394 μM for **20a**, named as 58A225 and containing a 2–atom linker, to 1322 μM for **20c**, named as 58A425 and containing a 4-atom linker (Table 5). Likewise, the AT affinity for the carboxylated 6,7–series ranged from 81 μM for **19a**; 67A225, containing the 2–atom linker, to 3883 μM for **19c**; 67A425, containing the 4-atom linker. Lastly, activators **7** and **8**, named as 67225 and 56425, and lacking 3–carboxylic acid group, demonstrated K_D of 753 μM and 1123 μM, respectively. The non-linear variation in affinity of these activators, more clearly demonstrated in the 6,7–series, probably suggests significant differences in binding mode despite their relatively similar structures.

4.3.4. Antithrombin Activation by Sulfated *N*-Arylacyl THIQ Derivatives— A characteristic of AT activation is the acceleration in the rate of FXa inhibition by heparins and heparin mimetics. Accordingly, the second-order rate constant of AT inhibition of FXa in presence (k_{ACT}) and absence (k_{UNCAT}) of sulfated *N*–arylacyl–THIQ derivatives was measured at pH 6.0, 25 mM NaCl and 25 °C, as described earlier in the previous work pertaining to the first and second

generations of AT activators.[83,110,219] In this technique, the residual FXa activity is measured at various time intervals at a fixed concentration of the activator to determine the pseudo-first order observed rate constant (k_{OBS}). Several k_{OBS} measurements at various concentrations of the activator are performed to assess the phenomenon of AT activation. Figure 23 shows representative profiles for **19a** (67A225) and **20b** (58A325) in the concentration ranges of 0 → 9 μM and 0 → 28 μM, respectively. At a qualitative level, the profiles suggest that 67A225 (Figure 23A) accelerates AT inhibition of FXa at a rate faster than 58A325 (Figure 23B).

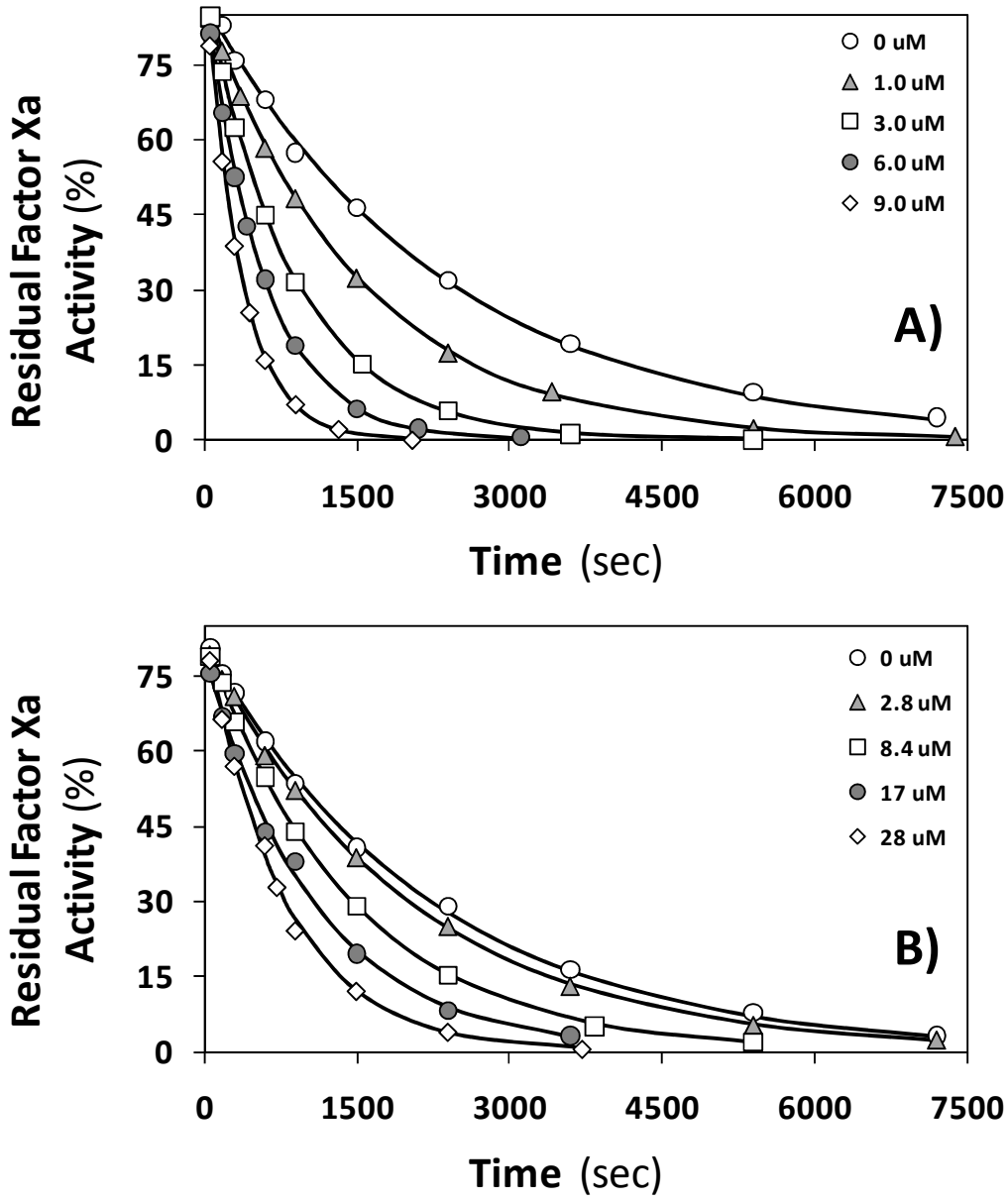

Figure 23. Kinetics of antithrombin inhibition of factor Xa in the presence of sulfated *N*-arylacyl-tetrahydroisoquinoline activators **19a** or 67A225 (A) and **20b** or 58A325 (B) at pH 6.0, *I* 0.05, 25 ^{O}C. The residual fXa activity was measured spectrophotometrically under pseudo-first order conditions through the initial rate of Spectrozyme FXa hydrolysis. The observed pseudo-first rate constant of fXa inhibition (k_{OBS}) at each activator concentration was calculated from the exponential decrease. The figure is adapted from reference 231.

To evaluate AT activation on a quantitative level, the increase in k_{OBS} as a function of the concentration of the each activator was analyzed using equation 6, as described earlier.[110] The slope of this plot provides the second order rate constant of FXa inhibition by AT-activator complex (k_{ACT}), while the intercept yields the second order rate constant of FXa inhibition by AT alone (k_{UNCAT}). The ratio of k_{ACT} to k_{UNCAT} provides the acceleration in AT inhibition of FXa, a measure of AT activation induced by the activator. Figure 24 shows the profiles measured for each *N*-arylacyl-THIQ activator and Table 6 lists the acceleration calculated from the linear fits to the data. The data indicate significant differences in the acceleration potential of each sulfated activator.

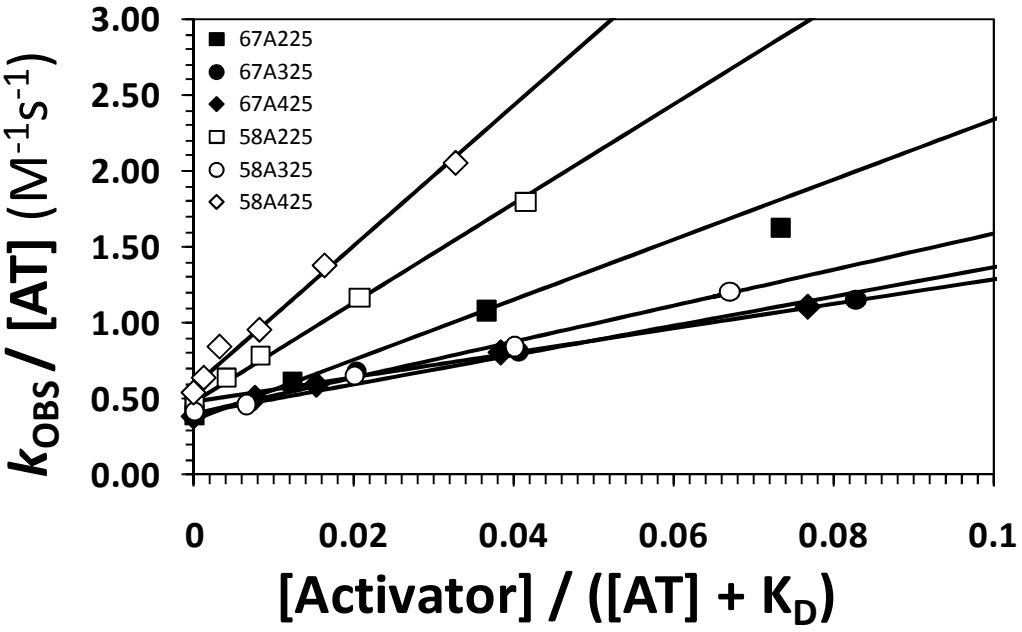

Figure 24. Acceleration in factor Xa inhibition by antithrombin - sulfated *N*-arylacyl-tetrahydroisoquinoline activator complexes**.** The observed rate constant (k_{OBS}) of fXa inhibition by AT in the presence of varying concentrations of the activator (o = **20b** (58A325); □ = **20a** (58A225); ◇ = **20c** (58A425), ◆ = **19c** (67A425); ● = **19b** (67A325); ■ = **19a** (67A225)) was measured in a spectrophotometric assay at pH 6.0, *I* 0.05 and 25 ^{O}C. Solid lines represent linear regressional fits to the data using equation 6 to calculate the second-order rate constants, k_{ACT} and k_{UNCAT}. The figure is adapted from reference 231.

Table 6. Acceleration in AT inhibition of FXa by sulfated THIQ activators.[a]

Activator	k_{UNCAT} ($M^{-1}s^{-1}$)	k_{ACT} ($M^{-1}s^{-1}$)	*Acceleration*
58A225	452 ± 17	32630 ± 1644	67.1 ± 5.9
58A325	374 ± 10	11800 ± 789	29.3 ± 2.8
58A425	543 ± 28[b]	46330 ± 2830	79.4 ± 8.9
67A225	345 ± 38	19740 ± 1290	53.2 ± 9.3
67A325	454 ± 21	8051 ± 751	16.5 ± 2.3
67A425	378 ± 15	9640 ± 748	23.7 ± 2.8
67225	386 ± 27	4582 ± 597	11.0 ± 2.2
56425	375 ± 22	3337 ± 265	8.3 ± 1.1
IAS_5[c]	~2300	69780 ± 580	~30.3
ECS[d]	~120	909 ± 40	~7.6

[a]Antithrombin activation was measured using the discontinuous slow kinetics assay of monitoring residual fXa following incubation in the presence of the activator at a fixed concentration in 20 mM sodium phosphate buffer, pH 6.0, containing 25 mM sodium chloride, 0.1 mM EDTA, and 0.1% PEG 8000 at 25 ^{O}C. [b]Error represents ±1 S. E. [c]Taken from ref. 110 and corresponds to results measured in 20 mM sodium phosphate buffer, pH 7.4, containing 100 mM NaCl, 0.1 mM EDTA and 0.1% PEG8000. [d]Taken from ref. 106 and corresponds to results measured in 20 mM sodium phosphate buffer, pH 6.0, containing 0.1 mM EDTA and 0.1% PEG8000.

The AT acceleration potential was found to be 79.4 for 58A425, 29.3 for 58A325, and 67.1 for 58A225, while it was 23.7 for 67A425, 16.5 for 67A325, and 53.2 for 67A225 under identical conditions (pH 6.0, 25 mM NaCl, 25 °C). These results put forward three molecules studied here as significantly better than the best non-saccharide aromatic AT activator designed earlier.[110] Specifically, 58A425, 58A225 and 67A225 accelerate AT inhibition of FXa much better than IAS5. More importantly, the acceleration induced by 58A425, i.e., 80–fold, is only 3.8–fold lower than the 300-fold acceleration induced by DEFGH. In terms of advance in activator design, 58A425 displays nearly 10-fold higher AT activation potential than the first designed non-saccharide aromatic activator.[106]

The results also indicate that the 5,8 series of activators is better than the 6,7 series of activators. Yet, the AT activation potential appears to follow a non-linear pattern with regard to the length of the linker in both series of molecules. For example, the 3-atom linker containing activator in both the series (5,8- and 6,7-series) displays weaker acceleration than the 2- and 4-atom counterparts. The reason for this behavior is not clear but may be due to different mode of binding of each activator. Finally, derivatives 56425 and 67225, which lack the 3-carboxylic acid group on the THIQ ring, exhibited AT acceleration of only 8.3 ± 1.1 and 11 ± 2.2, respectively. This implies that 3-carboxylic acid functionality of these activators is important for activation of AT.

Finally, to assess the importance of sulfate groups in these activators, several per-phenolic parents of the sulfated activators were evaluated for interaction with AT and FXa. None of the tested per-phenolic parents displayed any measurable interaction. Further, each sulfated activator was assessed for its direct interaction with FXa in the absence of AT and found to lack any direct inhibition effect. These results support the conclusion that the designed bicyclic–unicyclic sulfated

N-arylacyl THIQ derivatives function as indirect inhibitors of FXa through allosteric activation of AT.

4.4. Conclusion— Antithrombin is a key regulator of coagulation and prime target of heparins, clinically used anticoagulants. Heparins induce a two-step conformational activation of antithrombin, a process that has remained challenging to target with molecules devoid of the antithrombin binding pentasaccharide DEFGH. Computational screening of a focused library led to the design of two tetra-sulfated *N*-arylacyl tetrahydroisoquinoline variants as potential nonsaccharide activators of antithrombin. A high yielding synthetic scheme based on Horner–Wadsworth–Emmons or Pictet–Spengler reactions was developed to facilitate the functionalization of the tetrahydoisoquinoline ring, which upon further amidation, deprotection, and sulfation gave the targeted nonsaccharide activators. Spectrofluorometric measurement of affinity displayed antithrombin binding affinities in the low to high micromolar range. Measurement of second-order rate constants of antithrombin inhibition of factor Xa in the presence and absence of the designed activators showed antithrombin activation in the range of 8–80-fold. This work puts forward **20c**, a novel tetra-sulfated *N*-arylacyl tetrahydro–isoquinoline-based molecule that activates AT only 3.8-fold less than that achieved with DEFGH, suggesting a strong possibility of rationally designing sulfated organic molecules as clinically relevant AT activators.

4.5. Experimental Section—

4.5.1. Chemicals— Anhydrous CH_2Cl_2, THF, CH_3CN, and DMF were purchased from Sigma-Aldrich and used as such. All other solvents were of reagent gradient and used as purchased. Analytical TLC was performed using UNIPLATE^{TM} silica gel GHLF 250 μm pre-coated plates (ANALTECH, Newark, DE). TLC was visualized by electromagnetic wave of 254 nm and/or iodine. Column chromatography was performed using silica gel (200-400 mesh, 60 Å)

from Sigma Aldrich. Chemical reactions sensitive to air or moisture were carried out under nitrogen atmosphere in oven-dried glassware. All reagent solutions unless otherwise noted were handled under an inert nitrogen atmosphere using syringe techniques.

4.5.2. Proteins— Human plasma AT and human FXa were purchased from Haematologic Technologies (Essex Junction, VT). Molar concentration of AT was calculated from absorbance measurements at 280 nm using a ε_{max} of 37,700 $M^{-1}cm^{-1}$. AT was stored in 20 mM sodium phosphate buffer, pH 7.4, containing 100 mM NaCl, 0.1 mM EDTA and 0.1% (w/v) PEG8000 at -78 ^{0}C, while FXa was stored in 5 mM MES buffer, pH 6.0, containing 25 mM NaCl at -78 ^{0}C. Spectrozyme FXa was obtained from American Diagnostics (Greenwich, CT) and prepared in 20 mM sodium phosphate buffer, pH 7.4, containing 100 mM NaCl, 0.1 mM EDTA and 0.1% (w/v) PEG8000.

4.5.3. Modeling Antithrombin— Sybyl 8.1 (Tripos Associates, St. Louis, MO) was used for molecular modeling of AT – activator complexes. The structure of activated form of AT (ID: 2GD4) was acquired from protein data bank (www.rcsb.org). Chain I of the crystal structure, which corresponds to the inhibitory monomer was used as a model of the activated antithrombin conformation. This form does not report the side chains of R46, K125, R132, K136, and K275, probably due to their significant flexibility. These side chains were introduced through appropriate modifications in Sybyl. Hydrogen atoms were added to the 2GD4 structure, while inorganic ions and water molecules were removed. Individual atoms were assigned Gasteiger-Hŭckel charges. To prepare this structure for docking and scoring protocols, energy minimization was performed using Tripos force field so as to reach a terminating gradient of 0.5 kcal/mol $Å^2$ or a maximum of 100,000 iterations.

4.5.4. Modeling the Virtual Library of Sulfated *N*-arylacyl THIQ Derivatives— Ninety IAS_5-related potential AT activators were 'synthesized' *in silico* using LEGION combinatorial library design generator. For the sulfated activators, including IAS_5, that have carboxylic group at 3-position, both the enantiomers were modeled. The atom type of sulfur and oxygen atoms in sulfate groups was modified to S.o2 and O.co2, respectively, and an 'aromatic' bond type was modeled between these atoms. The molecules were assigned Gasteiger-Hŭckel charges and were then energetically minimized using Tripos force field until a terminating gradient of 0.5 kcal/mol $Å^2$ or a maximum of 100,000 iterations.

4.5.5. Docking and Scoring— Docking of the potential sulfated AT activators onto the EHBS of the activated form of AT (AT*) was performed with GOLD 4.1 (Cambridge Crystallographic Data Center, UK). The EHBS comprised of electropositive residues, R129, R132, K133, K136 and K275, and other residues around them, as reported earlier.[14,64] GOLD is a "soft docking" method that implicitly handles local protein flexibility by allowing a small degree of interpenetration, or van der Waals overlap, of ligand and protein atoms. GOLD also optimizes the positions of hydrogen-bond donating atoms on Ser, Thr, Tyr, and, most importantly, Lys and Arg residues as part of the docking process. Except for the automated number of iterations, the allowed amide bond flip, and the prohibited early termination, default parameters were employed during the GOLD docking runs. Docking was driven by the GOLD scoring function, while for ranking the docked solutions, a linear, modified form of the same scoring function (equation 3) was used, as reported earlier.[220]

$$GOLD_{Score} = HB_{EXT} + 1.375 \times VDW_{EXT} \qquad (3)$$

In this equation, HB_{EXT} and VDW_{EXT} are the "external" (non-bonded interactions taking place between the ligand and the target protein) hydrogen bonding and van der Waals terms, respectively.

In addition to GOLD score, Hydropathic INTeractions (HINT) (EduSoft LC, Ashland, VA) scoring function was also used to score AT – activator complexes. HINT scores each atom-atom interaction in the ligand – biomolecule complex using a parameter set derived from experimental solvation partition coefficients.[221] The interaction scores were calculated for each pose derived from docking using equation 4, which describes the overall interaction as a double sum over the atoms within each component.[106,107,220-222] In this equation, *S* is the solvent accessible surface area, *a* is the hydrophobic atom constant, *T* is a descriptor function, and *R* and *r* are functions of the distance between atoms *i* and *j*. From this equation, a binding score is calculated where *bij* describes specific interaction between atoms *i* and *j* and *B* describes the total interaction score between the two species.

$$B = \sum_{i=1}^{atom} \sum_{j=1}^{atom} b_{ij} = \sum \sum (S_i a_i S_j a_j R_{ij} T_{ij} + r_{ij}) \qquad (4)$$

For HINT scoring of AT – activator complexes, energy minimization was first performed using Tripos force field until a terminating gradient of 0.005 kcal/mol $Å^2$ was reached. AT and the activator were then partitioned as distinct molecules. AT was assigned HINT parameters from a dictionary of previously determined values. 'Essential' hydrogen atoms, i.e., only those attached to polar atoms, were explicitly considered in the models. Because HINT parameters for the sulfur atoms in higher oxidation states including sulfates are not well-established, sulfur interaction scores were removed from analysis.[106,107,109]

4.5.6. Chemical Characterization of Compounds— ^{1}H and ^{13}C NMR were recorded on Bruker-400 MHz spectrometer in either $CDCl_3$, CD_3OD, acetone-d_6, or D_2O. Signals, in part per

million (ppm), are either relative to the internal standard (tetramethyl silane, TMS) or to the residual peak of the solvent. The NMR data are reported as chemical shift (ppm), multiplicity of signal (s= singlet, d= doublet, t= triplet, q= quartet, dd= doublet of doublet, m= multiplet), coupling constants (Hz), and integration. ESI MS of unsulfated molecules were recorded using Waters Acquity TQD MS spectrometer in positive ion mode. Samples were dissolved in methanol and infused at a rate of 20 μL/min. Mass scans were obtained in the range of 200-700 amu with a scan time of 1s and a scan rate of 500 amu/s. The capillary voltage was varied between 3 and 4 kV, while the cone voltage ranged from 38 to103 V. For sulfated molecules, ESI MS were recorded in negative ion mode. Samples were dissolved in 0.5% (v/v) formic acid in water and infused at a rate of 20 μL/min. Mass scans were obtained in the range of 200-1000 amu with a scan time of 1s and a scan rate of 800 amu/s. The capillary voltage was varied between 2.2 and 3.9 kV, while the cone voltage ranged from 60 to 74 V. Ionization conditions were optimized for each compound to maximize the ionization of the parent ion. Generally, the extractor voltage was set to 3 V, the Rf lens voltage was 0.1 V, the source block temperature was set to 150 ºC, and the desolvation temperature was about 250 ºC.

4.5.7. Purification and Analytical Identification of Sulfated Compounds— Sulfated, non-saccharide, activators were purified using Sephadex G10 size exclusion chromatography. The quarternary ammonium counterion of sulfate groups present in the activators were exchanged for sodium ions using SP Sephadex-Na cation exchange chromatography. Sephadex G10 and SP Sephadex-Na chromatographies were performed using Flex columns (KIMBLE/KONTES, Vineland, NJ) of dimensions 170 × 1.5 cm and 75 × 1.5 cm, respectively. For regeneration of the cation exchange column, 1 L of 2 M NaCl solution was used. Water was used as eluent in both

chromatographies. Five mL fractions were collected and analyzed by reverse phase-HPLC (RP-HPLC) and/or capillary electrophoresis (CE).

Purity of compounds was assessed using RP-HPLC as well as CE. RP-HPLC analysis was carried out on a Shimadzu chromatography system using Waters Atlantis dC18 column (5 µm, 4.6 × 250 mm). The mobile phase consisted of a 100 mM NaCl aqueous solution-CH_3CN mixture (7:3 v/v) run at a constant flow rate of 0.5 mL/min. Compounds were detected at either 254 and/or 215 nm. The purity of each sulfated compound, as determined by RP-HPLC, was greater than 95%. CE experiments were performed using a Beckman P/ACE MDQ system (Fullerton, CA). Electrophoresis was performed at 25 ^{o}C and a constant voltage of 8 kV or a constant current of 75 µA using an uncoated fused silica capillary (ID 75 µm) with the total and effective lengths of 31.2 cm and 21 cm, respectively. A sequential wash of 1 M HCl (10 min), water (3 min), 1 M NaOH (10 min), and water (3 min) at 20 psi was used to activate the capillary. Before each run, the capillary was rinsed with the run buffer; 50 mM sodium phosphate buffer of pH=3, for 3 min at 20 psi. Sulfated compounds injected at the cathode (0.5 psi for 4 s) and detected at the anode (214 nm).

4.5.8. General Synthetic Procedures and Spectral Characterization Data—

General procedure for Horner-Wadsworth-Emmons reaction. To a solution of (±)-Boc-α-phosphono glycine trimethyl ester (1.2 equivalents) in dry THF (3 mL) was added DBU (1.2 equivalents), and the mixture was stirred for 30 min at 0 °C. A solution of 3,4-dimethoxy benzaldehyde **9** or 2,5-dimethoxy benzaldehyde **10** (1.0 equivalent) in dry THF (3 mL) was then added slowly, and the reaction mixture was warmed to RT and kept running overnight. After the solvent was removed under reduced pressure, the residue was dissolved in EtOAc (50 mL), quickly washed with saturated aqueous solutions of $NaHCO_3$ (2 × 20 mL), brine (20 mL), and then

dried over anhydrous Na_2SO_4. The solvent was evaporated and the crude product purified by flash chromatography on silica gel using (30:70 of EtOAc: hexanes) as mobile phase to yield the desired methyl acrylate in 77-85% yield.

Methyl 2-(*tert*-butoxycarbonylamino)-3-(3,4-dimethoxyphenyl)acrylate . ^{1}H-NMR ($CDCl_3$, 400 MHz): 7.20 (s, 1 H), 7.14 (s, 1 H), 7.07 (d, ^1J= 8.36 Hz, 1 H), 6.80-6.77 (dd, ^1J= 8.36 Hz, ^2J= 1.44 Hz, 1 H), 6.07 (s, br, 1 H), 3.83 (s, 3 H), 3.8 (s, 3 H), 3.77 (s, 3 H), 1.34 (s, 9H). ^{13}C-NMR ($CDCl_3$, 100 MHz): 166.22, 153.05, 150.15, 148.7, 131.5, 126.87, 124.09, 122.58, 112.28, 110.86, 80.79, 55.86, 55.73, 52.42, 28.13. MS (ESI) calculated for $C_{17}H_{23}NO_6$, $[M+H]^+$, *m/z* 338.15, found for $[M+Na]^+$, *m/z* 360.12.

Methyl 2-(*tert*-butoxycarbonylamino)-3-(2,5-dimethoxyphenyl)acrylate. ^{1}H-NMR ($CDCl_3$, 400 MHz): 7.21 (s, 1 H), 7.0 (s, 1H), 6.78 (t, ^1J= 0.92 H, 2 H), 6.41 (s, br, 1H), 3.77 (s, 3H), 3.76 (s, 3H), 3.68 (s, 3H), 1.32 (s, 9H). ^{13}C-NMR ($CDCl_3$, 100 MHz): 166.07, 153.44, 152.81, 151.51, 126.13, 123.79, 123.47, 116.11, 114.52, 112.61, 80.68, 56.45, 55.7, 52.44, 28.27. MS (ESI) calculated for $C_{17}H_{23}NO_6$, $[M+H]^+$, *m/z* 338.15, found for $[M+Na]^+$, *m/z* 360.18.

General procedure for catalytic hydrogenation of α-amino-β-aryl methyl acrylates. Methyl acrylate from the above reaction and 10% Pd/C were mixed in ethanol (10 mL). Hydrogen gas was then pumped into the mixture at RT. After stirring the solution for 5 h, the catalyst was filtered on Celite and the organic filtrate concentrated *in vacuo* to afford the reduced product in ~100% yield.

Methyl 2-(*tert*-butoxycarbonylamino)-3-(3,4-dimethoxyphenyl)propanoate (11). ^{1}H-NMR ($CDCl_3$, 400 MHz): 6.72 (d, ^1J= 8.08 Hz, 1 H), 6.59 (d, ^1J= 8.28 Hz, 1 H), 6.57 (d, ^1J= 1.36 Hz, 1 H), 4.89 (d, ^1J= 7 Hz, 1 H), 4.49-4.43 (dd, ^1J= 13.24 Hz, ^2J= 6.76 Hz, 1 H), 3.79 (s, 3 H), 3.78 (s, 3 H), 3.65 (s, 3 H), 2.96 (t, ^1J= 6.2 Hz, 2 H), 1.35 (s, 9H). ^{13}C-NMR ($CDCl_3$, 100 MHz):

172.39, 155.05, 148.91, 148.14, 128.44, 121.38, 112.45, 111.3, 79.89, 55.87, 55.8, 54.50, 52.16, 37.9, 28.3. MS (ESI) calculated for $C_{17}H_{25}NO_6$, $[M+H]^+$, *m/z* 340.17, found for $[M+Na]^+$, *m/z* 362.33.

Methyl 2-(*tert*-butoxycarbonylamino)-3-(2,5-dimethoxyphenyl)propanoate (12). ^{1}H-NMR ($CDCl_3$, 400 MHz): 6.7-6.68 (m, 2H), 6.605 (d, ^1J= 2.76 Hz, 1 H), 5.19 (d, ^1J= 7.08 Hz, 1 H), 4.45-4.39 (dd, ^1J= 13.24 Hz, ^2J= 7.04 Hz, 1 H), 3.71 (s, 3H), 3.67 (s, 3H), 3.64 (s, 3H), 2.96 (t, J= 4.84 Hz, 2H), 1.31 (s, 9H). ^{13}C-NMR ($CDCl_3$, 100 MHz): 172.7, 155.21, 153.5, 151.82, 125.73, 117.16, 112.7, 111.29, 79.47, 55.77, 55.6, 54.08, 51.97, 32.86, 28.22. MS (ESI) calculated for $C_{17}H_{25}NO_6$, $[M+H]^+$, *m/z* 340.17, found for $[M+Na]^+$, *m/z* 361.82.

General procedure for *N*-Boc deprotection. To a solution of *N*-Boc β-aryl amino ester (1.0 equivalent) in CH_2Cl_2 (5 mL), trifluoro-acetic acid (TFA, 5 mL) was added drop-wise at 0 ^{0}C, and the mixture was warmed to RT. After stirring for 4 h, the reaction mixture was diluted with CH_2Cl_2 (25 mL) and neutralized by drop-wise addition of saturated aqueous $NaHCO_3$ (20 mL). The organic layer was separated and the aqueous phase was extracted with EtOAc (2 × 25 mL). The organic extracts were combined, washed with saturated NaCl solution (25 mL), and dried over anhydrous Na_2SO_4. Removal of the solvent under reduced pressure left a residue, which was purified by silica gel chromatography (90:10 of EtOAc:hexanes) to afford the desired β-aryl amino ester in ~85% yield.

Methyl 3,4-dimethoxy phenylalanine. ^{1}H-NMR ($CDCl_3$, 400 MHz): 6.73 (d, J= 7.76 Hz,1 H), 6.66 (d, ^1J = 7.36 Hz, 1 H), 6.65 (s, 1 H), 3.79-3.65 (m, 1 H), 3.79 (s, 3 H), 3.78 (s, 3H), 3.64 (s, 3H), 2.99-2.95 (dd, ^1J= 13.6 Hz, ^2J= 4.84 Hz, 1H), 2.79-2.74 (dd, ^1J= 13.6 Hz, ^2J= 7.64 Hz, 1H), 1.86 (s, 1 H). ^{13}C-NMR ($CDCl_3$, 100 MHz): 175.22, 148.96, 147.99, 129.49,121.36, 112.4,

111.32, 55.87, 55.83, 55.8, 51.99, 40.41. MS (ESI) calculated for $C_{12}H_{17}NO_4$, $[M+H]^+$, *m/z* 240.12, found for $[M+Na]^+$, *m/z* 262.22.

Methyl 2,5-dimethoxy phenylalanine. ^{1}H-NMR ($CDCl_3$, 400 MHz): 6.71 (s, 3H), 4.28-4.25 (dd, ^1J= 8 Hz, ^2J= 5 Hz, 1H), 3.70 (s, 3H), 3.66 (s, 3H), 3.63 (s, 3H), 3.33-3.28 (dd, ^1J= 14.12 Hz, ^2J= 4.95 Hz, 1 H), 3.03-2.97 (dd, ^1J= 14.12 Hz, ^2J= 8.04 Hz, 1H). ^{13}C-NMR ($CDCl_3$, 100 MHz): 169.51, 153.41, 151.81, 123.01, 117.87, 113.92, 111.67, 55.77, 53.04, 52.77, 32.01. MS (ESI) calculated for $C_{12}H_{17}NO_4$, $[M+H]^+$, *m/z* 240.12, found for $[M+Na]^+$, *m/z* 262.15.

General procedure for Pictet-Spengler reaction of substituted methyl phenylalanine esters and substituted phenethylamine. A solution of methyl phenylalanine derivative or phenethylamine derivative (1 equivalent) in CH_2Cl_2 (2 mL) was treated at RT with formaldehyde (37% aqueous solution, 1.5 equivalents). TFA (2 equivalent) was then slowly added over 15 min. After stirring for 5 h, the reaction mixture was diluted with CH_2Cl_2 (2 mL) and neutralized with saturated $NaHCO_3$ solution (5 mL). The organic layer was separated and the aqueous phase was further extracted with CH_2Cl_2 (3 × 10 mL). The organic extracts were combined, washed with saturated NaCl solution (10 mL), and dried over anhydrous Na_2SO_4. Removal of the solvent under reduced pressure left a residue, which was purified by silica gel chromatography (60:40 of EtOAc: hexanes) to yield the desired tetrahydroisoquinoline derivative in 70-80 % yield.

Methyl 6,7-dimethoxy-1,2,3,4-tetrahydroisoquinoline-3-carboxylate (13). ^{1}H-NMR ($CDCl_3$, 400 MHz): 6.52 (s, 1 H), 6.46 (s, 1 H), 4.08-3.98 (dd, ^1J= 25.64 Hz, ^2J= 15.67 Hz, 2 H), 3.79-3.73 (m, 1 H), 3.78 (s, 3 H), 3.77 (s, 3 H), 3.72 (s, 3 H), 3.41 (s, br, 1 H), 3.00-2.95 (dd, ^1J= 16.08 Hz, ^2J = 4.76 Hz, 1 H), 2.91-2.84 (dd, ^1J= 16 Hz, ^2J= 9.68 Hz, 1 H). ^{13}C-NMR ($CDCl_3$, 100 MHz): 172.73, 147.83, 125.48, 124.35, 111.72, 108.91, 55.93, 55.57, 52.34, 46.37, 30.63. MS (ESI) calculated for $C_{13}H_{17}NO_4$, $[M+H]^+$, *m/z* 252.12, found for $[M+Na]^+$, *m/z* 274.19.

Methyl 5,8-dimethoxy-1,2,3,4-tetrahydroisoquinoline-3-carboxylate (14). ^{1}H-NMR ($CDCl_3$, 400 MHz): 6.53-6.52 (m, 2H), 3.94-3.81 (m, 3H), 3.69 (s, 3H), 3.67 (s, 3H), 3.48 (s, 3H), 3.15-3.06 (m, 1H), 2.87-2.79 (m, 1H). ^{13}C-NMR ($CDCl_3$, 100 MHz): 173.45, 151.16, 150.15, 124.81, 123.19, 107.12, 56.70, 55.67, 51.21, 45.55, 25.87. MS (ESI) calculated for $C_{13}H_{17}NO_4$, $[M+H]^+$, *m/z* 252.12, found *m/z* 252.14.

5,6-Dimethoxy-1,2,3,4-tetrahydroisquinoline (2). ^{1}H-NMR ($CDCl_3$, 400 MHz): 6.67-6.66 (m, 2 H), 3.75 (s, 3H), 3.73 (s, 3H), 3.59 (s, 1 H), 3.16 (s, 1 H), 2.8 (t, ^{1}J= 5.16 Hz, 2 H), 2.74 (t, ^{1}J= 5.08 Hz, 2 H). ^{13}C-NMR ($CDCl_3$, 100 MHz): 150.64, 146.63, 129.23, 128.41, 121.92, 110.41, 59.97, 55.92, 53.99, 48.88, 23.90. MS (ESI) calculated for $C_{11}H_{15}NO_2$, $[M+H]^+$, *m/z* 194.11, found for $[M+Na]^+$, *m/z* 216.11.

General procedure for *N*-arylacylation of 1,2,3,4-tetrahydroisoquinoline-3-carboxylic acid methyl ester (THIQ3CA ester) and 1,2,3,4-tetrahydroisoquinoline (THIQ). To a stirred solution of either 2,5-dimethoxylphenyl acetic, propionic, or butanoic acid (1 equivalent) in anhydrous CH_2Cl_2 (5 mL) was added 1-Ethyl-3-(3-dimethylaminopropyl) carbodiimide (EDCI, 1.1 equivalents) and DMAP (1.1 equivalents) at RT under nitrogen atmosphere. Dimethoxy-1,2,3,4-tetrahydroisoquinoline (either **1**, **2**, **13** or **14**) (1.1 equivalents) in anhydrous CH_2Cl_2 (5 mL) was then added drop-wise. After stirring overnight, the reaction mixture was partitioned between 2 N HCl solution (20 mL) and CH_2Cl_2 (30 mL). The organic layer was washed further with 2 N HCl (2 × 10 mL) and saturated NaCl solution (20 mL), dried using anhydrous Na_2SO_4, and concentrated to give a crude, which purified by silica gel chromatography (50:50 of EtOAc: hexanes) to give the desired coupled product in 70 – 95 % yield.

Methyl 2-(2-(2,5-dimethoxyphenyl)acetyl)-6,7-dimethoxy-1,2,3,4-tetrahydro-isoquinoline-3-carboxylate (15a). ^{1}H-NMR ($CDCl_3$, 400 MHz): 6.80 (d, ^{1}J= 2.64 Hz, 1 H), 6.75-

6.67 (m, 2 H), 6.56-6.40 (m, 2 H), 5.51-5.49 & 4.94-4.92 (dd & dd, ^{1}J= 3.32 Hz, ^{2}J= 6.04 Hz & ^{1}J= 2.32 Hz, ^{2}J= 5.76 Hz, 1 H) 4.91-4.30 (m, 2 H), 3.78 (s, 2 H), 3.76 (s, 3 H), 3.75 (s, 3 H), 3.72 (s, 3 H), 3.66 (s, 3H), 3.50 (d, ^{1}J= 51.52 Hz, 3 H), 3.14-3.06 (m, 1 H), 3.02-2.84 (m, 1 H). ^{13}C-NMR ($CDCl_3$, 100 MHz): 171.49, 171.36, 153.78, 151.18, 150.55, 148.22, 124.28, 123.92, 122.83, 115.91, 113.31, 112.90, 111.58, 109.28, 56.1, 55.95, 55.91, 55.73, 52.44, 52.29, 45.47, 35.30, 31.23. MS (ESI) calculated for $C_{23}H_{27}NO_7$, $[M+H]^+$, *m/z* 430.18, found for $[M+Na]^+$, *m/z* 452.36.

Methyl 2-(2-(2,5-dimethoxyphenyl)acetyl)-5,8-dimethoxy-1,2,3,4-tetrahydro-isoquinoline-3-carboxylate (16a). ^{1}H-NMR ($CDCl_3$, 400 MHz): 6.82-6.79 (m, 1 H), 6.73-6.66 (m, 2 H), 6.60-6.54 (m, 2 H), 5.64-5.62 & 4.96-4.94 (dd & dd, ^{1}J = 2.36 Hz, ^{2}J = 6.80 Hz & ^{1}J = 1.56 Hz, ^{2}J = 6.44 Hz, 1 H), 5.02-4.14 (m, 2 H), 3.76 (d,^{1}J= 23.76 Hz, 2H), 3.71 (s, 3H), 3.70 (s, 3 H), 3.67 (s, 3 H), 3.65 (s, 3 H), 3.49 (d, ^{1}J= 46.72 Hz, 3 H), 3.41-3.37 (m, 1 H), 2.78-2.49 (m, 1 H).^{13}C-NMR ($CDCl_3$, 100 MHz): 171.74, 171.45, 153.64, 151.30, 150.93, 149.57, 124.35, 122.29, 121.94, 116.04, 113.00, 111.39, 108.13, 107.43, 56.02, 55.83, 55.70, 55.42, 52.24, 49.92, 41.23, 35.06, 24.27. MS (ESI) calculated for $C_{23}H_{27}NO_7$, $[M+H]^+$, *m/z* 430.18, found for $[M+Na]^+$, *m/z* 452.3.

Methyl 2-(3-(2,5-dimethoxyphenyl)propanoyl)-6,7-dimethoxy-1,2,3,4-tetrahydro-isoquinoline-3-carboxylate (15b). ^{1}H-NMR ($CDCl_3$, 400 MHz): 6.72-6.69 (m, 3 H), 6.64-6.45 (m, 2 H), 5.52-5.50 & 4.87-4.85 (dd & dd, ^{1}J = 3 Hz, ^{2}J = 6.08 Hz & ^{1}J = 2.44 Hz, ^{2}J = 5.76 Hz, 1 H), 4.88-4.30 (m, 2 H), 3.78 (s, 3 H), 3.75 (s, 3 H), 3.73 (s, 3 H), 3.67 (s, 3 H), 3.56 (s, 3 H), 3.78-3.09 (m, 1 H), 2.99-2.84 (m, 3 H), 2.70-2.67 (m, 2 H).^{13}C-NMR ($CDCl_3$,100 MHz): 172.77, 171.62, 153.58, 151.76, 148.26, 147.80, 130.65, 124.10, 123.70, 116.74, 111.71, 111.26, 109.36,

108.91, 55.94, 55.91, 55.80, 55.67, 52.77, 50.97, 45.12, 34.18, 30.26, 26.69. MS (ESI) calculated for $C_{24}H_{29}NO_7$, $[M+H]^+$, *m/z* 444.19, found for $[M+Na]^+$, *m/z* 466.04.

Methyl 2-(3-(2,5-dimethoxyphenyl)propanoyl)-5,8-dimethoxy-1,2,3,4-tetrahydro-isoquinoline-3-carboxylate (16b). ^{1}H-NMR ($CDCl_3$, 400 MHz): 6.73-6.54 (m, 5 H), 5.65-5.63 & 4.96-4.94 (dd & dd, ^1J = 2.20 Hz, ^2J = 6.76 Hz & ^1J = 1.60 Hz, ^2J = 6.40 Hz, 1 H), 5.03-4.14 (m, 2 H), 3.73 (s, 3 H), 3.70 (s, 3 H), 3.69 (s, 3 H), 3.67 (s, 3 H), 3.55 (s, 3 H), 3.54-3.38 (m, 1 H), 2.94-2.85 (m, 2 H), 2.78-2.53 (m, 3 H). ^{13}C-NMR ($CDCl_3$, 100 MHz): 173.16, 171.58, 153.60, 151.81, 150.92, 149.59, 130.67, 122.43, 121.71, 116.50, 111.81, 111.20, 108.09, 107.63, 55.83, 55.70, 55.44, 55.31, 52.31, 49.61, 40.96, 34.16, 26.71, 24.31. MS (ESI) calculated for $C_{24}H_{29}NO_7$, $[M+H]^+$, *m/z* 444.19, found for $[M+Na]^+$, *m/z* 465.97.

Methyl 2-(4-(2,5-dimethoxyphenyl)butanoyl)-6,7-dimethoxy-1,2,3,4-tetrahydro-isoquinoline-3-carboxylate (15c). ^{1}H-NMR ($CDCl_3$, 400 MHz): 6.71-6.62 (m, 3 H), 6.55-6.47 (m, 2 H), 5.52-5.50 & 4.69-4.67 (dd & dd, ^1J = 2.88 Hz, ^2J =5.92 Hz & ^1J = 2.36 Hz, ^2J = 5.56 Hz, 1 H), 4.86-4.44 (m, 2 H), 3.78 (s, 3 H), 3.77 (s, 3 H), 3.69 (s, 3 H), 3.68 (s, 3 H), 3.55 (s, 3 H), 3.17-3.09 (m, 1 H), 3.04-2.93 (m, 1 H), 2.64 (m, 2 H), 2.44-2.40 (m, 2 H), 1.97-1.89 (m, 2 H). ^{13}C-NMR ($CDCl_3$, 100 MHz): 173.18, 171.55, 153.50, 151.88, 148.28, 147.84, 131.32, 124.11, 123.60, 116.45, 111.30, 110.97, 109.38, 108.99, 55.96, 55.94, 55.90, 55.70, 52.30, 50.94, 45.16, 33.10, 30.27, 29.76, 24.81. MS (ESI) calculated for $C_{25}H_{31}NO_7$, $[M+H]^+$, *m/z* 458.21, found for $[M+Na]^+$, *m/z* 479.96.

Methyl 2-(4-(2,5-dimethoxyphenyl)butanoyl)-5,8-dimethoxy-1,2,3,4-tetrahydro-isoquinoline-3-carboxylate (16c). ^{1}H-NMR ($CDCl_3$, 400 MHz): 6.70-6.55 (m, 5 H), 5.63-5.60 & 4.72 (dd & d, ^1J = 2.32 Hz, ^2J = 6.76 Hz & ^1J = 4.92 Hz, 1 H), 5.02-4.09 (m, 2 H), 3.71 (s, 3 H), 3.70 (s, 3 H), 3.69 (s, 3 H), 3.67 (s, 3 H), 3.55 (s, 3 H), 3.40-3.37 (m, 1 H), 2.75-2.68 (m, 1 H),

2.66-2.53 (m, 2 H), 2.51-2.31 (m, 2 H), 1.97-1.89 (m, 2 H). ^{13}C-NMR ($CDCl_3$, 100 MHz): 173.44, 171.62, 153.50, 151.85, 150.93, 149.58, 131.47, 122.5, 121.75, 116.38, 111.48, 111.18, 108.17, 107.38, 55.83, 55.75, 55.69, 55.40, 52.29, 49.64, 40.89, 33.26, 29.93, 25.12, 24.30. MS (ESI) calculated for $C_{25}H_{31}NO_7$, $[M+H]^+$, *m/z* 458.21, found for $[M+Na]^+$, *m/z* 480.4.

1-(6,7-dimethoxy-3,4-dihydroisoquinolin-2(1H)-yl)-2-(2,5-dimethoxy phenyl) ethanone (3). ^{1}H-NMR ($CDCl_3$, 400 MHz): 6.78-6.64 (m, 5H), 4.54 (d, ^1J= 48.84 Hz, 2H), 3.76 (s, 3H), 3.71(s, 3H), 3.69 (s, 3H), 3.67(s, 3H), 3.63-3.60 (m, 3H), 3.58-3.54 (m, 1H), 2.78 (t, ^1J = 5.96 Hz, 1 H), 2.64 (t, ^1J = 5.88 Hz, 1 H). ^{13}C-NMR ($CDCl_3$, 100 MHz): 170.40, 153.68, 151.00, 146.18, 128.52, 126.68, 124.67, 121.98, 117.10, 115.81, 112.94, 111.57, 110.88, 60.28, 56.09, 55.87, 55.68, 47.17, 43.89, 35.09, 23.64. MS (ESI) calculated for $C_{21}H_{25}NO_5$, $[M+H]^+$, *m/z* 372.17, found for $[M+Na]^+$, *m/z* 394.33.

1-(5,6-dimethoxy-3,4-dihydroisoquinolin-2(1H)-yl)-4-(2,5-dimethoxy phenyl) butan-1-one (4). ^{1}H-NMR ($CDCl_3$, 400 MHz): 6.79-6.60 (m, 5 H), 4.49 (d, ^1J= 74.72 Hz, 2 H), 3.77 (s, 3H), 3.73 (s, 3H), 3.67 (s, 3H), 3.66 (s, 3H), 3.67-3.66 (m, 1 H), 3.50 (t, ^1J= 5.68 Hz, 1 H), 2.80-2.76 (m, 2 H), 2.59 (t, ^1J= 7.6 Hz, 2 H), 2.34 (t, ^1J= 7.36 Hz, 2 H), 1.92-1.88 (m, 2H). ^{13}C-NMR ($CDCl_3$, 100 MHz): 171.92, 153.48, 151.83, 150.88, 146.21, 131.34, 128.44, 126.86, 126.00, 121.97, 121.27, 116.33, 111.22, 60.34, 55.90, 55.87, 55.68, 46.83, 42.92, 39.34, 33.05, 29.92, 25.19. MS (ESI) calculated for $C_{23}H_{29}NO_5$, $[M+H]^+$, *m/z* 400.20, found for $[M+Na]^+$, *m/z* 422.37.

General procedure for *O*-demethylation of *N*-arylacyl THIQ3CA esters and THIQs. To a stirred solution of the protected THIQ3CA ester (or THIQ derivative) in anhydrous CH_2Cl_2 (5 mL), BBr_3 (1M solution in CH_2Cl_2, 9-12 equivalents) was added drop-wise at -78 ^{0}C under nitrogen atmosphere over 10 min. After 2 h, the reaction mixture was brought to RT and allowed to equilibrate overnight. A mixture of (1:1) methanol/water (2 mL) was then added slowly at 0 ^{0}C

and vigorously stirred for 10 min to quench the reaction. The reaction mixture was then concentrated and partitioned between EtOAc (25 mL) and saturated solution of NH_4Cl (15 mL). The aqueous layer was further washed with EtOAc (2 × 20 mL). The combined organic layer was washed with brine solution (15 mL), dried using anhydrous Na_2SO_4 and, and finally concentrated *in vacuo*. The crude was purified by gradient silica gel chromatography using EtOAc in hexanes to give the desired poly-phenol of THIQ derivative in 65 – 85 % yield.

2-(2-(2,5-dihydroxyphenyl)acetyl)-6,7-dihydroxy-1,2,3,4-tetrahydroisoquinoline-3-carboxylic acid (17a). ^{1}H-NMR (acetone-d_6, 400 MHz): 6.65 (d, J= 2.92 Hz, 1 H), 6.54-6.50 (m, 3 H), 6.47-6.44 (dd, ^1J = 2.96 Hz, ^2J= 8.56 Hz, 1 H), 5.20-5.18 & 5.15-5.13 (dd & dd, ^1J= 3.60 Hz, ^2J = 5.92 Hz & ^1J = 2.60 Hz, ^2J = 5.68 Hz, 1 H), 4.79-4.19 (m, 2 H), 3.78-3.43 (m, 2 H), 3.07-3.00 (m, 1 H), 2.88-2.84 (m, 1 H). ^{13}C-NMR (acetone-d_6, 100 MHz): 173.3, 172.2, 151.33, 149.87, 149.53, 145.04, 124.65, 124.52, 123.98, 118.48, 117.87, 115.69, 115.53, 113.83, 56.18, 46.50, 36.49, 31.68. MS (ESI) calculated for $C_{18}H_{17}NO_7$, $[M+H]^+$, *m/z* 360.1, found for $[M+Na]^+$, *m/z* 382.24.

2-(2-(2,5-dihydroxyphenyl)acetyl)-5,8-dihydroxy-1,2,3,4-tetrahydroisoquinoline-3-carboxylic acid (18a). ^{1}H-NMR (acetone-d_6, 400 MHz): 6.64-6.54 (m, 3 H), 6.47-6.42 (m, 2 H), 5.49-5.47 & 5.26 (dd & d, ^1J = 2.20 Hz, ^2J = 6.32 Hz & ^1J = 5.00 Hz, 1 H), 4.91-4.19 (m, 2 H), 3.86-3.81 (dd, ^1J = 5.84 Hz, ^2J = 14.68 Hz, 1 H), 3.72-3.57 (m, 1 H), 3.46-3.41 (m, 1 H), 2.71-2.55 (m, 1 H).^{13}C-NMR (acetone-d_6, 100 MHz): 173.73, 172.51, 151.32, 149.58, 148.19, 147.02, 123.21, 121.08, 120.82, 118.53, 117.59, 116.68, 115.50, 113.46, 51.13, 42.68, 36.41, 25.43. MS (ESI) calculated for $C_{18}H_{17}NO_7$, $[M+H]^+$, *m/z* 360.1, found for $[M+Na]^+$, *m/z* 382.21.

2-(3-(2,5-dihydroxyphenyl)propanoyl)-6,7-dihydroxy-1,2,3,4-tetrahydroisoquinoline-3-carboxylic acid (17b). ^{1}H-NMR (400 MHz, acetone-d_6): 6.55-6.47 (m, 4 H), 6.40-6.38 (dd, ^1J =

2.88 Hz, ^{2}J = 8.56 Hz, 1 H), 5.22-5.20 & 4.94-4.93 (dd & dd, ^{1}J = 3.66 Hz, ^{2}J = 6.00 Hz & ^{1}J = 2.68 Hz, ^{2}J = 5.68 Hz, 1 H), 4.58-4.17 (m, 2 H), 3.07-2.94 (m, 1 H), 2.91-2.80 (m, 1 H), 2.79-2.66 (m, 4 H). ^{13}C-NMR (100 MHz, acetone-d_6): 174.36, 172.4, 151.36, 149.13, 145.02, 144.81, 129.95, 124.77, 124.58, 117.85, 117.66, 115.69, 114.7, 113.86, 55.41, 45.78, 35.63, 30.93. 26.11. MS (ESI) calculated for $C_{19}H_{19}NO_7$, $[M+H]^+$, *m/z* 374.12, found for $[M+Na]^+$, *m/z* 396.22.

2-(3-(2,5-dihydroxyphenyl)propanoyl)-5,8-dihydroxy-1,2,3,4-tetrahydroisoquinoline-3-carboxylic acid (18b). ^{1}H-NMR (CD_3OD, 400 MHz): 6.53-6.47 (m, 2H), 6.43-6.35 (m, 3 H), 5.34-5.32 & 5.01-5.00 (dd & dd, ^{1}J= 2.80 Hz, ^{2}J= 6.48 Hz & ^{1}J= 2.04 Hz, ^{2}J= 6.12 Hz, 1 H), 4.82-4.19 (m, 2 H), 3.46-3.31 (m, 1 H), 2.81-2.63 (m, 4 H), 2.56-2.46 (m, 1 H). ^{13}C-NMR (CD_3OD, 100 MHz): 175.91, 174.51, 151.24, 149.26, 148.40, 147.41, 129.59, 124.20, 121.19, 117.75, 117.17, 114.81, 114.25, 113.79, 52.05, 42.43, 35.20, 30.68, 27.25. MS (ESI) calculated for $C_{19}H_{19}NO_7$, $[M+H]^+$, *m/z* 374.12, found for $[M+Na]^+$, *m/z* 396.2.

2-(4-(2,5-dihydroxyphenyl)butanoyl)-6,7-dihydroxy-1,2,3,4-tetrahydroisoquinoline-3-carboxylic acid (17c). ^{1}H-NMR (acetone-d_6, 400 MHz): 6.55-6.46 (m, 4 H), 6.40-6.38 (m,1 H), 5.25-5.23 & 4.91-4.88 (dd & dd, ^{1}J= 3.44 Hz, ^{2}J= 6.00 Hz & ^{1}J= 2.60 Hz, ^{2}J= 5.52 Hz, 1 H), 4.64-4.17 (m, 2 H), 3.09-3.00 (m, 1 H), 2.98-2.83 (m, 1H), 2.49-2.17 (m, 4 H), 1.83-1.81 (m, 2 H). ^{13}C-NMR (acetone-d_6, 100 MHz): 174.09, 172.63, 151.06, 149.23, 145.05, 144.98, 129.65, 124.81, 124.7, 124.1, 117.45, 116.89, 115.73, 114.27, 113.88, 55.39, 45.72, 36.27, 33.12, 31.73, 26.14. MS (ESI) calculated for $C_{20}H_{21}NO_7$, $[M+H]^+$, *m/z* 388.13, found for $[M+Na]^+$, *m/z* 410.21.

2-(4-(2,5-dihydroxyphenyl)butanoyl)-5,8-dihydroxy-1,2,3,4-tetrahydroisoquinoline-3-carboxylic acid (18c). ^{1}H-NMR (acetone-d_6, 400 MHz): 6.53-6.43 (m, 4 H), 6.40-6.36 (m, 1 H), 5.50-5.48 & 5.03-5.01 (dd & dd, ^{1}J = 2.52 Hz, ^{2}J = 6.68 & ^{1}J = 1.88 Hz, ^{2}J = 6.32 Hz, 1 H), 4.90-4.14 (m, 2 H), 3.53-3.40 (m, 1 H), 2.81-2.66 (m, 1 H), 2.54-2.33 (m, 4 H), 1.83-1.75 (m, 2 H). ^{13}C-

NMR (acetone-d_6, 100 MHz): 174.17, 172.60, 150.99, 149.15, 148.28, 146.99, 129.62, 121.51, 117.30, 116.80, 114.17, 113.64, 113.33, 113.18, 54.44, 50.65, 41.81, 33.14, 26.24, 25.38. MS (ESI) calculated for $C_{20}H_{21}NO_7$, $[M+H]^+$, *m/z* 388.13, found for $[M+Na]^+$, *m/z* 410.34.

1-(6,7-dihydroxy-3,4-dihydroisoquinolin-2(1H)-yl)-2-(2,5-dihydroxyphenyl) ethanone (5). ^{1}H-NMR (acetone-d_6, 400 MHz): 6.60-6.53 (m, 2 H), 6.48-6.44 (m, 3 H), 4.5 (d, ^1J= 84.0 Hz, 2 H), 3.72 (t, ^1J= 5.72 Hz, 1 H), 3.63 (d, ^1J= 6.96 Hz, 2 H), 3.58 (t, ^1J= 5.96 Hz, 1 H), 2.56 (t, ^1J= 5.60 Hz, 1 H), 2.51 (t, ^1J= 5.88 Hz, 1 H). ^{13}C-NMR (acetone-d_6, 100 MHz): 172.25, 151.30, 150.12, 144.84, 144.65, 126.76, 125.22, 124.87, 123.44, 118.06, 115.84, 115.58, 113.79, 48.14, 45.17, 36.63, 28.33. MS (ESI) calculated for $C_{17}H_{17}NO_5$, $[M+H]^+$, *m/z* 316.11, found for $[M+Na]^+$, *m/z* 338.2.

1-(5,6-dihydroxy-3,4-dihydroisoquinolin-2(1H)-yl)-4-(2,5-dihydroxyyphenyl) butan-1-one (6). ^{1}H-NMR (CD_3OD, 400 MHz): 6.55-6.49 (m, 2 H), 6.46-6.43 (m, 1 H), 6.39-6.32 (m, 2 H), 4.39 (d, ^1J= 43.04 Hz, 2 H), 3.6 (t, ^1J= 6.16 Hz, 1 H), 3.49 (t, ^1J= 6.04 Hz, 1 H), 2.68 (t, ^1J= 5.92 Hz, 1 H), 2.63 (t, ^1J= 6.12 Hz, 1 H), 2.50-2.45 (m, 2 H), 2.35-2.30 (m, 2 H), 1.81-1.74 (m, 2 H). ^{13}C-NMR (CD_3OD, 100 MHz): 174.58, 151.10, 149.33, 144.64, 143.76, 130.19, 126.20, 125.94, 123.48, 118.24, 117.83, 116.93, 114.50, 45.03, 44.48, 41.11, 33.96, 30.85, 26.77. MS (ESI) calculated for $C_{19}H_{21}NO_5$, $[M+H]^+$, *m/z* 344.14, found for $[M+Na]^+$, *m/z* 366.23.

General procedure for *O*-sulfonation of polyphenolic THIQ3CA and THIQ derivatives. An equivolume mixture of anhydrous CH_3CN and DMF (3 mL) containing THIQ polyphenol and SO_3:NMe_3 complex (6 equivalents/-OH group of the polyphenol) was heated for 5 h at 80°C. Following reaction, the solution was cooled and concentrated *in vacuo* at less than 35 ^{0}C and the residue taken up in water for loading onto a Sephadex G10 column. The column was eluted with deionized water and fractions were combined based on RP-HPLC and/or CE profiles

(see above). The eluted fractions were lyophilized and re-loaded onto a SP Sephadex column for sodium exchange. Appropriate fractions were pooled, concentrated *in vacuo*, and lyophilized to obtain a white powder of per-sulfated THIQ-based antithrombin activators in 45 – 75 % yield.

Sodium 2-(2-(2,5-di-O-sulfonato-phenyl)acetyl)-6,7-di-O-sulfonato-1,2,3,4-tetrahydroisoquinoline-3-carboxylate tetrasodium (19a), 67A225. ^{1}H-NMR (D_2O, 400 MHz): 7.47-7.25 (m, 5 H), 5.02-4.99 & 4.93-4.91 (dd & dd, ^{1}J= 3.68 Hz, ^{2}J = 5.56 Hz & ^{1}J = 2.64 Hz, ^{2}J = 5.32 Hz, 1 H), 4.90-4.82 (m, 2 H), 4.27-3.56 (m, 2 H), 3.32-3.12 (m, 2 H). ^{13}C-NMR (D_2O, 100 MHz): 177.74, 172.94, 148.70, 147.52, 141.95, 132.61, 132.16, 131.31, 129.91, 124.43, 122.91, 122.35, 121.65, 121.05, 55.59, 45.86, 35.39, 31.88. MS (ESI) calculated for $C_{18}H1_2NNa_5O_{19}S_4$, $[M-H]^-$, *m/z* 787.84, found for $[M-Na]^-$, *m/z* 765.92.

Sodium 2-(2-(2,5-di-*O*-sulfonato-phenyl)acetyl)-5,8-di-*O*-sulfonato-1,2,3,4-tetrahydroisoquinoline-3-carboxylate tetrasodium (20a), 58A225. ^{1}H-NMR (D_2O, 400 MHz): 7.09-7.32 (m, 5 H), 4.87-5.18 (m, 1 H), 4.66-4.84 (m, 2 H), 3.52-4.14 (m, 2 H), 3.28-3.44 (m, 1 H), 2.88-2.99 (m, 1 H). ^{13}C-NMR (D_2O, 100 MHz): 176.65, 172.60, 148.65, 147.67, 146.05, 144.95, 129.91, 129.08, 127.82, 124.56, 122.89, 121.59, 120.99, 120.38, 54.08, 41.38, 35.37, 25.88. MS (ESI) calculated for $C_{18}H1_2NNa_5O_{19}S_4$, $[M-H]^-$, *m/z* 787.84, found for $[M-Na]^-$, *m/z* 766.05.

Sodium 2-(3-(2,5-di-*O*-sulfonato-phenyl)propanoyl)-6,7-di-*O*-sulfonato-1,2,3,4-tetrahydroisoquinoline-3-carboxylate tetrasodium (19b), 67A325. ^{1}H-NMR (D_2O, 400 MHz): 7.27-7.01 (m, 5 H), 5.16-5.13 & 4.98-4.95 (dd & dd, ^{1}J = 3.76 Hz, ^{2}J = 5.8 Hz & ^{1}J =3.32 Hz, ^{2}J 5.92 Hz, 1 H), 4.61-4.49 (m, 2 H), 3.18-2.82 (m, 5 H), 2.74-2.52 (m, 1 H). ^{13}C-NMR (D_2O, 100 MHz): 175.25, 174.50, 148.72, 147.26, 141.83, 141.57, 134.95, 132.34, 131.36, 130.93, 123.43, 122.65, 122.29, 120.97, 57.54, 45.51, 33.49, 30.79. 26.18. MS (ESI) calculated for $C_{19}H_{14}NNa_5O_{19}S_4$, $[M-H]^-$, *m/z* 801.85, found for $[M-Na]^-$, *m/z* 779.97.

Sodium 2-(3-(2,5-di-*O*-sulfonato-phenyl) propanoyl)-5,8-di-*O*-sulfonato-1,2,3,4-tetrahydroisoquinoline-3-carboxylate tetrasodium (20b), 58A325. ^{1}H-NMR (D_2O, 400 MHz): 7.45-7.03 (m, 5 H), 5.24-5.03 (m, 1 H), 4.91-4.51 (m, 2 H), 3.52-3.36 (m, 1 H), 3.15-3.08 (m, 3 H), 3.06-2.64 (m, 2 H). ^{13}C-NMR (D_2O, 100 MHz): 175.49, 174.57, 148.73, 147.33, 146.23, 145.17, 135.04, 128.84, 127.92, 127.56, 123.43, 122.79, 121.30, 120.53, 56.73, 52.42, 41.27, 33.33, 25.90. MS (ESI) calculated for $C_{19}H_{14}NNa_5O_{19}S_4$, $[M-H]^-$, *m/z* 801.85, found for $[M-Na]^-$, *m/z*. 780.07.

Sodium 2-(4-(2,5-di-*O*-sulfonato-phenyl)butanoyl)-6,7-di-*O*-sulfonato-1,2,3,4-tetrahydroisoquinoline-3-carboxylate tetrasodium (19c), 67A425. ^{1}H-NMR (D_2O, 400 MHz): 7.24-7.02 (m, 5 H), 5.02-4.99 & 4.94-4.91 (t & dd, ^{1}J = 5.64 Hz & ^{1}J = 4.24 Hz, ^{2}J = 5.92 Hz, 1 H), 4.49-4.35 (m, 2 H), 3.13-2.82 (m, 2 H), 2.66-2.63 (m, 2H), 2.49-2.06 (m, 2 H), 1.93-1.65 (m, 2 H). ^{13}C-NMR (D_2O, 100 MHz): 175.71, 172.92, 148.73, 147.35, 142.24, 141.55, 136.16, 132.29, 132.16, 123.51, 122.58, 122.04, 120.72, 120.33, 53.13, 45.87, 37.18, 32.33, 29.49, 25.01. MS (ESI) calculated for $C_{20}H_{16}NNa_5O_{19}S_4$, $[M-H]^-$, *m/z* 815.87, found for $[M-Na]^-$, *m/z* 793.7.

Sodium 2-(4-(2,5-di-*O*-sulfonato-phenyl)butanoyl)-5,8-di-*O*-sulfonato-1,2,3,4-tetrahydro isoquinoline- 3-carboxylate tetrasodium (20c), 58A425. ^{1}H-NMR (D_2O, 400 MHz): 7.42-7.30 (m, 3 H), 7.27-7.16 (m, 2 H), 5.17-4.91 (m, 1 H), 4.88-4.53 (m, 2 H), 3.56-3.33 (m, 1 H), 3.14-2.83 (m, 1 H), 2.8-2.37 (m, 4 H), 2.0-1.9 (m, 2 H). ^{13}C-NMR (D_2O, 100 MHz): 177.65, 175.86, 148.76, 147.27, 146.08, 144.89, 136.56, 129.31, 128.66, 127.93, 123.43, 122.54, 121.12, 120.25, 56.58, 41.2, 32.95, 29.1, 26.77, 25.86. MS (ESI) calculated for $C_{20}H_{16}NNa_5O_{19}S_4$, $[M-H]^-$, *m/z* 815.87, found for $[M-Na]^-$, *m/z* 793.92.

1-(6,7-di-*O*-sulfonato-3,4-dihydroisoquinolin-2(1H)-yl)-2-(2,5-di-*O*-sulfonato-phenyl) ethanone tetrasodium (7), 67225. ^{1}H-NMR (D_2O, 400 MHz): 7.32-7.29 (m, 2 H), 7.18-7.06 (m, 3 H), 4.59 (d, J= 48.8 Hz, 2 H), 3.84 (s, 2 H), 3.68 (t, ^{1}J = 5.84 Hz, 1 H), 3.63 (t, ^{1}J = 6.00 Hz, 1 H),

2.79-2.73 (m, 2 H). ^{13}C-NMR (D_2O, 100 MHz): 171.96, 148.73, 147.37, 141.51, 141.37, 133.57, 131.29, 130.01, 124.11, 122.94, 122.68, 121.6, 120.94, 47.08, 44.23, 35.0, 28.21. MS (ESI) calculated for $C_{17}H_{13}NNa_4O_{17}S_4$, $[M-H]^-$, *m/z* 721.87, found for $[M-Na]^-$, *m/z* 700.08.

1-(5,6-di-*O*-sulfonato-3,4-dihydroisoquinolin-2(1H)-yl)-4-(2,5-di-*O*-sulfonato-phenyl)butan-1-one tetrasodium (8), 56425. ^{1}H-NMR (D_2O, 400 MHz): 7.42-7.16 (m, 5 H), 5.05 (d, ^1J= 8.32 Hz, 2 H), 3.69-3.66 (m, 2 H), 3.07-3.03 (m, 2 H), 2.8-2.74 (m, 2 H), 2.58 (t, ^1J = 7.2 Hz, 1 H), 2.51 (t, ^1J = 7.28, 1 H), 1.96-1.92 (m, 2 H).^{13}C-NMR (D_2O, 100 MHz): 174.9, 148.73, 147.32, 143.05, 142.49, 137.64, 136.36, 134.21, 133.61, 130.12, 123.5, 122.52, 120.35, 42.49, 41.88, 39.87, 32.73, 29.01, 26.80. MS (ESI) calculated for $C_{19}H_{17}NNa_4O_{17}S_4$, $[M-H]^-$, *m/z* 749.9, found for $[M-Na]^-$, *m/z* 727.96.

4.5.9. Equilibrium Binding Studies— Fluorescence spectroscopy experiments were performed using a QM4 fluorometer (Photon Technology International, Birmingham, NJ) in 20 mM sodium phosphate buffer, pH 6.0, containing 25 mM NaCl, 0.1 mM EDTA, and 0.1 % PEG8000 at 25 °C in a manner following our previous work.[110,219] Equilibrium dissociation constants (K_D) for the interaction of non-saccharide aromatic activators with plasma AT were determined by titrating the activator (ACT) into a solution of serpin and monitoring the decrease in the fluorescence at 340 nm (λ_{EX} = 280 nm). Slit widths were 1 mm on both the excitation and emission sides. The saturable decrease in signal was fit to the quadratic equilibrium binding equation 5 to obtain the K_D of interaction. In this equation, ΔF represents the change in fluorescence following each addition of the ACT from the initial fluorescence F_O and ΔF_{MAX} represents the maximal change in fluorescence observed on saturation of AT.

$$\frac{\Delta F}{F_0} = \frac{\Delta F_{MAX}}{F_0} \times \frac{([AT]_0+[ACT]_0+K_D)-\sqrt{([AT]_0+[ACT]_0+K_D)^2-4[AT]_0[ACT]_0}}{2\,[AT]_0} \quad (5)$$

4.5.10. Factor Xa Inhibition Studies— The kinetics of inhibition of FXa by AT in the presence of the designed non-saccharide aromatic activators was measured spectrophotometrically under pseudo-first order conditions following our earlier work.[83,106,110,219] Briefly, a fixed concentration of FXa (20 nM) was incubated with fixed concentrations of plasma AT (1.075 μM) and sulfated activators (0 to 100 μM) in 20 mM sodium phosphate buffer, pH 6.0, containing 25 mM NaCl, 0.1 mM EDTA and 0.1% (w/v) PEG8000 at 25 ºC. At regular time intervals, an aliquot of the inhibition reaction was quenched with 900 μL of 100 μM Spectrozyme FXa in 20 mM sodium phosphate buffer, pH 7.4, containing 100 mM sodium chloride at 25 °C. To determine the residual FXa activity, the initial rate of substrate hydrolysis was measured from the increase in absorbance at 405 nm. The exponential decrease in the initial rate of substrate hydrolysis as a function of time was used to determine the observed pseudo-first rate constant of FXa inhibition (k_{OBS}). A plot of k_{OBS} at different concentrations of the activator could be described by equation 6 in which k_{UNCAT} is the second-order rate constant of FXa inhibition by AT alone and k_{ACT} is the second-order rate constant of FXa inhibition by AT–activator complex.

$$\frac{k_{OBS}}{[AT]_0} = k_{UNCAT} + k_{ACT} \times \frac{[ACT]_0}{[AT]_0 + K_D} \qquad (6)$$

CHAPTER 5: POTENT DIRECT FACTOR Xa INHIBITORS BASED ON TETRAHYDROISOQUINOLINE SCAFFOLD

5.1. Hypthesis— Anticoagulants represent the basis for treatment and prevention of thromboembolic disorders.[7] The inhibition of any coagulation enzyme can be expected to reduce or prevent clotting, yet most strategies have targeted two serine proteases, factor IIa (FIIa, or thrombin) and factor Xa (FXa), which belong to the common pathway of the coagulation cascade.[17] Of these, thrombin plays a major role in a number of physiologically relevant responses that rely on its catalytic activity.[225,226] Thus, inhibition of thrombin not only reduces cleavage of fibrinogen to fibrin, a key aspect of clotting, but also other processes such as platelet activation, platelet aggregation and angiogenesis. On the other hand, FXa has a rather limited role in comparison, which is only to generate thrombin.

Several lines of evidence suggest that FXa may represent a better target for anticoagulation. FXa's contribution to amplification of the coagulation signal is higher than that of thrombin.[18,19] Its occurrence earlier in the coagulation pathway suggests that a FXa inhibitor may be more effective in blocking progression of a coagulation signal than a thrombin inhibitor .[227,228] Recent results with indirect parenteral and direct oral FXa inhibitors have shown reduced bleeding complications.[25] Also, thrombin inhibitors have been associated with rebound hypercoagulability,[24,229] while peptidomimetic inhibitors have been shown to inhibit both free as well as clot-bound FXa.[142,230]

FXa can be inhibited through two major pathways including an indirect, antithrombin-dependent pathway [14,231] or a direct FXa targeting pathway.[6,232,233] Designing indirect FXa inhibitors that activate antithrombin is challenging and has been achieved primarily with heparin-based molecules,[14,234] although efforts are afoot to design effective non-saccharide-based antithrombin activators.[106,110, 231] In contrast, designing direct inhibitors of FXa has been much

more productive and has led to several clinically relevant peptidomimetics, e.g., rivaroxaban,[114,125] apixaban,[119] DPC423,[235] and others, that target FXa's active site.

A large number of scaffolds have been studied for direct inhibition of FXa including the aminopiperidines ,[236] piperazines,[237] diaminocycloalkanes,[238] lactams,[239,240] oxazolidinones,[125] amino acids (e.g., glycine, proline, and β-aminoproionate),[241,242] anthranilamides,[243] isoxazoles,[244] pyrazoles,[235,245] indazoles,[246] indoles,[247,248] and dihydropyrazolopyridinones.[119,249] The overall philosophy in the design of these scaffolds is to have a three-component system, which includes a core scaffold and two hydrophobic arms that provide a non-linear geometry considered important for FXa recognition. In addition, a key design principle has also been flexibility of the core scaffold. The core scaffolds studied to date can be classified into either a highly flexible class or a fairly rigid class.

It is known that trypsin's active site is much more open than FXa's, which in turn possesses an active site that is more open than that of thrombin. This allows trypsin to work upon practically any arginine containing sequence, while thrombin prefers a fairly rigid proline containing sequence. Thus, we hypothesized that an intermediate level of flexibility in the core scaffold will engineer high selectivity for FXa inhibition. Lastly, having an amino acid–like structure will allow us to apply the peptide chemistry in very straightforward manner to establish the SAR for the THIQ dicarboxamide class of FXa inhibitors.

5.2. Results and Discussion—

5.2.1. Designing the Tetrahydroisoquinoline-3-Carboxylic Acid Scaffold as a Potential Factor Xa Inhibitor Scaffold. The glycine and β-aminopropionate-based inhibitors are examples of a highly flexible core scaffold, while aromatic scaffolds, e.g., aminobenzoic acids, pyrazoles, and indazoles, are examples of fairly rigid scaffolds. An intermediate level of flexibility in the core

scaffold has not been studied to date for direct FXa inhibition. A large number of scaffolds possess intermediate level of flexibility including tetrahydroisoquinoline (THIQ), tetrahydroquinoline, tetrahydroquinazoline, dihydrocoumarin, and dihydroindole. In each of these, the five- or six-membered rings are flexible, yet full flexibility is restricted due to ring fusion. Of these, we focused on the THIQ scaffold, which is a widely explored privileged structure.[231,250-252] To enable a non-linear structure for FXa recognition, we introduced a carboxylic acid group at the 3-position of the THIQ scaffold to arrive at THIQ3CA scaffold.

The designed THIQ3CA scaffold was first investigated *in silico* to assess its potential in binding in factor Xa active site as well as to identify a potential inhibitor for synthesis. A virtual library of THIQ3CA structures was prepared by introducing substituents at positions 2 and 3. A large group of aromatic and non-aromatic carboxylic acid and amine arms at positions 2 and 3 were studied to identify potential 'hits'. The virtual library of resulting THIQ3CA dicarboxamides was then computationally docked into active site of human FXa and scored using genetic algorithm-based screening technique developed in our laboratory earlier.[231] As positive controls, two well-established direct FXa inhibitors, apixaban and rivaroxaban, were also studied in an identical manner.

The GOLD-based docking and scoring strategy identified several hits, of which THIQ3CA dicarboxamide **23**, containing a 5-chlorothiophen-2-yl moiety (also present in rivaroxaban), was identified as a promising candidate. Figure 25 shows a comparison of the predicted bound form of **23** with apixaban. Both molecules adopted a rather similar binding mode in which the 5-chlorothiophenyl-carbonyl group was found to be oriented toward the S1 subsite and the 4-(piperidin–2–one)–N^1–methylaniline moiety oriented into the S4 subsite. Comparison of the binding geometry with rivaroxaban suggested similar corresponding features. THIQ3CA

dicarboxamide **23** was synthesized in three high yield steps and evaluated for its direct human FXa inhibition potential. An IC_{50} of 55.9 μM, corresponding to a K_I of 28 μM, was measured, validating the potential of the THIQ3CA core scaffold in direct human FXa inhibition investigation.

5.2.2. Synthesis of THIQ3CA-Based Potential FXa Inhibitors. Based on the structure of **23**, a library of THIQ3CA dicarboxamides was designed. The synthesis of the targeted THIQ3CA analogs was achieved using a facile three-step strategy of amidation, deprotection, and amidation that relied on the availability of the two arms, A_N and A_C, at positions 2 and 3, respectively.[253] Each A_N structure designed as a part of the library was commercially available and was introduced using standard amidation reaction (see Scheme 6). In contrast, arm A_C at position 3 of THIQ3CA required pre-assembly. This arm was synthesized by aromatic nucleophilic substitution in which 4–bromoaniline derivatives **4a**–**4c** were reacted with either valerolactam **5a** or morpholin-3-one **5b** to quantitatively give the corresponding 4–substituted aniline derivatives **8a** – **8g**.[254] Likewise, substituted anilines **8h** – **8j** containing the piperazine side chain were also included in the study (Scheme 6).

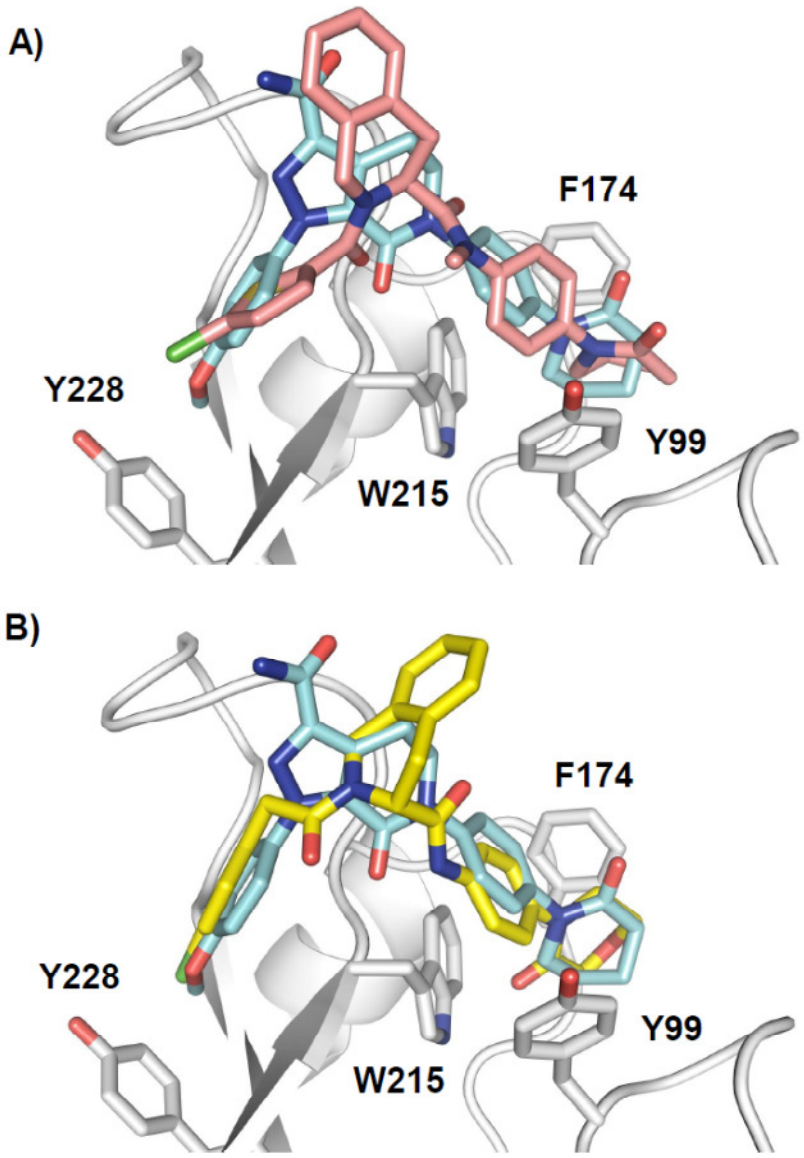

Figure 25. Virtual screening of a library of potential THIQ3CA-based inhibitors docked and scored onto the active site of FXa (PDB: 2P16) using GOLD resulted in the design of **23** (A: GOLD score of 69.3, Carbons in pink) that appeared to mimick the binding of well known potent FXa inhibitors. The virtual library of THIQ3CA–based dicarboxamides contained structural modifications in arms A_N and A_C. Apixaban (GOLD score of 93.7, Carbons in blue) and rivaroxaban (GOLD score of 87.2 , structure not shown) were also docked and scored as positive controls. Sytematic structural modifications led to the design of the most potent THIQ3CA dicarboxamide **47** (B: GOLD score of 77.2, Carbons in yellow).

To introduce either arm A_N or A_C through an amidation reaction, the THIQ3CA core was first appropriately protected, which involved either esterification of the 3-carboxylic acid or *t*-

butoxycarbonylation (Boc group) or carbonylbenzyloxylation (Cbz group) of the ring nitrogen. For example, THIQ3CAs **9** – **11** were amidated using amines **8a** – **8g** to yield Boc- or Cbz-protected THIQ3CA mono-carboxamides **12** – **21** in 73–89% yield (Scheme 7). The Boc or Cbz protecting group of **12** – **21** was then removed using either mild acid[255] or catalytic hydrogenation,[256] respectively, to afford the corresponding free form in 65-75% yield. The free form of **12** – **21** was then amidated at the 2 position with twenty one carboxylic acids in the presence of EDCI to yield the targeted THIQ3CA dicarboxamides **22** – **49** in 70–95% yield (Scheme 7). This strategy was also exploited for the synthesis of THIQ3CA dicarboxamides **50** – **55**, **59**, and **62** that contain additional variations on arms A_N and A_C (Schemes 8 and 9).

To assess the effect of flexibility for FXa inhibition, we targeted three core scaffolds that afford greater flexibility than the THIQ3CA scaffold as well as can help assess the importance of configurational geometry. These scaffolds were: 1) a ring opened variant of THIQ3CA core, the phenylalanine (PA) derivative **62**; 2) mono-cyclic dicarboxamides **69** – **73** belonging to the piperidine–3–carboxylic acid (P3CA) class; and 3) mono-cyclic dicarboxamides **78**, **79** and **81** belonging to the piperidine–2–carboxylic acid (P2CA) class (Scheme 10). These molecules were synthesized in a manner similar to the THIQ3CA scaffold using the amidation, deprotection, and amidation strategy.

To understand the importance of the aromatic ring of the THIQ3CA scaffold, and yet mimic its flexibility, we targeted 1) a partially unsaturated, cyclic ring system, i.e., *(S)*-1,2,3,6–tetrahydropyridine–2–carboxylic acid (THP2CA) and 2) a bridged system, i.e., (*1R,3S,4R*)-2-azabicyclo[2.2.1]heptane-3-carboxylic acid (ABH3CA) (Scheme 11). The synthesis of either scaffold started with the Boc-protected carboxylic acid **82** or **85**, which was converted in three steps to dicarboxamide **84** or **87**, respectively, in excellent yield.

Overall, we synthesized twenty eight THIQ3CA, one PA, five P3CA, three P2CA, one THP2CA and one ABH3CA dicarboxamides using a simple three-step protocol. The molecules were purified using standard flash chromatography system and were characterized using ^{1}H and ^{13}C NMR spectroscopy and ESI-MS.

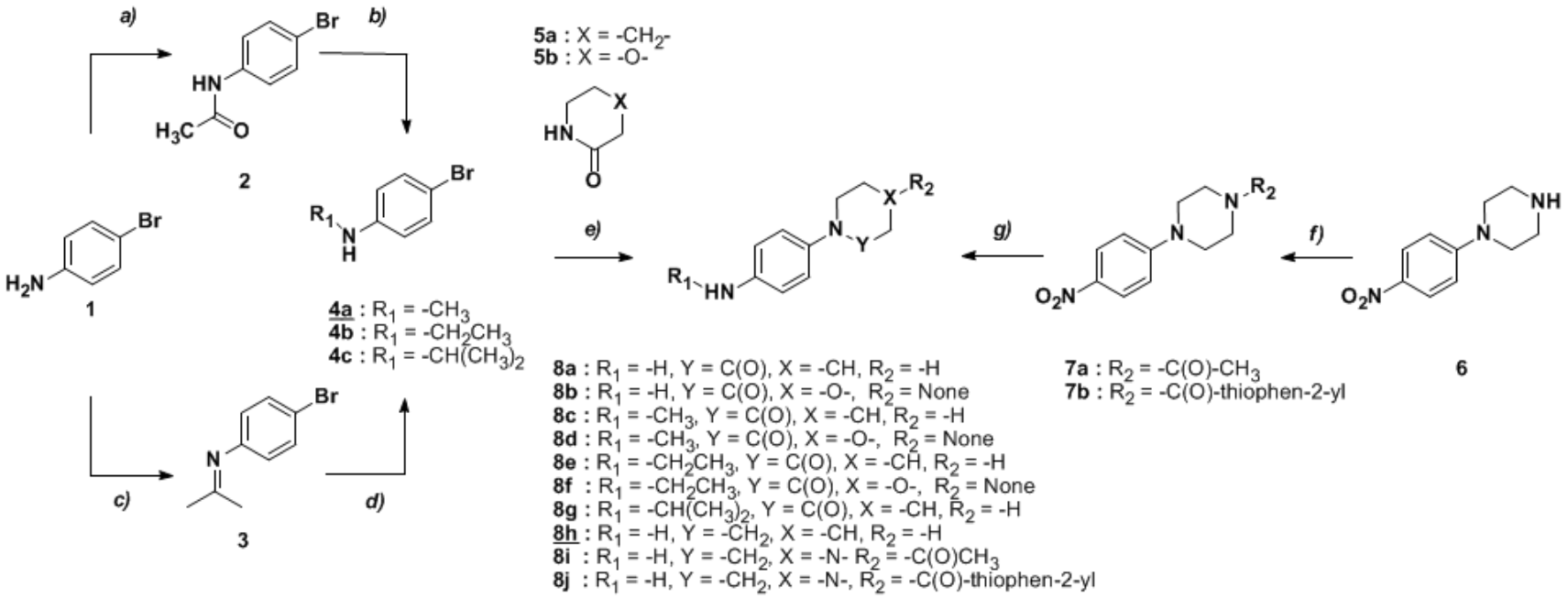

Scheme 6. ***a)*** Acetic anhydride, pyridine, CH_2Cl_2, rt/4 h, 92%, ***b)*** $LiAlH_4$, THF, rt/overnight, 60%, ***c)*** Acetone, Titanium (IV) isopropoxide, Ethanol, rt/12 h, ***d)*** $NaBH_4$, rt/2 h, 75%, ***e)*** Piperidin-2-one or morpholin-3-one, CuI, *N,N'*-Dimethylethylenediamine, K_2CO_3, Toluene, reflux/overnight, 65-90%, ***f)*** For **7a**: Acetic anhydride, pyridine, CH_2Cl_2, rt/4 h, 84%. For **7b**: Thiophene-2-carboxylic acid, EDCI, DMAP, CH_2Cl_2, rt/overnight, 70-95%, ***g)*** 10% Pd/C, CH_3OH/HCl, H_2, rt/5 h, 100%. ***Note:*** Underlined compounds are commercially available and are not products of the designated reactions.

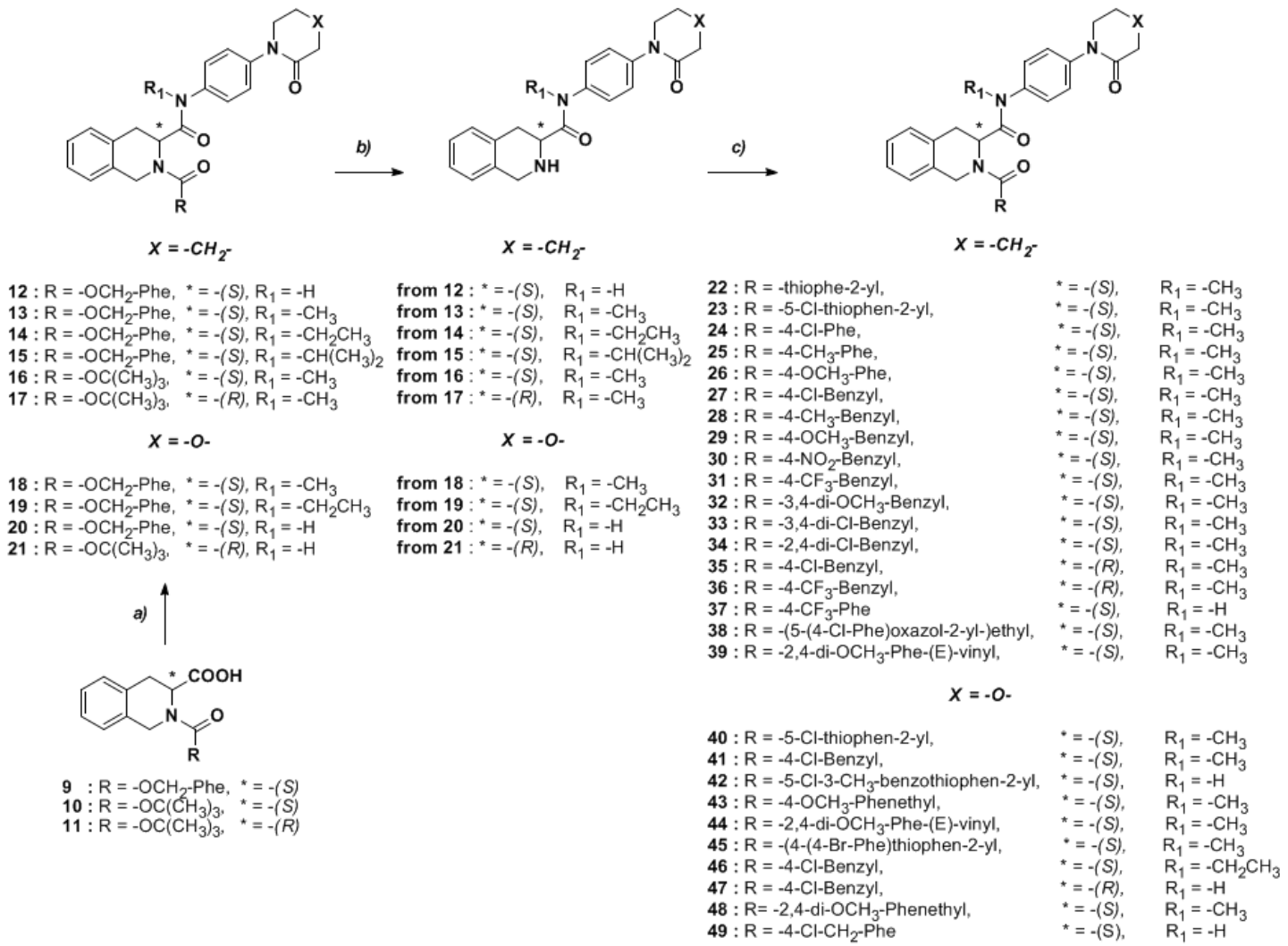

Scheme 7. ***a)*** Appropriate amine (**8a–8g**), $HOBt.H_2O$, DMAP, EDCI, CH_2Cl_2, rt/overnight, 73-89%, ***b)*** For Cbz-protected intermediates: 10% $Pd(OH)_2$, (1:1) CH_3OH: *t*-butanol, H_2, rt/overnight, 65-72%. For Boc-protected intermediates: (1:1) TFA:CH_2Cl_2, rt/4 h, 75%, ***c)*** Appropriate organic acid, EDCI, DMAP, CH_2Cl_2, rt/overnight, 70-95%.

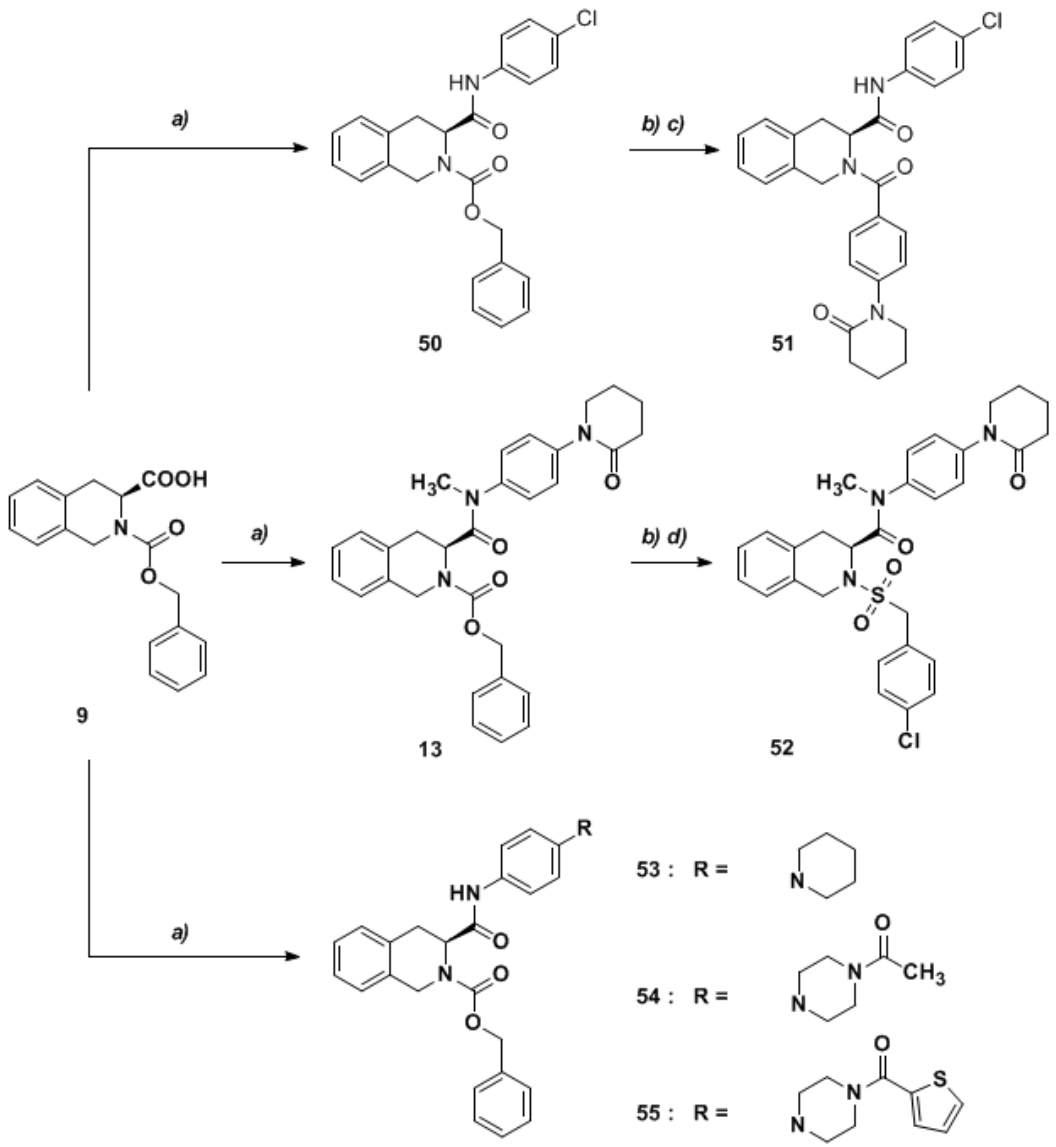

Scheme 8. ***a)*** Appropriate amine (**8c**, **8h–8j**, or **4-Chloroaniline**), HOBt.H_2O, DMAP, EDCI, CH_2Cl_2, rt/overnight, 73-89%, ***b)*** 10% $Pd(OH)_2$, (1:1) CH_3OH: *t*-butanol, H_2, rt/overnight, 65-72%, ***c)*** 4-(2-oxopiperidin-1-yl)benzoic acid , EDCI, DMAP, CH_2Cl_2, rt/overnight, 72%, ***d)*** (4-Chlorophenyl) methane sulfonyl chloride, pyridine, rt/overnight, 77%.

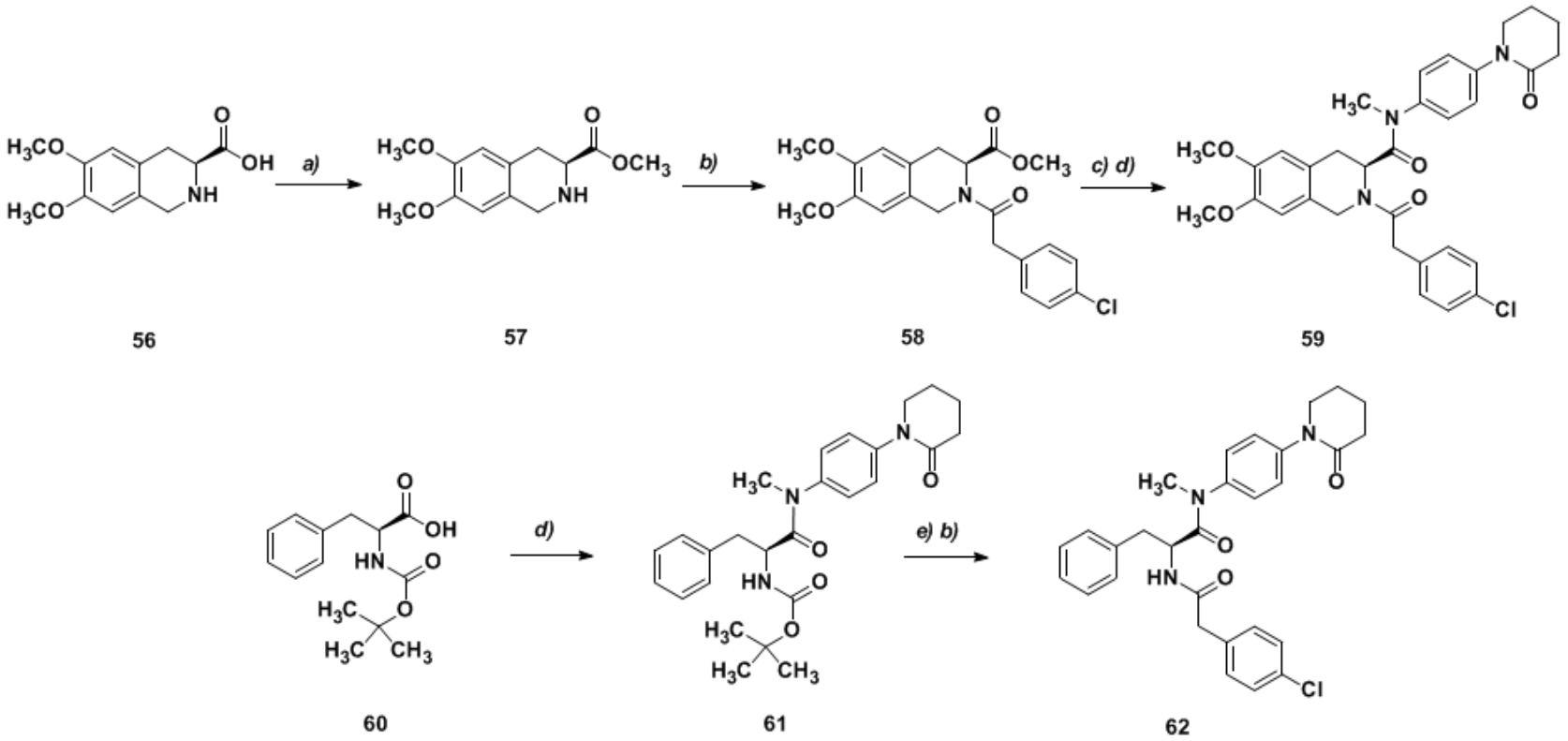

Scheme 9. ***a)*** $SOCl_2$, CH_3OH, reflux/4 h, 95%, ***b)*** 4-Chlorophenyl acetic acid , EDCI, DMAP, CH_2Cl_2, rt/overnight, 81%, ***c)*** $LiOH.H_2O$, CH_3OH, rt/24 h, 75%, ***d)*** **8c**, $HOBt.H_2O$, DMAP, EDCI, CH_2Cl_2, rt/overnight, 73-89%, ***e)*** (1:1) TFA:CH_2Cl_2, rt/4 h.

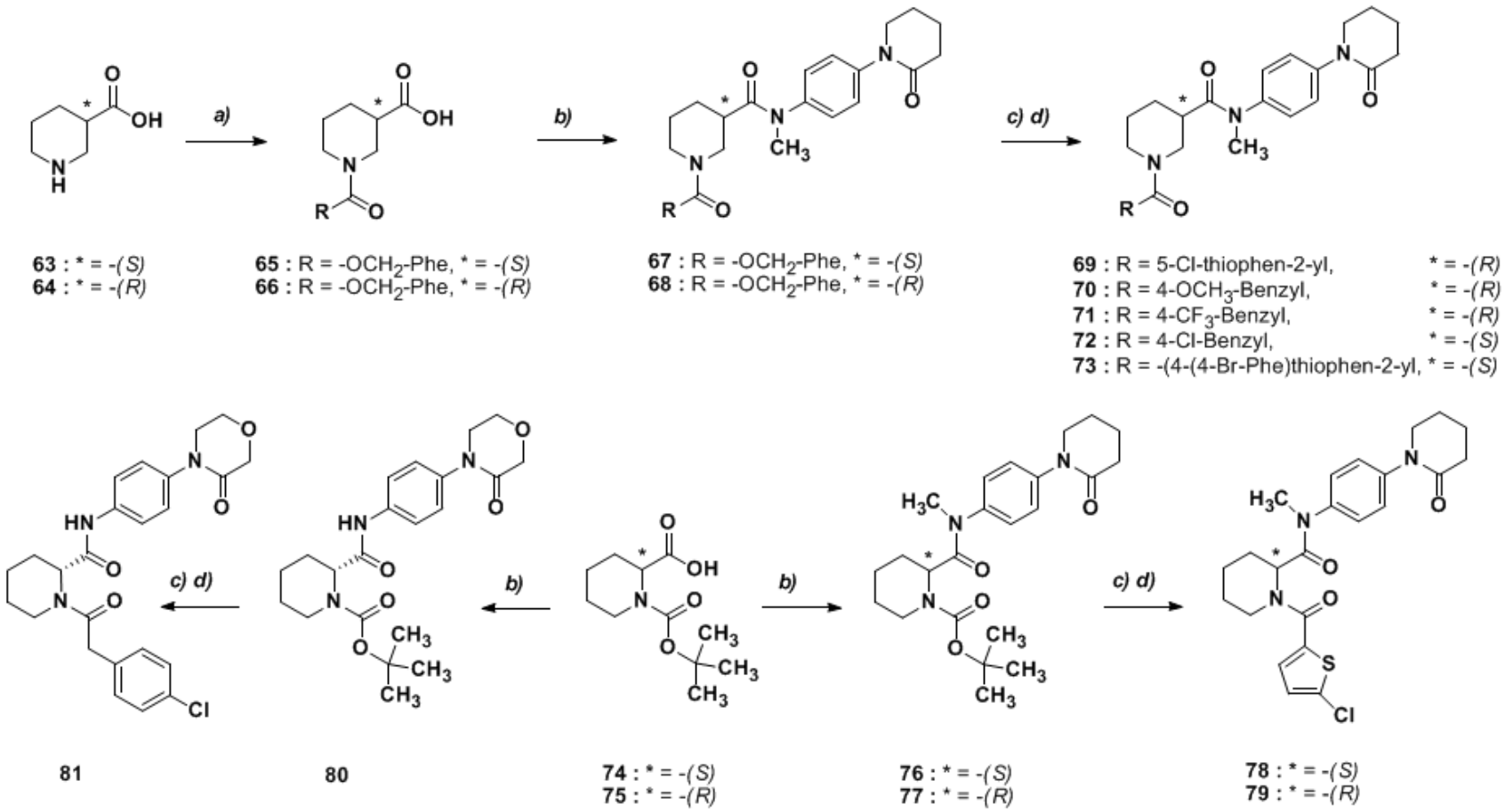

Scheme 10. ***a)*** Benzyl chloroformate, Et_3N, THF, rt/5 h, 70-73 %, ***b)*** **8b** or **8c** , $HOBt.H_2O$, DMAP, EDCI, CH_2Cl_2, rt/overnight, 73-89%, ***c)*** For Cbz-protected intermediates: 10% $Pd(OH)_2$, (1:1) CH_3OH: *t*-butanol, H_2, rt/overnight, 65-72%. For Boc-protected intermediates: (1:1) TFA:CH_2Cl_2, rt/4 h,75%, ***d)*** Appropriate organic acid, EDCI, DMAP, CH_2Cl_2, rt/overnight, 70-95%.

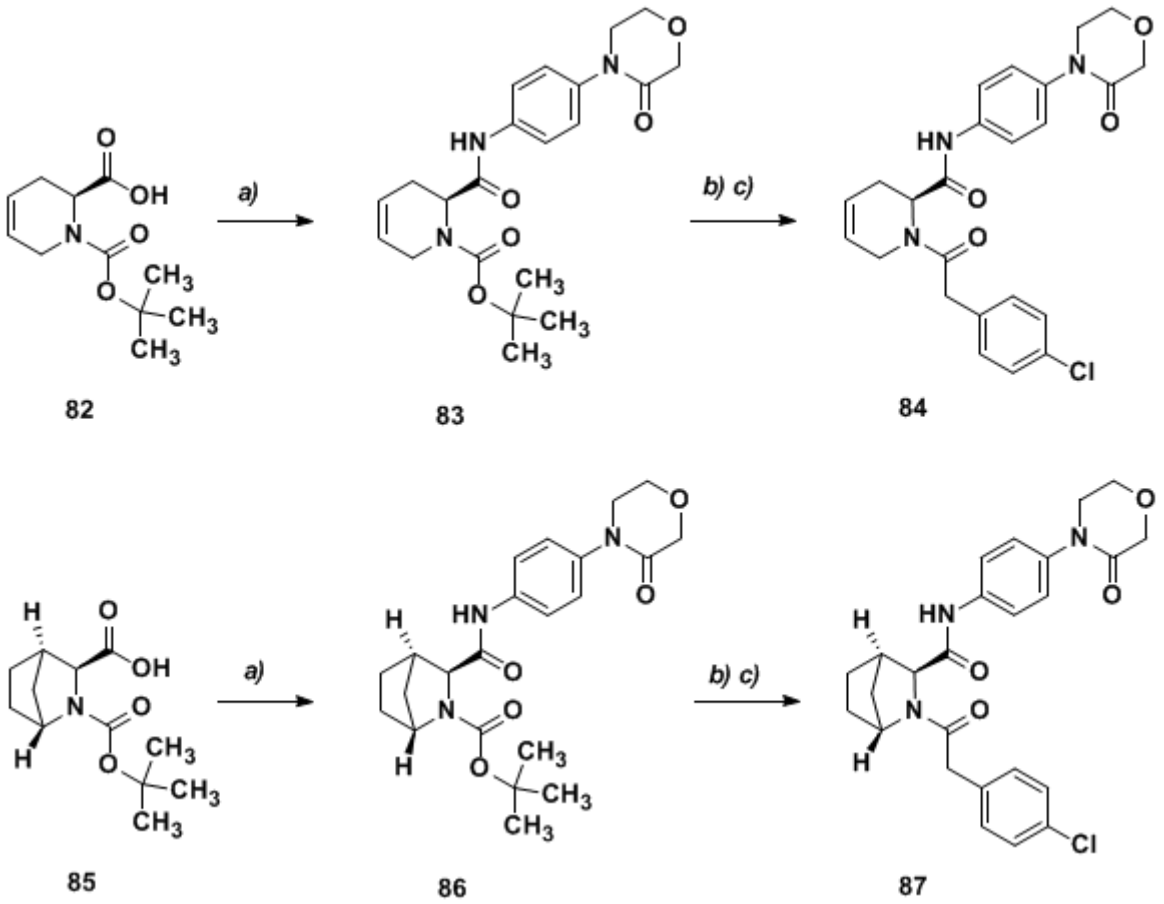

Scheme 11. ***a)*** **8b**, HOBt.H_2O, DMAP, EDCI, CH_2Cl_2, rt/overnight, ***b)*** (1:1) TFA:CH_2Cl_2, rt/4 h, ***c)*** 4-Chlorophenyl acetic acid , EDCI, DMAP, CH_2Cl_2, rt/overnight, 70-95%.

5.2.3. Inhibition Potential of the Library of FXa Inhibitors. Direct inhibition of FXa was measured by a chromogenic substrate hydrolysis assay in 20 mM TrisHCl buffer, pH 7.4, at 37 ºC, as reported earlier.[257] In this assay, hydrolysis of the substrate by FXa results in a linear increase in absorbance at 405 nm, the slope of which corresponds to residual enzyme activity. The change in residual enzyme activity as a function of the concentration of the potential inhibitor is plotted on a logarithmic scale and fitted by the logistic dose-response relationship 8 to derive the potency (IC_{50}), efficacy ($\Delta Y = Y_M - Y_0$) and Hill Slope (HS) of inhibition.[233,257] Figure 26 shows representative inhibition profiles for **20**, **47**, **49**, and **51**, which are THIQ3CA derivatives, and **62** and **81**, which are PA and P2CA derivatives, respectively. Similar profiles were measured for other THIQ3CA, P2CA, P3CA, THP2CA, and ABH3CA derivatives, except for the variation in potency of inhibition. The HS of inhibition was found to be in the range of 0.7 to 1.2, which suggests absence of the complications arising from non-specific binding or aggregation. The IC_{50} values of the FXa inhibitors studied in this work were found to exhibit a wide range of activity (high μM to nM), which provide valuable SAR.

5.2.4. Structural Optimization of Arm A_C of the THIQ3CA Scaffold. Our early molecular modeling studies suggested that arm A_C at the 3-position of the THIQ3CA core structure bound in the S4 subsite of the FXa active site. An intermediate **13**, synthesized early in the library and containing *N-(N*-methylanilin-4-yl)piperidin-2-one as the A_C arm, had shown a reasonable IC_{50} of 16.4 μM. This formed the starting point for studying the S4 subsite substitutions (Table 7). To optimize the structure of the A_C arm, two levels of structural modifications were introduced. These included 1) variation in the carboxamide *N*-substituent and 2) variation in the *para*-substituent of the aniline moiety. Replacing the *N*-methyl group of **13** with ethyl (inhibitor **14**) and isopropyl (inhibitor **15**) groups resulted in no significant change, however, *N*-

demethylation as in **12** reduced the IC_{50} by 1.7–fold suggesting the possibility of the formation of a hydrogen bond. This was however not substantiated by molecular modeling (not shown) and we speculated that the alkyl group on the nitrogen may be inducing a conformational preference that is not favorable for binding in the S4 subsite.

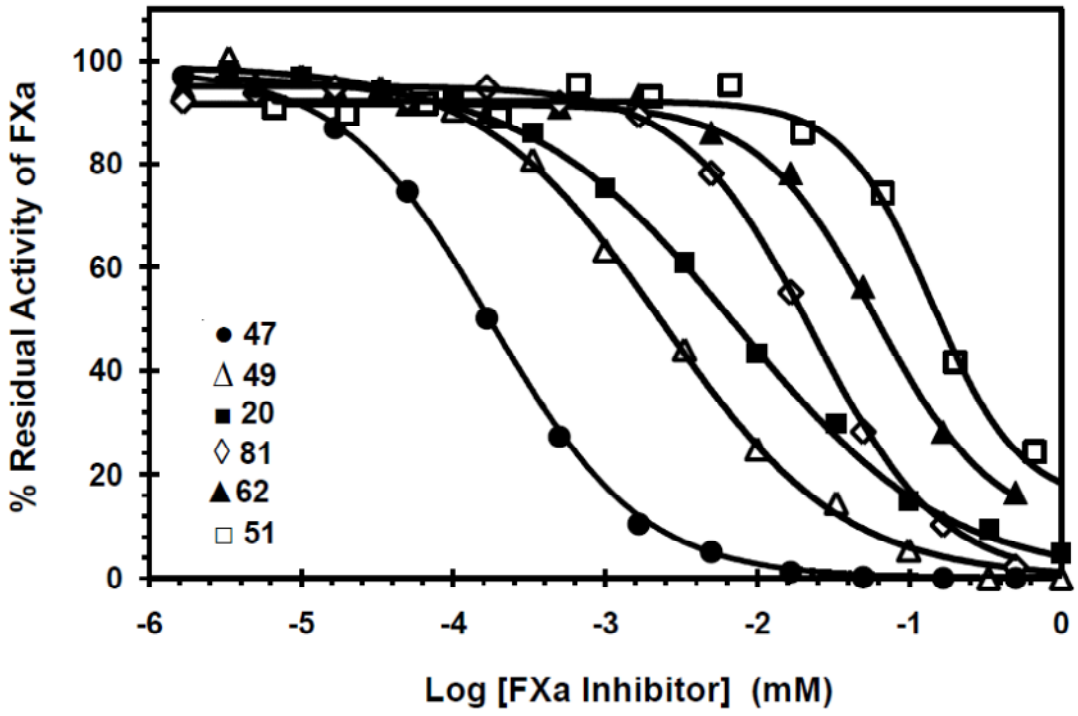

Figure 26. Direct inhibition of FXa by designed THIQ3CA and related dicarboxamides. The inhibition of human FXa was determined spectrophotometrically through the chromogenic substrate hydrolysis assay at pH 7.4 and 37ºC. Solid lines represent sigmoidal fits to the data to obtain IC_{50}, Y_M, Y_0, and HS, as described in the Experimental Methods section. Experiments were performed in duplicate or triplicate (SE < 20%).

Table 7. Optimization of the A_C arm (position 3) of THIQ3CA scaffold for FXa inhibition.

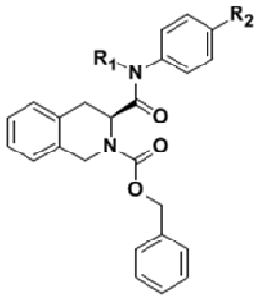

Inhibitor	R_1	R_2	IC_{50} *(μM)*
12	-H	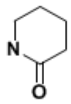	9.9 ± 0.2
13	$-CH_3$	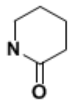	16.4 ± 0.4
14	$-CH_2CH_3$	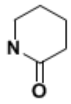	20 ± 1
15	$-CH(CH_3)_2$	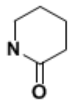	19 ± 2
18	$-CH_3$	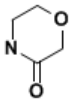	12.8 ± 0.2
19	$-CH_2CH_3$	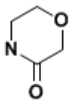	19 ± 6
20	-H	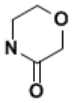	6.0 ± 0.8
50	-H	-Cl	>500
53	-H		>500
54	-H	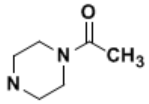	>500
55	-H	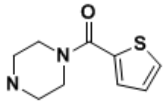	>500

To optimize the *para*–substituent of the aniline moiety, we relied on the extensive literature that abounds in such optimizations.[6,7,118] The moieties preferred at this position include the piperidone, morpholinone, piperidine, piperazine and other rings. Yet, introducing piperidine and piperazine moieties at the *para* position of the aniline was catastrophic. The piperidine–containing derivative **53** and the piperazine–containing derivatives **54** and **55** displayed an un-quantifiable IC_{50} of >500 μM (Table 7). Molecular modeling suggested that the *para* substituent helps orient the adjacent aromatic ring for better interaction with Tyr99, Phe174, and Trp215 of the S4 subsite (not shown), in a manner similar to that observed with rivaroxaban and apixaban .[119,125] Thus, we studied the morpholin-3-one moiety (derivative **20**, Table 7), which exhibited a much improved IC_{50} of 6.0 μM. The results indicated a significant contribution of the carbonyl group of morpholin-3-one for the THIQ3CA inhibitors.

5.2.5. Structural Optimization of Arm A_N of the THIQ3CA Scaffold. Molecular modeling suggested that the A_N arm at position 2 of the THIQ3CA core fits into S1 subsite of the FXa active site. The initial hit **13** (IC_{50} = 16.4 μM) containing the Cbz group as the A_N arm was used as the starting point for studying the S1 subsite substitutions. Considering that the A_N arm of **13** is structurally less defined than its A_C arm, we decided to explore a wider range of moieties to replace the Cbz group. Thus, the optimal chain length of A_N, the nature of its aromatic ring, and the position and number of substituents on the aromatic ring were studied.

Replacing the A_N arm of **13** with thiophenyl carbonyl (**22**), 5-chlorothiophenyl carbonyl (**23**), *p*-chlorophenyl carbonyl (**24**), *p*-methylphenyl carbonyl (**25**) or *p*-methoxyphenyl carbonyl (**26**) arm resulted in 1.2 – 12.7-fold reduction in potency (Table 8). Extending the length of the linker by one carbon atom resulted in significant improvement in IC_{50}. Dicarboxamide **27** containing a 4-chlorophenyl acetyl side chain exhibited an IC_{50} of 1.3 μM, which was the first high

affinity inhibitor (K_i = 0.65 μM) designed in the THIQ3CA series. Yet, most subsequent modifications failed to enhance potency further. For example, one or more electron donating (–CH_3, –OCH_3) as well as one or more electron withdrawing (–Cl, –CF_3, –NO_2) substituents on the phenylacetyl side chain weakened the potency by 1 – 262-fold (Table 8).

Considering the observations made with the A_C structural variants, we studied the morpholin-3-one containing THIQ3CA derivatives also for optimization of the A_N arm. Table 3 shows the results obtained in the morpholin-3-one series. Replacing the Cbz group of parent **18** (IC_{50} = 12.8 μM) with thiophenyl carbonyl (**40**), *p*-methoxyphenyl propanoyl (**43**), or *2,4*-dimethoxyphenyl propanoyl (**48**) resulted in considerable loss of activity. Yet, as in the piperidone series described above, introducing a 4-chlorophenyl acetyl side chain for the Cbz group resulted in an IC_{50} of 1.1 μM. Analysis of the above results indicated that the best inhibitors carried a 7–atom arm A_N (at position 2), e.g., **13**, **26**, **27**, **28**, and **41**. Within this category, a 7-atom arm containing a small, lipophilic electron–withdrawing group (–Cl) is optimal. This group appears to be the *p*-chlorophenylacetyl moiety, as exemplified by a considerable increase in affinity observed with **27**, **34** and **41,** and a loss in affinity for derivative **49** (Tables 8 and 9). Thus, FXa appears to preferentially recognize the chlorophenyl moiety in the THIQ3CA series of inhibitors.

Table 8. Optimization of the A_N arm (position 2) of THIQ3CA scaffold containing the piperidone moiety in the A_C arm for FXa inhibition.

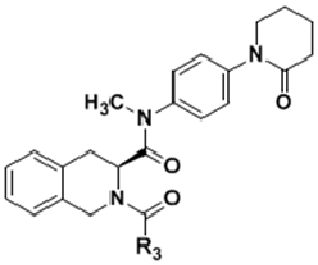

Inhibitor	R_3	IC_{50} (μM)
16	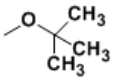	221 ± 19
22		42 ± 2
23	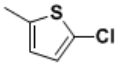	56 ± 2
24	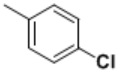	197 ± 39
25	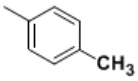	209 ± 31
26	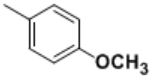	19 ± 2
27	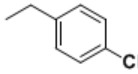	1.3 ± 0.1
28	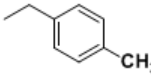	14 ± 3
29	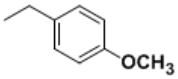	34 ± 1
30	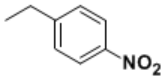	85 ± 19
31	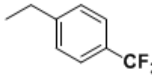	335 ± 50
32	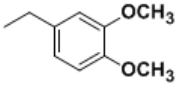	246 ± 58
33	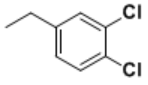	18 ± 2
34	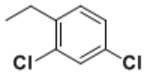	1.3 ± 0.2
38	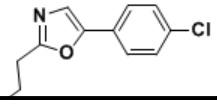	103 ± 8

Table 9. Optimization of the A_N arm (position 2) of THIQ3CA scaffold containing the morpholinone moiety in the A_C arm for FXa inhibition.

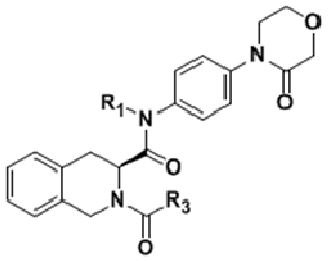

Inhibitor	R_1	R_3	IC_{50} *(μM)*
40	$-CH_3$	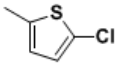	36 ± 3
41	$-CH_3$	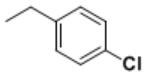	1.1 ± 0.1
42	-H	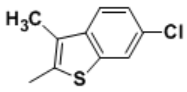	5.4 ± 0.9
43	$-CH_3$	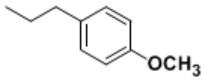	190 ± 16
45	$-CH_3$	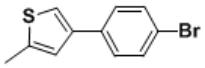	>500
48	$-CH_3$	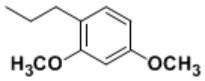	>500
49	-H	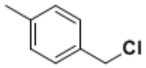	2.9 ± 0.4

5.2.6. Rational Design of Analog 47. The majority of inhibitors described above possessed (*S)*-chirality at position 3. To assess whether an (*R*)-isomer would be better, we studied THIQ3CA derivative **35**, which is a stereoisomer of **27** (IC_{50} = 1.3 μM). This stereochemical inversion resulted in a 1.5–fold increase in the activity (Table 10). This led to a hypothesis that introducing optimal features derived on arms A_N and A_C into a single THIQ3CA derivative may lead to the most potent FXa inhibitor designed so far. Thus, analog **47** was designed, which contained a morpholin-3-one moiety, a *p*-chlorophenylacetyl unit, (*R*)-chirality at the 3-position, and *NH*-

containing carboxamide at the 3-position. THIQ3CA derivative **47** displayed an IC_{50} of 0.27 μM (K_I = 0.135 μM) and presents the highest potency observed in the THIQ3CA series.

The design of **47** reflects a truly additive phenomenon. Inhibitor **47** exhibits ~60–fold decrease in IC_{50} relative to the starting inhibitor **13** (IC_{50} = 16.4 μM), which can be rationalized from the 1.5–fold (morpholin-3-one) × 2–fold (unsubstituted carboxamide) × 1.5–fold (stereochemical inversion) × 13–fold (4-chlorophenylacetyl moiety) increases found independently earlier. This is an interesting observation and appears to have considerable consistency across the series of molecules studied here.

Table 10. Simultaneous optimization of both A_N A_C arms of THIQ3CA scaffold for optimal FXa inhibition.

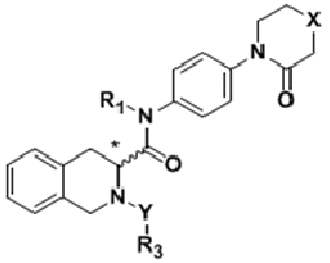

Inhibitor	R_1	X	Y	R_3	Chirality (*)	IC_{50} (μM)
35	$-CH_3$	$-CH_2-$	-C(O)-	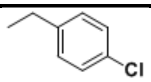	*(R)*-	0.9 ± 0.1
36	$-CH_3$	$-CH_2-$	-C(O)-	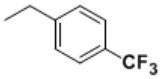	*(R)*-	311 ± 56
37	-H	$-CH_2-$	-C(O)-	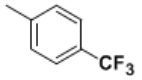	*(S)*-	13.3 ± 1.4
46	$-CH_2CH_3$	-O-	-C(O)-	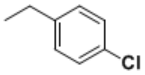	*(S)*-	1.6 ± 0.2
47	-H	-O-	-C(O)-	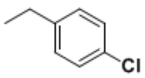	*(R)*-	0.27 ± 0.03
52	$-CH_3$	$-CH_2-$	$-SO_2-$	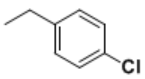	*(S)*-	151 ± 36

5.2.7. THIQ3CA Core is the Most Optimal Scaffold. Based on the number of flexible carbons constituting the core scaffold, we reasoned that the open-chain PA core will be more flexible than the six-membered cyclic P2CA and P3CA cores, which in turn will exhibit greater flexibility than the unsaturated or bridged THP2CA and ABH3CA cores. The THIQ3CA core was likely to be similar to the unsaturated or bridged cores in terms of conformational flexibility. Table 5 displays the potency of selected PA, P2CA, P3CA, THP2CA, ABH3CA, and THIQ3CA inhibitors. Overall, the potencies of PA, P2CA, and P3CA dicarboxamide inhibitors were found to be weak (23 – 371 μM), while those for THP2CA, ABH3CA and THIQ3CA inhibitors were higher (0.27 – 56 μM). Comparison of the unsaturated or bridged six-membered scaffold with the THIQ3CA scaffold shows that the latter is the optimal structure. For example, THP2CA derivative **84** and ABH3CA derivative **87** exhibit IC_{50}s of 9.1 and 10 μM, which are 33–37-fold greater than the 0.27 μM IC_{50} of the corresponding THIQ3CA derivative **47** (Table 11).

Within these broad results, we noticed interesting structure-activity dependence across the different core scaffolds studied here. Nearly all 5-chloro-thiophenyl containing derivatives, e.g., **23** and **40**, display weak inhibition potency in comparison to most *p*-chlorophenyl containing derivatives, e.g., **27** and **41** (Tables 8 and 9). This was against our expectation based on the well established high affinity of rivaroxaban, which contains the 5-chloro-thiophenyl side chain [22, 30]. Another interesting observation was that the morpholin-3-one ring consistently induces higher potency than the piperid-2-one ring. For example, morpholin-3-one-containing THIQ3CA derivatives **18**, **20**, and **40** have better activity than the corresponding piperid-2-one-containing derivatives **13**, **12**, and **23**, respectively (see Tables 7, 8 and 9).

Table 11. Comparison of the FXa inhibition potential of different scaffolds.

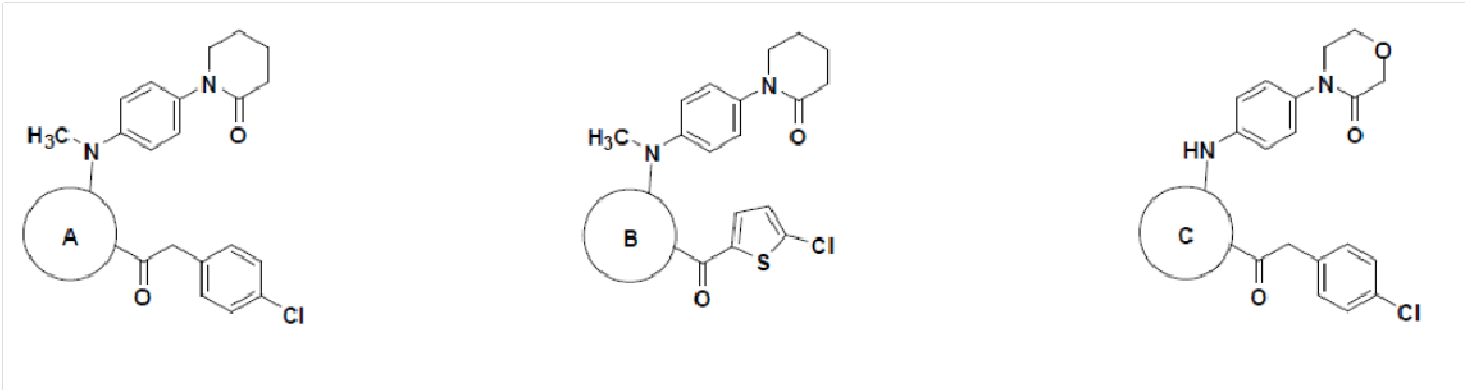

Inhibitor	A	IC_{50} *(μM)*
27	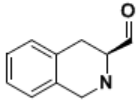	1.3 ± 0.1
59	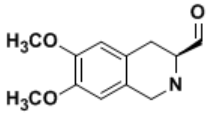	7.8 ± 0.4
62	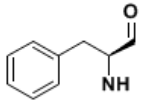	54 ± 5
72	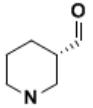	371 ± 59

Inhibitor	B	IC_{50} *(μM)*
23	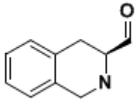	56 ± 2
78	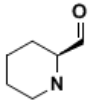	358 ± 16
79	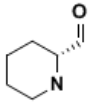	99 ± 7
69	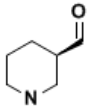	69 ± 7

Inhibitor	C	IC_{50} *(μM)*
47	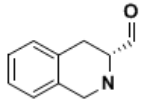	0.27 ± 0.03
81	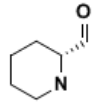	23 ± 2
84	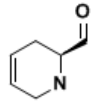	9 ± 2
87	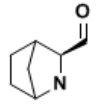	10 ± 3

The above results suggest that the THIQ3CA core scaffold was the optimal for FXa inhibition following optimization of its two arms A_N and A_C. Yet, the THP2CA and ABH3CA scaffolds are interesting. These scaffolds are new, readily synthesizable and are relatively unexplored. Screening of a wider chemical space would help better understand their true potential for FXa inhibition.

5.2.8. Dicarboxamide 47 Selectively Inhibits Factor Xa in Comparison to Other Proteases of the Coagulation and Digestive Systems. A critical goal of the molecular modeling-based rational design of THIQ3CA inhibitors was selectivity for targeting factor Xa. This enzyme is a trypsin-like serine protease with considerable homology with enzymes of the coagulation and digestive systems including FIIa, FVIIa, FIXa, FXIa, FXIIa, trypsin and chymotrypsin. Chromogenic substrate hydrolysis assays for each of these enzymes were performed in a manner similar to that for FXa. The assays were conducted at 37 ºC using literature reported buffer systems that are as close to physiological conditions as possible. Initial screening was performed at a high, fixed concentration of the inhibitor (100 – 1000 μM) and fractional residual enzyme activity was measured from the initial rate of hydrolysis in the presence of the inhibitor to that in its absence.

The THIQ3CA inhibitors showed high selectivity for FXa inhibition. No coagulation enzyme was found to be inhibited by THIQ3CA inhibitors at concentrations less than 100 μM. With regard to digestive enzymes, moderate inhibition of chymotrypsin (IC_{50} = 5–100 μM) was noted with 4-chlorophenyl side chain containing inhibitors. The most potent FXa inhibitor **47** demonstrated a selectivity of at least 1852–fold over FIIa, FVIIa, FIXa, FXIa, and FXIIa (Table 12). Against trypsin and chymotrypsin, the selectivity of **47** was found to be at least 370- and 279-

fold, respectively. Few rationally designed inhibitors have been able to achieve such high selectivity for factor Xa against other homologous enzymes.[258,259]

Table 12. Selectivity of inhibition by THIQ3CA dicarboxamide **47**.

Protease	IC_{50} *(μM)*	Selectivity Index
Human FIIa	>500	>1852
Human FVIIa	>1000	>3703
Human FIXa	>1000	>3703
Human FXIa	>500	>1852
Human FXIIa	>500	>1852
Bovine Trypsin	>100	>370
Bovine Chymotrypsin	75 ± 13	279

5.2.9. Prolongation of Plasma Clotting Times by THIQ3CA, THP2CA and ABH3CA Inhibitors. Clotting assays, prothrombin and activated partial thromboplastin time (PT and aPTT, respectively), are routinely used to assess anticoagulation potential of new enzyme inhibitors in an *in vitro* setting.[233,260,261] Whereas PT measures the effect of an inhibitor on the extrinsic pathway of coagulation, aPTT measures the effect on the intrinsic pathway. The prolongation of the human plasma clotting time as a function of the concentration of the inhibitors followed a pattern typical of other well-studied anticoagulants, except for the range of active concentrations. Table 13 lists the concentrations of selected potent FXa inhibitors required to double the PT and aPTT. Overall, for the inhibitors studied, doubling the PT required 17–2347 μM concentration, while doubling of aPTT required 20–810 μM, suggesting that most inhibitors essentially affect both pathways equally (Figure 27). This is to be expected because of their selectivity for targeting FXa, which is

an enzyme of the common pathway. The inhibitors studied included THIQ3CA derivatives **20**, **27**, **34**, **42**, **47**, and **49**, and THP2CA/ ABH3CA derivatives **84** and **87**. Inhibitor **47** doubled the PT clotting time at 17.1 μM, which is comparable to razaxaban (3.8 μM) and DPC423 (4.9 μM), two direct FXa inhibitors being pursued in clinical trials.[258]

Table 13. Effect of designed FXa dicarboxamide inhibitors on human plasma clotting time.

Inhibitor	**PT** *(μM)*	**aPTT** *(μM)*
20	1387	ND[a]
27	71	80
34	219	260
42	2160	ND[a]
47	17.1	20.2
49	645	614
84	952	810
87	2347	ND[a]

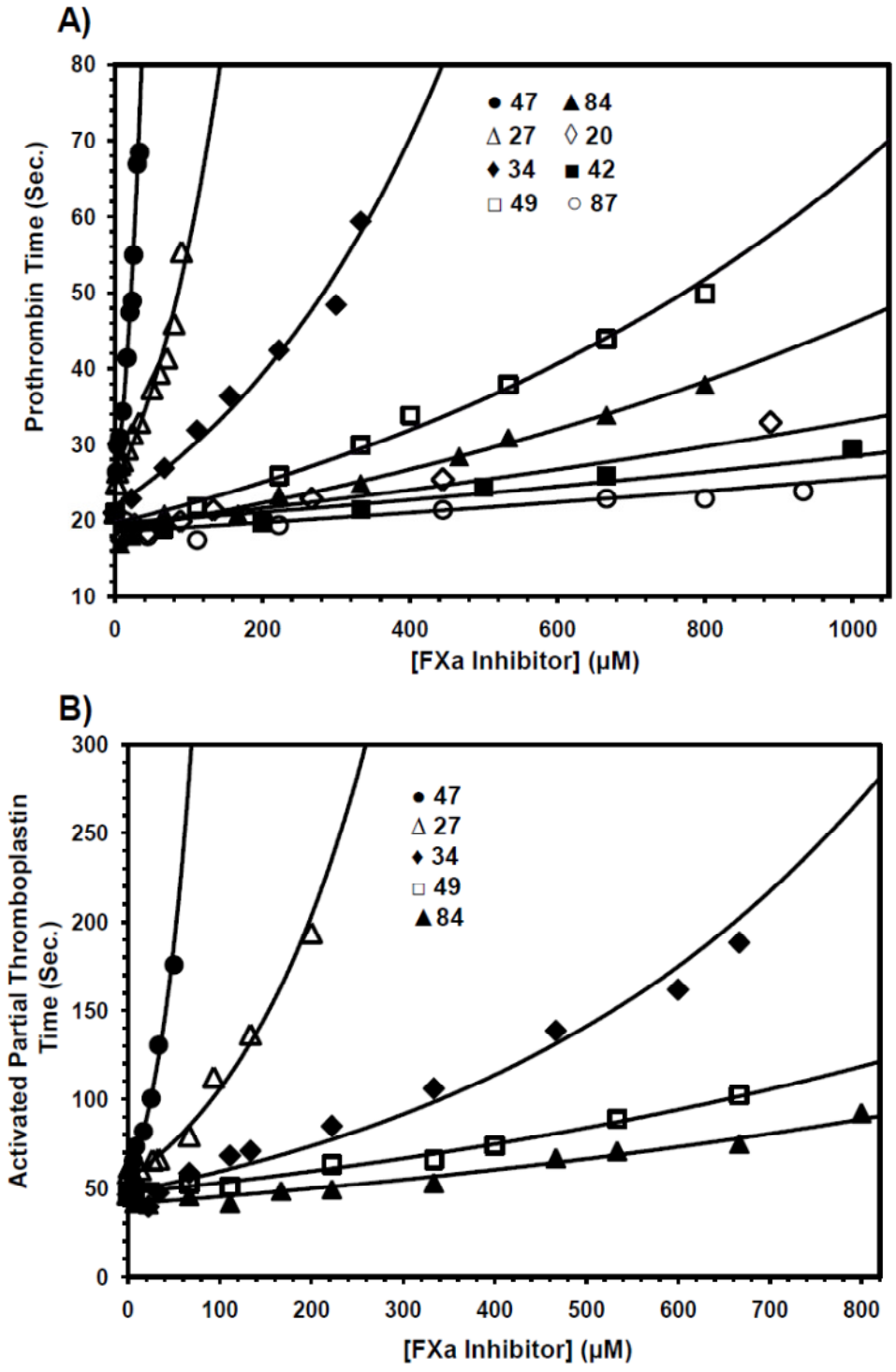

Figure 27. Prolongation of clotting time as a function of concentration of designed THIQ3CA and related dicarboxamides in either prothrombin time assay (PT) (A) or activated partial thromboplastin time assay (aPTT) (B). Solid lines are trend lines from which the concentration necessary to double clotting time was deduced. Clotting assays were performed in duplicate (SE ≤ 10%) as described in Experimental Methods.

5.3. Conclusion— Direct inhibition of FXa carries significant promise for developing effective and safe anticoagulants. Although a large number of FXa inhibitors have been studied, each can be classified as either possessing a highly flexible or a rigid core scaffold. We reasoned that an intermediate level of flexibility will provide high selectivity for FXa considering that its active site is less constrained in comparison to thrombin and more constrained as compared to trypsin. We studied several core scaffolds including 1,2,3,4-tetrahydroisoquinoline-3-carboxylic acid for direct FXa inhibition. Using docking and scoring with GOLD, a promising candidate **23** was identified, synthesized, and found to inhibit FXa with a K_i of 28 μM. Optimization of derivative **23** resulted in the design of a potent dicarboxamide **47**, which displayed a K_i of 0.135 μM. Dicarboxamide **47** displayed at least 1852-fold selectivity for FXa inhibition over other coagulation enzymes and doubled PT and aPTT of human plasma at 17.1 μM and 20.2 μM, respectively, which are comparable to those of clinically relevant agents. Dicarboxamide **47** is expected to serve as an excellent lead for further anticoagulant discovery.

5.4. Experimental Section—

5.4.1. Chemicals, Reagents, and Analytical Chemistry. Anhydrous CH_2Cl_2, THF, CH_3CN, DMF, toluene, and acetone were purchased from Sigma-Aldrich (Milwaukee, WI) or Fisher (Pittsburgh, PA) and used as such. Other solvents used were of reagent gradient and used as purchased. Analytical TLC was performed using UNIPLATE^{TM} silica gel GHLF 250 μm pre-coated plates (ANALTECH, Newark, DE). Column chromatography was performed using silica gel (200-400 mesh, 60 Å) from Sigma-Aldrich. Chemical reactions sensitive to air or moisture were carried out under nitrogen atmosphere in oven-dried glassware. Reagent solutions, unless otherwise noted, were handled under a nitrogen atmosphere using syringe techniques. Flash chromatography was performed using Teledyne ISCO (Lincoln, NE) Combiflash RF system and

disposable normal silica cartridges of 30–50 μm particle size, 230–400 mesh size and 60 Å pore size. The flow rate of the mobile phase was in the range of 18 to 35 mL/min and mobile phase gradients of ethyl acetate/hexanes and CH_2Cl_2/CH_3OH were used to elute compounds.

5.4.2. Chemical Characterization of Compounds. ^1H and ^{13}C NMR were recorded on Bruker-400 MHz spectrometer in either $CDCl_3$, CD_3OD, or acetone-d_6. Signals, in part per million (ppm), are either relative to the internal standard (tetramethyl silane, TMS) or to the residual peak of the solvent. The NMR data are reported as chemical shift (ppm), multiplicity of signal (s= singlet, d= doublet, t= triplet, q= quartet, dd= doublet of doublet, m= multiplet), coupling constants (Hz), and integration. Compounds with dicarboxamide functionalities exhibit amide rotamerism resulting in complexity of NMR signals. ESI-MS of compounds were recorded using Waters Acquity TQD MS spectrometer in positive ion mode. Samples were dissolved in methanol and infused at a rate of 20 μL/min. Mass scans were obtained in the range of 200-700 amu with a scan time of 1 s and a scan rate of 500 amu/s. The capillary voltage was varied between 3 and 4 kV, while the cone voltage ranged from 38 to 103 V. Ionization conditions were optimized for each compound to maximize the ionization of the parent ion. Generally, the extractor voltage was set to 3 V, the Rf lens voltage was 0.1 V, the source block temperature was set to 150 ºC, and the desolvation temperature was about 250 ºC. The purity of each final compound was greater than 95% as determined by uPLC-MS.

5.4.3. Proteins. Human plasma proteinases including FIIa, FXa, FXIa, FIXa, FVIIa, and recombinant tissue factor was obtained from Haematologic Technologies (Essex Junction, VT). FXIIa was purchased from Enzyme Research Laboratories (South Bend, IN). Bovine α-chymotrypsin and bovine trypsin were obtained from Sigma-Aldrich (St. Louis, MO). The substrates Spectrozyme TH, Spectrozyme FXa, Spectrozyme FXIIa, Spectrozyme FIXa,

Spectrozyme VIIa, and Spectrozyme CTY were obtained from American Diagnostica (Greenwich, CT). Factor IXa substrate, S-2366, trypsin substrate, S-2222, were obtained from Diapharma (West Chester, OH). Factor Xa and FVIIa were prepared in 20 mM TrisHCl buffer, pH 7.4, containing 100 mM NaCl, 2.5 mM $CaCl_2$, 0.1% PEG8000, and 0.02% Tween80. FIXa was prepared in 20 mM TrisHCl buffer, pH 7.4, containing 100 mM NaCl, 2.5 mM $CaCl_2$, 0.1% PEG8000, 0.02% Tween80, and 33% v/v Ethylene glycol. Other enzymes were prepared in 50 mM TrisHCl buffer, pH 7.4, containing 150 mM NaCl, 0.1% PEG8000, and 0.02% Tween80.

5.4.4. Modeling Factor Xa and the Virtual Library of (*S*)-THIQ3CA Dicarboxamides. Sybyl 8.1 (Tripos Associates, St. Louis, MO) was used for modeling of FXa–inhibitor complexes. The structure of human FXa (ID: 2P16)[119] was acquired from the Protein Data Bank (www.rcsb.org). To prepare the protein structure for modeling experiments, hydrogen atoms were added, while inorganic ions and water molecules were removed. Individual atoms were assigned Gasteiger –Hückel charges. Energy minimization was then performed using a Tripos force field so as to reach a terminating gradient of 0.5 kcal/mol $Å^2$ or a maximum of 100,000 iterations.

(S)–THIQ3CA was modified *in silico* at positions 2 and 3 with appropriate substituents to "synthesize" a virtual chemical library of nearly 150 dicarboxamide derivatives. The different combinations at 2- and 3-positions included substituted derivatives of aromatic carboxylic acids and aromatic amines, respectively. These acids and amines were further substituted at varying positions with halogen, *t*–butyl, cyclopropyl, methoxy, amino–methyl, substituted phenyl, substituted imidazole, pyridine, pyridine–2–one, *N*–oxide pyridine, *N*-methyl piperazine, or cyclic amides such as piperidone and morpholinone. The resulting molecules were assigned Gasteiger –Hückel charges and were then energetically minimized using a Tripos force field until a terminating gradient of 0.5 kcal/mol $Å^2$ or a maximum of 100,000 iterations.

5.4.5. Docking and Scoring. Docking of the *(S)*-THIQ3CA dicarboxamides onto the active site of FXa was performed with GOLD 5.1 (Cambridge Crystallographic Data Center, UK). The docking experiment was performed as reported earlier.[231] The binding site in human FXa was defined to include all atoms within 6 Å of the co–crystallized ligand. The docking protocol was validated by docking a ligand for which the adopted docking pose was found to have RMSD < 1 Å relative to that reported in the crystal structure.[119] Docking was driven by the GOLD scoring function, while for ranking the docked solutions; a linear, modified form of the same scoring function equation 7 was used, as reported earlier.[231] In this equation, HB_{EXT} and VDW_{EXT} are the "external" (nonbonded interactions taking place between the ligand and the target protein) hydrogen bonding and van der Waals terms, respectively.

$$GOLD_{Score} = HB_{EXT} + 1.375 \times VDW_{EXT} \qquad (7)$$

5.4.6. FXa Inhibition Studies. Direct inhibition of FXa was measured by a chromogenic substrate hydrolysis assay, as reported earlier [257] using a microplate reader (FlexStation III, Molecular Devices) at a wavelength of 405 nm and incubating temperature of 37 ºC. Generally, each well of the 96-well microplate had 185 µL pH 7.4 buffer to which 5 µL potential FXa inhibitor (or solvent reference) was added, to which 5 µL FXa (stock conc. 43.5 nM) was further added. After 10 min incubation at 37 ºC, 5 µL FXa substrate (stock conc. 5 mM) was rapidly added and the residual FXa activity was measured from the initial rate of increase in absorbance at 405 nm. The concentration of the organic solvent in which the inhibitors were dissolved was maintained constant and was less than 2.5% (v/v). Stocks of FXa inhibitors were prepared at 20 mM concentration and then serially diluted to give twelve different aliquots spanning a range of 0.015-500 µM in the plate wells. Each inhibitor was studied in duplicate or triplicate at each concentration. Relative residual FXa activity at each concentration of the inhibitor was calculated

from the ratio of FXa activity in the presence and absence of the inhibitor. Logistic Eq. 8 was used to fit the dose-dependence of residual proteinase activity to obtain the potency (IC_{50}) and efficacy (ΔY) of inhibition. In this equation, Y is the ratio of residual factor Xa activity in the presence of inhibitor to that in its absence (fractional residual activity), Y_M and Y_0 are the maximum and minimum possible values of the fractional residual proteinase activity, IC_{50} is the concentration of the inhibitor that results in 50% inhibition of enzyme activity, and HS is the Hill slope (which was between 0.7 and 1.2 in all measurements). Nonlinear curve fitting resulted in Y_M, Y_0, IC_{50} and HS values. The reported IC_{50} is an average of the two or three measurements with standard error (SE) of <20%. The efficacy of inhibition ΔY was found to be >80% for each studied FXa inhibitor.

$$Y = Y_0 + \frac{Y_M - Y_0}{1 + 10^{(Log[I]_0 - Log\ IC_{50})(HS)}} \qquad (8)$$

5.4.7. Inhibition of Proteases of the Coagulation and Digestive Systems. The potential of the FXa inhibitors against coagulation enzymes including FIIa, FVIIa, FIXa, FXIa, and FXIIa, and digestive enzymes including trypsin and chymotrypsin was performed using chromogenic substrate hydrolysis assays reported in the literature.[262] These assays were performed using substrates appropriate for the enzyme being studied under conditions closest to the physiological condition (37 ºC and pH 7.4), except for FIIa, which was performed at 25 ºC and pH 7.4. For selectivity analysis, single concentration point assay was utilized in which 0.5 – 1 mM FXa inhibitor was tested in duplicate. The fractional residual enzyme activity was measured and if found to be less than 50%, the inhibition profile was measured over a range of inhibitor concentrations to determine the IC_{50} of the enzyme–inhibitor complex. The K_M of the substrate for its enzyme was used to identify the concentration of the substrate to be used for inhibition studies. The concentrations of enzymes and substrates in microplate cells were: 6 nM and 50 μM for FIIa; 0.765 nM and 345 μM for FXIa; 5 nM and 125 μM for FXIIa; 89 nM and 850 μM for FIXa; 8 nM

and 1000 μM for FVIIa (along with 40 nM recombinant tissue factor); 72.5 ng/ml and 80 μM for bovine trypsin; and 500 ng/ml and 240 μM for bovine chymotrypsin.

5.4.8. Prothrombin Time (PT) and Activated Partial ThromboplastinTime (aPTT). Clotting time was measured in a standard one-stage recalcification assay with a BBL Fibrosystem fibrometer (Becton-Dickinson, Sparles, MD), as described previously.[233] For PT assays, thromboplastin was reconstituted according to the manufacturer's directions and warmed to 37 ºC. A 10 μL sample of the FXa inhibitor, to give the desired concentration, was brought up to 100 μL with citrated human plasma, incubated for 30 s at 37º C followed by addition of 200 μL of prewarmed thromboplastin. For the aPTT assay, 10 μL of inhibitor was mixed with 90 μL of citrated human plasma and 100 μL of prewarmed aPTT reagent (0.2% ellagic acid). After incubation for 4 min at 37 ºC, clotting was initiated by adding 100 μL of prewarmed 25 mM $CaCl_2$ and time to clot noted. The data were fit to a quadratic trendline, which was used to determine the concentration of the inhibitor necessary to double the clotting time. Clotting time in the absence of an anticoagulant was determined in similar fashion using 10 μL of deionized water and/or appropriate organic vehicle and was found to be 21.0 s for PT and 46.4 s for aPTT.

5.4.9. General Synthetic Procedures and Spectral Characterization Data—

***N*-(4-bromophenyl)acetamide (2).** To a stirred solution of 4-bromoaniline (**1**) (1 mmol) in anhydrous CH_2Cl_2 (4 mL) was added anhydrous pyridine (2 mmol) at RT, followed by drop-wise addition of acetic anhydride (1.5 mmol). After 4 h, the reaction mixture was diluted with CH_2Cl_2 (10 mL) and washed with 2.0 N HCl aqueous solution (2 × 10 mL). The organic phase was then concentrated by rotary evaporator and the resulting crude was purified by flash chromatography using gradient of EtOAc/hexanes as mobile phase to provide the titled acetylated product as violet solid in 92% yield. ^{1}H-NMR ($CDCl_3$, 400 MHz): 7.42 (d, J = 9.12 Hz, 2 H), 7.39 (d, J = 9.24 Hz,

2 H), 2.17 (s, 3 H). ^{13}C-NMR ($CDCl_3$, 100 MHz): 168.22, 136.94, 131.96, 121.37, 116.88, 24.57. MS (ESI) calculated for C_8H_8BrNO, $[M+H]^+$, *m/z* 213.99, found for $[M+H]^+$, *m/z* 214.11.

N-ethyl-4-bromoaniline (4b). To a stirred solution of N-(4-bromophenyl)acetamide (**2**) (1 mmol) in anhydrous THF (5 mL) was added $LiAlH_4$ (2.0 M in THF, 3 mmol) at 0 ^{0}C under nitrogen atmosphere. The reaction mixture was allowed to warm up to RT and was kept stirring overnight. The reaction mixture was then diluted with THF (10 mL). Water (1 mL) was added slowly, followed by 10% aqueous NaOH (2 mL), and followed finally by water (3 mL). The precipitating aluminum salts were filtered off on a pressed plug of Celite. The filtrate was concentrated *in vacuo* and purified by flash chromatography using gradient of EtOAc/hexanes to provide the titled product as brown solid in 60% yield. ^{1}H-NMR ($CDCl_3$, 400 MHz): 7.24 (d, J = 8.88 Hz, 2 H), 6.47 (d, J = 8.88 Hz, 2 H), 3.14 (d, J = 7.12 Hz, 1 H), 3.10 (d, J = 7.12 Hz, 1 H), 1.24 (t, J = 7.12 Hz, 3 H). ^{13}C-NMR ($CDCl_3$, 100 MHz): 147.39, 131.90, 114.26, 112.27, 38.49, 14.72. MS (ESI) calculated for $C_8H_{10}BrN$, $[M+H]^+$, *m/z* 200.01, found for $[M+H]^+$, *m/z* 200.1.

4-bromo-N-isopropylaniline (4c). A mixture of 4-bromoaniline (**1**) (1 mmol), acetone (1.5 mmol), titanium (IV) isopropoxide (1 mmol), and ethanol (4 mL) was stirred for 12 h at RT to give the brown solution of imine (**3**). To the light brown solution was added sodium borohydride ($NaBH_4$, 2 mmol) portion-wise over 10 min, and then the resulting solution was stirred for 2 h. The reaction mixture was cooled to 0 °C and quenched with 2.0 N aqueous NH_3 (10 mL). The resulting precipitate was filtered off and further washed with ether. The filtrate volume was reduced by rotary evaporator and extracted by ether (3 X 20 mL). The organic extracts were combined, washed with brine solution, dried over anhydrous Na_2SO_4, and finally filtered. The organic filtrate was concentrated *in vacuo* and the residue was purified by flash chromatography using gradient mobile phase of EtOAc/hexanes to afford the titled compound as brown solid in 75% yield. ^{1}H-

NMR ($CDCl_3$, 400 MHz): 7.22 (d, J = 8.92 Hz, 2 H), 6.44 (d, J = 8.92 Hz, 2 H), 3.59-3.53 (m, 1 H), 1.18 (d, J = 6.28 Hz, 6 H). ^{13}C-NMR ($CDCl_3$, 100 MHz): 146.52, 131.93, 114.76, 108.35, 44.32, 22.83. MS (ESI) calculated for $C_9H_{12}BrN$, $[M+H]^+$, *m/z* 214.02, found for $[M+H]^+$, *m/z* 214.11.

1-(4-(4-nitrophenyl)piperazin-1-yl)ethanone (7a). To a stirred solution of 1-(4-nitrophenyl) piperazine (**6**) (1 mmol) in anhydrous CH_2Cl_2 (4 mL) was added anhydrous pyridine (2 mmol) at RT, followed by drop-wise addition of acetic anhydride (1.5 mmol). After 4 h, the reaction mixture was diluted with CH_2Cl_2 (10 mL) and washed with 2.0 N HCl aqueous solution (2 X10 mL). The organic phase was then concentrated by rotary evaporator and the resulting crude was purified by flash chromatography using gradient of EtOAc/hexanes as mobile phase to provide the titled acetylated product in 84% yield. ^{1}H-NMR ($CDCl_3$, 400 MHz): 8.08 (d, J = 9.36 Hz, 2 H), 6.78 (d, J = 9.36 Hz, 2 H), 3.75-3.60 (m, 4 H), 3.40-3.37 (m, 4 H), 2.09 (s, 3 H). ^{13}C-NMR ($CDCl_3$, 100 MHz): 169.21, 154.19, 139.39, 125.95, 113.24, 47.15, 21.25. MS (ESI) calculated for $C_{12}H_{15}N_3O_3$, $[M+H]^+$, *m/z* 250.27, found for $[M+H]^+$, *m/z* 250.12.

(4-(4-nitrophenyl)piperazin-1-yl)(thiophen-2-yl)methanone (7b). ^{1}H-NMR ($CDCl_3$, 400 MHz): 8.07 (d, J = 9.40 Hz, 2 H), 7.44-7.42 (dd, J = 1.04 Hz, J = 5 Hz, 1 H), 7.30-7.29 (dd, J = 1.08 Hz, J = 3.68 Hz, 1 H), 3.03-3.01 (m, 1 H), 6.77 (d, J = 9.4 Hz, 2 H), 3.89 (t, J = 5.24 Hz, 4 H), 3.45 (t, J = 5.44 Hz, 4 H). ^{13}C-NMR ($CDCl_3$, 100 MHz): 163.81, 154.16, 139.39, 136.45, 129.39, 129.33, 126.95, 126.04, 125.96, 113.20, 112.55, 47.21, 46.25. MS (ESI) calculated for $C_{15}H_{15}N_3O_3S$, $[M+H]^+$, *m/z* 318.76, found for $[M+H]^+$, *m/z* 3.18.09.

General Procedure for Nucleophilic Amidation of Halogenated Aniline Derivatives 8a-8g. An oven-dried, two-neck round bottom flask fitted with a condenser was charged with CuI

(0.05 mmol) and K_2CO_3 (2.0 mmol) under nitrogen atmosphere. *N, N'*-dimethylethylenediamine (0.10 mmol), 4-haloaniline derivative (**4a**–**4c**) (1.0 mmol), piperidin-2-one (**5a**) or morpholin-3-one (**5b**) (1.5 mmol), and anhydrous toluene (1 mL) were added. The reaction mixture was stirred and refluxed overnight. The resulting mixture was allowed to reach RT and filtered through Celite, which was further washed with methanol (10 mL). The organic filtrate was concentrated *in vacuo* and the residue was purified by flash chromatography using gradient mobile phase of EtOAc/hexanes to afford the corresponding *para*-amidated aniline derivatives (**8a–8g**) as solid products in 65-90% yield.

1-(4-aminophenyl)piperidin-2-one (8a). ^{1}H-NMR ($CDCl_3$, 400 MHz): 7.00 (d, J = 8.76 Hz, 2 H), 6.56 (d, J = 8.76 Hz, 2 H), 3.56 (t, J = 5.44 Hz, 2 H), 2.52 (t, J = 5.24 Hz, 2 H), 1.92-1.89 (m, 4 H). ^{13}C-NMR ($CDCl_3$, 100 MHz): 170.11, 146.25, 132.89, 127.19, 113.35, 52.17, 32.88, 23.04, 21.20. MS (ESI) calculated for $C_{11}H_{14}N_2O$, $[M+H]^+$, *m/z* 191.25, found for $[M+H]^+$, *m/z* 191.98.

4-(4-aminophenyl)morpholin-3-one (8b). ^{1}H-NMR ($CDCl_3$, 400 MHz): 7.00 (d, J= 8.64 Hz, 2 H), 6.62 (d, J= 8.68 Hz, 2 H), 4.24 (s, 2 H), 3.93 (t, J= 5.2 Hz, 2 H), 3.61 (t, J = 5.24 Hz, 2 H). ^{13}C-NMR ($CDCl_3$, 100 MHz): 166.85, 147.59, 130.92, 127.00, 126.71, 113.25, 112.98, 68.62, 64.25, 50.27. MS (ESI) calculated for $C_{10}H_{12}N_2O_2$, $[M+H]^+$, *m/z* 193.22, found for $[M+H]^+$, *m/z* 193.26.

1-(4-(methylamino)phenyl)piperidin-2-one (8c). ^{1}H-NMR (acetone-d_6, 400 MHz): 6.84 (d, J= 8.68 Hz, 2 H), 6.42 (d, J = 8.72 Hz, 2 H), 3.43 (t, J = 5.44 Hz, 2 H), 2.62 (s, 3 H), 2.22 (t, J = 6.44 Hz, 2 H), 1.76-1.73 (m, 4 H). ^{13}C-NMR (acetone-d_6, 100 MHz): 169.23, 149.28, 134.28, 127.94, 112.57, 52.57, 33.66, 29.60, 24.51, 22.39. MS (ESI) calculated for $C_{12}H_{16}N_2O$, $[M+H]^+$, *m/z* 205.28, found for $[M+H]^+$, *m/z* 205.48.

4-(4-(methylamino)phenyl)morpholin-3-one (8d). ^{1}H-NMR ($CDCl_3$, 400 MHz): 7.10-7.08 (dd, J = 2.00 Hz, J = 8.60 Hz, 2 H), 6.62-6.59 (dd, J = 2.00 Hz, J = 8.60 Hz, 2 H), 4.31 (s, 2 H), 4.00 (t, J = 3.88 Hz, 2 H), 3.69 (t, J = 3.28 Hz, 2 H), 2.83 (s, 3 H). ^{13}C-NMR ($CDCl_3$, 100 MHz): 166.94, 148.50, 132.16, 130.94, 115.04, 68.57, 64.21, 50.27, 30.70. MS (ESI) calculated for $C_{11}H_{14}N_2O_2$, $[M+H]^+$, *m/z* 207.25, found for $[M+H]^+$, *m/z* 207.57.

1-(4-(ethylamino)phenyl)piperidin-2-one (8e). ^{1}H-NMR ($CDCl_3$, 400 MHz): 7.08 (d, J= 8.64 Hz, 2 H), 6.97 (d, J= 8.64 Hz, 2 H), 3.23 (t, J= 5.12 Hz, 2 H), 3.16-3.11 (q, J = 7.16 Hz, J = 14.28 Hz, 2 H), 2.27 (t, J= 6.36 Hz, 2 H), 1.73-1.67 (m, 4 H), 1.24 (t, J = 7.20 Hz, 3 H). ^{13}C-NMR ($CDCl_3$, 100 MHz): 169.35, 141.14, 126.33, 125.41, 117.35, 50.85, 41.96, 31.83, 22.52, 21.19, 12.55. MS (ESI) calculated for $C_{13}H_{18}N_2O$, $[M+H]^+$, *m/z* 219.30, found for $[M+H]^+$, *m/z* 219.15.

4-(4-(ethylamino)phenyl)morpholin-3-one (8f). ^{1}H-NMR ($CDCl_3$, 400 MHz): 7.01 (d, J= 8.76 Hz, 2 H), 6.53 (d, J = 8.72 Hz, 2 H), 4.24 (s, 2 H), 3.92 (t, J= 4.92 Hz, 2 H), 3.61 (t, J = 5.28 Hz, 2 H), 3.10-3.05 (q, J = 7.12 Hz, J = 14.28 Hz, 2 H), 1.18 (t, J = 7.16 Hz, 3 H). ^{13}C-NMR ($CDCl_3$, 100 MHz): 166.85, 147.59, 130.92, 127.00, 126.71, 113.25, 112.98, 68.62, 64.25, 50.27, 38.49, 41.83. MS (ESI) calculated for $C_{12}H_{16}N_2O_2$, $[M+H]^+$, *m/z* 221.28, found for $[M+H]^+$, *m/z* 221.26.

1-(4-(isopropylamino)phenyl)piperidin-2-one (8g). ^{1}H-NMR (acetone-d_6, 400 MHz): 6.82 (d, J= 8.84 Hz, 2 H), 6.43 (d, J = 8.84 Hz, 2 H), 3.52-3.50 (m, 1 H), 3.45 (t, J = 5.00 Hz, 2 H), 2.24 (t, J= 6.68 Hz, 2 H), 1.84-1.70 (m, 4 H), 1.11 (d, J = 6.32 Hz, 6 H). ^{13}C-NMR (acetone-d_6, 100 MHz): 169.63, 147.32, 134.14, 127.64, 113.52, 52.54, 44.70, 33.78, 24.51, 22.99, 22.37. MS (ESI) calculated for $C_{14}H_{20}N_2O$, $[M+H]^+$, *m/z* 233.33, found for $[M+H]^+$, *m/z* 233.08.

General Procedure for Catalytic Hydrogenation of Nitro Group for Synthesis of 8i and 8j. 4-Nitrophenylpiperazine (**7a** or **7b**) and 10% Pd/C was mixed in methanol (10 mL)

containing concentrated HCl (2 mL). Hydrogen gas was then pumped into the mixture at RT. After stirring the solution for 5 h, the catalyst was filtered on Celite and the organic filtrate concentrated *in vacuo* to afford the corresponding aniline derivative (**8i** and **8j**) in ~100% yield.

1-(4-(4-aminophenyl)piperazin-1-yl)ethanone (8i). ^{1}H-NMR ($CDCl_3$, 400 MHz): 6.81 (d, J = 8.76 Hz, 2 H), 6.66 (d, J = 8.76 Hz, 2 H), 3.75 (t, J = 5.08 Hz, 2 H), 3.60 (t, J = 4.92 Hz, 2 H), 3.01 (t, J = 5.20 Hz, 2 H), 2.98 (t, J = 5.12 Hz, 2 H), 2.13 (s, 3 H). ^{13}C-NMR ($CDCl_3$, 100 MHz): 168.98, 144.04, 140.90, 119.32, 116.17, 51.55, 51.14, 46.51, 41.61, 21.33. MS (ESI) calculated for $C_{12}H_{17}N_3O$, $[M+H]^+$, *m/z* 220.29, found for $[M+]^+$, *m/z* 220.15.

(4-(4-aminophenyl)piperazin-1-yl)(thiophen-2-yl)methanone (8j). ^{1}H-NMR (acetone-d_6, 400 MHz): 7.57 (d, J = 4.96 Hz, 1 H), 7.34 (d, J = 3.56 Hz, 1 H), 7.03 (d, J = 4.32 Hz, 1 H), 6.86 (d, J = 8.64 Hz, 2 H), 6.54 (d, J = 8.60 Hz, 2 H), 3.77 (t, J = 4.96 Hz, 4 H), 3.08 (t, J = 5.16 Hz, 4 H). ^{13}C-NMR (acetone-d_6, 100 MHz): 163.60, 148.27, 138.75, 129.72, 127.70, 122.94, 121.33, 120.06, 118.43, 116.14, 52.39, 51.20. MS (ESI) calculated for $C_{15}H_{17}N_3OS$, $[M+H]^+$, *m/z* 288.39, found for $[M+H]^+$, *m/z* 288.25.

General Procedure for Deprotection of *t*-Butyloxycarbonyl (Boc) Group of 16, 17, 21, 61, 76, 77, 80, 83, or 86. To a solution of 1,2,3,4-tetrahydroisoquinoline carboxamides (**16**, **17**, **21**), phenylalanine carboxamide (**61**), piperidine-2-carboxamides (**76**, **77**, **80**), 1,2,3,6-tetrahydropyridine-2-carboxamides (**83**), or 2-azabicyclo[2.2.1] heptane-3-carboxamides (**86**) (1.0 mmol) in CH_2Cl_2 (5 mL), trifluoroacetic acid (TFA, 5 mL) was added drop-wise at 0 ºC, and the mixture was warmed to RT. After stirring for 4 h, the reaction mixture was diluted with CH_2Cl_2 (25 mL) and neutralized by drop-wise addition of saturated aqueous $NaHCO_3$ (20 mL). The organic layer was separated and the aqueous phase was extracted with EtOAc (2 × 25 mL). The organic extracts were combined, washed with saturated NaCl solution (25 mL), and dried over

anhydrous Na_2SO_4. Removal of the solvent under reduced pressure afforded the desired unprotected carboxamides in quantitative yields and sufficient purity (as indicated by TLC) to be directly used in the next reactions without any further treatment.

***(S)-tert*-butyl 3-(methyl(4-(2-oxopiperidin-1-yl)phenyl)carbamoyl)-3,4-dihydro-isoquinoline-2(1H)-carboxylate (16).** ^{1}H-NMR ($CDCl_3$, 400 MHz): 7.37-7.27 (m, 4 H), 7.12-6.92 (m, 4 H), 7.15-7.11 (m, 3 H), 4.91-7.37 (m, 3 H), 3.62 (t, J= 5.44 Hz, 2 H), 3.14 (s, 3 H), 2.8-2.65 (m, 1 H), 2.50 (t, J= 6.44 Hz, 2 H), 2.0-1.90 (m, 4 H), 1.42 (s, 9 H) . ^{13}C-NMR ($CDCl_3$, 100 MHz): 171.99, 170.05, 154.30, 142.71, 141.31, 134.73, 132.21, 128.13, 127.69, 127.27, 126.63, 125.74, 79.98, 51.39, 45.49, 38.05, 32.88, 31.29, 29.65, 28.52, 23.48, 21.33. MS (ESI) calculated for $C_{27}H_{33}N_3O_4$, $[M+H]^+$, *m/z* 464.58, found for $[M+Na]^+$, *m/z* 486.29.

***(R)-tert*-butyl 3-(methyl(4-(2-oxopiperidin-1-yl)phenyl)carbamoyl)-3,4-dihydro-isoquinoline-2(1H)-carboxylate (17).** ^{1}H-NMR ($CDCl_3$, 400 MHz): 7.37-7.25 (m, 4 H), 7.12-6.90 (m, 4 H), 7.17-7.11 (m, 3 H), 4.91-7.37 (m, 3 H), 3.62 (t, J= 5.45 Hz, 2 H), 3.14 (s, 3 H), 2.82-2.65 (m, 1 H), 2.50 (t, J= 6.42 Hz, 2 H), 2.1-1.911 (m, 4 H), 1.41 (s, 9 H) . ^{13}C-NMR ($CDCl_3$, 100 MHz): 172.01, 170.09, 154.30, 142.71, 141.31, 134.72, 132.21, 128.15, 127.69, 127.27, 126.63, 125.74, 79.98, 51.39, 45.49, 38.05, 32.87, 31.29, 29.65, 28.52, 23.51, 21.35. MS (ESI) calculated for $C_{27}H_{33}N_3O_4$, $[M+H]^+$, *m/z* 464.58, found for $[M+Na]^+$, *m/z* 486.29.

(*R*)-tert-butyl 3-(4-(3-oxomorpholino)phenylcarbamoyl)-3,4-dihydroisoquinoline-2(1H)-carboxylate (21). ^{1}H-NMR ($CDCl_3$, 400 MHz): 7.50-7.30 (m, 2 H), 7.28-7.10 (m, 6 H), 5.00-4.45 (m, 3 H), 4.31 (s, 2 H), 4.00 (t, J = 4.84 Hz, 2 H), 3.69 (t, J = 5.68 Hz, 2 H), 3.40-3.27 (m, 1 H), 3.23-3.00 (m, 1 H), 1.50 (s, 9 H). ^{13}C-NMR ($CDCl_3$, 100 MHz): 171.40, 166.73, 155.65, 133.77, 128.13, 126.73, 126.08, 120.57, 81.81, 68.57, 64.13, 49.75, 44.85, 28.38. MS (ESI) calculated for $C_{28}H_{27}N_3O_5$, $[M+H]^+$, *m/z* 452.52, found for $[M+Na]^+$, *m/z* 474.37.

(*S*)-tert-butyl 1-(methyl(4-(2-oxopiperidin-1-yl)phenyl)amino)-1-oxo-3-phenylpropan-2-ylcarbamate (61). ^{1}H-NMR ($CDCl_3$, 400 MHz): 7.30-7.12 (m, 5 H), 6.86-6.76 (m, 2 H), 6.75-6.66 (m, 2 H), 4.49-4.44 (q, J = 7.16 Hz, J = 15.08 Hz, 1 H), 3.60 (t, J = 4.84 Hz, 2 H), 3.12 (s, 3 H), 2.83-2.77 (dd, J = 7.60 Hz, J = 13.12, 1 H), 2.66-2.61 (dd, J = 6.20 Hz, J = 12.52 Hz, 1 H), 2.50 (t, J = 6.36, 2 H), 1.90-1.85 (m, 4 H), 1.31 (s, 9 H). ^{13}C-NMR ($CDCl_3$, 100 MHz): 171.79, 170.00, 154.82, 142.77, 140.39, 136.59, 129.38, 128.35, 127.92, 127.10, 126.68, 79.46, 52.27, 51.69, 39.86, 37.45, 32.30, 28.30, 23.53, 21.39. MS (ESI) calculated for $C_{26}H_{33}N_3O_4$, $[M+H]^+$, *m/z* 452.57, found for $[M+H]^+$, *m/z* 452.42.

***(S)-tert*-butyl 2-(methyl(4-(2-oxopiperidin-1-yl)phenyl)carbamoyl)piperidine-1-carboxylate (76).** ^{1}H-NMR ($CDCl_3$, 400 MHz): 7.36-7.31 (m, 4 H), 7.06 (d, J = 3.04 Hz, 1 H), 6.83 (d, J = 3.92 Hz, 1 H), 4.85-4.86 (m, 1 H), 3.85-3.72 (m, 1 H), 3.60 (t, J = 5.16 Hz, 2 H), 3.55-3.46 (m, 1 H), 3.17 (s, 3 H), 2.50 (t, J = 5.76 Hz, 2 H), 1.89-1.84 (m, 4 H), 1.59-1.54 (m, 2 H), 1.53-1.38 (m, 2 H), 1.38 (s, 9 H), 1.26-1.18 (m, 2 H). ^{13}C-NMR ($CDCl_3$, 100 MHz): 172.98, 170.04, 154.20, 142.50, 141.49, 127.96, 127.13, 79.57, 51.41, 45.26, 42.43, 38.05, 32.92, 28.52, 26.62, 24.80, 23.60, 21.50, 19.49. MS (ESI) calculated for $C_{23}H_{33}N_3O_4$, $[M+H]^+$, *m/z* 416.53, found for $[M+Na]^+$, 438.29 *m/z*.

***(R)- tert*-butyl 2-(methyl(4-(2-oxopiperidin-1-yl)phenyl)carbamoyl)piperidine-1-carboxylate (77).** ^{1}H-NMR ($CDCl_3$, 400 MHz): 7.35-7.29 (m, 4 H), 7.06 (d, J = 3.05 Hz, 1 H), 6.84 (d, J = 3.91 Hz, 1 H), 4.85-4.86 (m, 1 H), 3.85-3.71 (m, 1 H), 3.60 (t, J = 5.15 Hz, 2 H), 3.55-3.46 (m, 1 H), 3.17 (s, 3 H), 2.50 (t, J = 5.75 Hz, 2 H), 1.90-1.85 (m, 4 H), 1.59-1.54 (m, 2 H), 1.54-1.38 (m, 2 H), 1.40 (s, 9 H), 1.26-1.18 (m, 2 H). ^{13}C-NMR ($CDCl_3$, 100 MHz): 172.95, 170.04, 154.20, 142.50, 141.49, 128.01, 127.13, 79.57, 51.41, 45.26, 42.43, 38.1, 32.92, 28.52,

26.63, 24.80, 23.60, 21.51, 19.50. MS (ESI) calculated for $C_{23}H_{33}N_3O_4$, $[M+H]^+$, *m/z* 416.53, found for $[M+Na]^+$, 438.24 *m/z*.

(*R*)-tert-butyl 2-(4-(3-oxomorpholino)phenylcarbamoyl)piperidine-1-carboxylate (80). ^{1}H-NMR ($CDCl_3$, 400 MHz): 7.46 (d, J = 8.80 Hz, 2 H), 7.19 (d, J = 8.36 Hz, 2 H), 4.80-4.72 (m, 1 H), 4.26 (s, 2 H), 4.14-4.04 (m, 2 H), 3.99 (t, J = 4.88 Hz, 2 H), 3.85 (t, J = 4.44 Hz, 2 H), 2.76 (t, J = 12.44 Hz, 1 H), 2.26-2.23 (m, 1 H), 1.77-1.50 (m, 4 H), 1.48 (s, 9 H). ^{13}C-NMR ($CDCl_3$, 100 MHz): 169.88, 166.88, 157.58, 137.04, 136.90, 126.27, 120.48, 81.26, 68.63, 64.16, 55.00, 49.92, 42.53, 28.42, 25.06, 20.37. MS (ESI) calculated for $C_{21}H_{29}N_3O_5$, $[M+H]^+$, *m/z* 404.48, found for $[M+Na]^+$, 426.34 *m/z* .

(*S*)-tert-butyl 6-(4-(3-oxomorpholino)phenylcarbamoyl)-5,6-dihydropyridine-1(2H)-carboxylate (83). ^{1}H-NMR ($CDCl_3$, 400 MHz): 7.50 (d, J = 8.80 Hz, 2 H), 7.22 (d, J = 8.64 Hz, 2 H), 5.85-5.80 (m, 1 H), 4.65-4.60 (m, 1 H), 5.00-4.93 (m, 1 H), 4.28 (s, 2 H), 4.20-4.07 (m, 1 H), 3.94 (t, J = 4.95 Hz, 2 H), 3.65 (t, J = 4.40 Hz, 2 H), 3.60-3.63 (m, 1 H), 2.60-3.72 (m, 1 H), 2.34-2.28 (m, 1 H). ^{13}C-NMR ($CDCl_3$, 100 MHz): 169.54, 166.82, 156.90, 137.99, 126.12, 123.36, 122.20, 120.36, 81.41, 68.54, 64.11, 61.4, 49.79, 41.50, 28.39, 24.10. MS (ESI) calculated for $C_{22}H_{29}N_3O_5$, $[M+H]^+$, *m/z* 402.46, found for $[M+Na]^+$, *m/z* 424.36.

(1*R*, 3*S*, 4*R*)-tert-butyl 3-(4-(3-oxomorpholino)phenylcarbamoyl)-2-azabicyclo[2.2.1] heptane -2-carboxylate (86). ^{1}H-NMR ($CDCl_3$, 400 MHz): 7.57 (d, J = 8.36 Hz, 2 H), 7.25 (d, J = 7.60 Hz, 2 H), 4.32 (s, 3 H), 4.14-4.11 (m, 1 H), 4.02 (t, J = 4.96 Hz, 2 H), 3.93-3.85 (m, 1 H), 3.73 (t, J = 4.84 Hz, 2 H), 3.03-2.96 (m, 1 H), 1.80-1.77 (m, 2 H), 1.67-1.65 (m, 2 H), 1.50 (s, 9 H), 1.39-1.36 (m, 2 H). ^{13}C-NMR ($CDCl_3$, 100 MHz): 169.30, 166.76, 157.58, 137.26, 136.90, 126.07, 120.42, 81.17, 68.57, 67.06, 64.35, 58.23, 49.78, 39.25, 36.65, 29.97, 28.43, 26.40. MS (ESI) calculated for $C_{22}H_{29}N_3O_5$, $[M+H]^+$, *m/z* 416.49, found for $[M+Na]^+$, *m/z* 438.20.

General Procedure for Deprotection of Carbobenzyloxy (Cbz) Group of 12-15, 18–20, 50, 67 or 68. 1,2,3,4-tetrahydroisoquinoline carboxamides (**12-15**, **18, 19, 50**) or piperidine-3-carboxamides (**67** or **68**) and 10% $Pd(OH)_2$ on activated charcoal were mixed in CH_3OH: *tert*-butanol (1:1) mixture (10 mL). Hydrogen gas was then pumped into the mixture at RT. After stirring the solution overnight, the catalyst was filtered on Celite and the organic filtrate concentrated *in vacuo* to afford the corresponding desired unprotected carboxamides in quantitative yields and sufficient purity (as indicated by TLC) to be directly used in the next reactions without any further treatment.

(*S*)-benzyl 3-(4-(2-oxopiperidin-1-yl)phenylcarbamoyl)-3,4-dihydroisoquinoline-2(1H)-carboxylate (12). ^{1}H-NMR ($CDCl_3$, 400 MHz): 7.50-7.27 (m, 6 H), 7.25-7.08 (m, 5 H), 7.06 (d, J = 8.44, 2 H), 5.23-5.12 (m, 2 H), 4.96-4.54 (m, 3 H), 3.55 (t, J = 5.00 Hz, 2 H), 3.40-3.30 (m, 1 H), 3.20-3.09 (m, 1 H), 2.52 (t, J = 5.00 Hz, 2 H), 2.00-1.87 (m, 4 H). ^{13}C-NMR ($CDCl_3$, 100 MHz): 170.23, 169.22, 156.94, 139.31, 136.09, 135.47, 134.33, 133.32,128.64, 128.32, 128.07, 127.76, 127.23, 126.90, 126.58,125.99, 120.87, 68.04, 64.35, 51.75, 45.08, 32.82, 30.31, 23.51, 21.41. MS (ESI) calculated for $C_{29}H_{29}N_3O_4$, $[M+H]^+$, *m/z* 484.57, found for $[M+Na]^+$, *m/z* 506.3.

(*S*)-benzyl 3-(methyl(4-(2-oxopiperidin-1-yl)phenyl)carbamoyl)-3,4-dihydroiso-quinoline-2(1H)-carboxylate (13). ^{1}H-NMR ($CDCl_3$, 400 MHz): 7.47 (d, J = 7.64 Hz, 1 H), 7.39-7.31 (m, 6 H), 7.18 (m, 4 H), 7.06-6.82 (m, 2 H), 5.23 (d, J = 45.56 Hz, 1 H), 5.16 (d, J = 19.68 Hz, 1 H), 5.03-4.50 (m, 3 H), 3.67 (t, J = 5.20 Hz, 1 H), 3.59 (t, J = 5.20 Hz, 1 H), 3.17 (d, J = 50.36 Hz, 3 H), 2.87-2.83 (m, 2 H), 2.58 (t, J = 6.20 Hz, 2 H), 2.00-1.93 (m, 4 H). ^{13}C-NMR ($CDCl_3$, 100 MHz): 170.91, 169.46, 154.74, 141.69, 140.31, 139.82, 135.47, 134.33, 133.44, 131.75, 128.01, 127.60, 127.23, 126.78, 126.12, 125.97, 124.88, 66.92, 52.41, 50.50, 44.23, 37.01,

31.70, 30.81, 22.42, 20.22. MS (ESI) calculated for $C_{30}H_{31}N_3O_4$, $[M+H]^+$, *m/z* 498.59, found for $[M+Na]^+$, *m/z* 520.32.

(*S*)-benzyl 3-(ethyl(4-(2-oxopiperidin-1-yl)phenyl)carbamoyl)-3,4-dihydroisoquinoline-2(1H)-carboxylate (14). ^{1}H-NMR ($CDCl_3$, 400 MHz): 7.44-7.41 (m, 1 H), 7.38-7.32 (m, 6 H), 7.21-7.10 (m, 4 H), 7.05-6.70 (m, 2 H), 5.20-5.02 (m, 2 H), 4.93-4.44 (m, 3 H), 3.83-3.76 (m, 1 H), 3.66-3.60 (m, 2 H), 3.58-3.46 (m, 1 H), 2.86-2.81 (dd, J = 3.76 Hz, J = 6.76 Hz, 2 H), 2.59 (d, J = 5.48 Hz, 2 H), 2.00-1.90 (m, 4 H), 1.11-0.97 (m, 3 H). ^{13}C-NMR ($CDCl_3$, 100 MHz): 171.33, 170.51, 155.70, 142.68, 139.79, 139.30, 136.53, 135.43, 134.52, 132.79, 132.35, 129.19, 128.63, 127.77, 127.14, 126.94, 125.89, 67.91, 60.38, 52.58, 51.47, 45.29, 32.66, 29.70, 23.41, 21.18, 12.84. MS (ESI) calculated for $C_{31}H_{33}N_3O_4$, $[M+H]^+$, *m/z* 512.62, found for $[M+Na]^+$, *m/z* 534.33.

(*S*)-benzyl 3-(isopropyl(4-(2-oxopiperidin-1-yl)phenyl)carbamoyl)-3,4-dihydroisoquinoline-2(1H)-carboxylate (15). ^{1}H-NMR ($CDCl_3$, 400 MHz): 7.45-7.28 (m, 7 H), 7.24-7.08 (m, 4 H), 7.02-6.46 (m, 2 H), 5.16-5.03 (m, 2 H), 4.93-4.27 (m, 4 H), 3.68 (t, J = 5.90 Hz, 1 H), 3.62 (t, J = 5.92 Hz, 1 H), 2.89-2.82 (m, 2 H), 2.54 (d, J = 7.12 Hz, 2 H), 1.96-1.85 (m, 4 H), 1.20-0.80 (m, 6 H). ^{13}C-NMR ($CDCl_3$, 100 MHz): 171.43, 170.05, 155.26, 143.37, 136.59, 135.68, 135.23, 132.94, 131.15, 130.19, 129.05, 128.64, 127.77, 127.13, 126.82, 126.46, 125.87, 67.83, 60.37, 53.06, 51.34, 46.99, 32.96, 31.94, 23.65, 21.52, 20.39. MS (ESI) calculated for $C_{32}H_{35}N_3O_4$, $[M+H]^+$, *m/z* 526.65, found for $[M+Na]^+$, *m/z* 548.35.

(*S*)-benzyl 3-(methyl(4-(3-oxomorpholino)phenyl)carbamoyl)-3,4-dihydroisoquinoline-2(1H)-carboxylate (18). ^{1}H-NMR ($CDCl_3$, 400 MHz): 7.51-7.44 (dd, J = 6.68 Hz, J = 20.32, 2 H), 7.38-7.36 (m, 4 H), 7.34-7.30 (m, 1 H), 7.22-7.09 (m, 4 H), 7.06-6.84 (m, 2 H), 5.24 (d, J = 28.32 Hz, 1 H), 5.16 (d, J = 5.88 Hz, 1 H), 5.03-4.63 (m, 3 H), 4.34 (d, J = 6.72 Hz, 2 H),

4.02 (t, J = 4.80 Hz, 2 H), 3.79 (t, J = 4.72 Hz, 1 H), 3.72 (t, J = 3.76 Hz, 1 H), 3.17 (d, J = 51.12 Hz, 3 H), 2.90-2.83 (m, 2 H). ^{13}C-NMR ($CDCl_3$, 100 MHz): 171.92, 166.71, 155.76, 141.64, 140.80, 136.46, 135.32, 132.69, 129.05, 128.64, 128.14, 127.79, 12718, 127.00, 126.92, 126.51, 125.93, 68.58, 67.43, 64.09, 52.40, 49.42, 45.24, 37.96, 31.83. MS (ESI) calculated for $C_{29}H_{29}N_3O_5$, $[M+H]^+$, *m/z* 500.57, found for $[M+Na]^+$, *m/z* 522.30.

(*S*)-benzyl 3-(ethyl(4-(3-oxomorpholino)phenyl)carbamoyl)-3,4-dihydroisoquinoline-2(1H)-carboxylate (19). ^{1}H-NMR ($CDCl_3$, 400 MHz): 7.48-7.44 (m, 2 H), 7.42-7.34 (m, 4 H), 7.33-7.30 (m, 1 H), 7.25-7.10 (m, 4 H), 7.09-6.80 (m, 2 H), 5.20-5.04 9m, 2 H), 4.94-4.44 (m, 3 H), 4.35 (d, J = 5.28 Hz, 2 H), 4.03 (t, J = 4.04 Hz, 2 H), 3.81-3.72 (m, 2 H), 3.67-3.47 (m, 2 H), 2.87-2.83 (m, 2 H), 1.12-0.97 (m, 3 H). ^{13}C-NMR ($CDCl_3$, 100 MHz): 171.31, 166.65, 155.71, 140.90, 139.99, 136.52, 135.40, 134.52, 132.72, 129.31, 128.65, 128.01, 127.77, 127.16, 126.90, 126.28, 125.92, 68.60, 67.92, 64.10, 60.37, 52.56, 49.40, 45.28, 31.44, 12.83. MS (ESI) calculated for $C_{30}H_{31}N_3O_5$, $[M+H]^+$, *m/z* 514.59, found for $[M+Na]^+$, *m/z* 537.37.

***(S)*-benzyl 3-(4-(3-oxomorpholino)phenylcarbamoyl)-3,4-dihydroisoquinoline-2(1H)-carboxylate (20).** ^{1}H-NMR (acetone-d_6, 400 MHz): 7.55 (d, J = 8.92 Hz, 2 H), 7.49-7.34 (m, 4 H), 7.29 (d, J = 8.80, 2 H), 7.27-7.22 (m, 5 H), 5.25-5.09 (m, 2 H), 5.01-4.61 (m, 3 H), 4.18 (s, 2 H), 3.76 (s, br, 2 H), 3.32 (t, J = 4.00 Hz, 2 H), 3.29-3.24 (m, 2 H). ^{13}C-NMR ($CDCl_3$, 100 MHz): 171.95, 166.73, 155.76, 141.65, 140.78, 136.46, 135.31, 132.69, 129.05, 128.66, 128.14, 127.79, 127.18, 127.00, 126.92, 126.51, 125.95, 68.61, 67.43, 64.09, 52.40, 49.42, 45.24, 31.80. MS (ESI) calculated for $C_{28}H_{27}N_3O_5$, $[M+H]^+$, *m/z* 486.20, found for $[M+Na]^+$, *m/z* 508.18.

(*S*)-benzyl 3-(4-chlorophenylcarbamoyl)-3,4-dihydroisoquinoline-2(1H)-carboxylate (50). ^{1}H-NMR ($CDCl_3$, 400 MHz): 7.50-7.35 (m, 3 H), 7.34-7.26 (m, 2 H), 7.25-7.18 (m, 4 H), 7.17-7.00 (m, 4 H), 5.39-5.10 (m, 2 H), 4.96-4.49 (m, 3 H), 3.35-3.21 (m, 1 H), 3.20-3.3.03 (m, 1

H). ^{13}C-NMR ($CDCl_3$, 100 MHz): 169.12, 157.30, 136.24, 135.95, 133.44, 132.70, 129.08, 128.81, 128.70, 128.57, 128.43, 128.11, 127.77, 126.78, 125.94, 121.13, 68.19, 57.04, 45.11, 28.30. MS (ESI) calculated for $C_{24}H_{21}ClN_2O_3$, $[M+H]^+$, *m/z* 421.90, found for $[M+Na]^+$, *m/z* 443.26.

(*S*)-benzyl 3-(methyl(4-(2-oxopiperidin-1-yl)phenyl)carbamoyl)piperidine-1-carboxylate (67). ^{1}H-NMR ($CDCl_3$, 400 MHz): 7.40-7.34 (m, 2 H), 7.33-7.31 (m, 2 H), 7.30-7.23 (m, 2 H), 7.22-7.04 (m, 3 H), 5.20-5.00 (m, 2 H), 4.14 (t, J = 6.60 Hz, 1 H), 4.06 (t, J = 6.72 Hz, 1 H), 3.70-3.50 (m, 2 H), 3.21 (s, 3 H), 2.99 (t, J = 11.92 Hz, 1 H), 2.76 (t, J = 11.84 Hz, 1 H), 2.58 (t, J = 6.00 Hz, 2 H), 2.50-2.40 (m, 1 H), 2.00-1.94 (m, 4 H), 1.76-1.71 (m, 2 H), 1.61-1.58 (m, 1 H), 1.27-1.24 (m, 1 H). ^{13}C-NMR ($CDCl_3$, 100 MHz): 173.22, 170.26, 154.96, 142.71, 141.40, 136.80, 128.46, 127.98, 127.80, 127.64, 127.25, 67.04, 51.41, 46.60, 44.08, 39.71, 37.50, 32.84, 27.77, 24.12, 23.48, 21.32. MS (ESI) calculated for $C_{26}H_{31}N_3O_4$, $[M+H]^+$, *m/z* 450.55, found for $[M+Na]^+$, *m/z* 472.35.

(*R*)-benzyl 3-(methyl(4-(2-oxopiperidin-1-yl)phenyl)carbamoyl)piperidine-1-carboxylate (68). ^{1}H-NMR ($CDCl_3$, 400 MHz): ^{13}C-NMR ($CDCl_3$, 100 MHz): ^{1}H-NMR ($CDCl_3$, 400 MHz): 7.40-7.34 (m, 2 H), 7.33-7.31 (m, 2 H), 7.30-7.23 (m, 2 H), 7.22-7.04 (m, 3 H), 5.20-5.00 (m, 2 H), 4.14 (t, J = 6.60 Hz, 1 H), 4.06 (t, J = 6.72 Hz, 1 H), 3.70-3.50 (m, 2 H), 3.21 (s, 3 H), 2.99 (t, J = 11.92 Hz, 1 H), 2.76 (t, J = 11.84 Hz, 1 H), 2.58 (t, J = 6.00 Hz, 2 H), 2.50-2.40 (m, 1 H), 2.00-1.94 (m, 4 H), 1.76-1.71 (m, 2 H), 1.61-1.58 (m, 1 H), 1.27-1.24 (m, 1 H). ^{13}C-NMR ($CDCl_3$, 100 MHz): 173.22, 170.26, 154.96, 142.71, 141.40, 136.80, 128.46, 127.98, 127.80, 127.64, 127.25, 67.04, 51.41, 46.60, 44.08, 39.71, 37.50, 32.84, 27.77, 24.12, 23.48, 21.32. MS (ESI) calculated for $C_{26}H_{31}N_3O_4$, $[M+H]^+$, *m/z* 450.55, found for $[M+Na]^+$, *m/z* 472.35.

General Procedure for Amine Protection by Carbobenzyloxy (Cbz) Group in the Synthesis of 65 or 66. Piperidine-3-carboxylic acid (**63** or **64**) (1 mmol) was dissolved in dry THF

(10 mL) and stirred at RT. Tri-ethylamine (Et_3N) (2 mmol) was then added followed by benzyl chloroformate (1.5 mmol). The reaction mixture became initially cloudy and turned to clear solution after 5 h. The reaction mixture was then partitioned between acidified water (15 mL) and EtOAc (20 mL). The aqueous layer was further washed with EtOAc (2 × 20 mL). The organic extracts were combined, dried over anhydrous Na_2SO_3, filtered, and concentrated *in vacuo*. The *N*-Cbz protected product (**65** or **66**) was isolated as white solids by flash chromatography using gradient of EtOAc/hexanes as eluant in 70-73 % yield.

(*S*)-1-(benzyloxycarbonyl)piperidine-3-carboxylic acid (65). ^{1}H-NMR (acetone-d_6, 400 MHz): 7.43-7.30 (m, 5 H), 5.15 (s, 2 H), 4.35-4.04 (m, 1 H), 3.93 (d, J = 12.08 Hz, 1 H), 3.18-3.02 (m, 1 H), 3.01-2.92 (m, 1 H), 2.53-2.46 (m, 1 H), 2.09-2.062 (m, 1 H), 1.75-1.66 (m, 2 H), 1.53-1.45 (m, 1 H). ^{13}C-NMR (acetone-d_6, 100 MHz): 174.88, 155.77, 138.25, 129.30, 128.70, 128.60, 67.49, 46.62, 44.90, 41.64, 27.87, 24.98. MS (ESI) calculated for $C_{14}H_{17}NO_4$, $[M+H]^+$, *m/z* 264.30, found for $[M+H]^+$, *m/z* 264.37.

(*R*)-1-(benzyloxycarbonyl)piperidine-3-carboxylic acid (66). ^{1}H-NMR (acetone-d_6, 400 MHz): 7.43-7.30 (m, 5 H), 5.15 (s, 2 H), 4.35-4.04 (m, 1 H), 3.93 (d, J = 12.08 Hz, 1 H), 3.18-3.02 (m, 1 H), 3.01-2.92 (m, 1 H), 2.53-2.46 (m, 1 H), 2.09-2.062 (m, 1 H), 1.75-1.66 (m, 2 H), 1.53-1.45 (m, 1 H). ^{13}C-NMR (acetone-d_6, 100 MHz): 174.88, 155.77, 138.25, 129.30, 128.70, 128.60, 67.49, 46.62, 44.90, 41.64, 27.87, 24.98. MS (ESI) calculated for $C_{14}H_{17}NO_4$, $[M+H]^+$, *m/z* 264.30, found for $[M+Na]^+$, *m/z* 286.28.

General Procedure for Amidation of 3-Carboxylic Acid to Yield 12-21, **50**, **53-55**, **59**, **61**, **67**, **68**, **76**, **77**, **80**, **83**, or **86.** To a stirred solution of the free carboxylic acid of (**9-11**, **58**, **60**, **65**, **66**, **74**, **75**, **82**, or **85**) (1.0 mmol) in anhydrous CH_2Cl_2 (5 mL) was added hydrated *N*-hydroxybenzotrizole ($HOBT.H_2O$, 1.1 mmol), DMAP (1.1 mmol), and 1-ethyl-3-(3-dimethyl

aminopropyl)carbodiimide (EDCI, 1.1 mmol) at RT under nitrogen atmosphere. Appropriate amine (**8a – 8j** or 4-chloroaniline) (1.1 mmol) in anhydrous CH_2Cl_2 (5 mL) was then added dropwise. After stirring overnight, the reaction mixture was partitioned between 2.0 N HCl solution (20 mL) and CH_2Cl_2 (30 mL). The organic layer was washed further with 2 N HCl (2 × 10 mL) and saturated NaCl solution (20 mL), dried using anhydrous Na_2SO_4, and concentrated to give a crude, which purified by flash chromatography using gradient of CH_2Cl_2/CH_3OH as eluant to give the desired carboxamide product in 73 – 89 % yield.

(*S*)-benzyl 3-(4-(2-oxopiperidin-1-yl)phenylcarbamoyl)-3,4-dihydroisoquinoline-2(1H)-carboxylate (12). ^{1}H-NMR ($CDCl_3$, 400 MHz): 7.50-7.27 (m, 6 H), 7.25-7.08 (m, 5 H), 7.06 (d, J = 8.44, 2 H), 5.23-5.12 (m, 2 H), 4.96-4.54 (m, 3 H), 3.55 (t, J = 5.00 Hz, 2 H), 3.40-3.30 (m, 1 H), 3.20-3.09 (m, 1 H), 2.52 (t, J = 5.00 Hz, 2 H), 2.00-1.87 (m, 4 H). ^{13}C-NMR ($CDCl_3$, 100 MHz): 170.23, 169.22, 156.94, 139.31, 136.09, 135.47, 134.33, 133.32,128.64, 128.32, 128.07, 127.76, 127.23, 126.90, 126.58,125.99, 120.87, 68.04, 64.35, 51.75, 45.08, 32.82, 30.31, 23.51, 21.41. MS (ESI) calculated for $C_{29}H_{29}N_3O_4$, $[M+H]^+$, *m/z* 484.57, found for $[M+Na]^+$, *m/z* 506.3.

(*S*)-benzyl 3-(methyl(4-(2-oxopiperidin-1-yl)phenyl)carbamoyl)-3,4-dihydroisoquinoline-2(1H)-carboxylate (13). ^{1}H-NMR ($CDCl_3$, 400 MHz): 7.47 (d, J = 7.64 Hz, 1 H), 7.39-7.31 (m, 6 H), 7.18 (m, 4 H), 7.06-6.82 (m, 2 H), 5.23 (d, J = 45.56 Hz, 1 H), 5.16 (d, J = 19.68 Hz, 1 H), 5.03-4.50 (m, 3 H), 3.67 (t, J = 5.20 Hz, 1 H), 3.59 (t, J = 5.20 Hz, 1 H), 3.17 (d, J = 50.36 Hz, 3 H), 2.87-2.83 (m, 2 H), 2.58 (t, J = 6.20 Hz, 2 H), 2.00-1.93 (m, 4 H). ^{13}C-NMR ($CDCl_3$, 100 MHz): 170.91, 169.46, 154.74, 141.69, 140.31, 139.82, 135.47, 134.33, 133.44, 131.75, 128.01, 127.60, 127.23, 126.78, 126.12, 125.97, 124.88, 66.92, 52.41, 50.50, 44.23, 37.01,

31.70, 30.81, 22.42, 20.22. MS (ESI) calculated for $C_{30}H_{31}N_3O_4$, $[M+H]^+$, *m/z* 498.59, found for $[M+Na]^+$, *m/z* 520.32.

(*S*)-benzyl 3-(ethyl(4-(2-oxopiperidin-1-yl)phenyl)carbamoyl)-3,4-dihydroisoquinoline-2(1H)-carboxylate (14). ^{1}H-NMR ($CDCl_3$, 400 MHz): 7.44-7.41 (m, 1 H), 7.38-7.32 (m, 6 H), 7.21-7.10 (m, 4 H), 7.05-6.70 (m, 2 H), 5.20-5.02 (m, 2 H), 4.93-4.44 (m, 3 H), 3.83-3.76 (m, 1 H), 3.66-3.60 (m, 2 H), 3.58-3.46 (m, 1 H), 2.86-2.81 (dd, J = 3.76 Hz, J = 6.76 Hz, 2 H), 2.59 (d, J = 5.48 Hz, 2 H), 2.00-1.90 (m, 4 H), 1.11-0.97 (m, 3 H). ^{13}C-NMR ($CDCl_3$, 100 MHz): 171.33, 170.51, 155.70, 142.68, 139.79, 139.30, 136.53, 135.43, 134.52, 132.79, 132.35, 129.19, 128.63, 127.77, 127.14, 126.94, 125.89, 67.91, 60.38, 52.58, 51.47, 45.29, 32.66, 29.70, 23.41, 21.18, 12.84. MS (ESI) calculated for $C_{31}H_{33}N_3O_4$, $[M+H]^+$, *m/z* 512.62, found for $[M+Na]^+$, *m/z* 534.33.

(*S*)-benzyl 3-(isopropyl(4-(2-oxopiperidin-1-yl)phenyl)carbamoyl)-3,4-dihydroisoquinoline-2(1H)-carboxylate (15). ^{1}H-NMR ($CDCl_3$, 400 MHz): 7.45-7.28 (m, 7 H), 7.24-7.08 (m, 4 H), 7.02-6.46 (m, 2 H), 5.16-5.03 (m, 2 H), 4.93-4.27 (m, 4 H), 3.68 (t, J = 5.90 Hz, 1 H), 3.62 (t, J = 5.92 Hz, 1 H), 2.89-2.82 (m, 2 H), 2.54 (d, J = 7.12 Hz, 2 H), 1.96-1.85 (m, 4 H), 1.20-0.80 (m, 6 H). ^{13}C-NMR ($CDCl_3$, 100 MHz): 171.43, 170.05, 155.26, 143.37, 136.59, 135.68, 135.23, 132.94, 131.15, 130.19, 129.05, 128.64, 127.77, 127.13, 126.82, 126.46, 125.87, 67.83, 60.37, 53.06, 51.34, 46.99, 32.96, 31.94, 23.65, 21.52, 20.39. MS (ESI) calculated for $C_{32}H_{35}N_3O_4$, $[M+H]^+$, *m/z* 526.65, found for $[M+Na]^+$, *m/z* 548.35.

***(S)-tert*-butyl 3-(methyl(4-(2-oxopiperidin-1-yl)phenyl)carbamoyl)-3,4-dihydroisoquinoline-2(1H)-carboxylate (16).** ^{1}H-NMR ($CDCl_3$, 400 MHz): 7.37-7.27 (m, 4 H), 7.12-6.92 (m, 4 H), 7.15-7.11 (m, 3 H), 4.91-7.37 (m, 3 H), 3.62 (t, J= 5.44 Hz, 2 H), 3.14 (s, 3 H), 2.8-2.65 (m, 1 H), 2.50 (t, J= 6.44 Hz, 2 H), 2.0-1.90 (m, 4 H), 1.42 (s, 9 H) . ^{13}C-NMR ($CDCl_3$, 100 MHz):

171.99, 170.05, 154.30, 142.71, 141.31, 134.73, 132.21, 128.13, 127.69, 127.27, 126.63, 125.74, 79.98, 51.39, 45.49, 38.05, 32.88, 31.29, 29.65, 28.52, 23.48, 21.33. MS (ESI) calculated for $C_{27}H_{33}N_3O_4$, $[M+H]^+$, *m/z* 464.58, found for $[M+Na]^+$, *m/z* 486.29.

***(R)-tert*-butyl 3-(methyl(4-(2-oxopiperidin-1-yl)phenyl)carbamoyl)-3,4-dihydro-isoquinoline-2(1H)-carboxylate (17).** ^{1}H-NMR ($CDCl_3$, 400 MHz): 7.37-7.25 (m, 4 H), 7.12-6.90 (m, 4 H), 7.17-7.11 (m, 3 H), 4.91-7.37 (m, 3 H), 3.62 (t, J= 5.45 Hz, 2 H), 3.14 (s, 3 H), 2.82-2.65 (m, 1 H), 2.50 (t, J= 6.42 Hz, 2 H), 2.1-1.911 (m, 4 H), 1.41 (s, 9 H) . ^{13}C-NMR ($CDCl_3$, 100 MHz): 172.01, 170.09, 154.30, 142.71, 141.31, 134.72, 132.21, 128.15, 127.69, 127.27, 126.63, 125.74, 79.98, 51.39, 45.49, 38.05, 32.87, 31.29, 29.65, 28.52, 23.51, 21.35. MS (ESI) calculated for $C_{27}H_{33}N_3O_4$, $[M+H]^+$, *m/z* 464.58, found for $[M+Na]^+$, *m/z* 486.29.

(*S*)-benzyl 3-(methyl(4-(3-oxomorpholino)phenyl)carbamoyl)-3,4-dihydroiso-quinoline-2(1H)-carboxylate (18). ^{1}H-NMR ($CDCl_3$, 400 MHz): 7.51-7.44 (dd, J = 6.68 Hz, J = 20.32, 2 H), 7.38-7.36 (m, 4 H), 7.34-7.30 (m, 1 H), 7.22-7.09 (m, 4 H), 7.06-6.84 (m, 2 H), 5.24 (d, J = 28.32 Hz, 1 H), 5.16 (d, J = 5.88 Hz, 1 H), 5.03-4.63 (m, 3 H), 4.34 (d, J = 6.72 Hz, 2 H), 4.02 (t, J = 4.80 Hz, 2 H), 3.79 (t, J = 4.72 Hz, 1 H), 3.72 (t, J = 3.76 Hz, 1 H), 3.17 (d, J = 51.12 Hz, 3 H), 2.90-2.83 (m, 2 H). ^{13}C-NMR ($CDCl_3$, 100 MHz): 171.92, 166.71, 155.76, 141.64, 140.80, 136.46, 135.32, 132.69, 129.05, 128.64, 128.14, 127.79, 12718, 127.00, 126.92, 126.51, 125.93, 68.58, 67.43, 64.09, 52.40, 49.42, 45.24, 37.96, 31.83. MS (ESI) calculated for $C_{29}H_{29}N_3O_5$, $[M+H]^+$, *m/z* 500.57, found for $[M+Na]^+$, *m/z* 522.30.

(*S*)-benzyl 3-(ethyl(4-(3-oxomorpholino)phenyl)carbamoyl)-3,4-dihydroisoquinoline-2(1H)-carboxylate (19). ^{1}H-NMR ($CDCl_3$, 400 MHz): 7.48-7.44 (m, 2 H), 7.42-7.34 (m, 4 H), 7.33-7.30 (m, 1 H), 7.25-7.10 (m, 4 H), 7.09-6.80 (m, 2 H), 5.20-5.04 9m, 2 H), 4.94-4.44 (m, 3 H), 4.35 (d, J = 5.28 Hz, 2 H), 4.03 (t, J = 4.04 Hz, 2 H), 3.81-3.72 (m, 2 H), 3.67-3.47 (m, 2 H),

2.87-2.83 (m, 2 H), 1.12-0.97 (m, 3 H). ^{13}C-NMR ($CDCl_3$, 100 MHz): 171.31, 166.65, 155.71, 140.90, 139.99, 136.52, 135.40, 134.52, 132.72, 129.31, 128.65, 128.01, 127.77, 127.16, 126.90, 126.28, 125.92, 68.60, 67.92, 64.10, 60.37, 52.56, 49.40, 45.28, 31.44, 12.83. MS (ESI) calculated for $C_{30}H_{31}N_3O_5$, $[M+H]^+$, *m/z* 514.59, found for $[M+Na]^+$, *m/z* 537.37.

***(S)*-benzyl 3-(4-(3-oxomorpholino)phenylcarbamoyl)-3,4-dihydroisoquinoline-2(1H)-carboxylate (20).** ^{1}H-NMR (acetone-d_6, 400 MHz): 7.55 (d, J = 8.92 Hz, 2 H), 7.49-7.34 (m, 4 H), 7.29 (d, J = 8.80, 2 H), 7.27-7.22 (m, 5 H), 5.25-5.09 (m, 2 H), 5.01-4.61 (m, 3 H), 4.18 (s, 2 H), 3.76 (s, br, 2 H), 3.32 (t, J = 4.00 Hz, 2 H), 3.29-3.24 (m, 2 H). ^{13}C-NMR ($CDCl_3$, 100 MHz): 171.95, 166.73, 155.76, 141.65, 140.78, 136.46, 135.31, 132.69, 129.05, 128.66, 128.14, 127.79, 127.18, 127.00, 126.92, 126.51, 125.95, 68.61, 67.43, 64.09, 52.40, 49.42, 45.24, 31.80. MS (ESI) calculated for $C_{28}H_{27}N_3O_5$, $[M+H]^+$, *m/z* 486.20, found for $[M+Na]^+$, *m/z* 508.18.

(*R*)-tert-butyl 3-(4-(3-oxomorpholino)phenylcarbamoyl)-3,4-dihydroisoquinoline-2(1H)-carboxylate (21). ^{1}H-NMR ($CDCl_3$, 400 MHz): 7.50-7.30 (m, 2 H), 7.28-7.10 (m, 6 H), 5.00-4.45 (m, 3 H), 4.31 (s, 2 H), 4.00 (t, J = 4.84 Hz, 2 H), 3.69 (t, J = 5.68 Hz, 2 H), 3.40-3.27 (m, 1 H), 3.23-3.00 (m, 1 H), 1.50 (s, 9 H). ^{13}C-NMR ($CDCl_3$, 100 MHz): 171.40, 166.73, 155.65, 133.77, 128.13, 126.73, 126.08, 120.57, 81.81, 68.57, 64.13, 49.75, 44.85, 28.38. MS (ESI) calculated for $C_{28}H_{27}N_3O_5$, $[M+H]^+$, *m/z* 452.52, found for $[M+Na]^+$, *m/z* 474.37.

(*S*)-benzyl 3-(4-chlorophenylcarbamoyl)-3,4-dihydroisoquinoline-2(1H)-carboxylate (50). ^{1}H-NMR ($CDCl_3$, 400 MHz): 7.50-7.35 (m, 3 H), 7.34-7.26 (m, 2 H), 7.25-7.18 (m, 4 H), 7.17-7.00 (m, 4 H), 5.39-5.10 (m, 2 H), 4.96-4.49 (m, 3 H), 3.35-3.21 (m, 1 H), 3.20-3.3.03 (m, 1 H). ^{13}C-NMR ($CDCl_3$, 100 MHz): 169.12, 157.30, 136.24, 135.95, 133.44, 132.70, 129.08, 128.81, 128.70, 128.57, 128.43, 128.11, 127.77, 126.78, 125.94, 121.13, 68.19, 57.04, 45.11, 28.30. MS (ESI) calculated for $C_{24}H_{21}ClN_2O_3$, $[M+H]^+$, *m/z* 421.90, found for $[M+Na]^+$, *m/z* 443.26.

(*S*)-benzyl 3-(4-(piperidin-1-yl)phenylcarbamoyl)-3,4-dihydroisoquinoline-2(1H)-carboxylate (53). ^{1}H-NMR ($CDCl_3$, 400 MHz): 7.39-7.26 (m, 5 H), 7.26-7.22 (m, 4 H), 7.12-7.04 (m, 2 H), 6.87-6.85 (m, 2 H), 5.25-5.14 (m, 2 H), 5.00-4.49 (m, 3 H), 3.39-3.31 (m, 1 H), 3.25-3.07 (m, 1 H), 3.08 (t, J = 5.36 Hz, 4 H), 1.73-1.70 (m, 4 H), 1.56 (t, J = 5.24 Hz, 2 H). ^{13}C-NMR ($CDCl_3$, 100 MHz): 169.41, 157.01, 148.18, 136.07, 133.54, 132.71, 128.65, 128.30, 128.05, 127.65, 127.09, 126.65, 125.89, 121.57, 121.26, 117.39, 68.01, 56.84, 51.75, 45.07, 31.91, 25.54, 23.99. MS (ESI) calculated for $C_{29}H_{31}N_3O_3$, $[M+H]^+$, *m/z* 470.58, found for $[M+Na]^+$, *m/z* 492.35.

(*S*)-benzyl 3-(4-(4-acetylpiperazin-1-yl)phenylcarbamoyl)-3,4-dihydroisoquinoline-2(1H)-carboxylate (54). ^{1}H-NMR ($CDCl_3$, 400 MHz): 7.39-7.26 (m, 5 H), 7.26-7.22 (m, 4 H), 7.12-7.04 (m, 2 H), 6.87-6.85 (m, 2 H), 5.23-5.11 (m, 2 H), 4.97-4.56 (m, 3 H), 3.84-3.80 (m, 2 H), 3.71-3.68 (m, 2 H), 3.33-3.30 (m, 1 H), 3.17-3.14 (m, 1 H), 3.15-3.09 (m, 4 H), 2.09 (s, 3 H). ^{13}C-NMR ($CDCl_3$, 100 MHz): 169.36, 168.99, 156.97, 145.20, 136.09, 133.35, 132.93, 128.64, 128.30, 127.98, 127.63, 126.81, 125.97, 121.65, 121.35, 118.44, 67.99, 55.45, 51.69, 45.14, 40.55, 30.54, 21.26. MS (ESI) calculated for $C_{30}H_{32}N_4O_4$, $[M+H]^+$, *m/z* 513.61, found for $[M+Na]^+$, *m/z* 535.33.

(*S*)-benzyl 3-(4-(4-(thiophene-2-carbonyl)piperazin-1-yl)phenylcarbamoyl)-3,4-dihydro-isoquinoline-2(1H)-carboxylate (55). ^{1}H-NMR ($CDCl_3$, 400 MHz): 7.47-7.45 (dd, J = 0.92 Hz, J = 4.96 Hz, 1 H), 7.42-7.27 (m, 6 H), 7.25-7.19 (m, 3 H), 7.18-7.08 (m, 2 H), 7.07-7.04 (m, 2 H), 6.99-6.85 (m, 2 H), 5.29-5.10 (m, 2 H), 5.05-4.53 (m, 3 H), 3.95-3.85 (m, 4 H), 3.35-3.20 (m, 2 H), 3.16-3.10 (m, 4 H). ^{13}C-NMR ($CDCl_3$, 100 MHz): 168.92, 163.65, 155.85, 145.20, 136.75, 136.04, 133.59, 133.17, 132.95, 129.11, 128.92, 128.53, 128.06, 127.99, 126.91, 126.48, 126.05, 125.92, 121.44, 117.71, 116.86, 68.05, 58.45, 55.37, 50.72, 45.09, 31.80. MS (ESI) calculated for $C_{33}H_{32}N_4O_4S$, $[M+H]^+$, *m/z* 581.70, found for $[M+Na]^+$, *m/z* 603.36.

(*S*)-2-(2-(4-chlorophenyl)acetyl)-6,7-dimethoxy-N-methyl-N-(4-(2-oxopiperidin-1-yl)phenyl)-1,2,3,4-tetrahydroisoquinoline-3-carboxamide (59). ^{1}H-NMR ($CDCl_3$, 400 MHz): 7.45 (d, J = 7.80 Hz, 2 H), 7.29 (d, J = 8.48 Hz, 2 H), 7.11 (d, J = 8.80 Hz, 2 H), 6.49 (s, 1 H), 6.31 (s, 1 H), 4.97 (t, J= 6.16 Hz, 1 H), 4.60-4.40 (dd, J = 14.60 Hz, J = 64.28 Hz, 2 H), 3.76 (s, 3 H), 3.75 (s, 2 H), 3.72 (s, 3 H), 3.59 (t, J = 5.48 Hz, 2 H), 3.17 (s, 3 H), 2.72 (t, J = 6.24 Hz, 2 H), 2.51 (t, J = 6.20 Hz, 2 H), 1.90-1.85 (m, 4 H). ^{13}C-NMR ($CDCl_3$, 100 MHz): 171.85, 170.27, 170.06, 148.22, 147.81, 142.82, 141.19, 133.25, 132.71, 130.37, 128.83, 127.93, 125.75, 124.55, 56.05, 55.95, 51.54, 51.44, 46.77, 40.76, 38.09, 32.87, 30.09, 23.50, 21.33. MS (ESI) calculated for $C_{32}H_{34}ClN_3O_5$, $[M+H]^+$, *m/z* 577.09, found for $[M+Na]^+$, *m/z* 598.37.

(*S*)-tert-butyl 1-(methyl(4-(2-oxopiperidin-1-yl)phenyl)amino)-1-oxo-3-phenylpropan-2-ylcarbamate (61). ^{1}H-NMR ($CDCl_3$, 400 MHz): 7.30-7.12 (m, 5 H), 6.86-6.76 (m, 2 H), 6.75-6.66 (m, 2 H), 4.49-4.44 (q, J = 7.16 Hz, J = 15.08 Hz, 1 H), 3.60 (t, J = 4.84 Hz, 2 H), 3.12 (s, 3 H), 2.83-2.77 (dd, J = 7.60 Hz, J = 13.12, 1 H), 2.66-2.61 (dd, J = 6.20 Hz, J = 12.52 Hz, 1 H), 2.50 (t, J = 6.36, 2 H), 1.90-1.85 (m, 4 H), 1.31 (s, 9 H). ^{13}C-NMR ($CDCl_3$, 100 MHz): 171.79, 170.00, 154.82, 142.77, 140.39, 136.59, 129.38, 128.35, 127.92, 127.10, 126.68, 79.46, 52.27, 51.69, 39.86, 37.45, 32.30, 28.30, 23.53, 21.39. MS (ESI) calculated for $C_{26}H_{33}N_3O_4$, $[M+H]^+$, *m/z* 452.57, found for $[M+H]^+$, *m/z* 452.42.

(*S*)-benzyl 3-(methyl(4-(2-oxopiperidin-1-yl)phenyl)carbamoyl)piperidine-1-carboxylate (67). ^{1}H-NMR ($CDCl_3$, 400 MHz): 7.40-7.34 (m, 2 H), 7.33-7.31 (m, 2 H), 7.30-7.23 (m, 2 H), 7.22-7.04 (m, 3 H), 5.20-5.00 (m, 2 H), 4.14 (t, J = 6.60 Hz, 1 H), 4.06 (t, J = 6.72 Hz, 1 H), 3.70-3.50 (m, 2 H), 3.21 (s, 3 H), 2.99 (t, J = 11.92 Hz, 1 H), 2.76 (t, J = 11.84 Hz, 1 H), 2.58 (t, J = 6.00 Hz, 2 H), 2.50-2.40 (m, 1 H), 2.00-1.94 (m, 4 H), 1.76-1.71 (m, 2 H), 1.61-1.58 (m, 1 H), 1.27-1.24 (m, 1 H). ^{13}C-NMR ($CDCl_3$, 100 MHz): 173.22, 170.26, 154.96, 142.71, 141.40,

136.80, 128.46, 127.98, 127.80, 127.64, 127.25, 67.04, 51.41, 46.60, 44.08, 39.71, 37.50, 32.84, 27.77, 24.12, 23.48, 21.32. MS (ESI) calculated for $C_{26}H_{31}N_3O_4$, $[M+H]^+$, *m/z* 450.55, found for $[M+Na]^+$, *m/z* 472.35.

(*R*)-benzyl 3-(methyl(4-(2-oxopiperidin-1-yl)phenyl)carbamoyl)piperidine-1-carboxylate (68). ^{1}H-NMR ($CDCl_3$, 400 MHz): ^{13}C-NMR ($CDCl_3$, 100 MHz): ^{1}H-NMR ($CDCl_3$, 400 MHz): 7.40-7.34 (m, 2 H), 7.33-7.31 (m, 2 H), 7.30-7.23 (m, 2 H), 7.22-7.04 (m, 3 H), 5.20-5.00 (m, 2 H), 4.14 (t, J = 6.60 Hz, 1 H), 4.06 (t, J = 6.72 Hz, 1 H), 3.70-3.50 (m, 2 H), 3.21 (s, 3 H), 2.99 (t, J = 11.92 Hz, 1 H), 2.76 (t, J = 11.84 Hz, 1 H), 2.58 (t, J = 6.00 Hz, 2 H), 2.50-2.40 (m, 1 H), 2.00-1.94 (m, 4 H), 1.76-1.71 (m, 2 H), 1.61-1.58 (m, 1 H), 1.27-1.24 (m, 1 H). ^{13}C-NMR ($CDCl_3$, 100 MHz): 173.22, 170.26, 154.96, 142.71, 141.40, 136.80, 128.46, 127.98, 127.80, 127.64, 127.25, 67.04, 51.41, 46.60, 44.08, 39.71, 37.50, 32.84, 27.77, 24.12, 23.48, 21.32. MS (ESI) calculated for $C_{26}H_{31}N_3O_4$, $[M+H]^+$, *m/z* 450.55, found for $[M+Na]^+$, *m/z* 472.35.

***(S)-tert*-butyl 2-(methyl(4-(2-oxopiperidin-1-yl)phenyl)carbamoyl)piperidine-1-carboxylate (76).** ^{1}H-NMR ($CDCl_3$, 400 MHz): 7.36-7.31 (m, 4 H), 7.06 (d, J = 3.04 Hz, 1 H), 6.83 (d, J = 3.92 Hz, 1 H), 4.85-4.86 (m, 1 H), 3.85-3.72 (m, 1 H), 3.60 (t, J = 5.16 Hz, 2 H), 3.55-3.46 (m, 1 H), 3.17 (s, 3 H), 2.50 (t, J = 5.76 Hz, 2 H), 1.89-1.84 (m, 4 H), 1.59-1.54 (m, 2 H), 1.53-1.38 (m, 2 H), 1.38 (s, 9 H), 1.26-1.18 (m, 2 H). ^{13}C-NMR ($CDCl_3$, 100 MHz): 172.98, 170.04, 154.20, 142.50, 141.49, 127.96, 127.13, 79.57, 51.41, 45.26, 42.43, 38.05, 32.92, 28.52, 26.62, 24.80, 23.60, 21.50, 19.49. MS (ESI) calculated for $C_{23}H_{33}N_3O_4$, $[M+H]^+$, *m/z* 416.53, found for $[M+Na]^+$, 438.29 *m/z*.

***(R)- tert*-butyl 2-(methyl(4-(2-oxopiperidin-1-yl)phenyl)carbamoyl)piperidine-1-carboxylate (77).** ^{1}H-NMR ($CDCl_3$, 400 MHz): 7.35-7.29 (m, 4 H), 7.06 (d, J = 3.05 Hz, 1 H), 6.84 (d, J = 3.91 Hz, 1 H), 4.85-4.86 (m, 1 H), 3.85-3.71 (m, 1 H), 3.60 (t, J = 5.15 Hz, 2 H), 3.55-

3.46 (m, 1 H), 3.17 (s, 3 H), 2.50 (t, J = 5.75 Hz, 2 H), 1.90-1.85 (m, 4 H), 1.59-1.54 (m, 2 H), 1.54-1.38 (m, 2 H), 1.40 (s, 9 H), 1.26-1.18 (m, 2 H). ^{13}C-NMR ($CDCl_3$, 100 MHz): 172.95, 170.04, 154.20, 142.50, 141.49, 128.01, 127.13, 79.57, 51.41, 45.26, 42.43, 38.1, 32.92, 28.52, 26.63, 24.80, 23.60, 21.51, 19.50. MS (ESI) calculated for $C_{23}H_{33}N_3O_4$, $[M+H]^+$, *m/z* 416.53, found for $[M+Na]^+$, 438.24 *m/z*.

(*R*)-tert-butyl 2-(4-(3-oxomorpholino)phenylcarbamoyl)piperidine-1-carboxylate (80). ^{1}H-NMR ($CDCl_3$, 400 MHz): 7.46 (d, J = 8.80 Hz, 2 H), 7.19 (d, J = 8.36 Hz, 2 H), 4.80-4.72 (m, 1 H), 4.26 (s, 2 H), 4.14-4.04 (m, 2 H), 3.99 (t, J = 4.88 Hz, 2 H), 3.85 (t, J = 4.44 Hz, 2 H), 2.76 (t, J = 12.44 Hz, 1 H), 2.26-2.23 (m, 1 H), 1.77-1.50 (m, 4 H), 1.48 (s, 9 H). ^{13}C-NMR ($CDCl_3$, 100 MHz): 169.88, 166.88, 157.58, 137.04, 136.90, 126.27, 120.48, 81.26, 68.63, 64.16, 55.00, 49.92, 42.53, 28.42, 25.06, 20.37. MS (ESI) calculated for $C_{21}H_{29}N_3O_5$, $[M+H]^+$, *m/z* 404.48, found for $[M+Na]^+$, 426.34 *m/z* .

(*S*)-tert-butyl 6-(4-(3-oxomorpholino)phenylcarbamoyl)-5,6-dihydropyridine-1(2H)-carboxylate (83). ^{1}H-NMR ($CDCl_3$, 400 MHz): 7.50 (d, J = 8.80 Hz, 2 H), 7.22 (d, J = 8.64 Hz, 2 H), 5.85-5.80 (m, 1 H), 4.65-4.60 (m, 1 H), 5.00-4.93 (m, 1 H), 4.28 (s, 2 H), 4.20-4.07 (m, 1 H), 3.94 (t, J = 4.95 Hz, 2 H), 3.65 (t, J = 4.40 Hz, 2 H), 3.60-3.63 (m, 1 H), 2.60-3.72 (m, 1 H), 2.34-2.28 (m, 1 H). ^{13}C-NMR ($CDCl_3$, 100 MHz): 169.54, 166.82, 156.90, 137.99, 126.12, 123.36, 122.20, 120.36, 81.41, 68.54, 64.11, 61.4, 49.79, 41.50, 28.39, 24.10. MS (ESI) calculated for $C_{22}H_{29}N_3O_5$, $[M+H]^+$, *m/z* 402.46, found for $[M+Na]^+$, *m/z* 424.36.

(1*R*, 3*S*, 4*R*)-tert-butyl 3-(4-(3-oxomorpholino)phenylcarbamoyl)-2-azabicyclo[2.2.1] heptane -2-carboxylate (86). ^{1}H-NMR ($CDCl_3$, 400 MHz): 7.57 (d, J = 8.36 Hz, 2 H), 7.25 (d, J = 7.60 Hz, 2 H), 4.32 (s, 3 H), 4.14-4.11 (m, 1 H), 4.02 (t, J = 4.96 Hz, 2 H), 3.93-3.85 (m, 1 H), 3.73 (t, J = 4.84 Hz, 2 H), 3.03-2.96 (m, 1 H), 1.80-1.77 (m, 2 H), 1.67-1.65 (m, 2 H), 1.50 (s, 9

H), 1.39-1.36 (m, 2 H). ^{13}C-NMR ($CDCl_3$, 100 MHz): 169.30, 166.76, 157.58, 137.26, 136.90, 126.07, 120.42, 81.17, 68.57, 67.06, 64.35, 58.23, 49.78, 39.25, 36.65, 29.97, 28.43, 26.40. MS (ESI) calculated for $C_{22}H_{29}N_3O_5$, $[M+H]^+$, *m/z* 416.49, found for $[M+Na]^+$, *m/z* 438.20.

General Procedure for Amidation at the Ring Nitrogen of the Core Structure to Yield 7b, **22-49**, **51**, **58**, **62**, **69-73**, **78**, **79**, **81**, **84**, **or 87.** To a stirred solution of organic acid (1.0 mmol) in anhydrous CH_2Cl_2 (5 mL) was added 1-Ethyl-3-(3-dimethylaminopropyl) carbodiimide (EDCI, 1.1 mmol) and DMAP (1.1 mmol) at RT under nitrogen atmosphere. The unprotected form (free amine) of (**6**, **12-21**, **50**, **57**, **61**, **67**, **68**, **76**, **77**, **80**, **83**, or **86**) (1.1 mmol) in anhydrous CH_2Cl_2 (5 mL) was then added drop-wise. After stirring overnight, the reaction mixture was partitioned between 2.0 N HCl solution (20 mL) and CH_2Cl_2 (30 mL). The organic layer was washed further with 2 N HCl (2 × 10 mL) and saturated NaCl solution (20 mL), dried using anhydrous Na_2SO_4, and concentrated to give a crude, which purified by flash chromatography using gradient of CH_2Cl_2/CH_3OH as eluting phase to give the desired dicarboxamide product in 70 – 95 % yield.

(4-(4-nitrophenyl)piperazin-1-yl)(thiophen-2-yl)methanone (7b). ^{1}H-NMR ($CDCl_3$, 400 MHz): 8.07 (d, J = 9.40 Hz, 2 H), 7.44-7.42 (dd, J = 1.04 Hz, J = 5 Hz, 1 H), 7.30-7.29 (dd, J = 1.08 Hz, J = 3.68 Hz, 1 H), 3.03-3.01 (m, 1 H), 6.77 (d, J = 9.4 Hz, 2 H), 3.89 (t, J = 5.24 Hz, 4 H), 3.45 (t, J = 5.44 Hz, 4 H). ^{13}C-NMR ($CDCl_3$, 100 MHz): 163.81, 154.16, 139.39, 136.45, 129.39, 129.33, 126.95, 126.04, 125.96, 113.20, 112.55, 47.21, 46.25. MS (ESI) calculated for $C_{15}H_{15}N_3O_3S$, $[M+H]^+$, *m/z* 318.76, found for $[M+H]^+$, *m/z* 318.09.

(*S*)-N-methyl-N-(4-(2-oxopiperidin-1-yl)phenyl)-2-(thiophene-2-carbonyl)-1,2,3,4-tetrahydroisoquinoline-3-carboxamide (22). ^{1}H-NMR ($CDCl_3$, 400 MHz): 7.51-7.42 (m, 2 H), 7.41 (d, J = 0.88 Hz, 1 H), 7.4-7.39 (m, 1 H), 7.37 (d, J = 20.08 Hz, 2 H), 7.12-7.09 (m, 2 H), 7.04-7.00 (m, 3 H), 4.97-4.76 (dd, J = 14.96 Hz, J = 69.36 Hz, 2 H), 4.9-4.82 (m, 1 H), 3.55 (t, J= 5.44

Hz, 2 H), 3.21 (s, 3 H), 2.98-2.85 (m, 2 H), 2.50 (t, J= 6.44 Hz, 2 H), 1.90-1.84 (m, 4 H) . ^{13}C-NMR ($CDCl_3$, 100 MHz): 171.32, 170.07, 162.67, 142.93, 141.12, 137.40, 134.54, 133.10, 129.36, 129.01, 128.17, 127.60, 127.36, 126.88, 126.74, 125.48, 53.06, 51.37, 48.92, 38.00, 32.90, 31.24, 23.50, 21.36. MS (ESI) calculated for $C_{27}H_{27}N_3O_3S$, $[M+H]^+$, *m/z* 474.59, found for $[M+Na]^+$, *m/z* 496.21.

(*S*)-2-(5-chlorothiophene-2-carbonyl)-N-methyl-N-(4-(2-oxopiperidin-1-yl)phenyl)-1,2,3,4-tetrahydroisoquinoline-3-carboxamide (23). ^{1}H-NMR ($CDCl_3$, 400 MHz): 7.51-7.35 (m, 2 H), 7.28 (d, J = 8.28 Hz, 2 H), 7.15-7.11 (m, 3 H), 7.04-7.02 (m, 2 H), 6.83 (d, J= 3.92 Hz, 1 H), 4.95-4.76 (dd, J = 14.84 Hz, J = 63.4 Hz, 2 H), 4.90-4.80 (m, 1 H), 3.56 (t, J= 5.44 Hz, 2 H), 3.19 (s, 3 H), 3.00-2.94 (dd, J = 8.4 Hz, J = 15.24, 1 H), 2.89-2.84 (dd, J = 5.96 Hz, J = 15.16 Hz, 1 H), 2.50 (t, J= 6.44 Hz, 2 H), 1.92-1.80 (m, 4 H) . ^{13}C-NMR ($CDCl_3$, 100 MHz): 171.07, 170.05, 162.65, 143.0, 141.0, 136.22, 134.49, 134.17, 129.09, 128.09, 127.64, 127.37, 126.97, 126.11, 125.48, 53.16, 51.36, 48.71, 38.02, 32.92, 31.20, 23.51, 21.37. MS (ESI) calculated for $C_{27}H_{26}ClN_3O_3S$, $[M+H]^+$, *m/z* 509.04, found for $[M+Na]^+$, *m/z* 530.17.

(*S*)-2-(4-chlorobenzoyl)-N-methyl-N-(4-(2-oxopiperidin-1-yl)phenyl)-1,2,3,4-tetrahydro-isoquinoline-3-carboxamide (24). ^{1}H-NMR ($CDCl_3$, 400 MHz): 7.53 (d, J = 6.04 Hz, 2 H), 7.39-7.29 (m, 5 H), 7.15-7.09 (m, 3 H), 7.06 (d, J = 10.24 Hz, 1 H), 6.87 (d, J = 7.00 Hz, 1 H), 4.71 (t, J = 7.40 Hz, 1 H), 4.59-4.39 (dd, J = 14.84 Hz, J = 63.76 Hz, 2 H), 3.60 (t, J= 5.28 Hz, 2 H), 3.26 (s, 3 H), 3.03-2.97 (dd, J = 9.60 Hz, J = 14.84 Hz, 1 H), 2.91-2.86 (dd, J = 5.88 Hz, J = 14.92 Hz, 1 H), 2.57 (t, J = 5.92 Hz, 2 H), 1.90-1.84 (m, 4 H). ^{13}C-NMR ($CDCl_3$, 100 MHz): 171.92, 171.69, 170.36, 142.52, 141.47, 136.38, 134.60, 133.75, 133.53, 131.45, 128.91, 128.70, 128.41, 127.96, 127.53, 127.10, 125.24, 51.74, 49.05, 38.11, 32.24, 31.19, 29.69, 23.22, 20.92. MS (ESI) calculated for $C_{29}H_{28}ClN_3O_3$, $[M+H]^+$, *m/z* 503.01, found for $[M+Na]^+$, *m/z* 524.22 .

(*S*)-N-methyl-2-(4-methylbenzoyl)-N-(4-(2-oxopiperidin-1-yl)phenyl)-1,2,3,4-tetrahydro-isoquinoline-3-carboxamide (25). ^{1}H-NMR ($CDCl_3$, 400 MHz): 7.53 (d, J = 6.76 Hz, 2 H), 7.30-7.26 (m, 4 H), 7.17-7.07 (m, 4 H), 7.03 (d, J = 6.52 Hz, 1 H), 6.87 (d, J = 6.84 Hz, 1 H), 4.76 (t, J = 8.08 Hz, 1 H), 4.60-4.48 (dd, J = 14.72 Hz, J = 33.24 Hz, 2 H), 3.58 (t, J= 5.28 Hz, 2 H), 3.24 (s, 3 H), 3.02-2.96 (dd, J = 9.12 Hz, J = 15.00 Hz, 1 H), 2.91-2.85 (dd, J = 5.80 Hz, J = 14.72 Hz, 1 H), 2.52 (t, J = 5.92 Hz, 2 H), 2.33 (s, 3 H), 1.90-1.84 (m, 4 H). ^{13}C-NMR ($CDCl_3$, 100 MHz): 170.94, 170.21, 169.63, 141.73, 140.36, 139.17, 134.11, 132.99, 131.58, 129.06, 128.07, 127.35, 126.63, 126.49, 126.28, 125.84, 124.22, 51.68, 50.51, 47.95, 36.98, 31.64, 30.25, 28.78, 22.39, 20.19. MS (ESI) calculated for $C_{30}H_{31}N_3O_3$, $[M+H]^+$, *m/z* 482.59, found for $[M+Na]^+$, *m/z* 504.27.

(*S*)-2-(4-methoxybenzoyl)-N-methyl-N-(4-(2-oxopiperidin-1-yl)phenyl)-1,2,3,4-tetrahydroisoquinoline-3-carboxamide (26). ^{1}H-NMR ($CDCl_3$, 400 MHz): 7.51 (d, J = 6.76 Hz, 2 H), 7.35 (d, J = 7.52 Hz, 2 H), 7.28 (d, J = 6.08 Hz, 2 H), 7.11-7.02 (m, 4 H), 6.86 (d, J = 8.68 Hz, 2 H), 4.79 (t, J = 7.12 Hz, 1 H), 4.63-4.52 (dd, J = 14.44 Hz, J = 31.08 Hz, 2 H), 3.78 (s, 3 H), 3.57 (t, J= 5.28 Hz, 2 H), 3.24 (s, 3 H), 3.02-2.96 (m,1 H), 2.90-2.86 (dd, J = 5.76 Hz, J = 14.64 Hz, 1 H), 2.50 (t, J = 5.92 Hz, 2 H), 1.90-1.84 (m, 4 H). ^{13}C-NMR ($CDCl_3$, 100 MHz): 171.92, 170.66, 170.08, 160.90, 142.90, 141.27, 135.23, 134.12, 129.26, 128.28, 128.04, 127.54, 127.29, 126.79, 125.22, 113.70, 55.36, 52.59, 51.39, 49.06, 37.94, 32.90, 31.28, 23.51, 21.36. MS (ESI) calculated for $C_{30}H_{31}N_3O_4$, $[M+H]^+$, *m/z* 498.59, found for $[M+Na]^+$, *m/z* 520.29.

***(S)*-2-(2-(4-chlorophenyl)acetyl)-N-methyl-N-(4-(2-oxopiperidin-1-yl)phenyl)-1,2,3,4-tetrahydroisoquinoline-3-carboxamide (27).** ^{1}H-NMR ($CDCl_3$, 400 MHz): 7.47 (d, J = 7.76 Hz, 2 H), 7.28 (d, J = 8.32 Hz, 2 H), 7.20 (d, J = 8.24 Hz, 2 H), 7.12-7.07 (m, 4 H), 6.98 (d, J = 6.08 Hz, 1 H), 6.86 (d, J = 6.44 Hz, 1 H), 4.86 (t, J = 6.68 Hz, 1 H), 4.63-4.48 (dd, J = 14.68 Hz, J =

47.76 Hz, 2 H), 3.74 (s, 2 H), 3.58 (t, J = 5.08 Hz, 2 H), 3.16 (s, 3 H), 2.85-2.73 (m, 2 H), 2.51 (t, J = 5.92 Hz, 2 H), 1.90-1.85 (m, 4 H) . ^{13}C-NMR ($CDCl_3$, 100 MHz): 170.71, 169.17, 168.99, 141.86, 140.16, 133.14, 132.16, 131.93, 129.39, 127.80, 127.56, 126.88, 126.23, 125.85, 124.92, 50.97, 50.41, 46.16, 39.60, 36.98, 31.86, 30.15, 22.48, 20.32. MS (ESI) calculated for $C_{30}H_{30}ClN_3O_3$, $[M+H]^+$, *m/z* 517.04, found for $[M+Na]^+$, *m/z* 538.23.

(*S*)-N-methyl-N-(4-(2-oxopiperidin-1-yl)phenyl)-2-(2-p-tolylacetyl)-1,2,3,4-tetrahydro-isoquinoline-3-carboxamide (28). ^{1}H-NMR ($CDCl_3$, 400 MHz): 7.45 (d, J = 7.32 Hz, 2 H), 7.26 (d, J = 8.20 Hz, 2 H), 7.09-6.95 (m, 7 H), 6.82 (d, J = 6.92 Hz, 1 H), 4.85 (t, J = 6.56 Hz, 1 H), 4.60-4.53 (m, 2 H), 3.73 (s, 2 H), 3.58 (t, J = 5.28 Hz, 2 H), 3.16 (s, 3 H), 2.84-2.75 (m, 2 H), 2.50 (t, J = 5.92 Hz, 2 H), 2.23 (s, 3 H), 1.90-1.85 (m, 4 H) . ^{13}C-NMR ($CDCl_3$, 100 MHz): 172.80, 171.87, 170.34, 142.77, 141.27, 136.47, 135.29, 134.40, 133.17, 132.66, 131.52, 129.47, 128.73, 127.94, 126.85, 126.74, 125.94, 51.83, 47.11, 46.12, 40.07, 37.89, 32.74, 31.21, 30.70, 23.36, 21.06. MS (ESI) calculated for $C_{31}H_{33}N_3O_3$, $[M+H]^+$, *m/z* 496.62, found for $[M+Na]^+$, *m/z* 518.36.

(*S*)-2-(2-(4-methoxyphenyl)acetyl)-N-methyl-N-(4-(2-oxopiperidin-1-yl)phenyl)-1,2,3,4-tetrahydroisoquinoline-3-carboxamide (29). ^{1}H-NMR ($CDCl_3$, 400 MHz): 7.47 (d, J = 7.76 Hz, 2 H), 7.28 (d, J = 8.36 Hz, 2 H), 7.11-7.03 (m, 4 H), 6.97 (d, J = 6.72 Hz, 1 H), 6.84 (d, J = 6.8 Hz, 1 H), 6.77 (d, J= 8.64 Hz, 2 H), 4.88 (t, J = 6.80 Hz, 1 H), 4.63-4.52 (dd, J = 14.76 Hz, J = 30.56 Hz, 2 H), 3.72 (s, 2 H), 3.70 (s, 3 H), 3.59 (t, J = 5.28 Hz, 2 H), 3.17 (s, 3 H), 2.81-2.73 (m, 2 H), 2.50 (t, J = 5.92 Hz, 2 H), 1.90-1.85 (m, 4 H) . ^{13}C-NMR ($CDCl_3$, 100 MHz): 170.82, 169.75, 169.06, 157.43, 141.84, 140.26, 133.41, 132.16, 128.81, 127.30, 126.46, 126.37, 125.75, 124.39, 113.19, 54.25, 50.83, 50.41, 46.11, 39.60, 36.96, 31.90, 30.21, 22.51, 20.37. MS (ESI) calculated for $C_{31}H_{33}N_3O_4$, $[M+H]^+$, *m/z* 512.62, found for $[M+Na]^+$, *m/z* 534.3.

(*S*)-N-methyl-2-(2-(4-nitrophenyl)acetyl)-N-(4-(2-oxopiperidin-1-yl)phenyl)-1,2,3,4-tetrahydroisoquinoline-3-carboxamide (30). ^{1}H-NMR ($CDCl_3$, 400 MHz): 8.12 (d, J = 8.72 Hz, 2 H), 7.44 (d, J = 8.44 Hz, 2 H), 7.38 (d, J = 8.72 Hz, 2 H), 7.29 (d, J = 8.52 Hz, 2 H), 7.19-7.07 (m, 2 H), 7.00 (d, J= 7.04 Hz, 1 H), 6.92 (d, J = 6.60 Hz, 1 H), 4.90 (t, J = 6.92 Hz, 1 H), 4.69-4.49 (dd, J = 14.72 Hz, J = 63.36 Hz, 2 H), 3.93-3.83 (dd, J = 16.12 Hz, J = 22.80, 2 H), 3.59 (t, J = 5.64 Hz, 2 H), 3.17 (s, 3 H), 2.85-2.77 (m, 2 H), 2.50 (t, J = 6.00 Hz, 2 H), 1.90-1.85 (m, 4 H) . ^{13}C-NMR ($CDCl_3$, 100 MHz): 171.53, 170.09, 168.99, 147.01, 142.98, 141.06, 133.86, 132.99, 130.75, 130.13, 129.84, 128.21, 127.72, 127.51, 127.18, 126.98, 125.81, 123.85, 123.52, 51.40, 47.31, 40.85, 38.02, 32.93, 31.13, 29.70, 23.52, 21.38. MS (ESI) calculated for $C_{30}H_{30}N_4O_5$, $[M+H]^+$, *m/z* 527.59, found for $[M+Na]^+$, *m/z* 549.34.

(*S*)-N-methyl-N-(4-(2-oxopiperidin-1-yl)phenyl)-2-(2-(4-(trifluoromethyl) phenyl)acetyl)-1,2,3,4-tetrahydroisoquinoline-3-carboxamide (31). ^{1}H-NMR ($CDCl_3$, 400 MHz): 7.49 (d, J = 8.80 Hz, 2 H), 7.45 (d, J = 8.32 Hz, 2 H), 7.31, (d, J = 8.4 Hz, 2 H), 7.29 (d, J = 9.88 Hz, 2 H), 7.10-7.03 (m, 2 H), 6.98 (d, J = 7.84 Hz, 1 H), 6.85 (d, J = 6.72 Hz, 1 H), 4.89 (t, J = 6.88 Hz, 1 H), 4.66-4.48 (dd, J = 14.76 Hz, J = 55.44 Hz, 2 H), 3.84 (s, 2 H), 3.59 (t, J = 5.44 Hz, 2 H), 3.17 (s, 3 H), 2.82-2.71 (m, 2 H), 2.50 (t, J = 6.00 Hz, 2 H), 1.91-1.85 (m, 4 H). ^{13}C-NMR ($CDCl_3$, 100 MHz): 171.64, 170.08, 169.56, 142.94, 141.13, 138.82, 134.08, 133.06, 130.48, 129.65, 129.40, 129.21, 128.25, 127.82, 127.35, 126.89, 125.65, 125.32, 60.39, 51.41, 47.25, 41.05, 37.41, 32.93, 31.16, 23.52, 21.38. MS (ESI) calculated for $C_{31}H_{30}F_3N_3O_3$, $[M+H]^+$, *m/z* 550.59, found for $[M+Na]^+$, *m/z* 572.32.

(*S*)-2-(2-(3,4-dimethoxyphenyl)acetyl)-N-methyl-N-(4-(2-oxopiperidin-1-yl)phenyl)-1,2,3,4-tetrahydroisoquinoline-3-carboxamide (32). ^{1}H-NMR ($CDCl_3$, 400 MHz): 7.47 (d, J = 6.64 Hz, 2 H), 7.27 (d, J = 7.76 Hz, 2 H), 7.09-6.97 (m, 3 H), 6.84 (d, J = 6.84 Hz, 1 H), 6.75-6.69

(m, 3 H), 4.85 (t, J = 6.80 Hz, 1 H), 4.60-4.50 (dd, J = 14.68 Hz, J = 26.08 Hz, 2 H), 3.78 (s, 3 H), 3.75 (s, 3 H), 3.73 (s, 2 H), 3.58 (t, J = 5.28 Hz, 2 H), 3.16 (s, 3 H), 2.85-2.73 (m, 2 H), 2.51 (t, J = 5.92 Hz, 2 H), 1.90-1.85 (m, 4 H). ^{13}C-NMR ($CDCl_3$, 100 MHz): 170.86, 169.74, 169.33, 148.18, 146.87, 141.79, 140.26, 133.44, 132.20, 131.55, 127.43, 126.99, 126.32, 125.78, 124.39, 120.53, 119.90, 110.98, 110.48, 54.94, 54.86, 50.89, 46.20, 45.16, 39.95, 36.96, 31.80, 30.18, 22.46, 20.29. MS (ESI) calculated for $C_{32}H_{35}N_3O_5$, $[M+H]^+$, *m/z* 542.27, found for $[M+Na]^+$, *m/z* 564.33.

(*S*)-2-(2-(3,4-dichlorophenyl)acetyl)-N-methyl-N-(4-(2-oxopiperidin-1-yl)phenyl)-1,2,3,4-tetrahydroisoquinoline-3-carboxamide (33). ^{1}H-NMR ($CDCl_3$, 400 MHz): 7.47 (d, J = 7.76 Hz, 2 H), 7.37-7.28 (m, 4 H), 7.11-6.99 (m, 4 H), 6.91 (d, J = 8.36 Hz, 1 H), 4.87 (t, J = 6.88 Hz, 1 H), 4.65-4.47 (dd, J = 14.64 Hz, J = 59.20 Hz, 2 H), 3.71 (s, 2 H), 3.59 (t, J = 5.56 Hz, 2 H), 3.16 (s, 3 H), 2.87-2.78 (m, 2 H), 2.53 (t, J = 5.92 Hz, 2 H), 1.90-1.85 (m, 4 H). ^{13}C-NMR ($CDCl_3$, 100 MHz): 170.66, 170.38, 169.46, 142.84, 141.10, 135.16, 134.73, 133.94, 132.52, 131.74, 131.07, 130.56, 128.61, 128.21, 127.61, 127.11, 126.77, 125.39, 123.61, 51.46, 47.17, 40.8, 38.05, 32.78, 31.73, 30.66, 23.45, 21.29. MS (ESI) calculated for $C_{30}H_{29}Cl_2N_3O_3$, $[M+H]^+$, *m/z* 551.48, found for $[M+Na]^+$, *m/z* 572.27.

(*S*)-2-(2-(2,4-dichlorophenyl)acetyl)-N-methyl-N-(4-(2-oxopiperidin-1-yl)phenyl)-1,2,3,4-tetrahydroisoquinoline-3-carboxamide (34). ^{1}H-NMR ($CDCl_3$, 400 MHz): 7.47 (d, J = 7.76 Hz, 2 H), 7.28-7.19 (m, 4 H), 7.14-7.07 (m, 3 H), 6.99-6.93 (m, 2 H), 4.93 (t, J = 6.52 Hz, 1 H), 4.66-4.48 (dd, J = 14.80 Hz, J = 56.84 Hz, 2 H), 3.88-3.76 (dd, J = 16.24 Hz, J = 31 Hz, 2 H), 3.58 (t, J = 5.24 Hz, 2 H), 3.16 (s, 3 H), 2.85-2.75 (m, 2 H), 2.50 (t, J = 6.12 Hz, 2 H), 1.90-1.85 (m, 4 H) . ^{13}C-NMR ($CDCl_3$, 100 MHz): 171.57, 170.07, 169.21, 142.90, 141.15, 134.58, 134.05, 133.47, 132.94, 131.72, 129.14, 128.25, 127.58, 127.54, 127.50, 127.35, 126.91, 125.46. MS (ESI) calculated for $C_{30}H_{29}Cl_2N_3O_3$, $[M+H]^+$, *m/z* 551.48, found for $[M+Na]^+$, *m/z* 572.27.

***(R)*-2-(2-(4-chlorophenyl)acetyl)-N-methyl-N-(4-(2-oxopiperidin-1-yl)phenyl)-1,2,3,4-tetrahydroisoquinoline-3-carboxamide (35).** ^{1}H-NMR ($CDCl_3$, 400 MHz): 7.47 (d, J = 7.75 Hz, 2 H), 7.28 (d, J = 8.30 Hz, 2 H), 7.20 (d, J = 8.25 Hz, 2 H), 7.13-7.07 (m, 4 H), 6.98 (d, J = 6.08 Hz, 1 H), 6.86 (d, J = 6.45 Hz, 1 H), 4.86 (t, J = 6.70 Hz, 1 H), 4.64-4.48 (dd, J = 14.70 Hz, J = 47.80 Hz, 2 H), 3.74 (s, 2 H), 3.58 (t, J = 5.09 Hz, 2 H), 3.16 (s, 3 H), 2.85-2.72 (m, 2 H), 2.51 (t, J = 5.91 Hz, 2 H), 1.90-1.85 (m, 4 H) . ^{13}C-NMR ($CDCl_3$, 100 MHz): 170.71, 169.17, 169.0, 141.86, 140.16, 133.14, 132.20, 131.93, 129.39, 127.80, 127.57, 126.88, 126.23, 125.85, 124.92, 50.97, 50.40, 46.16, 39.60, 36.98, 31.87, 30.15, 22.48, 20.32. MS (ESI) calculated for $C_{30}H_{30}ClN_3O_3$, $[M+H]^+$, *m/z* 517.04, found for $[M+Na]^+$, *m/z* 538.28.

(*R*)-N-methyl-N-(4-(2-oxopiperidin-1-yl)phenyl)-2-(2-(4-(trifluoromethyl)phenyl) acetyl)-1,2,3,4-tetrahydroisoquinoline-3-carboxamide (36). ^{1}H-NMR ($CDCl_3$, 400 MHz): 7.45-7.31 (m, 4 H), 7.28-7.21 (m, 4 H), 7.17-7.08 (m, 2 H), 7.06-6.84 (m, 2 H), 4.87 (m, 1 H), 4.63-4.47 (dd, J = 14.80 Hz, J = 47.72 Hz, 2 H), 3.84 (d, J = 5.32 Hz, 2 H), 3.59 (t, J = 5.32 Hz, 2 H), 3.18 (s, 3 H), 2.86-2.75 (m, 2 H), 2.50 (t, J = 6.00 Hz, 2 H), 1.90-1.85 (m, 4 H) . ^{13}C-NMR ($CDCl_3$, 100 MHz): 171.67, 170.87, 169.87, 142.66, 141.30, 138.62, 133.87, 133.04, 129.72, 129.08, 128.31, 127.69, 127.45, 126.93, 125.67, 125.51, 122.81, 51.57, 47.24, 40.93, 38.06, 32.57, 31.06, 29.70, 23.36, 21.15. MS (ESI) calculated for $C_{30}H_{30}N_4O_5$, $[M+H]^+$, *m/z* 550.59, found for $[M+Na]^+$, *m/z* 572.32.

***(S)*-N-(4-(2-oxopiperidin-1-yl)phenyl)-2-(4-(trifluoromethyl)benzoyl)-1,2,3,4-tetrahydro-isoquinoline-3-carboxamide (37).** ^{1}H-NMR ($CDCl_3$, 400 MHz): 8.97 (s, 1 H), 7.73 (d, J = 7.88Hz, 2 H), 7.57 (d, J = 11.45 Hz, 2 H), 7.55 (d, J = 8.12 Hz, 2 H), 7.35-7.27 (m, 3 H), 7.24-7.18 (m, 2 H), 6.94 (d, J = 7.00 Hz, 1 H), 5.25 (t, J = 6.64 Hz, 1 H), 4.51-4.40 (dd, J = 15.16 Hz, J = 27.04 Hz, 2 H), 4.32 (s, 2 H), 4.02 (t, J = 4.80 Hz, 2 H), 3.72 (t, J =5.00 Hz, 2 H), 3.61-

3.55 (dd, J = 6.96 Hz, J = 16.40 Hz, 1 H), 3.22-3.17 (dd, J = 6.68 Hz, J = 15.68 Hz, 1 H). ^{13}C-NMR ($CDCl_3$, 100 MHz): 171.24, 168.26, 166.89, 138.58, 136.83, 133.83, 133.25, 132.30, 128.33, 128.24, 127.56, 126.18, 125.84, 125.21, 124.98, 120.69, 68.58, 64.37, 54.46, 49.81, 48.28, 29.02. MS (ESI) calculated for $C_{28}H_{24}F_3N_3O_4$, $[M+H]^+$, *m/z* 524.51, found for $[M+Na]^+$, *m/z* 546.30.

(*S*)-2-(3-(5-(4-chlorophenyl)oxazol-2-yl)propanoyl)-N-methyl-N-(4-(2-oxopiperidin-1-yl)phenyl)-1,2,3,4-tetrahydroisoquinoline-3-carboxamide (38). ^{1}H-NMR ($CDCl_3$, 400 MHz): 7.50 (d, J = 7.32 Hz, 2 H), 7.41 (d, J = 8.20 Hz, 2 H), 7.31-7.19 (m, 4 H), 7.12-7.07 (m, 3 H), 7.05-6.95 (m, 2 H), 4.97 (t, J = 5.88 Hz, 1 H), 4.71-4.62 (dd, J = 14.48 Hz, J = 21.64 Hz, 2 H), 3.59 (t, J = 5.28 Hz, 2 H), 3.59-2.90 (m, 4 H), 3.14 (s, 3 H), 2.84-2.74 (m, 2 H), 2.50 (t, J = 5.92 Hz, 2 H),1.90-1.85 (m, 4 H) . ^{13}C-NMR ($CDCl_3$, 100 MHz): 171.64, 170.25, 164.13, 150.50, 142.87, 141.13, 134.34, 133.82, 132.80, 131.76, 129.49, 129.19, 128.63, 127.89, 127.45, 126.92, 125.68, 125.37, 123.68, 51.62, 46.55, 38.04, 32.86, 31.07, 30.53, 29.1, 27.30, 23.49, 21.33. MS (ESI) calculated for $C_{34}H_{33}N_4O_4$, $[M+H]^+$, *m/z* 598.11, found for $[M+Na]^+$, *m/z* 619.33.

(*S,E*)-2-(3-(2,4-dimethoxyphenyl)acryloyl)-N-methyl-N-(4-(2-oxopiperidin-1-yl)phenyl)-1,2,3,4-tetrahydroisoquinoline-3-carboxamide (39). ^{1}H-NMR ($CDCl_3$, 400 MHz): 7.77 (d, J = 15.52 Hz,1 H), 7.55-7.43 (m, 2 H), 7.38 (d, J = 8.48 Hz, 1 H), 7.36-7.27 (m, 2 H), 7.11-7.02 (m, 4 H), 6.89 (d, J= 15.52 Hz, 1 H), 6.45-6.42 (dd, J = 2 Hz, J = 8.56 Hz, 1 H), 6.39 (s, 1 H), 5.08-5.06 (m, 1 H), 4.78 (s, 3 H), 3.79 (s, 3 H), 3.77 (s, 3 H), 3.64 (t, J = 5.44 Hz, 2 H), 3.17 (s, 3 H), 2.93-2.87 (dd, J = 6.48 Hz, J = 15.56 Hz, 1 H), 2.83-2.78 (dd, J = 4.76 Hz, J = 14.76 Hz, 1H), 2.49 (t, J = 6.44 Hz, 2 H), 1.88-1.80 (m, 4 H) . ^{13}C-NMR ($CDCl_3$, 100 MHz): 170.73, 169.04, 166.33, 161.16, 158.71, 140.36, 137.42, 133.22, 132.22, 129.39, 127.23, 126.68, 126.29, 125.72, 124.61, 116.53, 115.03, 104.13, 97.50, 54.47, 54.44, 50.64, 50.40, 45.86, 36.96, 31.90, 30.25,

22.49, 20.37. MS (ESI) calculated for $C_{33}H_{35}N_3O_5$, $[M+H]^+$, *m/z* 554.66, found for $[M+Na]^+$, *m/z* 576.3.

(*S*)-2-(5-chlorothiophene-2-carbonyl)-N-methyl-N-(4-(3-oxomorpholino)phenyl)-1,2,3,4-tetra-hydroisoquinoline-3-carboxamide (40). ^{1}H-NMR ($CDCl_3$, 400 MHz): 7.49-7.44 (m, 2 H), 7.37 (d, J = 8.16 Hz, 2 H), 7.14-7.11 (m, 3 H), 7.04-7.02 (m, 2 H), 6.84 (d, J= 3.96 Hz,1 H), 4.96-4.76 (dd, J = 14.80 Hz, J = 65.08 Hz, 2 H), 4.82-4.79 (m, 1 H), 4.28 (s, 2 H), 3.96 (t, J= 5.36 Hz, 2 H), 3.69 (t, J = 5.20 Hz, 2H), 3.20 (s, 3 H), 3.01-2.95 (dd, J = 8.36 Hz, J = 15.28, 1 H), 2.89-2.84 (dd, J = 5.56 Hz, J = 15.16 Hz, 1 H). ^{13}C-NMR ($CDCl_3$, 100 MHz): 171.11, 166.68, 162.71, 141.48, 140.94, 136.12, 134.62, 134.17, 133.41, 129.12, 128.31, 127.72, 127.61, 127.02, 126.51, 126.12, 125.50, 68.58, 64.08, 55.99, 53.16, 49.38, 38.03, 31.23. MS (ESI) calculated for $C_{26}H_{24}ClN_3O_4S$, $[M+H]^+$, *m/z* 511.01, found for $[M+Na]^+$, *m/z* 532.22.

(*S*)-2-(2-(4-chlorophenyl)acetyl)-N-methyl-N-(4-(3-oxomorpholino)phenyl)-1,2,3,4-tetrahydroisoquinoline-3-carboxamide (41). ^{1}H-NMR ($CDCl_3$, 400 MHz): 7.49 (d, J = 7.76 Hz, 2 H), 7.37 (d, J = 8.44 Hz, 2 H), 7.22 (d, J= 8.00 Hz, 2 H), 7.14-7.06 (m, 4 H), 6.98 (d, J = 5.80 Hz, 1 H), 6.87 (d, J = 6.28 Hz, 1 H), 4.85 (t, J = 6.90 Hz, 1 H), 4.64-4.49 (dd, J = 14.68 Hz, J = 46.6 Hz, 2 H), 4.28 (s, 2 H), 3.97 (t, J = 4.72 Hz, 2 H), 3.75 (s, 2 H), 3.71 (t, J = 5.20 Hz, 2 H), 3.17 (s, 3 H), 2.85-2.74 (m, 2 H). ^{13}C-NMR ($CDCl_3$, 100 MHz): 171.08, 170.00, 166.70, 141.64, 140.95, 134.16, 133.12, 133.04, 132.76, 130.31, 129.35, 128.84, 128.47, 127.52, 126.91, 126.45, 125.37, 68.59, 64.09, 51.96, 49.41, 47.18, 40.63, 37.99, 31.19, 21.02. MS (ESI) calculated for $C_{29}H_{28}ClN_3O_4$, $[M+H]^+$, *m/z* 519.01, found for $[M+Na]^+$, *m/z* 540.25.

***(S)*-2-(5-chloro-3-methylbenzo[b]thiophene-2-carbonyl)-N-(4-(3-oxomorpholino) phenyl)-1,2,3,4-tetrahydroisoquinoline-3-carboxamide (42).** ^{1}H-NMR ($CDCl_3$, 400 MHz): 7.69–7.65 (m, 2 H), 7.43–7.32 (m, 3H), 7.18–6.91 (m, 6 H), 6.17–5.15 (m, 1H), 4.65–4.42 (m,

2H), 4.24 (s, 2 H), 3.94 (t, J = 4.8 Hz, 2 H), 3.62 (t, J = 4.92 Hz, 2 H), 3.44–3.39 (dd, J = 5.88 Hz, J = 16.16 Hz, 1 H), 3.16–3.11 (dd, J = 6.6 Hz, J = 15.88 Hz, 1 H), 2.32 (s, 3 H). ^{13}C-NMR (CD_3OD, 100 MHz):168.33, 166.89, 166.45, 140.60, 137.36, 136.65, 132.83, 132.05, 131.31, 128.68, 128.39, 128.17, 127.98, 126.88, 126.36, 126.06, 125.94, 125.65, 123.70, 122.53, 120.81, 68.55, 64.11, 55.96, 49.80, 47.20, 29.92, 12.77.MS (ESI) calculated for $C_{30}H_{26}ClN_3O_4S$, $[M+H]^+$, *m/z* 560.14, found for $[M+Na]^+$, *m/z* 582.33.

(*S*)-2-(3-(4-methoxyphenyl)propanoyl)-N-methyl-N-(4-(3-oxomorpholino)phenyl)-1,2,3,4-tetra-hydroisoquinoline-3-carboxamide (43). ^{1}H-NMR ($CDCl_3$, 400 MHz): 7.51 (d, J = 7.40 Hz, 2 H), 7.40 (d, J = 8.20 Hz, 2 H), 7.12-7.09 (m, 2 H), 7.07 (d, J = 8.56 Hz, 2 H), 7.00-6.98 (m, 2 H), 6.76 (d, J= 8.56 Hz, 1 H), 4.90 (t, J = 6.90 Hz, 1 H), 4.64-4.47 (dd, J = 14.88 Hz, J = 54.92 Hz, 2 H), 4.29 (s, 2 H), 3.98 (t, J = 4.60 Hz, 2 H), 3.73 (t, J = 5.04 Hz, 2 H), 3.71 (s, 3 H), 3.18 (s, 3 H), 2.88-2.73 (m, 4 H), 2.71-2.62 (m, 2 H). ^{13}C-NMR ($CDCl_3$, 100 MHz): 171.90, 171.84, 166.70, 158.08, 141.73, 140.80, 134.22, 133.24, 133.00, 129.29, 128.45, 127.60, 127.44, 126.86, 126.45, 125.49, 114.00, 68.60, 64.10, 55.28, 51.50, 49.43, 46.66, 37.97, 36.36, 31.18, 30.27. MS (ESI) calculated for $C_{31}H_{33}N_3O_5$, $[M+H]^+$, *m/z* 528.62, found for $[M+Na]^+$, *m/z* 550.34.

(*S,E*)-2-(3-(2,4-dimethoxyphenyl)acryloyl)-N-methyl-N-(4-(3-oxomorpholino)phenyl)-1,2,3,4-tetrahydroisoquinoline-3-carboxamide (44). ^{1}H-NMR ($CDCl_3$, 400 MHz): 7.77 (d, J = 15.52 Hz,1 H), 7.54 (d, J = 6.84 Hz, 2 H), 7.38 (d, J = 8.48 Hz, 3 H), 7.13-7.06 (m, 3 H), 7.03 (d, J = 4.76 Hz, 1 H), 6.89 (d, J= 15.56 Hz, 1 H), 6.45-6.43 (dd, J = 2.28 Hz, J = 8.48 Hz, 1 H), 6.39 (d, J = 2.28 Hz, 1 H), 5.08-5.06 (m, 1 H), 4.77 (s, 2 H), 4.27 (s, 2 H), 3.93 (t, J = 2.72 Hz, 2 H), 3.80 (s, 3 H), 3.77 (s, 3 H), 3.71 (t, J = 4.72 Hz, 2 H), 3.18 (s, 3 H), 2.94-2.89 (dd, J = 7.08 Hz, J = 15.56 Hz, 1 H), 2.86-2.80 (dd, J = 4.44 Hz, J = 14.04 Hz, 1H). ^{13}C-NMR ($CDCl_3$, 100 MHz): 170.69, 166.34, 165.65, 161.19, 158.70, 140.79, 137.48, 133.15, 132.17, 129.40, 127.38, 126.67,

126.30, 125.76, 125.46, 124.62, 116.44, 114.89, 104.13, 97.49, 67.55, 63.06, 54.47, 54.44, 50.68, 48.41, 45.83, 36.98, 30.23. MS (ESI) calculated for $C_{32}H_{33}N_3O_5$, $[M+H]^+$, *m/z* 556.63, found for $[M+Na]^+$, *m/z* 578.34.

(S)-2-(4-(4-bromophenyl)thiophene-2-carbonyl)-N-methyl-N-(4-(3-oxomorpholino) phenyl)-1,2,3,4-tetrahydroisoquinoline-3-carboxamide (45). ^{1}H-NMR ($CDCl_3$, 400 MHz): 7.59-7.47 (m, 7 H), 7.38 (d, J = 8.44 Hz, 2 H), 7.16-7.10 (m, 2 H), 7.05-7.02 (m, 2 H), 5.00-4.79 (m, 3 H), 4.27 (s, 2 H), 3.94 (t, J = 4.92 Hz, 2 H), 3.67 (t, J = 5.01, 2 H), 3.22 (s, 3 H), 2.98-2.97 (m, 1 H), 2.92-2.87 (dd, J= 5.88 Hz, J = 15.0 Hz, 1 H). ^{13}C-NMR ($CDCl_3$, 100 MHz):171.30, 166.69, 163.76, 141.54, 140.94, 140.82, 138.26, 134.46, 134.0, 132.12, 128.41, 127.90, 127.75, 127.58, 127.03, 126.50, 125.50, 123.99, 121.63, 68.58, 64.07, 53.26, 49.36, 38.03, 31.32, 26.50. MS (ESI) calculated for $C_{32}H_{28}BrN_3O_4S$, $[M+H]^+$, *m/z* 631.56, found for $[M+Na]^+$, *m/z* 652.24.

(*S*)-2-(2-(4-chlorophenyl)acetyl)-N-ethyl-N-(4-(3-oxomorpholino)phenyl)-1,2,3,4-tetrahydroisoquinoline-3-carboxamide (46). ^{1}H-NMR ($CDCl_3$, 400 MHz): 7.49 (d, J = 7.76 Hz, 2 H), 7.37 (d, J = 8.44 Hz, 2 H), 7.22 (d, J= 8.00 Hz, 2 H), 7.14-7.06 (m, 4 H), 6.98 (d, J = 5.80 Hz, 1 H), 6.87 (d, J = 6.28 Hz, 1 H), 4.77 (t, J = 6.88 Hz, 1 H), 4.63-4.48 (dd, J = 14.76 Hz, J = 47.08 Hz, 2 H), 4.28 (s, 2 H), 3.96 (t, J = 4.72 Hz, 2 H), 3.74 (s, 2 H), 3.71 (t, J = 5.12 Hz, 2 H), 3.74-3.25 (m, 2 H), 2.80-2.69 (m, 2 H), 1.04 (t, J = 7.08 Hz, 3 H). ^{13}C-NMR ($CDCl_3$, 100 MHz): 171.08, 169.90, 166.67, 140.95, 140.01, 134.21, 133.19, 132.72, 130.64, 130.46, 130.29, 129.35, 128.97, 128.74, 127.52, 126.87, 125.36, 68.59, 64.09, 52.15, 49.39, 47.22, 45.02, 40.67, 31.24, 30.05, 12.93. MS (ESI) calculated for $C_{30}H_{30}ClN_3O_4$, $[M+H]^+$, *m/z* 533.04, found for $[M+Na]^+$, *m/z* 556.35.

(*R*)-2-(2-(4-chlorophenyl)acetyl)-N-(4-(3-oxomorpholino)phenyl)-1,2,3,4-tetrahydro-isoquinoline-3-carboxamide (47). ^{1}H-NMR ($CDCl_3$, 400 MHz): 7.57-7.30 (m, 2 H), 7.26-7.20

(m, 2 H), 7.19-7.17 (m, 2 H), 7.16-7.00 (m, 4 H), 6.99-6.68 (m, 2 H). 5.14-4.12 (m, 1 H), 4.75-4.50 (m, 2 H), 4.25 (s, 2 H), 3.95 (t, J = 4.72 Hz, 2 H), 3.81 (d, J = 10.40 Hz, 2 H), 3.66 (t, J = 5.20 Hz, 2 H), 3..38-3.29 (m, 1 H), 3.14-2.92 (m, 1 H). ^{13}C-NMR ($CDCl_3$, 100 MHz): 172.23, 169.13, 167.34, 136.97, 136.81, 133.53, 133.09, 132.45, 130.72, 130.28, 130.11, 129.54, 129.00, 128.01, 127.46, 126.75, 125.95, 125.39, 124.21, 122.79, 120.63, 68.29, 63.94, 60.56, 52.53, 49.78, 46.88, 40.45, 28.12. MS (ESI) calculated for $C_{28}H_{26}ClN_3O_4$, $[M+H]^+$, *m/z* 504.98, found for $[M+Na]^+$, *m/z* 526.21.

(*S*)-2-(3-(2,4-dimethoxyphenyl)propanoyl)-N-methyl-N-(4-(3-oxomorpholino)phenyl)-1,2,3,4-tetrahydroisoquinoline-3-carboxamide (48). ^{1}H-NMR ($CDCl_3$, 400 MHz): 7.51 (d, J = 6.24 Hz, 2 H), 7.39 (d, J = 8.2 Hz, 2 H), 7.12-7.09 (m, 2 H), 7.02-6.97 (m, 3 H), 6.38 (d, J = 23.20 Hz, 1 H), 6.35-6.33 (dd, J= 2.36 Hz, J = 8.20 Hz, 1 H), 4.86 (t, J = 6.80 Hz, 1 H), 4.61 (s, 2 H), 4.28 (s, 2 H), 3.97 (t, J = 4.72 Hz, 2 H), 3.75 (s, 2 H), 3.72 (s, 6 H), 3.18 (s, 3 H), 2.86-2.74 (m, 4 H), 2.72-2.61 (m, 1 H). ^{13}C-NMR ($CDCl_3$, 100 MHz): 172.41, 172.01, 166.70, 159.58, 158.37, 141.73, 140.80, 134.64, 133.24, 130.43, 128.50, 127.58, 126.99, 126.45, 125.83, 121.77, 103.99, 98.60, 68.59, 64.10, 55.38, 55.23, 51.46, 49.44, 46.56, 37.94, 34.93, 31.22, 26.02. MS (ESI) calculated for $C_{32}H_{35}N_3O_6$, $[M+H]^+$, *m/z* 558.64, found for $[M+Na]^+$, *m/z* 580.29.

***(S)*-2-(4-(chloromethyl)benzoyl)-N-(4-(2-oxopiperidin-1-yl)phenyl)-1,2,3,4-tetrahydro-isoquinoline-3-carboxamide (49).** ^{1}H-NMR ($CDCl_3$, 400 MHz):7.60-7.42 (m, 6 H), 7.28-7.05 (m, 6 H), 5.21-5.15 (m, 1 H), 4.80 (s, 2 H), 4.74 (s, 2 H), 3.65 (t, J = 6.00 Hz, 2 H), 3.42-3.33 (m, 2 H), 2.41 (t, J = 6.52 Hz, 2 H), 1.95-1.90 (m, 4 H). ^{13}C-NMR ($CDCl_3$, 100 MHz): 171.47, 170.05, 169.52, 140.56, 138.8, 137.81, 135.11, 129.67, 128.87, 128.73, 128.22, 127.48, 127.31, 126.47, 120.69, 55.75, 52.05, 49.12, 46.25, 33.63, 31.38, 24.34, 22.22. MS (ESI) calculated for $C_{29}H_{28}ClN_3O_3$, $[M+H]^+$, *m/z* 503.01, found for $[M+Na]^+$, *m/z* 526.30.

(*S*)-N-(4-chlorophenyl)-2-(4-(2-oxopiperidin-1-yl)benzoyl)-1,2,3,4-tetrahydro-isoquinoline-3-carboxamide (51). ^{1}H-NMR ($CDCl_3$, 400 MHz): 8.00-7.39 (m, 4 H), 7.31-7.12 (m, 6 H), 7.02-6.90 (m, 2 H), 5.23-5.22 (m, 1 H), 4.65-4.37 (dd, J= 15.44 Hz, J = 95.12 Hz, 2 H), 3.61 (t, J = 5.24 Hz, 2 H), 3.52-3.47 (dd, J = 3.60 Hz, J = 15.52 Hz, 2 H), 3.14-3.09 (dd, J = 5.72 Hz, J = 15.16 Hz, 2 H), 2.53 (t, J = 5.10 Hz, 2 H), 1.90-1.88 (m, 4 H). ^{13}C-NMR ($CDCl_3$, 100 MHz): 172.05, 170.43, 168.57, 147.54, 145.18, 138.05, 133.91, 133.36, 130.99, 128.91, 128.27, 127.93, 127.81, 126.68, 126.14, 125.14, 125.41, 124.24, 119.92, 54.50, 51.43, 48.35, 32.81, 29.70, 23.41, 21.25. MS (ESI) calculated for $C_{28}H_{26}ClN_3O_3$, $[M+H]^+$, *m/z* 488.99, found for $[M+Na]^+$, *m/z* 510.32.

(*S*)-methyl 2-(2-(4-chlorophenyl)acetyl)-6,7-dimethoxy-1,2,3,4-tetrahydroisoquinoline-3-carboxylate (58). To a stirred solution of methyl esters (**57**) (1.0 mmol) in CH_3OH (20 mL) was added LiOH-H_2O (5.0 mmol) at RT. Water (5 mL) was added after 24 to the reaction mixture which was kept stirring for further 30 min. The reaction mixture was then concentrated *in vacuo* to about 10 mL and acidified by 1.0 N HCl. The mixture was extracted with EtOAc (2 × 10 mL). The organic extracts were combined, dried over anhydrous Na_2SO_4, filtered, and finally concentrated by rotary evaporation. The corresponding carboxylic acid derivative was obtained as yellowish white solid in ~75% yield and high purity (as indicated by TLC) and accordingly it was used directly in the next reaction (General procedure for amidation at the carboxylic group of the core structure) without any further treatment to afford the titled compound. ^{1}H-NMR ($CDCl_3$, 400 MHz): 7.23-7.11 (m, 4 H), 6.56 (s, 1 H), 6.40 (s, 1 H), 5.48-5.46 & 4.74-4.72 (dd, J = 3.32 Hz, J = 6.04 Hz & J = 2.36 Hz, J = 5.72 Hz, 1 H), 4.89-4.32 (m, 2 H), 3.78 (s, 3 H), 3.76 (s, 2 H), 3.75 (s, 3 H), 3.55-3.46 (d, 3 H), 3.14-3.05 (m, 1 H), 3.01-2.83 (m, 1 H). ^{13}C-NMR ($CDCl_3$, 100 MHz): 171.31, 170.57, 148.22, 147.88, 132.94, 132.83, 130.32, 128.87, 124.04, 123.29, 111.23, 108.85,

55.95, 55.90, 52.39, 51.39, 45.66, 40.50, 29.69. MS (ESI) calculated for $C_{21}H_{22}ClNO_4$, $[M+H]^+$, *m/z* 404.86, found for $[M+Na]^+$, *m/z* 422.16.

(*S*)-2-(2-(4-chlorophenyl)acetamido)-N-methyl-N-(4-(2-oxopiperidin-1-yl)phenyl)-3-phenyl propanamide (62). ^{1}H-NMR ($CDCl_3$, 400 MHz): 7.30-7.22 (m, 4 H), 7.21-7.19 (m, 3 H), 7.11 (d, J= 8.36 Hz, 2 H), 6.93 (d, J = 7.72 Hz, 2 H), 6.84 (d, J = 7.12 Hz, 2 H), 4.87-4.82 (q, J = 7.16 Hz, J = 15.08 Hz, 1 H), 3.69 (t, J = 4.96 Hz, 2 H), 3.47 (s, 2 H), 3.22 (s, 3 H), 2.90-2.85 (dd, J = 7.16 Hz, J = 13.32, 1 H), 2.71-2.66 (dd, J = 7.00 Hz, J = 13.36 Hz, 1 H), 2.59 (t, J = 6.40, 2 H), 2.05-1.95 (m, 4 H) . ^{13}C-NMR ($CDCl_3$, 100 MHz): 171.30, 170.07, 169.63, 143.01, 140.21, 136.00, 133.15, 130.62, 129.24, 128.95, 128.44, 127.95, 127.25, 126.90, 51.42, 51.19, 42.76, 38.91, 37.60, 32.93, 23.53, 21.40. MS (ESI) calculated for $C_{29}H_{30}ClN_3O_3$, $[M+H]^+$, *m/z* 505.03, found for $[M+Na]^+$, *m/z* 526.33.

(*R*)-1-(5-chlorothiophene-2-carbonyl)-N-methyl-N-(4-(2-oxopiperidin-1-yl)phenyl) piperidine-3-carboxamide (69). ^{1}H-NMR ($CDCl_3$, 400 MHz): 7.32 (d, J = 8.28 Hz, 2 H), 7.14 (d, J = 6.68 Hz, 2 H), 6.94 (d, J = 3.36 Hz, 1 H), 6.85 (d, J = 3.84 Hz, 1 H), 4.40-4.20 (m, 2 H), 3.71 (t, J = 5.44 Hz, 2 H), 3.22 (s, 3 H), 3.21-3.16 (m, 1 H), 3.01-2.89 (m, 1 H), 2.58 (t, J = 6.52 Hz, 2 H), 2.56-2.48 (m, 1 H), 2.05-1.95 (m, 4 H), 1.92-1.84 (m, 2 H), 1.73-1.63 (m, 1 H), 1.39-1.22 (m, 1 H). ^{13}C-NMR ($CDCl_3$, 100 MHz): 172.69, 170.14, 162.20, 143.02, 141.07, 135.98, 133.58, 128.14, 127.58, 127.36, 125.86, 51.36, 46.60, 44.08, 39.71, 37.55, 32.94, 27.82, 24.33,23.52, 21.37. MS (ESI) calculated for $C_{23}H_{26}ClN_3O_3S$, $[M+H]^+$, *m/z* 461.00, found for $[M+Na]^+$, *m/z* 482.23.

(*R*)-1-(2-(4-methoxyphenyl)acetyl)-N-methyl-N-(4-(2-oxopiperidin-1-yl)phenyl) piperidine-3-carboxamide (70). ^{1}H-NMR ($CDCl_3$, 400 MHz): 7.36-7.30 (dd, J = 8.32 Hz, J = 15.04 Hz, 2 H), 7.23 (d, J = 8.48 Hz, 1 H), 7.08 (d, J = 8.28 Hz, 1 H), 7.02 (t, J = 6.72 Hz, 2 H),

6.85-6.78 (dd, J = 8.48 Hz, J = 19.72 Hz, 2 H), 4.60-4.52 (m, 1 H), 3.79 (d, J = 18.6 Hz, 3 H), 3.75-3.68 (m, 1 H), 3.66 (t, J = 5.72 Hz, 2 H), 3.56-3.46 (m, 2 H), 3.14 (d, J = 14.96 Hz, 3 H), 3.18-2.89 (m, 1 H), 2.79-2.43 (m, 1 H), 2.58 (t, J = 5.70 Hz, 2 H), 2.39-2.16 (m, 1 H), 2.00-1.90 (m, 4 H), 1.77-1.54 (m, 4 H). ^{13}C-NMR ($CDCl_3$, 100 MHz): 173.19, 170.14, 169.54, 158.40, 143.08, 141.35, 129.60, 127.71, 127.30, 114.24, 55.32, 51.42, 48.47, 46.36, 44.62, 42.03, 40.32, 39.47, 37.53, 32.93, 23.52, 21.37. MS (ESI) calculated for $C_{27}H_{33}N_3O_4$, $[M+H]^+$, *m/z* 464.58, found for $[M+Na]^+$, *m/z* 486.33.

(*R*)-N-methyl-N-(4-(2-oxopiperidin-1-yl)phenyl)-1-(2-(4-(trifluoromethyl)phenyl) acetyl) piperidine-3-carboxamide (71). ^{1}H-NMR ($CDCl_3$, 400 MHz): 7.56-7.51 (dd, J = 7.96 Hz, J = 14.60 Hz, 2 H), 7.33 (t, J = 8.12 Hz, 2 H), 7.27 (t, J = 7.12 Hz, 2 H), 7.22 (d, J = 8.40 Hz, 1 H), 7.07 (d, J = 8.24 Hz, 1 H), 4.57-4.49 (m, 1 H), 3.77-3.51 (m, 5 H), 2.39-2.95 (m, 1 H), 3.21 (d, J = 6.96 Hz, 3 H), 2.85-2.49 (m, 1 H), 2.57 (t, J = 5.88 Hz, 2 H),2.41-2.28 (m, 1 H), 2.00-1.86 (m, 4 H), 1.76-1.62 (m, 4 H). ^{13}C-NMR ($CDCl_3$, 100 MHz): 172.98, 170.21, 168.73, 142.86, 141.32, 139.26, 129.52, 128.88, 127.64, 127.34, 125.53, 122.84, 51.39, 48.51, 46.32, 44.66, 42.19, 40.24, 39.34, 37.54, 32.89, 23.47, 21.33. MS (ESI) calculated for $C_{27}H_{30}F_3N_3O_3$, $[M+H]^+$, *m/z* 502.55, found for $[M+Na]^+$, *m/z* 524.35.

(*S*)-1-(2-(4-chlorophenyl)acetyl)-N-methyl-N-(4-(2-oxopiperidin-1-yl)phenyl) piperidine-3-carboxamide (72). ^{1}H-NMR ($CDCl_3$, 400 MHz): 7.28 (d, J = 5.28 Hz, 1 H), 7.26 (d, J = 9.32 Hz, 1 H), 7.21-7.19 (m, 1 H), 7.16 (d, J = 8.04 Hz, 2 H), 7.03 (d, J = 8.40 Hz, 1 H), 7.00 (d, J = 8.24 Hz, 1 H), 6.94 (d, J = 8.28 Hz, 1 H), 4.48 (t, J = 12.32 Hz, 1 H), 3.64 (t, J = 16.08 Hz, 1 H), 3.60 (t, J = 5.72 Hz, 2 H), 3.50 (d, J = 17.60 Hz, 2 H), 3.21-2.85 (m, 1 H), 3.14 (d, J = 14.96 Hz, 3 H), 2.75-2.29 (m, 1 H), 2.52 (t, J = 5.70 Hz, 2 H), 2.24-2.08 (m, 1 H), 1.90-1.85 (m, 4 H), 1.72-1.54 (m, 4 H). ^{13}C-NMR ($CDCl_3$, 100 MHz): 173.04, 170.14, 168.69, 143.08, 140.87,

133.72, 132.53, 130.14, 128.85, 127.29, 51.42, 48.44, 46.33, 44.61, 42.03, 40.28, 39.38, 37.55, 32.95, 23.51, 21.36. MS (ESI) calculated for $C_{26}H_{30}ClN_3O_3$, $[M+H]^+$, *m/z* 469.00, found for $[M+Na]^+$, *m/z* 490.33.

(*S*)-1-(4-(4-bromophenyl)thiophene-2-carbonyl)-N-methyl-N-(4-(2-oxopiperidin-1-yl)phenyl) piperidine-3-carboxamide (73). ^{1}H-NMR ($CDCl_3$, 400 MHz): 7.51 (d, J = 8.20 Hz, 2 H), 7.49 (s, 1 H), 7.41 (d, J = 8.88Hz, 2 H), 7.40 (s, 1 H), 7.24-7.20 (m, 2 H), 7.13-7.09 (m, 2 H), 3.62-4.10 (m, 2 H), 3.62 (t, J = 5.28 Hz, 2 H), 3.20-2.95 (m, 2 H), 3.19 (s, 3 H), 2.55 (t, J = 5.28 Hz, 2 H), 2.54-2.50 (m, 1 H), 1.95-1.85 (m, 4 H), 1.84-1.81 (m, 2 H), 1.73-1.69 (m, 1 H), 1.39-1.33 (m, 1 H). ^{13}C-NMR ($CDCl_3$, 100 MHz): 172.83, 170.09, 163.19, 142.93, 141.11, 140.74, 138.05, 134.09, 132.07, 127.98, 127.53, 127.34, 123.12, 121.59, 51.34, 41.00, 40.05, 37.57, 32.94, 27.93, 24.46, 23.51, 21.37. MS (ESI) calculated for $C_{29}H_{30}BrN_3O_3S$, $[M+H]^+$, *m/z* 581.54, found for $[M+Na]^+$, *m/z* 602.24.

(*S*)-1-(5-chlorothiophene-2-carbonyl)-N-methyl-N-(4-(2-oxopiperidin-1-yl)phenyl) piperidine -2-carboxamide (78). ^{1}H-NMR ($CDCl_3$, 400 MHz): 7.36-7.34 (m, 2 H), 7.31(d, J = 8.36 Hz, 2 H), 7.06 (d, J = 3.04 Hz, 1 H), 6.83 (d, J = 3.92 Hz, 1 H), 5.15-5.08 (m, 1 H), 4.04-3.87 (m, 2 H), 3.57 (t, J = 5.32 Hz, 2 H), 3.18 (s, 3 H), 2.50 (t, J = 5.80 Hz, 2 H), 1.89-1.84 (m, 4 H), 1.78-1.74 (m, 1 H), 1.69-1.60 (m, 2 H), 1.54-1.51 (m, 1 H), 1.50-1.45 (m, 2 H). ^{13}C-NMR ($CDCl_3$, 100 MHz): 170.92, 169.07, 162.84, 141.79, 140.07, 135.21, 132.76, 127.61, 127.02, 126.28, 124.88, 50.37, 44.40, 36.97, 31.89, 28.68, 25.45, 24.07, 22.50, 20.36, 18.42. MS (ESI) calculated for $C_{23}H_{26}ClN_3O_3S$, $[M+H]^+$, *m/z* 461.00, found for $[M+Na]^+$, *m/z* 482.20.

***(R)*-1-(5-chlorothiophene-2-carbonyl)-*N*-methyl-*N*-(4-(2-oxopiperidin-1-yl)phenyl) piperidine-2-carboxamide (79).** ^{1}H-NMR ($CDCl_3$, 400 MHz): 7.38-7.30 (m, 4 H), 7.06 (d, J = 3.08 Hz, 1 H), 6.82 (d, J = 3.92 Hz, 1 H), 5.15-5.08 (m, 1 H), 4.04-3.88 (m, 2 H), 3.57 (t, J = 5.28

Hz, 2 H), 3.18 (s, 3 H), 2.50 (t, J = 5.80 Hz, 2 H), 1.89-1.86 (m, 4 H), 1.78-1.75 (m, 1 H), 1.69-1.64 (m, 2 H), 1.63-1.58 (m, 1 H), 1.57-1.53 (m, 2 H). ^{13}C-NMR ($CDCl_3$, 100 MHz): 171.93, 170.10, 163.86, 142.79, 141.08, 136.21, 133.78, 128.61, 128.02, 127.29, 125.88, 51.38, 44.39, 37.98, 32.89, 32.12, 26.47, 25.08, 23.51, 21.36, 19.43.MS (ESI) calculated for $C_{23}H_{26}ClN_3O_3S$, $[M+H]^+$, *m/z* 461.00, found for $[M+Na]^+$, *m/z* 482.20.

(*R*)-1-(2-(4-chlorophenyl)acetyl)-N-(4-(3-oxomorpholino)phenyl)piperidine-2-carboxamide (81). ^{1}H-NMR ($CDCl_3$, 400 MHz): 7.46 (d, J = 8.80 Hz, 2 H), 7.33 (d, J = 8.56 Hz, 2 H), 7.26 (d, J = 8.76 Hz, 2 H), 7.19 (d, J = 8.16 Hz, 2 H), 4.30-5.28 (m, 1 H), 4.33 (s, 2 H), 4.02 (t, J = 3.88 Hz, 2 H), 4.03-3.72 (m, 2 H), 3.79 (s, 2 H), 3.73 (t, J = 4.68 Hz, 2 H), 3.08 (t, J = 13.20 Hz, 1 H), 2.31-2.27 (m, 1 H), 1.92-1.85 (m, 2 H), 1.82-1.63 (m, 2 H). ^{13}C-NMR ($CDCl_3$, 100 MHz): 171.92, 169.04, 166.76, 137.15, 133.16, 131.06, 130.02, 129.09, 128.70, 126.13, 120.60, 68.59, 64.14, 52.83, 49.77, 44.45, 40.22, 25.18, 24.76. MS (ESI) calculated for $C_{24}H_{26}ClN_3O_4$, $[M+H]^+$, *m/z* 456.94, found for $[M+Na]^+$, *m/z* 478.30.

(*S*)-1-(2-(4-chlorophenyl)acetyl)-N-(4-(3-oxomorpholino)phenyl)-1,2,3,6-tetrahydro-pyridine-2-carboxamide (84). ^{1}H-NMR (CD_3OD, 400 MHz): 7.60-7.49 (dd, J = 7.40 Hz, J = 36.52 Hz, 2 H), 7.33 (d, J = 8.80 Hz, 2 H), 7.32-7.29 (m, 2 H), 7.27 (d, J = 9.32 Hz, 2 H), 5.87-5.47 (m, 2 H), 4.50-4.27 (m, 1 H), 4.28 (s, 2 H), 4.04 (t, J = 4.40 Hz, 2 H), 3.94-3.84 (m, 2 H), 3.76 (t, J = 4.40 Hz, 2 H), 2.71-2.55 (m, 2 H). ^{13}C-NMR (CD_3OD, 100 MHz): 172.74, 170.42, 168.12, 137.31, 133.67, 132.33, 130.53, 128.23, 126.00, 124.02, 123.08, 121.98, 120.84, 67.67, 63.68, 50.89, 49.81, 43.61, 39.61, 26.40. MS (ESI) calculated for $C_{24}H_{24}ClN_3O_4$, $[M+H]^+$, *m/z* 454.93, found for $[M+H]^+$, *m/z* 454.30.

(1*R*, 3*S*, 4*R*)-2-(2-(4-chlorophenyl)acetyl)-N-(4-(3-oxomorpholino)phenyl)-2-azabicyclo [2.2.1]heptane-3-carboxamide (87). ^{1}H-NMR ($CDCl_3$, 400 MHz): 7.52 (d, J = 8.64

Hz, 2 H), 7.32 (d, J = 8.32 Hz, 2 H), 7.23 (d, J = 8.36 Hz, 2 H), 7.22 (d, J = 8.20 Hz, 2H), 4.32 (s, 2 H), 4.26 (s, 2 H), 4.01 (t, J = 4.96 Hz, 2 H), 3.76-3.65 (m, 4 H), 3.11-3.95 (m, 1 H), 2.04-1.99 (m, 1 H), 1.89-1.74 (m, 3 H), 1.63-1.45 (m, 3 H). ^{13}C-NMR (CD_3OD, 100 MHz): 171.24, 170.63, 169.48, 138.89, 138.48, 135.06, 133.86, 132.02, 129.63, 127.56, 122.03, 69.07, 67.43, 65.09, 60.21, 51.20, 43.46, 41.58, 36.43, 32.14, 28.55. MS (ESI) calculated for $C_{25}H_{26}ClN_3O_4$, $[M+H]^+$, *m/z* 468.95, found for $[M+Na]^+$, *m/z* 490.27.

CHAPTER 6: SIGNIFICANCE OF THE CURRENT WORK

6.1. Synthesis of 1,2,3,4–tetrahydroisoquinoline–3–carboxylic acid (THIQ3CA)— Despite the fact that the THIQ3CA scaffold is widely involved in structures of many medicinal agents, the reported synthetic options to construct this interesting scaffold are limited. This is especially true for electronically activated THIQ3CA derivatives. One of the key reasons is the shortage of availability of appropriate precursors and/or the lengthy schemes involved in precursor synthesis. The protocol reported in chapter III utilizes commercially available benzaldehydes and optimized Horner–Wadsworth–Emmons/Pictet–Spengler reactions and *(±)–Z–α–phosphono–glycine trimethyl ester*. The approach is mild, expeditious and high yielding. In fact, the approach helped pave the way for the synthesis of a novel library of bicyclic–unicyclic and bicyclic–unicyclic–bicyclic methyl–protected poly–phenolic THIQ3CA derivatives in a straightforward manner. A specific advantage of this protocol is that it is flexible and is likely to be generally applicable.

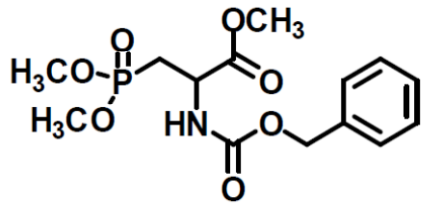

6.2. Implications of Conformational Isomerism—NMR spectroscopic studies highlighted an important structural property of *N*–arylacyl THIQ3CA derivatives that is of considerable significance. Two major rotamers –*trans* and *cis* –were found to be present in solution arising from hindered rotation around the amide bond. From the drug design perspective, this observation carries significant implications. Most structure–based drug design studies typically utilize only one conformer. The expectation is that rapid inter–conversion between the different rotamers (or conformers) will eventually induce dynamic equilibrium in favor of the form of that eventually binds to target site.[263] This work suggests that such inter–

conversion may not occur for *N*–arylacyl THIQ3CA derivatives because of the high rotational barrier of ~17 kcal/mol. Thus, both conformers will have to be explicitly studied in structure–based drug design.

6.3. Indirect FXa Inhibitors: Antithrombin Activators— Heparins form one of the two major classes of anticoagulant drugs in use today. Although heparin–based therapy is continuously advancing, the advancements in terms of medicinal chemistry have not led to structures beyond the heparin pentasaccharide. Fundamental research is necessary for scaffold hopping so as to derive clinically viable candidates. Yet, scaffold hopping is challenging, as demonstrated by our earlier work[106-110] as well as by recent efforts from the Pinto group,[264,265] both of which indicate relatively weak affinity of the designed molecules.

Despite this difficulty, our molecular docking and scoring protocol indicates a reasonable level of success. The two molecules identified through virtual screening, sodium 2-(2-(2,5-di-O-sulfonato-phenyl)acetyl)-6,7-di-O-sulfonato-1,2,3,4-tetrahydroisoquinoline-3-carboxylate tetrasodium (67A225) and sodium 2-(2-(2,5-di-O-sulfonato-phenyl)acetyl)-5,8-di-O-sulfonato-1,2,3,4-tetrahydroisoquinoline-3-carboxylate tetrasodium (58A225) showed K_D of 81 and 394 μM, respectively, while their AT acceleration potentials were 53– and 67–fold, respectively. These results indicate significant improvements over our second-generation AT activator IAS5. This work highlights a critical aspect of allosteric conformational activation of AT. Whereas the affinity of the AT activators studied in this work was lower than that studied in our earlier work,[106,110] the activation potential measured was found to be higher. This shows a segregation of affinity and activation potential, as expected on the basis of the theory of two–step allosteric activation. Affinity reflects the strength with which an activator binds in the EHBS, whereas activation potential is a measure of the stability of the conformational change induced in AT.

This work also shows that the two molecules listed above, although not fitting perfectly in the EHBS, are able to induce sufficient conformational change in AT to inhibit FXa at a higher rate. Because our analysis evaluates the properties of the AT–activator complex, we are able to parse affinity and activation parameters, which provides a unique insight into the mechanism of allosteric activation. Yet, detailed mechanistic and structural biology studies are necessary to ascertain whether the new molecules bind in the EHBS. Overall, the results support the concept that targeting the pre–equilibrium pathway may be a viable route to new AT activators.

An important point that our study affords is the correlation of GOLD and HINT scores with affinity measured for the series of sulfated *N*–arylacyl tetrahydroisoquinoline derivatives. A qualitative correlation was evident from this limited study, but upon detailed quantitative evaluation, the correlation is not strong. Molecular modeling studies of highly sulfated carbohydrates and noncarbohydrates have also been challenging,[106-110,220] especially because appropriate docking and scoring tools have not been developed for sulfated molecules as they have been for traditional hydrophobic small molecules. Sulfated *N*–arylacyl tetrahydroisoquinolines appear to have an added complication. These molecules display conformational isomerism, as evident from the NMR studies which raises the possibility of complications arising from selectivity of recognition.

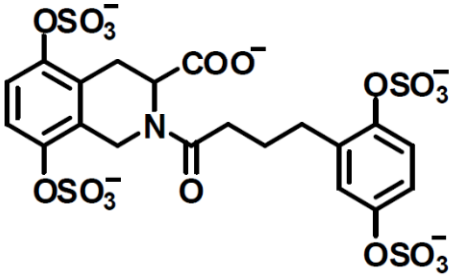

The best molecule in the series studied here, i.e., *sodium 2-(4-(2,5-di-O-sulfonato-phenyl)butanoyl)-5,8-di-O-sulfonato-1,2,3,4-tetrahydro isoquinoline- 3-carboxylate tetrasodium (58A425)*, is only 3.8–fold less efficient at AT activation than the "gold" standard, DEFGH. This is a considerable advance. However, this does not imply that the design of a clinically viable nonsaccharide AT activator is

within rapid reach. One, the potency of this molecule is inadequate. Two, an AT activation higher than the 80–fold achieved thus far may be necessary. This does not imply that 300–fold activation, as for the "gold" standard DEFGH, is an absolute necessity for clinical viability. The important parameter that will govern clinical relevance is likely to be activation to toxicity ratio, which should favor activation by a high margin. In this regard, toxicity studies with liver HepG2 and lung A549 cells lines show minimal toxicity for these types of highly water–soluble molecules at levels as high as 50 mg/L. This implies that activation less than 300–fold may not be a major limitation.

It is expected that molecule 58A425 will serve as an excellent scaffold for further design modifications. A specific advantage of the nonsaccharide AT activators is that their synthesis is much simpler than the heparin–based activators.[266] This implies that a library of diverse analogues around this molecule can be prepared without much difficulty to identify more potent and efficacious molecules. This work is in progress.

6.4. Direct FXa Inhibitors— This work explores the dependence of direct FXa inhibition on the flexibility of core scaffold and attempts to optimize the structure of two arms A_N and A_C of a bifunctional cyclic ring system. We discovered interesting structural preference for both arms and a fine additive relationship that culminated in the design of THIQ3CA analog; *(R)-2-(2-(4-chlorophenyl)acetyl)-N-(4-(3-oxomorpholino)phenyl)-1,2,3,4-tetrahydroisoquinoline-3-carboxamide*, which displays direct inhibition with IC_{50} of 270 nM (K_i = 135 nM) and more than 279–fold selectivity over related proteases in the coagulation and digestive systems. The potency and selectivity profiles of this molecule are

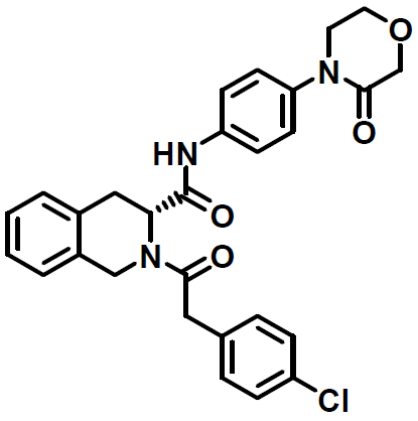

comparable to other direct FXa inhibitors designed and reported in the literature. For example, rivaroxaban and apixaban have K_i*'s* in the subnanomolar range,[119,125] TAK-442 has K_i of 1.8 nM,[124] LY517717 has K_i of 6.6 nM,[118] YM150 possesses K_i of 31 nM,[123] and DX-9065a has K_i of 41 nM.[267] Not only that, but also this molecule doubles the PT and aPTTT clotting times at concentrations of 17–20 μM, 4–fold less than those of drug candidates in clinical trials. The scaffolds of these inhibitors are significantly different from what has been reported here. Synthetically, THIQ3CA–based FXa inhibitors and related derivatives reported here were assembled by only three, well-established, and high yielding steps of amidation and protection/deprotection reactions which were executed at room temperature avoiding the harsh conditions included in the synthesis of other reported FXa inhibitors.

Our work suggests that the morpholinone ring engineers better inhibition potential than any other ring system; that the nitrogen of the carboxamide group at position–3 should be optimally unsubstituted; that a (*R*)–stereochemistry at position-3 is more preferred than its *(S)*–enantiomer; and that a 7–atom A_N arm containing a *para*-chloro substituted aromatic ring is critical for potent, direct FXa inhibition. It is also worth mentioning that the A_N and A_C arms should be adjacent to each other (1,2-substitution) rather than one carbon away (1,3-disubstitution). These conclusions may help design more potent molecules based on the THIQ3CA scaffold.

Literature Cited

(1) Macfarlane, R. G. An enzyme cascade in the blood clotting mechanism, and its function as a biochemical amplifier. *Nature* **1964**, *202*, 498–499.

(2) Davie, E. W.; Ratnoff, O. D. Waterfall sequence for intrinsic blood clotting. *Science* **1964**, *145*, 1310–1312.

(3) Riddel, J. P. Jr.; Aouizerat, B. E.; Miaskowski, C.; Lillicrap, D. P. Theories of blood coagulation. *J. Pediatr. Oncol. Nurs.* **2007**, *24*, 123–131.

(4) Davie, E. W.; Fujikawa, K.; Kisiel, W. The coagulation cascade: Initiation, maintenance, and regulation. *Biochemistry* **1991**, *30*, 10363–10370.

(5) Davie, E. W. A brief historical review of the waterfall/cascade of blood coagulation. *J. Biol. Chem.* **2003**, *278*, 50819–50832.

(6) Straub, A.; Roehrig, S.; Hillisch, A. Oral, direct thrombin and factor Xa inhibitors: The replacement for warfarin, leeches, and pig intestines? *Angew. Chem. Int. Ed.* **2011**, *50*, 4574–4590.

(7) Henry, B. L., Desai, U.R. Anticoagulants: Drug discovery and development. In *Burger's Medicinal Chemistry*, 7th ed.; D. Rotella, D.J. Abraham, Eds.; John Wiley and Sons: New York, **2010**; pp. 365–408.

(8) Bjork, I.; Olson, S. T. Antithrombin. A bloody important serpin. *Adv. Exp. Med. Biol.* **1997**, *425*, 17-33.

(9) Griffin, J. H.; Fernandez, J. A.; Gale, A. J.; Mosnier, L. O. Activated protein C. *J. Thromb. Haemost.* **2007**, 5 Suppl 1, 73-80.

(10) Crawley, J. T.; Lane, D. A. The haemostatic role of tissue factor pathway inhibitor. *Arterioscler. Thromb. Vasc. Biol.* **2008**, *28*, 233-242.

(11) Olson, S. T.; Swanson, R.; Raub-Segall, E.; Bedsted, T.; Sadri, M.; Petitou, M.; Herault, J. P.; Herbert, J. M.; Bjork I. Accelerating ability of synthetic oligosaccharides on antithrombin inhibition of proteinases of the clotting and fibrinolytic systems. Comparison with heparin and low-molecular–weight heparin. *Thromb Haemost.* **2004**, *92*, 929–939.

(12) Larsen, K. S.; Ostergaard, H.; Bjelke, J. R.; Olsen, O. H.; Rasmussen, H. B.; Christensen, L.; Kragelund, B. B.; Stennicke, H. R. Engineering the substrate and inhibitor specificities of human coagulation Factor VIIa. *Biochem. J.* **2007**, *405*, 429-438.

(13) Zhao, M.; Abdel-Razek, T.; Sun, M.; Gailani, D. Characterization of a heparin binding site on the heavy chain of factor XI. *J. Biol. Chem.* **1998**, *273*, 31153-31159.

(14) Desai, U. R. New antithrombin-based anticoagulants. *Med. Res. Rev.* **2004**, *24*, 151-181.

(15) The Surgeon General's Call to Action To Prevent Deep Vein Thrombosis and Pulmonary Embolism. http://www.surgeongeneral. gov/topics/deepvein/index.html, **2008**.

(16) Debourdeau, P.; Beckers, M.; Gérôme, P.; Durant, C.; Lacoin, Q.; Debourdeau, A.; Bancel, D. F. How to improve the implementation of guidelines on cancer-related thrombosis. *Expert. Rev. Anticancer. Ther.* **2011**, *11*, 473–483.

(17) Lee, Y-K.; Player, M. R. Developments in factor Xa inhibitors for the treatment of thromboembolic disorders. *Med. Res. Rev.* **2011**, *31*, 202–283.

(18) Yin, E.T.; Wessler, S. Investigation of the apparent thrombogenicity of thrombin. *Thromb. Diath. Haemorrh.* **1968**, *20*, 465–468.

(19) Mann, K.G.; Brummel, K.; Butenas, S. What is all that thrombin for? *J. Thromb. Haemost.* **2003**, *1*, 1504–1514.

(20) Turpie, A. G. G.; Bauer, K. A.; Eriksson, B.I.; Lassen, M. R. Fondaparinux vs enoxaparin for the prevention of venous thromboembolism in major orthopedic surgery. A meta-analysis of 4 randomized double-blind studies. *Arch. Intern. Med.* **2002**, *162*, 1833–1840.

(21) OASIS-5 Trial Group. Comparison of fondaparinux and enoxaparin in acute coronary syndromes. *N. Engl. J. Med.* **2006**, *354*, 1464–1476.

(22) Jenny, N. S.; Lundblad, R. L.; Mann, K. G. Thrombin. *In*: Colman, R.W.; Mardeer, V. J.; Clowes, A.W.; George, J. N.; Goldhaber, S. Z, eds. Hemostasis and Thrombosis: Basic Principles and Clinical Practice, (5th edition). Philadelphia, PA: Lippincott, Williams, & Wilkins, **2006**, 193–214.

(23) Davie, E. W.; Kulman, J. D. An overview of the structure and function of thrombin. *Semin. Thromb. Hemost.* **2006***, 32*, 3–15.

(24) Merlini, P. A.; Ardissino, D.; Bauer, K. A.; Oltrona, L.; Pezzano, A.; Bottasso, B.; Rosenberg, R. D.; Mannucci, P. M. Persistent thrombin generation during heparin therapy in patients with acute coronary syndromes. *Arterioscler. Thromb. Vasc. Biol.* **1997**, *17*, 1325–1330.

(25) Ansell, J. Factor Xa or thrombin: Is factor Xa a better target? *J. Thromb. Haemost.* **2007**, *5 (Suppl. 1)*, 60–64.

(26) Nutt, E.; Gasic, T.; Rodkey, J.; Gasic, G. J.; Jacobs, J. W.; Friedman, P. A.; Simpson, E. The amino acid sequence of antistasin. A potent inhibitor of factor Xa reveals a repeated internal structure. *J. Biol. Chem.* **1988**, *263*, 10162–10167.

(27) Tuszynski, G. P.; Gasic, T. B.; Gasic, G. J. Isolation and characterization of antistasin. An inhibitor of metastasis and coagulation. *J. Biol. Chem.* **1987**, *262*, 9718–9723.

(28) Dunwiddie, C.; Thornberry, N. A.; Bull, H. G.; Sardana, M.; Friedman, P. A.; Jacobs, J. W.; Simpson, E. Antistasin, a leech-derived inhibitor of factor Xa. Kinetic analysis of enzyme inhibition and identification of the reactive site. *J. Biol. Chem.* **1989**, *264*, 16694–16699.

(29) Waxman, L.; Smith, D. E.; Arcuri, K. E.; Vlasuk, G. P. Tick anticoagulant peptide (TAP) is a novel inhibitor of blood coagulation factor Xa. *Science* **1990**, *248*, 593–596.

(30) Nicolini, F. A.; Lee, P.; Malycky, J. L.; Lefkovits, J.; Kottke-Marchant, K.; Plow, E. F.; Topol, E. J. Selective inhibition of factor Xa during thrombolytic therapy markedly improves coronary artery patency in a canine model of coronary thrombosis. *Blood Coagul. Fibrinolysis* **1996**, *7*, 39–48.

(31) Vlasuk, G. P.; Ramjit, D.; Fujita, T.; Dunwiddie, C. T.; Nutt, E. M.; Smith, D. E.; Shebuski, R. J. Comparison of the *in vivo* anticoagulant properties of standard heparin and the highly selective factor Xa inhibitors antistasin and tick anticoagulant peptide (TAP) in a rabbit model of venous thrombosis. *Thromb. Haemost.* **1991**, *65*, 257–262.

(32) Lynch, J. J Jr.; Sitko, G. R.; Mellott, M. J.; Nutt, E. M.; Lehman, E. D.; Friedman, P. A.; Dunwiddie, C. T.; Vlasuk, G. P. Maintenance of canine coronary artery patency following thrombolysis with front loaded plus low dose maintenance conjunctive therapy. A comparison of factor Xa versus thrombin inhibition. *Cardiovasc. Res.* **1994**, *28*, 78–85.

(33) Sitko, G. R.; Ramjit, D. R.; Stabilito, I. I.; Lehman, D.; Lynch, J. J.; Vlasuk, G. P. Conjunctive enhancement of enzymatic thrombolysis and prevention of thrombotic reocclusion with the selective factor Xa inhibitor, tick anticoagulant peptide. Comparison to hirudin and heparin in a canine model of acute coronary artery thrombosis. *Circulation* **1992**, *85*, 805–815.

(34) Lefkovits, J.; Malycky, J. L.; Rao, J. S.; Hart, C. E.; Plow, E. F.; Topol, E. J.; Nicolini, F. A. Selective inhibition of factor Xa is more efficient than factor VIIa-tissue factor complex blockade at facilitating coronary thrombolysis in the canine model. *J. Am. Coll. Cardiol.* **1996**, *28*, 1858–1865.

(35) Gettins, P. G. W. Serpin structure, mechanism and function. *Chem. Rev.* **2002**, *102,* 4751–4803.

(36) Olson, S.T.; Bjork, I.; Shore, J. D. Kinetic characterization of heparin-catalyzed and uncatalyzed inhibition of blood coagulation proteinases by antithrombin. *Methods Enzymol.* **1993**, *222,* 525–559.

(37) Rosenberg, R. D.; Damus, P. S. The purification and mechanism of action of human antithrombin–heparin cofactor. *J. Biol. Chem.* **1973**, *248*, 6490–6505.

(38) Schreuder, H. A.; de Boer, B.; Dijkema, R.; Mulders, J.; Theunissen, H. J. M.; Grootenhuis, P. D. J.; Hol, W. G. J. The intact and cleaved human antithrombin III complex as a model for serpin-proteinase interactions. *Nat. Struct. Biol.* **1994**, *1*, 48–54.

(39) Carrell, R. W.; Stein, P. E.; Fermi, G.; Wardell, M. R. Biological implications of a 3 Å structure of dimeric antithrombin. *Structure* **1994**, *2*, 257–270.

(40) Skinner, R.; Abrahams, J-P.; Whisstock, J. C.; Lesk, A. M.; Carrell, R. W.; Wardell, M. R. The 2.6 Å structure of antithrombin indicates a conformational change at the heparin binding site. *J. Mol. Biol.* **1997**, *266*, 601–609.

(41) Bruch, M.; Weiss, V.; Engel, J. Plasma serine proteinase inhibitors (serpins) exhibit major conformational changes and a large increase in conformational stability upon cleavage at their reactive sites. *J. Biol. Chem.* **1988**, *263*, 16626–16630.

(42) Huntington, J. A.; Read, R. J.; Carrell, R. W. Structure of a serpin–protease complex shows inhibition by deformation. *Nature* **2000**, *407*, 923–926.

(43) Plotnick, M. I.; Mayne, L.; Schechter, N. M.; Rubin, H. Distortion of the active site of chymotrypsin complexed with a serpin. *Biochemistry* **1996**, *35*, 7586–7590.

(44) Calugaru, S. V.; Swanson, R.; Olson, S. T. The pH dependence of serpin-proteinase complex dissociation reveals a mechanism of complex stabilization involving inactive and active conformational states of the proteinases which are perturbable by calcium. *J. Biol. Chem.* **2001**, *276*, 32446–32455.

(45) Bjork, I.; Olson, S. T. Antithrombin: A bloody important serpin. *In*: Church, F. C.; Cunningham, D. D.; Ginsburg, D.; Hoffman, M.; Tollefsen, D. M.; Stone, S. R, editors. *Chemistry and biology of serpins.* New York: Plenum Press; **1997**. pp 17–33.

(46) Olson, S. T.; Shore, J. D. Demonstration of a two-step reaction mechanism for inhibition of α-thrombin by antithrombin III and identification of the step affected by heparin. *J. Biol. Chem.* **1982**, *257*, 14891–14895.

(47) Latallo, Z. S.; Jackson, C. M. Reaction of thrombins with human antithrombin III. II. Dependence of rate of inhibition on molecular form and origin of thrombin. *Thromb. Res.* **1986**, *43*, 523–537.

(48) Wong, R. F.; Windwer, S. R.; Feinman, R. D. Interaction of thrombin and antithrombin. Reaction observed by intrinsic fluorescence measurements. *Biochemistry* **1983**, *22*, 3994–3999.

(49) Jordan, R.E.; Oosta, G. M.; Gardner, W. T.; Rosenberg, R. D. The kinetics of haemostatic enzyme- antithrombin interactions in the presence of low molecular weight heparin. *J. Biol. Chem.* **1980**, *255*, 10081–10090.

(50) Griffith, M. J. Kinetics of the heparin-enhanced antithrombin III/thrombin reaction. Evidence for a template model for the mechanism of action of heparin. *J. Biol. Chem.* **1982**, *257*, 7360–7365.

(51) Olson, S. T.; Bjork, I. Predominant contribution of surface approximation to the mechanism of heparin acceleration of the antithrombin-thrombin reaction. Elucidation from salt concentration effects. *J. Biol. Chem.* **1991**, *266*, 6353–6364.

(52) Olson, S. T.; Bjork, I.; Sheffer, R.; Craig, P. A.; Shore, J. D.; Choay, J. Role of the antithrombin-binding pentasaccharide in heparin acceleration of antithrombin-proteinase reactions. Resolution of the antithrombin conformational change contribution to heparin rate enhancement. *J. Biol. Chem.* **1992**, *267*, 12528–12538.

(53) Duchaussoy, P.; Jaurand, G.; Driguez, P-A.; Lederman, I.; Ceccato, M-L.; Gourvenec, F.; Strassel, J-M.; Sizun, P.; Petitou, M.; Herbert, J-M. Assessment through chemical synthesis of the size of the heparin sequence involved in thrombin inhibition. *Carbohydr. Res.* **1999**, *317*, 85–99.

(54) Craig, P. A.; Olson, S. T.; Shore, J. D. Transient kinetics of heparin-catalyzed protease inactivation by antithrombin III. Characterization of assembly, product formation, and heparin dissociation steps in the factor Xa reaction. *J. Biol. Chem.* **1989**, *264*, 5452–5461.

(55) Chuang,Y-J.; Swanson, R.; Raja, S. M.; Olson, S. T. Heparin enhances the specificity of antithrombin for thrombin and factor Xa independent of the reactive center loop sequence. Evidence for an exosite determinant of factor Xa specificity in heparin-activated antithrombin. *J. Biol. Chem.* **2001**, *276*, 14961–14971.

(56) Petitou, M.; Herault, J-P.; Bernat, A.; Driguez, P-A.; Duchaussoy, P.; Lormeau, J-C.; Herbert, J-M. Synthesis of thrombin-inhibiting heparin mimetics without side effects. *Nature* **1999**, *398*, 417–422.

(57) Rezaie, A. R. Calcium enhances heparin catalysis of the antithrombin-factor Xa reaction by a template mechanism. *J. Biol. Chem.* **1998**, *273*, 16824–16827.

(58) Jin, L.; Abrahams, J-P.; Skinner, R.; Petitou, M.; Pike, R. N.; Carrell, R. W. The anticoagulant activation of antithrombin by heparin. *Proc. Natl. Acad. Sci. USA* **1997**, *94*, 14683–14688.

(59) Ersdal-Badju, E.; Lu, A.; Zuo,Y.; Picard,V.; Bock, S. C. Identification of the antithrombin III heparin binding site. *J. Biol. Chem.* **1997**, *272*, 19393–19400.

(60) Desai, U. R.; Swanson, R. S.; Bock, S. C.; Bjork, I.; Olson, S. T. The role of arginine 129 in heparin binding and activation of antithrombin. *J. Biol. Chem.* **2000**, *275*, 18976–18984.

(61) Schedin-Weiss, S.; Desai, U. R.; Bock, S. C.; Gettins, P. G. W.; Olson, S. T.; Bjork, I. The importance of lysine 125 for heparin binding and activation of antithrombin. *Biochemistry* **2002**, *41*, 4779–4788.

(62) Arocas, V.; Bock, S. C.; Raja, S.; Olson, S. T.; Bjo¨rk, I. Lysine 114 of antithrombin is of crucial importance for the affinity and kinetics of heparin pentasaccharide binding. *J. Biol. Chem.* **2001**, *276*, 43809–43817.

(63) Schedin-Weiss, S.; Arocas, V.; Bock, S. C.; Olson, S. T.; Bjo¨rk, I. Specificity of the basic side chains of Lys114, Lys125 and Arg129 of antithrombin in heparin binding. *Biochemistry* **2002**, *41,* 12369–12376.

(64) Arocas, V.; Turk, B.; Bock, S. C.; Olson, S. T.; Bjo¨rk, I. The region of antithrombin interacting with full-length heparin chains outside the high-affinity pentasaccharide sequence extends to Lys136 but not to Lys139. *Biochemistry* **2000**, *39*, 8512–8518.

(65) Huntington, J. A.; Olson, S. T.; Fan, B.; Gettins, P. G. W. Mechanism of heparin activation of antithrombin: Evidence for reactive center loop preinsertion with expulsion upon heparin binding. *Biochemistry* **1996**, *35*, 8495–8503.

(66) Streusand, V. J.; Bjork, I.; Gettins, P.; Petitou, M.; Olson, S.T. Mechanism of acceleration of antithrombin proteinase reactions by low affinity heparin: Role of the antithrombin binding pentasaccharide in heparin rate enhancement. *J. Biol. Chem.* **1995**, *270*, 9043–9051.

(67) Hirsh, J.; Levine, M. N. Low molecular weight heparins. *Blood* **1992**, *79*, 1–17.

(68) Cosmi, B.; Hirsh, J. Low molecular weight heparins. *Curr. Opin. Cardiol.* **1994**, *9,* 612–618.

(69) Sundaram, M.; Qi, Y.; Shriver, Z.; Liu, D.; Zhao, G.; Venkataraman, G.; Langer, R.; Sasisekharan, R. Rational design of low-molecular weight heparins with improved in vivo activity. *Proc. Natl. Acad. Sci. USA* **2003**, *100*, 651–656.

(70) Desai, U. R.; Wang, H-M.; Linhardt, R. J. Substrate specificity of the heparin lyases from Flavobacterium heparinum. *Arch. Biochem. Biophys.* **1993**, *306*, 461–468.

(71) Desai, U. R.; Wang, H-M.; Linhardt, R. J. Specificity studies on the heparin lyases from Flavobacterium heparinum. *Biochemistry* **1993**, *32*, 8140–8145.

(72) Shriver, Z.; Sundaram, M.; Venkataraman, G.; Fareed, J.; Linhardt, R. J.; Biemann, K.; Sasisekharan, R. Clearage of the antithrombin III binding site in heparin by heparinases and its implication in the generation of low molecular weight heparins. *Proc. Natl. Acad. Sci. USA* **2000**, *97*, 10365–10370.

(73) Horne, A.; Gettins, P. 1HNMRspectroscopic studies on the interaction between human plasma antithrombin III and defined low molecular weight heparin fragments. *Biochemistry* **1992**, *31*, 2286–2294.

(74) Lin, P.; Sinha, U.; Betz, A. Antithrombin binding of low molecular weight heparins and inhibition of factor Xa. *Biochim. Biophys. Acta.* **2001**, *1526*, 105–113.

(75) Hirsh, J.; Warkentin, T. E.; Raschke, R.; Granger, C.; Ohman, E. M.; Dalen, J. E. Heparin and low-molecular-weight heparin: Mechanisms of action, pharmacokinetics, dosing considerations, monitoring, efficacy and safety. *Chest* **1998**, *114(Suppl 5)*, 489S–510S.

(76) Boneu, B. Low molecular weight heparins: Are they superior to unfractionated heparins to prevent and to treat deep vein thrombosis? *Thromb. Res.* **2000**, *100*, V113–V120.

(77) Nurmohamed, M. T.; ten Cate, H.; ten Cate, J. W. Low molecular weight heparin(oid)s: Clinical investigations and practical recommendations. *Drugs* **1997**, *53*, 736–751.

(78) Thomas, D. P. Does low molecular weight heparin cause less bleeding? *Thromb. Haemost.* **1997**, *78*, 1422– 1425.

(79) Leizorovicz, A.; Haugh, M. C.; Chapuis, F. R.; Samama, M. M.; Boissel, J. P. Low molecular weight heparin in prevention of perioperative thrombosis. *Br. Med. J.* **1992**, *305*, 913–920.

(80) Olson, S. T.; Srinivasan, K. R.; Bjork, I.; Shore, J. D. Binding of high affinity heparin to antithrombin III: Stopped flow kinetic studies of the binding interaction. *J. Biol. Chem.* **1981**, *256*, 11073–11079.

(81) Olson, S. T.; Richard, B.; Izaguirre, G.; Schedin-Weiss, S.; Gettins, P. G. W. Molecular mechanisms of antithrombineheparin regulation of blood clotting proteinases. A paradigm for understanding proteinase regulation by serpin family protein proteinase inhibitors. *Biochimie* **2010**, *92*, 1587–1596.

(82) Petitou, M.; Barzu, T.; Herault, J. P.; Herbert, J. M. A unique trisaccharide sequence in heparin mediates the early step of antithrombin III activation. *Glycobiology* **1997**, *7,* 323–327.

(83) Desai, U. R.; Petitou, M.; Bjork, I.; Olson, S. T. Mechanism of heparin activation of antithrombin: Role of individual residues of the pentasaccharide activating sequence in

the recognition of native and activated states of antithrombin. *J. Biol. Chem.* **1998**, *273*, 7478–7487.

(84) Eriksson, B. I.; Bauer, K. A.; Lassen, M. R.; Turpie, A. G. G. Fondaparinux compared with enoxaparin for the prevention of venous thromboembolism after hip-fracture surgery. *N. Engl. J. Med.* **2001**, *345*, 1298–1304.

(85) Eriksson, B. I.; Bauer, K. A.; Lassen, M. R.; Turpie, A. G. G. Fondaparinux compared with enoxaparin for the prevention of venous thromboembolism after elective major knee surgery. *N. Engl. J. Med.* **2001**, *345*, 1305–1310.

(86) Fareed, J.; Hoppensteadt, D. A.; Bick, R. L. An update on heparins at the beginning of the new millenium. *Sem. Thromb. Hemost.* **2000**, *26(Suppl 1),* 5–21.

(87) Herbert, J-M.; Herault, J. P.; Bernat, A.; van Amsterdam, R. G. M.; Vogel, G. M. T.; Lormeau, J. C.; Petitou, M.; Meuleman, D. G. Biochemical and pharmacological properties of SANORG 32701: Comparison with the synthetic pentasaccharide (SR90107/Org 31540) and standard heparin. *Circulation Res.* **1996**, *79,* 590–600.

(88) Petitou, M.; Duchaussoy, P.; Jaurand, G.; Gourvenec, F.; Lederman, I.; Strassel, J-M.; Barzu, T.; Crepon, B.; Herault, J. P.; Lormeau, J. C.; Bernat, A.; Herbert, J-M. Synthesis and pharmacological properties of a close analogue of an antithrombotic pentasaccharide (SR 90107A/ORG 31540). *J. Med. Chem.* **1997**, *40,* 1600–1607.

(89) Herbert, J-M.; Herault, J. P.; Bernat, A.; van Amsterdam, R. G. M.; Lormeau, J. C.; Petitou, M.; van Boeckel, C.; Hoffman, P.; Meuleman, D. G. Biochemical and pharmacological properties of SANORG 34006, a potent and long-acting synthetic pentasaccharide. *Blood* **1998**, *91*, 4197–4205.

(90) Duchaussoy, P.; Lei, P. S.; Petitou, M.; Sinay, P.; Lormeau, J. C.; Choay, J. The first total synthesis of the antithrombin III binding site of porcine mucosa heparin. *Bioorg. Med. Chem. Lett.* **1991***, 2*, 99–102.

(91) van Boeckel, C. A. A.; Petitou, M. The unique antithrombin III binding domain of heparin: A lead to new synthetic antithrombotics. *Angew. Chem. Int. Ed. Engl.* **1993**, *32,* 1671–1818.

(92) Richard, B.; Swanson, R.; Olson, S.T. The signature 3-O-sulfo group of the anticoagulant heparin sequence is critical for heparin binding to antithrombin but is not required for allosteric activation. *J. Biol. Chem.* **2009**, *284*, 27054 – 27064.

(93) Westerduin, P.; van Boeckel, C. A. A.; Basten, J. E. M.; Broekhoven, M. A.; Lucas, H.; Rood, A.; van der Heijden, H.; van Amsterdam, R. G. M.; van Dinther, T. G.; Meuleman, D. G.; Visser, A.; Vogel, G. M. T.; Damm, J. B. L.; Overklift, G. T. Feasible synthesis and biological properties of six 'non-glycosamino' glycan analogues of the antithrombin III binding heparin pentasaccharide. *Bioorg. Med. Chem.* **1994**, *2*, 1267–1280.

(94) Gross, P. L.; Weitz, J. I. New anticoagulants for treatment of venous thromboembolism. *Arterioscler. Thromb. Vasc. Biol.* **2008**, *28*, 380–386.

(95) Savi, P.; Herault, J. P.; Duchaussoy, P.; Millet, L.; Schaeffer, P.; Petitou, M.; Bono, F.; Herbert, J. M. Reversible biotinylated oligosaccharides: a new approach for a better management of anticoagulant therapy. *J. Thromb. Haemostasis* **2008**, *6*, 1697–1706.

(96) Petitou, M.; Herault, J. P.; Lormeau, J. C.; Helmboldt, A.; Mallet, J-M.; Sinay, P.; Herbert, J-M. Introducing a C-interglycosidic bond in a biologically active pentasaccharide hardly affects its biological properties. *Bioorg. Med. Chem.* **1998***, 6,* 1509–1516.

(97) Minix, R.; Doctor, V. Interaction of fucoidan with proteases and inhibitors of coagulation and fibrinolysis. *Thromb. Res.* **1997**, *87*, 419-429.

(98) Pereira, M. S.; Mulloy, B.; Mourao, P. A. S. Structure and anticoagulant activity of sulfated fucans: Comparison between the regular, repetitive, and linear fucans from echniderms with the more heterogeneous and branched polymers from brown algae. *J. Biol. Chem.* **1999**, *274*, 7656-7667.

(99) Alban, S.; Franz, G. Characterization of the anticoagulant actions of a semisynthetic curdlan sulfate. *Thromb. Res.* **2000**, *99*, 377-388.

(100) Drozd, N. N.; Sher, A. I.; Makarov, V. A.; Galbraikh, L. S.; Vikhoreva, G. A.; Gorbachiova, I. N. Comparison of antithrombin activity of the polysulphate chitosan derivatives in *in vivo and in vitro* system. *Thromb. Res.* **2001**, *102*, 445-455.

(101) Pires, L.; Gorin, P. A. J.; Reicher, F.; Sierakowski, M.-R. An active heparinoid obtained by sulphation of a galactomannan extracted from the endosperm of *Senna macranthera s*eeds. *Carbohydr. Polym.* **2001**, *46*, 165-169.

(102) Majdoub, H.; Ben Mansour, M.; Chaubet, F.; Roudesli, M. S.; Maaroufi, R. M. Anticoagulant activity of a sulfated polysaccharide from the green alga Arthrospira platensis. *Biochim. Biophys. Acta.* **2009**, *1790*, 1377-1381.

(103) Pawlaczyk, I.; Czerchawski, L.; Kuliczkowski, W.; Karolko, B.; Pilecki, W.; Witkiewicz, W.; Gancarz, R. Anticoagulant and anti-platelet activity of polyphenolic-polysaccharide preparation isolated from the medicinal plant Erigeron canadensis L. *Thromb. Res.* **2011**, *127*, 328-340.

(104) de Kort, M.; Buijsman, R. C.; van Boeckel, C. A. Synthetic heparin derivatives as new anticoagulant drugs. *Drug Discov. Today.* **2005**, *10*, 769-779.

(105) Avci, F. Y.; Karst, N. A.; Linhardt, R. J. Synthetic oligosaccharides as heparin-mimetics displaying anticoagulant properties. *Curr Pharm Des.* **2003**, *9*, 2323-2335.

(106) Gunnarsson, G. T.; Desai, U. R. Designing small, non-sugar activators of antithrombin using hydropathic interaction analyses. *J. Med. Chem.* **2002**, *45*, 1233–1243.

(107) Gunnarsson, G. T.; Desai, U. R. Interaction of sulfated flavanoids with antithrombin: Lessons on the design of organic activators. *J. Med. Chem*. **2002**, *45*, 4460–4470.

(108) Gunnarsson, G. T.; Desai, U. R. Exploring new non-sugar sulfated molecules as activators of antithrombin. *Bioorg. Med. Chem. Lett.* **2003**, *13*, 579–583.

(109) Gunnarsson, G. T.; Desai, U. R. Hydropathic interaction analyses of small organic activators binding to antithrombin. *Bioorg. Med. Chem.* **2004***, 12*, 633-640.

(110) Raghuraman, A.; Liang, A.; Krishnasamy, C.; Lauck, T.; Gunnarsson, C. T.; Desai, U. R. On designing non-saccharide, allosteric activators of antithrombin. *Eur. J. Med. Chem.* **2009**, *44*, 2626-2631.

(111) Liang, A.; Thakkar, J. N.; Desai, U. R. Study of physico-chemical properties of novel highly sulfated, aromatic, mimetics of heparin and heparan sulfate. *J. Pharm. Sci.* **2010**, *99*, 1207-1216.

(112) Al-Horani, R. A.; Desai, U. R. Chemical sulfation of small molecules–Advantages and challenges. *Tetrahedron* **2010**, *66*, 2907–2918.

(113) Raghuraman, A.; Riaz, M.; Hindle, M.; Desai, U. R. Rapid, high-yielding microwave-assisted per-sulfation of organic scaffolds. *Tetrahedron Lett.* **2007**, *48*, 6754–6758.

(114) Perzborn, E.; Roehrig, S.; Straub, A.; Kubitza, D.; Misselwitz, F. The discovery and development of rivaroxaban, an oral, direct factor Xa inhibitor. *Nat. Rev. Drug Discov.* **2011**, *10*, 61–75.

(115) Leadley, R. J. Coagulation factor Xa inhibition: biological background and rationale. *Curr. Top. Med. Chem.* **2011***, 1*, 151–159.

(116) Brown, D. L.; Kouides, P. A. Diagnosis and treatment of inherited factor X deficiency. *Haemophilia* **2008**, *14*, 1176–1182.

(117) Padmanabhan, K.; Padmanabhan, K. P.; Tulinsky, A.; Park, C. H.; Bode, W.; Huber, R.; Blankenship, D.T.; Cardin, A. D.; Kisiel, W. Structure of human des(1–45) factor Xa at 2.2 Å resolution. *J. Mol. Bio.***1993**, 232, 947–966.

(118) Pinto, D. J. P.; Smallheer, J. M.; Cheney, D. L.; Knabb, R. M.; Wexler, R. R. Factor Xa inhibitors: Next–generation antithrombotic agents. *J. Med. Chem.* **2010**, *53*, 6243–6274.

(119) Pinto, D. J.P.; Orwat, M. J.; Koch, S.; Rossi, K. A.; Alexander, R. S.; Smallwood, A.; Wong, P. C.; Rendina, A. R.; Luettgen, J. M.; Knabb, R. M.; He, K.; Xin, B.; Wexler, R.

R.; Lam, P. Y. S. Discovery of 1-(4-methoxyphenyl)-7-oxo-6-(4-(2-oxopiperidin-1-yl)-phenyl)-4,5,6,7-tetrahydro-1H-pyrazolo[3,4-c]pyridine-3-carboxamide (apixaban, BMS-562247), a highly potent, selective, efficacious, and orally bioavailable inhibitor of blood coagulation factor Xa. *J. Med. Chem.* **2007**, 50, 5339–5356.

(120) Zhang, P.; Huang, W.; Wang, L.; Bao, L.; Jia, Z. J.; Shawn M. Bauer, S. M.; Goldman, E. A.; Probst, G. D.; Song, Y.; Su, T.; Fan, J.; Wu, Y.; Li, W.; Woolfrey, J.; Sinha, U.; Wong, P. W.; Edwards, S. T.; Arfsten, A. E.; Lane A. Clizbe, L. A.; Kanter, J.; Pandey, A.; Gary Park, G.; Hutchaleelaha, A.; Lambing, J. L.; Hollenbach, S. J.; Scarborough, R. M.; Zhu, B.-Y. Discovery of betrixaban (PRT054021), N-(5-chloropyridin-2-yl)-2- (4-(N,N-dimethylcarbamimidoyl) benzamido)-5-methoxybenzamide, a highly potent, selective, and orally efficacious factor Xa inhibitor. *Bioorg. Med. Chem. Lett.* **2009**, *19*, 2179–2185.

(121) Kohrt, J.T.;Bigge,C.F.;Bryant, J.W.;Casimiro-Garcia,A.;Chi,L.; Cody, W. L.;Dahring, T.; Dudley, D. A.; Filipski, K. J.;Haarer, S.; Heemstra, R.; Janiczek, N.; Narasimhan, L.; McClanahan, T.; Peterson, J. T.; Sahasrabudhe, V.; Schaum, R.; Van Huis, C. A.; Welch, K. M.; Zhang, E.; Leadley, R. J.; Edmunds, J. J. The discovery of (2R,4R)-N-(4-chlorophenyl)-N-(2-fluoro-4-(2-oxopyridin- 1(2H)-yl)phenyl)-4-methoxypyrrolidine-1,2-dicarboxamide (PD 0348292), an orally efficacious factor Xa inhibitor. *Chem. Biol. Drug. Des.* **2007**, *70*, 100–112.

(122) Furugohri, T.; Isobe, K.; Honda, Y.; Kamisato-Matsumoto, C.; Sugiyama, N.; Nagahara, T.; Morishima, Y.; Shibano, T. DU-176b, a potent and orally active factor Xa inhibitor: in vitro and in vivo pharmacological profiles. *J. Thromb. Haemostasis* **2008**, *6*, 1542–1549.

(123) Hirayama, F.; Koshio, H.; Ishihara, T.; Hachiya, S.; Sugasawa, K.; Koga, Y.; Seki, N.; Shiraki, R.; Shigenaga, T.; Iwatsuki, Y.; Moritani, Y.; Mori, K.; Kadokura, T.; Kawasaki, T.; Matsumoto, Y.; Sakamoto, S.; Tsukamoto, S. Discovery of N-[2-Hydroxy-6-(4-methoxybenzamido)phenyl]-4-(4-methyl-1,4-diazepan-1-yl)benzamide (Darexaban, YM150) as a potent and orally available factor Xa inhibitor. *J. Med. Chem*. **2011**, *54*, 8051–8065.

(124) Fujimoto, T.; Imaeda, Y.; Konishi, N.; Hiroe, K.; Kawamura, M.; Textor, G. P.; Aertgeerts, K.; Kubo, K. Discovery of a tetrahydropyrimidin-2(1H)-one derivative (TAK-442) as a potent, selective, and orally active factor Xa inhibitor. *J. Med. Chem*. **2010**, *53*, 3517–3531.

(125) Roehrig, S.; Straub, A.; Pohlmann, J.; Lampe, T.; Pernerstorfer, S.; Schlemmer, K.-H.; Reinemer, P.; Perzborn, E. Discovery of the novel antithrombotic agent 5-chloro-*N*-({(5*S*)-2-oxo-3- [4-(3-oxomorpholin-4-yl)phenyl]-1,3-oxazolidin-5-yl}methyl)thiophene-2-carboxamide (BAY 59-7939): An oral, direct factor Xa inhibitor. *J. Med. Chem*. **2005**, *48*, 5900 – 5908.

(126) Eriksson, B. I.; Quinlan, D. J.; Weitz, J. I. Comparative pharmacodynamics and pharmacokinetics of oral direct thrombin and factor Xa inhibitors in development. *Clin. Pharmacokinet.* **2009**, *48*, 1–22.

(127) Wysowski, D. K.; Nourjah, P.; Swartz, L. Bleeding complications with warfarin use: a prevalent adverse effect resulting in regulatory action. *Arch. Intern. Med.* **2007**, *167*, 1414–1419.

(128) Blick, S. K.; Orman, J. S.; Wagstaff, A. J.; Scott, L. J. Spotlight on fondaparinux sodium in acute coronary syndromes. *BioDrugs* **2008**, *22*, 413–415.

(129) Antman, E. M.; Morrow, D. A.; McCabe, C. H.; Murphy, S. A.; Ruda, M.; Sadowski, Z.; Budaj, A.; Lopez-Sendon, J. L.; Guneri, S.; Jiang, F.; White, H. D.; Fox, K. A.; Braunwald, E. Enoxaparin versus unfractionated heparin with fibrinolysis for ST-elevation myocardial infarction. *New Eng. J. Med.* **2006**, *354*, 1477–1488.

(130) Senaran, H.; Acaroglu, E.; Ozdemir, H. M.; Atilla, B. Enoxaparin and heparin comparison of deep vein thrombosis prophylaxis in total hip replacement. *Arch. Orthop. Trauma Surg.* **2006**, *126*, 1–5.

(131) Fanikos, J.; Tsilimingras, K.; Kucher, N.; Rosen, A. B.; Hieblinger, M. D.; Goldhaber, S. Z. Comparison of efficacy, safety, and cost of low-molecular-weight heparin with continuous-infusion unfractionated heparin for initiation of anticoagulation after mechanical prosthetic valve implantation. *Am. J. Cardiol.* **2004**, *93*, 247-250.

(132) Yusuf, S.; Mehta, S. R.; Chrolavicius, S.; Afzal, R.; Pogue, J.; Granger, C. B.; Budaj, A.; Peters, R. J.; Bassand, J. P.; Wallentin, L.; Joyner, C.; Fox, K. A. Comparison of fondaparinux and enoxaparin in acute coronary syndromes. *New Eng. J. Med.* **2006**, *354*, 1464–1476.

(133) Chung, T. L.; Holton, L. H 3rd.; Silverman, R. P. The effect of fondaparinux versus enoxaparin in the survival of a congested skin flap in a rabbit model. *Ann. Plast. Surg.* **2006**, *56*, 312–315.

(134) Samama, M. M.; Gerotziafas, G. T. Evaluation of the pharmacological properties and clinical results of the synthetic pentasaccharide (fondaparinux). *Thromb. Res.* **2003**, *109*, 1–11.

(135) Turpie, A. G.; Eriksson, B. I.; Lassen, M. R.; Bauer, K. A. Fondaparinux, the first selective factor Xa inhibitor. *Curr. Opin. Hematol.* **2003**, *10*, 327–332.

(136) Juurlink, D. N. Drug interactions with warfarin: what clinicians need to know. *CMAJ* **2007**, *177*, 369–371.

(137) Delaney, J. A.; Opatrny, L.; Brophy, J. M.; Suissa, S. Drug drug interactions between antithrombotic medications and the risk of gastrointestinal bleeding. *CMAJ* **2007**, *177*, 347–351.

(138) Carroll, D. N.; Carroll, D. G. Interactions between warfarin and three commonly prescribed fluoroquinolones. *Ann. Pharmacother.* **2008**, *42*, 680–685.

(139) Thijssen, H. H.; Soute, B. A.; Vervoort, L. M.; Claessens, J. G. Paracetamol (acetaminophen) warfarin interaction: NAPQI, the toxic metabolite of paracetamol, is an inhibitor of enzymes in the vitamin K cycle. *Thromb. Haemost.* **2004**, *92*, 797–802.

(140) Hornsby, L. B.; Hester, E. K.; Donaldson, A. R. Potential interaction between warfarin and high dietary protein intake. *Pharmacotherapy* **2008**, *28*, 536–539.

(141) Cheng, T. O. Not only green tea but also green leafy vegetables inhibit warfarin. *Int. J. Cardiol.* **2008**, *125*, 101.

(142) Weitz, J. I.; Hudoba, M.; Massel, D.; Maraganore, J.; Hirsh, J. Clot-bound thrombin is protected from inhibition by heparin-antithrombin III but is susceptible to inactivation by antithrombin III-independent inhibitors. *J. Clin. Invest.* **1990**, *86*, 385–391.

(143) Weitz, J. I.; Leslie, B.; Hudoba, M. Thrombin binds to soluble fibrin degradation products where it is protected from inhibition by heparin-antithrombin but susceptible to inactivation by antithrombin-independent inhibitors. *Circulation* **1998**, *97*, 544–552.

(144) Kumar, R.; Beguin, S.; Hemker, H. C. The influence of fibrinogen and fibrin on thrombin generation–evidence for feedback activation of the clotting system by clot bound thrombin. *Thromb. Haemost.* **1994**, *72,* 713–721.

(145) Shikata, E.; Ieiri, I.; Ishiguro, S.; Aono, H.; Inoue, K.; Koide, T.; Ohgi, S.; Otsubo, K. Association of pharmacokinetic (CYP2C9) and pharmacodynamic (factors II, VII, IX, and X; proteins S and C; and gamma-glutamyl carboxylase) gene variants with warfarin sensitivity. *Blood* **2004**, *103*, 2630–2635.

(146) Schwarz, U. I.; Ritchie, M. D.; Bradford, Y.; Li, C.; Dudek, S. M.; Frye-Anderson, A.; Kim, R. B.; Roden, D. M.; Stein, C. M. Genetic determinants of response to warfarin during initial anticoagulation. *N. Engl. J. Med.* **2008**, *358*, 999–1008.

(147) Greinacher, A.; Alban, S.; Omer-Adam, M. A.; Weitschies, W.; Warkentin, T. E. Heparin-induced thrombocytopenia: a stoichiometry-based model to explain the differing immunogenicities of unfractionated heparin, low molecular weight heparin, and fondaparinux in different clinical settings. *Thromb. Res.* **2008**, *122*, 211–220.

(148) Morris, T. A.; Castrejon, S.; Devendra, G.; Gamst, A. C. No difference in risk for thrombocytopenia during treatment of pulmonary embolism and deep venous thrombosis with either low molecular weight heparin or unfractionated heparin: a metaanalysis. *Chest* **2007**, *132*, 1131–1139.

(149) Warkentin, T. E.; Greinacher, A. Heparin-induced thrombocytopenia: recognition, treatment, and prevention: the Seventh ACCP Conference on Antithrombotic and Thrombolytic Therapy. *Chest* **2004**, *126*, 311S–337S.

(150) Guerrini, M.; Beccati, D.; Shriver, Z.; Naggi, A.; Viswanathan, K.; Bisio, A.; Capila, I.; Lansing, J. C.; Guglieri, S.; Fraser, B.; Al-Hakim, A.; Gunay, N. S.; Zhang, Z.; Robinson, L.; Buhse, L.; Nasr, M.; Woodcock, J.; Langer, R.; Venkataraman, G.; Linhardt, R. J.; Casu, B.; Torri, G.; Sasisekharan, R. Oversulfated chondroitin sulfate is a contaminant in heparin associated with adverse clinical events. *Nat. Biotechnol.* **2008**, *26*, 669–675.

(151) Kishimoto, T. K.; Viswanathan, K.; Ganguly, T.; Elankumaran, S.; Smith, S.; Pelzer, K.; Lansing, J. C.; Sriranganathan, N.; Zhao, G.; Galcheva-Gargova, Z.; Al-Hakim, A.; Bailey, G. S.; Fraser, B.; Roy, S.; Rogers-Cotrone, T.; Buhse, L.; Whary, M.; Fox, J.; Nasr, M.; Dal Pan, G. J.; Shriver, Z.; Langer, R.S.; Venkataraman, G.; Austen, K. F.; Woodcock, J.; Sasisekharan, R. Contaminated heparin associated with adverse clinical events and activation of the contact system. *N. Engl. J. Med.* **2008**, *358*, 2457–2467.

(152) Le Templier, G.; Rodger, M. A. Heparin-induced osteoporosis and pregnancy. *Curr. Opin. Pulm. Med.* **2008**, *14*, 403–407.

(153) Lubenow, N.; Greinacher, A. Hirudin in heparin-induced thrombocytopenia. *Semin Throm. Hemost.* **2002**, *28*, 431–438.

(154) Coons, J. C.; Battistone, S. 2007 Guideline update for unstable angina/non-ST-segment elevation myocardial infarction: focus on antiplatelet and anticoagulant therapies. *Ann. Pharmacother.* **2008**, *42*, 989–1001.

(155) Warkentin, T. E. Bivalent direct thrombin inhibitors: hirudin and bivalirudin. *Best Pract. Res. Clin. Haematol.* **2004**, *17*, 105–125.

(156) Römisch, J.; Diehl, K. H.; Hoffmann, D.; Krahl-Mateblowski, U.; Reers, M.; Stüber, W.; Pâques, E. P. Comparison of in vitro and in vivo properties of rhirudin (HBW 023) and a synthetic analogous peptide. *Haemostasis* **1993**, *23*, 249–258.

(157) Braun, P. J.; Dennis, S.; Hofsteenge, J.; Stone, S. R. Use of site-directed mutagenesis to investigate the basis for the specificity of hirudin. *Biochemistry* **1988**, *27*, 6517–6522.

(158) Mohapatra, R.; Tran, M.; Gore, J. M.; Spencer, F. A. A review of the oral direct thrombin inhibitor ximelagatran: not yet the end of the warfarin era. *Am. Heart J.* **2005**, *150*, 19–26.

(159) Stempelj, M.; Zorko, M.; Peternel, L.; Urleb, U.; Ferjan, I. Histamine release, an undesired effect of thrombin inhibitors with basic character, is mediated through direct activation of G(i) proteins. *Eur. J. Pharmacol.* **2006**, *538*, 182–187.

(160) Peternel, L.; Stempelj, M.; Cerne, M.; Zega, A.; Obreza, A.; Oblak, M.; Drevensek, G.; Budihna, M. V.; Stanovnik, L.; Urleb, U. Direct thrombin inhibitors built on the azaphenylalanine scaffold provoke degranulation of mast cells. *Thromb. Haemost.* **2006**, *95*, 294–300.

(161) Food and Drug Administration. Pradaxa (dabigatran etexilate mesylate): Drug safety communication--Safety review of post-market reports of serious bleeding events. December 7, 2011. Available at: http:/www.fda.gov/Safety/ MedWatch/ Safety Information/SafetyAlertsforHumanMedicalProducts/ucm282820.htm

(162) Steiner, T.; Rosand, J.; Diringer, M.; Intracerebral Hemorrhage associated with oral anticoagulant therapy: Current practices and unresolved questions. *Stroke*, **2006**, *37*, 256–262.

(163) Zhang, Y.; Feng, J.; Liu, C.; Zhang, L.; Jiao, J.; Fang, H.; Su, L.; Zhang, X.; Zhang, J.; Li, M.; Wang, B.; Xu, W. Design, synthesis and preliminary activity assay of 1,2,3,4-tetrahydroisoquinoline-3-carboxylic acid derivatives as novel Histone deacetylases (HDACs) inhibitors. *Bioorg. Med. Chem.* **2010**, *18*, 1761-1772.

(164) Cheng, S.; Zhang, X.; Wang, W.; Zhao, M.; Zheng, M.; Chang, H. W.; Wu, J.; Peng, S. A class of novel N-(3S-1,2,3,4-tetrahydroisoquinoline-3-carbonyl)-L-amino acid derivatives: their synthesis, anti-thrombotic activity evaluation, and 3D QSAR analysis. *Eur .J. Med. Chem.* **2009**, *44*, 4904-4919.

(165) Azukizawa, S.; Kasai, M.; Takahashi, K.; Miike, T.; Kunishiro, K.; Kanda, M.; Mukai, C.; Shirahase, H. Synthesis and biological evaluation of (*S*)-1,2,3,4-tetrahydroisoquinoline-3-carboxylic acids: A novel series of PPARγ agonists. *Chem. Pharm. Bull.* **2008**, *56*, 335-345.

(166) Cai, T. B.; Zou, Z.; Thomas, J. B.; Brieaddy, L.; Navarro, H. A.; Carroll, F. I. Synthesis and In vitro opioid receptor functional antagonism of analogues of the selective Kappa opioid receptor antagonist (3*R*)-7-Hydroxy-*N*-((1*S*)-1-{[(3*R*,4*R*)-4-(3-hydroxyphenyl)-3,4-dimethyl-1-piperidinyl]methyl}-2-methylpropyl)-1,2,3,4-tetrahydro-3-isoquinolinecarboxamide (JDTic). *J. Med. Chem.* **2008**, *51*, 1849–1860.

(167) Cox, E.D., Cook, J. M. The Pictet-Spengler condensation: a new direction for an old reaction. *Chem. Rev.* **1995**, *95*, 1797–1842.

(168) Whaley, W.M.; Govindachari, T.R. The Pictet–Spengler synthesis of tetrahydro–isoquinolines and related compounds. In *Organic Reactions*: Adams, R., Ed.; Wiley: New York, **1951**, *6*, 74–150.

(169) Liu, J-M.; Young, J-J.; Li, Y-J.; Sha, C-K. Synthesis of substituted 1,2 dihydro–isoquinolines by the intramolecular 1,3-dipolar alkyl azide-olefin cycloaddition. *J. Org. Chem.* **1986**, *51*, 1120-1123.

(170) Kotha, S.; Sreenivasachary, N. Tetrahydroisoquinoline-3-carboxylic Acid (Tic) derivatives via a [2 + 2 + 2] cycloaddition reaction. *Bioorg. Med. Chem. Lett.* **2000**, *10*, 1413-1415.

(171) Kotha, S.; Sreenivasachary, N. A new synthetic approach to 1,2,3,4-tetrahydro–isoquinoline-3-carboxylic acid (Tic) derivatives *via* enyne metathesis and the Diels–Alder reaction. *Chem. Commun.* **2000**, 503–504.

(172) Toda, J.; Matsumoto, S.; Saitoh, T.; Sano, T. *Chem.* A Chiral synthesis of four stereoisomers of 1,3-dimethyl-1,2,3,4-tetrahydroisoquinoline, an inducer of Parkinson-like syndrome. *Pharm. Bull.* **2000**, *48*, 91-98.

(173) Hirsenkorn, R. Short-cut in the pomeranz-fritsch synthesis of 1-benzyl-isoquinolines; short and efficient syntheses of norrecticuline derivatives and of papaverine. *Tetrahedron Lett.* **1991**, *32*, 1775-1778.

(174) Kommidi, H.; Balasubramaniam, S.; Aidhen, I. S. Weinreb amide-based synthetic equivalents for convenient access to 4-aryl-1,2,3,4-tetrahydroquinolines. *Tetrahedron* **2010**, *66*, 3723-3729.

(175) Kihara, M.; Kashimoto, M.; Kobayashi, Y. A Convenient synthesis of 4-substituted 1,2,3,4-tetrahydroisoquinolin-4-ols by a novel intramolecular Barbier reaction and by an insertion reaction. Reaction scope and limitations. *Tetrahedron* **1992**, *48*, 67–78.

(176) Gremmen, C.; Wanner, M. J.; Koomen, G.-J. Enantiopure tetrahydroisoquinolines via N-sulfinyl Pictet–Spengler reactions. *Tetrahedron Lett*. **2001**, *42*, 8885–8888.

(177) Connors, R. V.; Zhang A. J.; Shuttleworth, S.J. Pictet-Spengler synthesis of tetrahydro-β-carbolines using vinylsulfonylmethyl resin. *Tetrahedron Lett*. **2002**, *43*, 6661–6663.

(178) Miles, W. H.; Heinsohn, S. K.; Brennan, M. K.; Swarr, D. T.; Eidam, P. M.; Gelato, K. A. The oxa-Pictet-Spengler reaction of 1-(3-furyl)-2-alkanols. *Synthesis* **2002**, 1541-1545.

(179) Nielsen, T.E.; Diness, F.; Meldal, M.The Pictet-Spengler reaction in solid-phase combinatorial chemistry. *Curr. Opin. Drug Discov. Devel.* **2003**, *6*, 801-814.

(180) Pal, B.; Jaisankar, P.; Giri, V. S. Microwave assisted Pictet-Spengler and Bischler-Napieralski reactions. *Synth. Commun.* **2003**, *33*, 2339-2348.

(181) Nielsen T. E.; Meldal, M. Solid-phase intramolecular *N*-acyliminium Pictet–Spengler reactions as crossroads to scaffold diversity. *J. Org. Chem.* **2004**, *69*, 3765-3773.

(182) Taylor, M.S.; Jacobsen, E. N. Highly enantioselective catalytic acyl-Pictet-Spengler reactions. *J. Am. Chem. Soc.* **2004**, *126*, 10558-10559.

(183) Maryanoff, B. E.; Zhang, H.-C.; Cohen, J. H.; Turchi, I. J.; Maryanoff C. A. *Cyclizations* of *N*–acyliminium ions. *Chem. Rev.* **2004**, *104*, 1431–1628.

(184) Lesma, G.; Danieli, B.; Lodroni, F.; Passarella, D.; Sacchetti, A.; Silvani, A. Microwave–assisted, solid-phase synthesis of a chiral 1,2,3,4–tetrahydroquinoline library. *Comb. Chem. & High Thr. Scr.* **2006**, *9,* 691-701.

(185) Meutermans, W. D. F.; Alewood, P. F. The solid phase synthesis of dihydro- and tetrahydro-isoquinolines. *Tetrahedron Lett.* **1995***, 36*, 7709–7712.

(186) Nicoletti, M.; O'Hagan, D.; Slawin, A. M. Z. The asymmetric Bischler–Napieralski reaction: preparation of 1,3,4-trisubstituted 1,2,3,4-tetrahydroisoquinolines. *J. Chem. Soc. Perkin Trans. 1* **2002**, 116–121.

(187) Judeh, Z. M. A.; Ching, C. B.; Bu, J.; McCluskey, A. The first Bischler-Napieralski cyclization in a room temperature ionic liquid. *Tetrahedron Lett.* **2002**, *43*, 5089-5091.

(188) Schollkopf, U.; Hinrchs, R.; Lonsky, R. Asymmetric synthesis of cyclic α-amino acids by the bislactim ether method. *Angew. Chem., Int. Engl. Ed.* **1987***, 26*, 143-145.

(189) Seebach, D.; Dziadulewicz, E.; Behrendt, L.; Cantoreggi, S.; Fitzi, R. Synthesis of Nonproteinogenic (*R*)- or (*S*)-Amino Acids Analogues of Phenylalanine, Isotopically Labeled and Cyclic Amino Acids from *tert*-Butyl 2-(*tert*-Butyl)-3-methyl-4-oxo-1-imidazolidinecarboxylate (Boc-BMI). *Liebigs Ann. der Chem.* **1989**, *12*, 1215-1232.

(190) Kammermeier, T.; Lerch, U.; Sommer, C. Efficient synthesis of racemic and enantiomerically pure 1,2,3,4–tetrahydroisoquinoline–3–carboxylic acid and esters. *Synthesis* **1992**, 1157–1160.

(191) Wang, C.; Moseberg, H. I. Synthesis of a novel series of topographically constrained amino acids: Benzo–1,2,3,4–tetrahydroisoquinoline–3–carboxylic Acids. *Tetrahedron Lett.* **1995**, *36*, 3623–3626.

(192) Mash, E. A.; Williams, L. J.; Pfeiffer, S. S. Synthesis of ethyl *N*-(diphenyl)methyl-1,2,3,4-tetrahydro-isoquinoline-3-carboxylates. *Tetrahedron Lett*. **1997**, *38*, 6977-6988.

(193) Chinchilla, R.; Galindo, N.; Najera, C. Chiral 3,6-dihydro-2H-1,4-oxazin-2-ones as alanine equivalents for the asymmetric synthesis of α-methyl α-amino Acids (AMAAs) under mild reaction conditions. *Synthesis* **1999**, 704–717.

(194) Fukuyama, T.; Linton, S. D.; Tun, M. M. A stereocontrolled total synthesis of (±)-renieramycin A. *Tetrahedron Lett.* **1990**, *31*, 5989–5992.

(195) Kazmierski, W. M.; Urbanczyk-Lipkowska, Z.; Hruby, V. J. New amino acids for the topographical control of peptide conformation: synthesis of all the isomers of α,β-

dimethylphenylalanine and α,β-dimethyl-1,2,3,4-tetrahydroisoquinoline-3-carboxylic acid of high optical purity. *J. Org. Chem.* **1994**, *59*, 1789-1795.

(196) Singh, R. B.; Rai, D. K. Potential curves and bond strength of PO. *J. Phys. Chem.* **1965**, 69, 3461–3462.

(197) Knor, S.; Laufer, B.; Kessler, H. Efficient enantioselective synthesis of condensed and aromatic-ring-substituted tyrosine derivatives. *J. Org. Chem.* **2006**, 71, 5625–5630.

(198) Schmidt, U.; Lieberknecht, A.; Wild, J. Amino acids and peptides; XLIII. Dehydroamino acids; XVIII. Synthesis of dehydroamino acids and amino acids from *N*-Acyl-2-(dialkyloxyphosphinyl)-glycin Esters; II. *Synthesis* 1984, 53–60.

(199) Knowles, W. S. Asymmetric hydrogenations (Nobel Lecture). *Angew. Chem., Int. Engl. Ed.* **2002**, 41, 1998–2007.

(200) Wang, W.; Li, H. An efficient synthesis of the intrinsic fluorescent peptide labels, (*S*)- and (*R*)-(6,7-dimethoxy-4-coumaryl)alanines via asymmetric hydrogenations. *Tetrahedron Lett.* **2004**, 45, 8479–8481.

(201) Bringmann, G.; Ochse, M.; Michel, M. Gentrymine B, an *N*-quaternary Ancistrocladus alkaloid: stereoanalysis, synthesis, and biomimetic formation from Gentrymine A [1]. *Tetrahedron* **2000**, 56, 581–585.

(202) Kitamura, M.; Tsukamoto, M.; Takaya, H.; Noyori, R. Conformational study on 2-Acyl-1-alkylidene-1,2,3,4-tetrahydroisoquinolines. *Bull. Chem. Soc. Jpn.* **1996**, 69, 1695–1700.

(203) Fraenkel, G.; Cava, M. P.; Dalton, D. R. Hindered Rotation in 1-Benzyl-1,2,3,4-tetrahydro-6-7-dimethoxyisoquinolines. *J. Am. Chem. Soc.***1967**, 89, 329–332.

(204) de Koning, C.B.; van Otterlo, W. A. L., Michael, J. P. Amide rotamers of N-acetyl-1,3-dimethyltetrahydroisoquinolines: synthesis, variable temperature NMR spectroscopy and molecular modeling. *Tetrahedron* **2003**, 59, 8337-8345.

(205) Wouters, J.; Elassad, K.; Norberg, B.; Graulich, A.; Liegeois, J-F. *Bis*-tetrahydro-isoquinoline derivatives: structure analysis of the three stereoisomers of 1,1′-(propane-1,3-diyl)-bis-(6,7-dimethoxy-2-methyl-1,2,3,4-tetrahydroisoquinoline). *Eur. J. Med. Chem.* **2010**, 45, 3240-3244.

(206) Bishop, G. J.; Price, B. J.; Sutherland, I. O. Torsional barriers in *NN*′-diacylhydrazines**.** *J. Chem. Soc., Chem. Commun.* **1967**, 672–674.

(207) Shanan-Atidi, H.; Bar-Eli, K. H. A Convenient method for obtaining free energies of activation by the coalescence temperature of an unequal doublet. *J. Phys. Chem.* **1970**, 74, 961–963.

(208) Kost, D.; Carlson, E. H.; Raban, M. The validity of approximate equations for k_c in dynamic nuclear magnetic resonance**.** *J. Chem. Soc., Chem. Commun.* **1971**, 656–657.

(209) Hirsh, J.; Anand, S. S.; Halperin, J. L.; Fuster, V. Guide to anticoagulant therapy: Heparin. *Circulation* **2001**, *103*, 2994–3018.

(210) Blossom, D. B.; Kallen, A. J.; Patel, P. R.; Elward, A.; Robinson, L.; Gao, G.; Langer, R.; Perkins, K. M.; Jaeger, J. L.; Kurkjian, K. M.; Jones, M.; Schillie, S. F.; Shehab, N.; Ketterer, D.; Venkataraman, G.; Kishimoto, T. K.; Shriver, Z.; McMahon, A. W.; Austen, K. F.; Kozlowski, S.; Srinivasan, A.; Turabelidze, G.; Gould, C. V.; Arduino, M. J.; Sasisekharan, R. Outbreak of adverse reactions associated with contaminated heparin. *N. Engl. J. Med.* **2008**, *359*, 2674–2684.

(211) Gray, E.; Mulloy, B.; Barrowcliffe, T. W. Heparin and low-molecular-weight heparin. *Thromb. Haemost.* **2008***, 99*, 807–818.

(212) Rabenstein, D. L. Heparin and heparin sulfate: Structure and function. *Nat. Prod. Rep.* **2002***, 19*, 312–331.

(213) Tran, A. H.; Lee, G. Fondaparinux for prevention of venous thromboembolism in major orthopedic surgery. *Ann. Pharmacother.* **2003**, *37*, 1632-1643.

(214) Tsiridis, E.; Gamie, Z.; George, M. J.; Hamilton-Baille, D.; West, R. M.; Giannoudis, P. V. Early postoperative bleeding in polytrauma patients treated with fondaparinux: literature review and institutional experience. *Curr. Vasc. Pharmacol.* **2011**, *9*, 42-47.

(215) Akl, E. A.; Vasireddi, S. R.; Gunukula, S.; Barba, M.; Sperati, F.; Terrenato, I.; Muti, P.; Schünemann, H. Anticoagulation for the initial treatment of venous thromboembolism in patients with cancer. *Cochrane Database Syst. Rev.* **2011**, *6*, CD006649.

(216) Brito, V.; Ciapponi, A.; Kwong, J. Factor Xa inhibitors for acute coronary syndromes. *Cochrane Database Syst Rev.* **2011**, *1*, CD007038.

(217) Freeman, C.; Liu, L.; Banwell, M. G.; Brown, K. J.; Bezos, A.; Ferro, V.; Parish, C. R. Use of sulfated linked cyclitols as heparan sulfate mimetics to probe the heparin/heparan sulfate binding specificity of proteins. *J. Biol. Chem.* **2005**, *280*, 8842–8849.

(218) Kim, S. K.; Huh, J.; Kim, S. Y.; Byun, Y.; Lee, D. Y.; Moon, H. T. Physicochemical conjugation with deoxycholic acid and dimethylsulfoxide for heparin oral delivery. *Bioconjugate Chem.* **2011**, *22*, 1451–1458.

(219) Desai, U. R.; Petitou, M.; Bjork, I.; Olson, S. T. Mechanism of heparin activation of antithrombin: evidence for an induced fit model of allosteric activation involving two interaction subsites. *Biochemistry* **1998**, *37*, 13033–13041.

(220) Raghuraman, A.; Mosier, P. D.; Desai, U. R. Finding a needle in a haystack. Development of a combinatorial virtual screening approach for identifying high specificity heparin/heparan sulfate sequence(s). *J. Med. Chem.* **2006**, *49*, 3553-3562.

(221) Kellogg, G. E.; Abraham, D. J. Hydrophobicity: is LogP(o/w) more than the sum of its parts? *Eur. J. Med Chem.* **2000**, *35*, 651-661.

(222) Tripathi, A.; Surface, J. A.; Kellogg, G. E. Using active site mapping and receptor-based pharmacophore tools: prelude to docking and de novo/fragment-based ligand design. *Methods Mol. Biol.* **2011**, *716*, 39-54.

(223) Raghuraman, A.; Mosier, P. D.; Desai, U. R. Understanding dermatan sulfate_heparin cofactor II interaction through virtual library screening. *ACS Med. Chem. Lett.* **2010**, *1*, 281–285.

(224) Liang, A.; Raghuraman, A.; Desai, U. R. Capillary electrophoretic study of small, highly sulfated, non-sugar molecules interacting with antithrombin. *Electrophoresis* **2009**, *30*, 1544-1551.

(225) Huntington, J. A.; Baglin, T. P. Targeting thrombin–rational drug design from natural mechanisms, *Trends Pharmacol. Sci.* **2003**, *24*, 589–595.

(226) Popović, M.; Smiljanić, K.; Dobutović, B.; Syrovets, T.; Simmet, T.; Isenović, E. R. Thrombin and vascular inflammation. *Mol. Cell. Biochem.* **2012**, 359, 301–313.

(227) Yin, E. T.; Wessler, S. Heparin-accelerated inhibition of activated factor X by its natural inhibitor. *Biochem. Biophys. Acta.* **1970**, *201*, 387–390.

(228) Wessler, S.; Yin, E. T. Theory and practice of minidose heparin in surgical patients. *Circulation.* **1973**, *47*, 671–676.

(229) Hermans, C.; Claeys, D. Review of the rebound phenomenon in new anticoagulant treatments, *Curr. Med. Res. Opin*. **2006**, *22*, 471–481.

(230) Rezaie, R. A. Prothrombin protects factor Xa in the prothrombinase complex from inhibition by the heparin-antithrombin complex. *Blood* **2001**, *97*, 2308–2313.

(231) Al-Horani, R. A., Liang, A.; Desai, U. R. Designing nonsaccharide allosteric activators of antithrombin for accelerated inhibition of factor Xa. *J. Med. Chem.* **2011**, *54*, 6125–6138.

(232) Henry, B. L.; Monien, B. H.; Bock, P. E.; Desai, U. R. A novel allosteric pathway of thrombin inhibition. Exosite II mediated potent inhibition of thrombin by chemo-enzymatic, sulfated dehydropolymers of 4-hydroxycinnamic acids. *J. Biol. Chem.* **2007**, *282*, 31891–31899.

(233) Sidhu, P. S.; Liang, A.; Mehta, A. Y.; Abdel Aziz, M. H.; Zhou, Q.; Desai, U. R. Rational design of potent, small, synthetic allosteric inhibitors of thrombin, *J. Med. Chem.* **2011**, *54*, 5522–5531.

(234) Xu, Y.; Masuko, S.; Takieddin, M.; Xu, H.; Liu, R.; Jing, J.; Mousa, S. A.; Linhardt, R. J.; Liu, J. Chemoenzymatic synthesis of homogeneous ultralow molecular weight heparins. *Science* **2011**, *334*, 498–501.

(235) Pinto, D. J.; Orwat, DM. J.; Wang, S.; Fevig, J. M.; Quan, M. L.; Amparo, E.; Cacciola, J.; Rossi, K. A.; Alexander, R. S.; Smallwood, A. M.; Luettgen, J. M.; Liang, L.; Aungst, B. J.; Wright, M. R.; Knabb, R. M.; Wong, P. C.; Wexler, R. R.; Lam, P. Y. Discovery of 1-[3-(aminomethyl)phenyl]-*N*-[3-fluoro-2‘-(methylsulfonyl)- [1,1‘-biphenyl]-4-yl]-3-(trifluoromethyl)-1*H*-pyrazole-5-carboxamide (DPC423), a highly potent, selective, and orally bioavailable inhibitor of blood coagulation factor Xa, *J. Med. Chem.* **2001**, *44*, 566–578.

(236) Imaeda, Y.; Kuroita, T.; Sakamoto, H.; Kawamoto, T.; Tobisu, M.; Konishi, N.; Hiroe, K.; Kawamura, M.; Tanaka, T.; Kubo, K. Discovery of imidazo[1,5-c]imidazol-3-ones: Weakly basic, orally active factor Xa inhibitors, *J. Med. Chem.* **2008**, *51*, 3422–3436.

(237) Maignan, S.; Guilloteau, J. P.; Choi-Sledeski, Y. M.; Becker , M. R.; Ewing, W. R.; Pauls, H. W.; Spada, A. P.; Mikol, V. Molecular structures of human factor Xa complexed with ketopiperazine inhibitors: Preference for a neutral group in the S1 pocket. *J. Med. Chem.* **2003**, *46*, 685–690.

(238) Nagata, T.; Yoshino, T.; Haginoya, N.; Yoshikawa, K.; Nagamochi, M.; Kobayashi, S.; Komoriya, S.; Yokomizo, A.; Muto, R.; Yamaguchi, M.; Osanai, K.; Suzuki, M.; Kanno, H. Discovery of *N*- [(1R,2S,5S)-2-{[(5-chloroindol-2-yl)carbonyl]amino}-5-(dimethylcarbamoyl)cyclohexyl]-5-methyl- 4,5,6,7-tetrahydrothiazolo[5,4-c]pyridine-2-carboxamide hydrochloride: A novel, potent and orally active direct inhibitor of factor Xa. *Bioorg. Med. Chem.* **2009**, *17*, 1193–1206.

(239) Young, R. J.; Borthwick, A. D.; Brown, D.; Burns-Kurtis, C. L.; Campbell, M.; Chan, C.; Charbaut, M.; Chung, C. W.; Convery, M. A.; Kelly, H. A.; King, N.P.; Kleanthous, S.; Mason, A. M.; Pateman, A. J.; Patikis, A. N.; Pinto, I. L.; Pollard, D. R.; Senger, S.; Shah, G. P.; Toomey, J. R.; Watson, N. S.; Weston, H. E. Structure and property based design of factor Xa inhibitors: Pyrrolidin-2-ones with biaryl P4 motifs. *Bioorg. Med. Chem. Lett.* **2008**, *18*, 23–27.

(240) Smallheer, J. M.; Wang, S.; Laws, M. L.; Nakajima, S.; Hu, Z.; Han, W.; Jacobson, I.; Luettgen, J. M.; Rossi, K. A.; Rendina, A. R.; Knabb, R. M.; Wexler, R. R.; Lam, P. Y. S., Quan, M. L. Sulfonamidolactam inhibitors of coagulation factor Xa, *Bioorg. Med. Chem. Lett.* **2008**, *18*, 2428–2433.

(241) Kohrt, J. T.; Filipski, K. J.; Cody, W. L.; Bigge, C. F.; La, F.; Welch, K.; Dahring, T.; Bryant, J. W.; Leonard, D.; Bolton, G.; Narasimhan, L.; Zhang, E.; Peterson, J. T.;

Haarer, S.; Sahasrabudhe, V.; Janiczek, N.; Desiraju, S.; Hena, M.; Fiakpui, C.; Saraswat, N.; Sharma, R.; Sun, S.; Maiti, S. N.; Leadley, R.; Edmunds, J. J. The discovery of glycine and related amino acid-based factor Xa inhibitors. *Bioorg. Med. Chem.* **2006**, *14*, 4379–4392.

(242) Van Huis, C. A.; Casimiro-Garcia, A.; Bigge, C. F.; Cody, W. L.; Dudley, D. A.; Filipski, K. J.; Heemstra, R. J.; Kohrt, J. T.; Leadley, R. J. Jr.; Narasimhan, L. S.; McClanahan, T.; Mochalkin, I.; Pamment, M.; Thomas Peterson J.; Sahasrabudhe, V.; Schaum, R. P.; Edmunds, J. J. Exploration of 4,4-disubstituted pyrrolidine-1,2-dicarboxamides as potent, orally active factor Xa inhibitors with extended duration of action. *Bioorg. Med. Chem.* **2009**, *17*, 2501–2511.

(243) Ye, B.; Arnaiz, D. O.; Chou, Y. –L.; Griedel, B. D.; Karanjawala, R.; Lee, W.; Morrissey, M. M.; Sacchi, K. L.; Sakata, S. T.; Shaw, K. J.; Wu, S. C.; Zhao, Z.; Adler, M.; Cheeseman, S.; Dole, W. P.; Ewing, J.; Fitch, R.; Lentz, D.; Liang, A.; Light, D.; Morser, J.; Post, J.; Rumennik, G.; Subramanyam, B.; Sullivan, M. E.; Vergona, R.; Walters, J.; Wang, Y.-X.; White, K. A.; Whitlow, M.; Kochanny, M. J. Thiophene-anthranilamides as highly potent and orally available factor Xa inhibitors. *J. Med. Chem.* **2007**, *50*, 2967 – 2980.

(244) Pruitt, J. R.; Pinto, D. J.; Estrella, M. J.; Bostrom, L. L.; Knabb, R. M.; Wong, P. C.; Wright, M. R.; Wexler, R. R. Isoxazolines and isoxazoles as factor Xa inhibitors. *Bioorg. Med. Chem. Lett*. **2000**, *10*, 685–689.

(245) Quan, M. L.; Lam, P. Y. S.; Han, Q.; Pinto, D. J. P.; He, M. Y.; Renhua, E.; Christopher, D.; Clark, C. G.; Teleha, C. A.; Sun, J. –H.; Alexander, R. S.; Bai, S.; Luettgen, J. M.; Knabb, R. M.; Wong, P. C.; Wexler, R.R. Discovery of 1-(3′-Aminobenzisoxazol-5′-yl)-3-trifluoromethyl-*N*-[2-fluoro-4- [(2‘-dimethylamino-methyl)imidazol-1-yl]phenyl]-1*H*-pyrazole-5-carboxyamide Hydrochloride (Razaxaban), a highly potent, selective, and orally bioavailable factor Xa inhibitor. *J. Med. Chem.* **2005**, *48*, 1729 – 1744.

(246) Lee, Y.-K.; Parks, D. J.; Lu, T.; Thieu, T. V.; Markotan, T.; Pan, W.; McComsey, D. F.; Milkiewicz, K. L.; Crysler, C. S.; Ninan, N.; Abad, M. C.; Giardino, E. C.; Maryanoff, B. E.; Damiano, B. P.; Player, M. R. 7-Fluoroindazoles as potent and selective inhibitors of factor Xa. *J. Med. Chem.* **2008**, *51*, 282–297.

(247) Matter, H.; Defossa, E.; Heinelt, U.; Blohm, P. M.; Schneider, D.; Müller, A.; Herok, S.; Schreuder, H.; Liesum, A.; Brachvogel, V.; Lönze, P.; Walser, A.; Al-Obeidi, F.; Wildgoose, P. Design and quantitative structure-activity relationship of 3-amidinobenzyl-1H-indole-2-carboxamides as potent, nonchiral, and selective inhibitors of blood coagulation factor Xa. *J. Med. Chem.* **2002**, *45*, 2749–2769.

(248) Nazaré, M.; Will, D. W.; Matter, H.; Schreuder, H.; Ritter, K.; Urmann, M.; Essrich, M.; Bauer, A.; Wagner, M.; Czech, J.; Lorenz, M.; Laux, V.; Wehner, V. Probing the subpockets of factor Xa reveals two binding modes for inhibitors based on

a 2-carboxyindole scaffold: a studycombining structure-activity relationship and X-ray crystallography. *J. Med. Chem.* **2005**, *48*, 4511–4525.

(249) Pinto, D. J. P.; Galemmo, R. A. Jr.; Quan, M. L.; Orwat, M. J.; Clark, C.; Li, R.; Wells, B.; Woerner, F.; Alexander, R. S.; Rossi, K. A.; Smallwood, A.; Wong, P. C.; Luettgen, J. M.; Rendina, A. R.; Knabb, R. M.; He, K.; Wexler, R. R.; Lam, P. Y. S. Discovery of potent, efficacious, and orally bioavailable inhibitors of blood coagulation factor Xa with neutral P1 moieties. *Bioorg. Med. Chem. Lett.* **2006**, *16*, 5584–5589.

(250) Cheng, S.; Zhang, X.; Wang, W.; Zhao, M.; Zheng, M.; Chang, H. W.; Wu, J.; Peng, S. A class of novel *N*-(3S-1,2,3,4-tetrahydroisoquinoline-3-carbonyl)-L-amino acid derivatives: Their synthesis, antithrombotic activity evaluation, and 3D QSAR analysis. *Eur. J. Med. Chem*. **2009**, *44*, 4904-4919.

(251) Azukizawa, S.; Kasai, M.; Takahashi, K.; Miike, T.; Kunishiro, K.; Kanda, M.; Mukai, C.; Shirahase, H. Synthesis and biological evaluation of (S)-1,2,3,4-tetrahydroisoquinoline-3-carboxylic acids: A novel series of PPARγ agonists. *Chem. Pharm. Bull*. **2008**, *56*, 335-345.

(252) Cai, T. B.; Zou, Z.; Thomas, J. B.; Brieaddy, L.; Navarro, H. A.; Carroll, F. I. Synthesis and in vitro opioid receptor functional antagonism of analogues of the selective kappa opioid receptor antagonist (3R)-7-hydroxy-N-((1S)-1-{[(3R,4R)-4-(3-hydroxyphenyl)-3,4-dimethyl-1-piperidinyl] methyl}-2-methylpropyl)-1,2,3,4-tetrahydro-3-isoquinolinecarboxamide (JDTic). *J. Med. Chem*. **2008**, *51*, 1849-1860.

(253) Montalbetti, C. A.G. N.; Falque, V. Amide bond formation and peptide coupling. *Tetrahedron* **2005**, 61, 10827–10852.

(254) Klapars, A.; Huang, X.; Buchwald, S. L. A general and efficient copper catalyst for the amidation of aryl halides. *J. Am. Chem. Soc.* **2002**, *124*, 7421–7428.

(255) Shendage, D. M.; Froehlich, R.; Haufe, G. Highly efficient stereoconservative amidation and deamidation of α-Amino Acids, *Org. Lett.* **2004**, *6*, 3675–3678.

(256) Mathias, L. J.; Fuller, W. D.; Nissen, D.; Goodman, M. Polydepsipeptides. 6. Synthesis of sequential polymers containing varying ratios of L-alanine and L-lactic Acid. *Macromolecules* **1978**, *11*, 534–539.

(257) Verghese, J.; Liang, A.; Sidhu, P. P.; Hindle, M.; Zhou, Q.; Desai, U. R. First steps in the direction of synthetic, allosteric, direct inhibitors of thrombin and factor Xa, *Bioorg. Med. Chem. Lett.* **2009**, *19,* 4126–4129.

(258) Young, R. J. The successful quest for oral factor Xa inhibitors; Learnings for all of medicinal chemistry? *Bioorg. Med. Chem. Lett.* **2011**, *21*, 6228–6235.

(259) Rupprecht, H-J.; Blank, R. Clinical pharmacology of direct and indirect factor Xa inhibitors. *Drugs* **2010**, *70*, 2153–2170.

(260) Henry, B. L.; Thakkar, J. N.; Martin, E. J.; Brophy, D. F.; Desai, U. R. Characterization of the plasma and blood anticoagulant potential of structurally and mechanistically novel oligomers of 4-hydroxycinnamic acids. *Blood Coagulation Fibrinolysis* **2009**, *20*, 27–34.

(261) Monien, B. H.; Henry, B. L.; Raghuraman, A.; Hindle, M.; Desai, U. R. Novel chemo-enzymatic oligomers of cinnamic acids as direct and indirect inhibitors of coagulation proteinases. *Bioorg. Med. Chem.* **2006**, *14*, 7988–7998.

(262) Schumacher, W. A.; Seiler, S. E.; Steinbacher, T. E.; Stewart, A. B.; Bostwick, J. S.; Hartl, K. S.; Liu, E. C.; Ogletree, M. L. Antithrombotic and hemostatic effects of a small molecule factor XIa inhibitor in rats. *Eur. J. Pharmacol.* **2007**, *570*, 167–174.

(263) Clayden, J.; Moran, W. J.; Edwards, P. J.; LaPlante, S. R. The challenge of atropisomerism in drug discovery. *Angew. Chem. Int. Ed.* **2009**, *48*, 6398 – 6401.

(264) Correia-da-Silva, M.; Sousa, E.; Duarte, B.; Marques, F.; Carvalho, F.; Cunha-Ribeiro, L. M.; Pinto, M. M. Flavonoids with an oligopolysulfated moiety: A new class of anticoagulant agents. *J. Med. Chem.* **2011**, *54*, 95–106.

(265) Correia-da-Silva, M.; Sousa, E.; Duarte, B.; Marques, F.; Cunha-Ribeiro, L. M.; Pinto, M. M. Dual anticoagulant/antiplatelet persulfated small molecules. *Eur. J. Med. Chem.* **2011**, *46*, 2347–2358.

(266) Petitou, M.; van Boeckel, C. A. A synthetic antithrombin III binding pentasaccharide is now a drug! What comes next? *Angew. Chem., Int. Ed. Engl.* **2004**, *43*, 3118–3133.

(267) Kaiser, B. DX-9065a, a direct inhibitor of factor Xa. *Cardiovasc. Drug Rev.* **2003**, 21, 91–104.

(268) Al-Horani, R. A.; Desai, U. R. Electronically rich *N*-substituted tetrahydroisoquinoline-3-carboxylic acid esters: Concise synthesis and conformational studies. *Tetrahedron* **2012**, 68, 2027–2040.

VITA

Rami A. Al–Horani is a Jordanian citizen who was born on 13 June, 1977 in Al–Madinah Al–Munawwarah, Saudi Arabia. He earned his B.Sc. in Pharmacy in 2000 and later in 2003 he obtained his M.Sc. in Pharmaceutical Sciences. Both degrees were from University of Jordan in Amman, Jordan. From 2003 through 2007, he worked as an academic lecturer at different universities in Jordan including University of Jordan, Applied Science Private University of Jordan, and Al–Zytoonah Private University of Jordan. In 2007, he was granted a Fulbright scholarship to pursue his PhD in Medicinal Chemistry at Virginia Commonwealth University, Richmond–Virginia, USA. The Fulbright scholarship was sponsored by US Department of State and was granted based on merit.